

Design for Cost Methodology Applied to High Temperature Gas-Cooled Reactors

by

Lorenzo Venneri

BS Astrophysics (2018) Rice University

SUBMITTED TO THE
DEPARTMENT OF NUCLEAR SCIENCE AND ENGINEERING

IN PARTIAL FULFILLMENT OF THE REQUIREMENTS FOR THE DEGREE OF MASTER
OF SCIENCE IN NUCLEAR SCIENCE AND ENGINEERING AT THE MASSACHUSETTS
INSTITUTE OF TECHNOLOGY

SEPTEMBER 2023

© 2023 Lorenzo Venneri All rights reserved.

The author hereby grants to MIT a nonexclusive, worldwide, irrevocable, royalty-free license to exercise any and all rights under copyright, including to reproduce, preserve, distribute and publicly display copies of the thesis, or release the thesis under an open-access license.

Authored By: Lorenzo Venneri
Department of Nuclear Science and Engineering
August 26th, 2023

Certified by: Koroush Shirvan
Atlantic Richfield Career Development Professor in Energy Studies
Thesis Supervisor

Accepted by: Ju Li
Department of Nuclear Science and Engineering
Chair, Department Committee on Graduate Students

Design for Cost Methodology Applied to High Temperature Gas-Cooled Reactors

by

Lorenzo Venneri

Submitted to the Department of Nuclear Science and Engineering
on August 26th, 2023, in partial fulfillment of the
requirements for the degree of

MASTER OF SCIENCE IN NUCLEAR SCIENCE AND ENGINEERING

SEPTEMBER 2023

Abstract

SpaceX's Falcon 9 is like a Toyota Corolla – an order of magnitude cheaper than competitor's "high performance" rocket systems, the Ferraris, but achieving the same basic transport requirements with greater reliability and safety. Before Falcon, space launch was a Ferrari-like industry, with handmade, highly specialized, extremely expensive vehicles targeting government customers and fully complicit in the inefficiencies of government contracting. Similarly, the nuclear industry produces and still designs Ferrari-like fission reactors, with high performance metrics in terms of power density and unit power, at a megaproject scale, but with high system and operational complexity, extreme development cost, numerous part counts, and very low production and deployment rates that still require human-machine interface to meet societal safety objectives. The demand for nuclear Ferraris in the U.S., particularly within non-traditional energy utilities is very low, as few competent utilities want unique reactors with such high capital costs, running at such high power that low probability accidents can have offsite consequences. Where is the nuclear Corolla?

In the pursuit of energy systems that are cost effective and widely deployable, this thesis specifies a nuclear reactor architecture called the Class A HTGR (CA-HTGR), where Class A refers to the passive safety class during decay heat cooling. The architecture is used in a coupled design and cost approach to search for Levelized Cost of Electricity (LCOE) minimizing designs. The feasibility and utility of this design for cost (DFC) methodology, also termed economics by design, is shown through assessment of advanced manufacturing opportunities and LCOE minimizing designs.

Section 1 introduces the history and status quo of fission energy, providing a perspective on the stalled industry and possible paths forward, motivated by the rapid expansion and success of the space launch industry. A comparison is made between nuclear and natural gas, suggesting possible cost reductions in a rebooted nuclear industry. Because of the unusual, black swan risk associated with nuclear, the starting point for massive cost reductions and widescale deployment is a new safety paradigm that reduces risk through consequence reduction. Through a technology description and down selection in Section 2, the CA-HTGR is shown to be the most effective architecture available for reducing consequence and mitigating hazards pertinent to nuclear fission reactors.

Nuclear reactor design has historically been a painful, one-off process with limited opportunity for optimization, iteration, and design exploration. Connections between design parameters and value functions like LCOE are often unclear or missing altogether. The wide-ranging disciplines, the timelines and development costs involved, and the barriers to change, combine to form a complex design process that often leads to siloed subsystem teams, and leaving little room for optimization, iteration, or integrated design, and more easily favors design by regulation, tradition, and sunk cost.

As an alternative to the traditional nuclear design approach, Section 2 introduces DFC methods made up of design, cost, and search codes. Instead of one-off labor-intensive estimates, DFC aims to automate estimates over a wide range of the design space with the end goal of LCOE minimization. Section 3 presents the design code and describes the models and assumptions used to specify an HTGR concept design, including models for core energy content, power rating, reactor vessel geometry, and balance of plant. Section 4 presents the cost code which includes estimates for CAPEX, OPEX, and project LCOE. Section 5 describes model uncertainty and design rankings, discussing the utility of each and possible methods for their estimation.

Advanced manufacturing (AM) and its potential use cases for nuclear fission are introduced in Section 6. DFC methods are used to evaluate the cost effects on an HTGR baseline. Rather than attempt detailed and high uncertainty cost estimation of advanced manufacturing methods, ranges of costs and performance factors were reported together with dependent LCOE changes. The results suggest various opportunities for AM and the utility of coupled design and cost estimation for evaluating the potential impacts of AM opportunities.

Finally, Section 7 presents the use of DFC methods to examine the design and cost space. A wide range of cost outcomes were found through random sampling of the design space. Genetic algorithms were used to search the design space for LCOE minimizing designs, establishing the feasibility of DFC methods for HTGRs.

The DFC methods developed and utilized for this thesis can be used to improve the delivery of cost competitive nuclear fission reactors for planet-wide deployment. DFC methods provide a system-focused approach that considers design interdependencies, allowing for optimization. The main shortcomings of the reported DFC methods include low fidelity design and cost approximations that may not match the reality of an HTGR. Optimizing on a simplified model can be useful because financial commitments are often made using similar or even simpler models. DFC methods could be used to quickly produce cost minimizing designs for a given population of end users and projects. In the future, nuclear projects can be accelerated by using DFC methods in conjunction with nuclear analysis codes, templating codes, and language models to automatically produce design and licensing documentation.

Thesis Supervisor: Koroush Shirvan

Title: John Clark Hardwick (1986) Career Development Professor of Nuclear Science and Engineering

Acknowledgments

Many thanks to Professor Shirvan who gave me the time, freedom, and guidance to explore various aspects of HTGR design and cost estimation. I also thank previous thought and research in the field, particularly the developers of HTGR technologies and cost estimation methods for chemical and nuclear facilities.

The Class A Passively Safe HTGR described in this thesis parallels the design objectives and architecture of the commercial USNC MMR, conceived and championed by Francesco Venneri.

Contents

1	INTRODUCTION.....	14
1.1	PERSPECTIVES ON A STALLED INDUSTRY & PATH FORWARD	14
1.2	A SPACE LAUNCH PARALLEL FOR THE NUCLEAR INDUSTRY	15
1.3	POSSIBLE LIMITING COST FOR FISSION AND FUSION	20
1.3.1	<i>Fission like CCNG Limiting Cases</i>	20
1.3.2	<i>Fusion Limiting Cases</i>	21
1.3.2.1	Conventional Fusion w/ Conventional Nuke Basis	22
1.3.2.2	Conventional Fusion with CCNG basis	22
1.3.2.3	Direct Conversion Fusion with Solar or CCNG basis	22
1.4	RISK REDUCTION APPROACH FOR WIDESCALE ADOPTION	23
1.4.1	<i>Energetic Driving Force Creates Consequence from Fission Products</i>	23
1.4.2	<i>Risk = Probabilities • Consequences</i>	24
1.4.2.1	Risk Reduction Via Lower Probabilities	25
1.4.2.2	Risk Reduction Via Lower Consequences	26
2	DESIGN APPROACH AND TECHNOLOGY DOWN SELECTION.....	27
2.1	DESIGN PRINCIPLES.....	27
2.2	COST REDUCTION AND REVENUE GENERATING STRATEGIES DEPEND ON RISK REDUCTION	28
2.3	HAZARDS AND MITIGATING DESIGN CHOICES	29
2.3.1	<i>Fuel</i>	31
2.3.1.1	Conventional Fuel.....	32
2.3.1.2	TRISO/FCM Fuel	32
2.3.1.3	TRISO in Graphite.....	32
2.3.1.4	TRISO in SiC Matrix – FCM Fuel	33
2.3.1.5	Fuel Enrichment.....	33
2.3.2	<i>Coolant</i>	34
2.3.2.1	Water.....	34
2.3.2.2	Helium.....	34
2.3.3	<i>Moderator</i>	35
2.3.3.1	Safety Aspects.....	35
2.3.3.2	Neutronic and Dimensional Aspects.....	35
2.3.4	<i>Coolant and Reactor Temperatures</i>	35
2.3.4.1	Enhanced Power Conversion Efficiency	35
2.3.4.2	Larger Stored Energy Raises Afterheat Temperatures	36
2.3.4.3	Enhanced Passive Cooling	36
2.3.5	<i>HTGR Type and RX Geometry</i>	36
2.3.6	<i>Power and Size – General Considerations and Metrics</i>	36
2.3.6.1	Decay Heat Hazard	37
2.3.6.2	Power Density	37
2.3.6.3	Surface Area to Power Ratio.....	38
2.3.6.4	First Order Power Rating Constraints.....	39
2.3.6.5	Biological Parallel.....	40
2.3.6.6	Different Reactor Architectures under Passive Cooling Constraint	41
2.3.7	<i>Power and Size – Economies</i>	42
2.3.7.1	Economies of Heat Production in Larger Reactors	43
2.3.7.2	Economies of RX Production	43
2.3.7.3	Serving Diverse End-Users.....	44
2.3.7.4	Transport and Manufacturability Constraint	45
2.3.7.5	Safety Constraints	45
2.3.7.6	Burnup, fuel loading, enrichment	46
2.3.8	<i>Technology down selection: Class A HTGR</i>	48
2.4	DESIGN FOR COST OPPORTUNITIES.....	48
2.4.1	<i>Motivation and Prior Work</i>	48
2.4.2	<i>Code Architecture</i>	49
2.4.3	<i>Use Modes</i>	50
3	DESIGN CODE.....	51
3.1	APPROACH.....	51
3.1.1	<i>Reduced order models with parameter specific adjustments</i>	51
3.1.2	<i>Incorporating external tools</i>	51
3.1.3	<i>Applicable Codes</i>	51
3.2	CORE ENERGY CONTENT	53
3.3	POWER RATING	55
3.3.1	<i>Maximum Fuel Power Density</i>	55
3.3.2	<i>Passive Safety Power Rating</i>	56
3.3.3	<i>Other Power Rating Estimates</i>	57
3.3.3.1	Equilibrated Lumped Capacitance	57
3.3.3.2	Lumped Capacitance w/ Time Dependence	59
3.3.3.3	Finite Difference	61
3.3.4	<i>Note on Reactivity Insertion</i>	62

3.4	REACTOR.....	62
3.4.1	RPV.....	62
3.4.1.1	PV Sizing.....	63
3.4.1.2	PV Support.....	63
3.4.1.3	RX Enclosure.....	63
3.4.2	TH Design and Pressure Drops.....	63
3.5	BALANCE OF PLANT.....	68
3.5.1	BoP Types.....	69
3.5.2	Power Conversion and Thermal Cycle Efficiency.....	69
3.5.3	Heat Transfer Loops.....	69
3.5.4	Net Electric Power.....	70
3.5.5	Piping.....	70
3.5.5.1	Pipe Dimensions.....	70
3.5.5.2	Piping Pressure Drop.....	71
3.5.6	Fluid Inventory.....	71
3.5.7	Fluid Purification.....	71
3.5.8	Heat Exchangers.....	71
3.5.9	Pumping Power and Pump.....	71
3.5.10	Heat Rejection.....	72
3.6	CIVIL.....	74
3.6.1	Building Specification.....	74
3.6.2	Site Area.....	75
4	COST CODE.....	76
4.1	PAST MODELS.....	76
4.2	CAPITAL COST.....	76
4.2.1	Approach.....	76
4.2.1.1	List of accounts and rules.....	76
4.2.1.2	Arbitrarily specific account toggles and cost estimation functions.....	76
4.2.1.3	Accommodating new reference designs and cost bases.....	76
4.2.1.4	Boundary Cases.....	77
4.2.1.4.1	Over specification or incorrect scaling.....	77
4.2.1.4.2	Too much or too little cost data.....	77
4.2.2	Baseline Design and Cost Data.....	78
4.2.3	Direct Costs Rules.....	79
4.2.3.1	Inflation.....	79
4.2.3.2	Parameter or Count Scaling Rules.....	79
4.2.3.3	Other Cost Estimates.....	79
4.2.3.4	Balance of Plant Accounts.....	79
4.2.3.5	Special Rules.....	80
4.2.3.5.1	Special Rules from Prior Work.....	80
4.2.3.5.2	Vertical Integration.....	80
4.2.3.5.3	Country of Manufacture.....	80
4.2.3.5.4	Nuclear Quality.....	81
4.2.3.5.5	Standard Licensing.....	81
4.2.3.6	Modularization.....	81
4.2.3.6.1	Factory Costs.....	82
4.2.3.7	Capital Costs Learning.....	82
4.2.3.7.1	Base Unit Choice.....	83
4.2.3.7.2	Comments on Learning Rates.....	83
4.2.4	Construction Duration.....	83
4.2.5	Indirect Costs.....	84
4.2.6	Transmission and Delivery.....	84
4.3	OPERATING COST.....	84
4.3.1	Reactor Expendables: Fuel, Moderator, Vessel.....	84
4.3.2	Fuel Costs.....	85
4.3.3	RPV Cost and Lifetime.....	88
4.3.4	NRC Fees.....	89
4.3.5	Cost of Land.....	89
4.3.6	Insurance and Property Tax.....	89
4.3.7	Spares and Maintenance Cost.....	89
4.3.8	Refueling Activity Cost.....	89
4.3.9	Used Nuclear Fuel Costs.....	90
4.3.9.1	Pool Dimension and Wet Storage.....	90
4.3.9.2	Dry Cask Costs.....	91
4.3.10	Staff Scaling.....	91
4.3.11	Staff Salary.....	93
4.3.12	Operations Learning.....	94
4.4	PROJECT.....	94
4.4.1	Timelines.....	94
4.4.2	Decommissioning Cost.....	95

4.4.3	Tax Credits and Expense	95
4.4.4	Financing	95
4.4.5	Nominal LCOE.....	97
5	MODEL UNCERTAINTY VS DESIGN RANKINGS.....	100
6	2D-TRADES TO EXPLORE AM OPPORTUNITIES	101
6.1	GENERAL AM OPPORTUNITIES	101
6.2	BASELINE DESIGN	103
6.3	PARAMETER SENSITIVITY RESULTS.....	103
6.4	FUEL.....	104
6.4.1	Fuel Loading through Higher packing fraction, UN Kernels, Larger Kernels, Multi-Size Kernels	104
6.4.2	Fuel Capability: Higher Temperature Fuels w/ Enhanced Radiation Tolerance	107
6.4.3	Fuel Shuffling.....	109
6.5	MODERATOR	109
6.6	CORE	110
6.6.1	Core Dimensions.....	110
6.6.2	AM-Enabled Core Design.....	113
6.7	HEAT EXCHANGER.....	114
6.7.1	Topological Optimization for Mass and Pressure Drop.....	115
6.7.2	Part Integration	115
6.7.3	Alloy freedom.....	115
6.8	VESSELS AND LARGE METAL COMPONENTS	115
6.8.1	Part Integration and Weld Removal	116
6.8.2	Topological Design for Mass Reduction.....	116
6.8.3	Topological Design for flow (CBA, plenums, orificing, veins).....	116
6.8.4	On-site RPV or large steel component manufacturing	116
6.8.5	Heat Transfer Features.....	117
6.8.6	Vessel Replacement Cost vs Damage Threshold	118
6.9	2D TRADE CONCLUSIONS	118
7	DESIGN SEARCH AND POPULATIONS.....	119
7.1	PROBLEM STATEMENT	119
7.2	RANDOM SAMPLING AND GENETIC ALGORITHM POPULATIONS	119
7.3	GENETIC ALGORITHM SEARCH	125
8	CONCLUSIONS	128
8.1	MODEL SHORTCOMINGS AND FUTURE WORK	128
8.1.1	Design Code Shortcomings.....	128
8.1.2	Cost Code Shortcomings.....	128
8.1.3	Search Code Shortcomings.....	129
8.2	ENVISIONED USE.....	129
8.2.1	DFC Based on End-Users and Project Lists	129
8.2.2	R&D and Technology Roadmaps.....	129
8.2.3	Integration with Standardized Modeling and Reporting Processes to Automate and Accelerate Reactor Design, Analysis, Licensing, and Business Development	129
9	REFERENCES.....	131
10	APPENDIX.....	138
10.1	BASE INPUTS	138
10.2	CAPITAL COST COA RULES.....	141
10.2.1	Scaling Rules.....	141
10.2.2	Special Rules.....	144
10.3	GA POPULATION ON FULL SET	145
10.4	MATERIALS AND FLUIDS.....	148
10.5	AM COMPONENT COST ESTIMATION.....	149
10.5.1	Bottom-Up Approaches.....	149
10.6	ULTIMATE COST LIMITS.....	152
10.6.1	Cost Limit by Basic Inputs	153
10.6.2	Cost limit by Crustal Abundance	153
10.7	LEVELIZED COST ON LONG TIME HORIZONS	153
10.8	GENERALIZED WRIGHT'S LAW	155
10.9	ACCIDENT PATHWAYS IN CA-HTGR	155
10.10	SPHERICAL VESSEL OPPORTUNITY	156
10.11	COMPACT HEAT EXCHANGER DESIGN.....	156
10.11.1	CHX Specification.....	156
10.11.2	CHX Design Solutions	159
10.11.3	Cuboid Solution	159
10.11.4	Integrating Over the Channel Lengths	159
10.11.5	HX dimensions and HX Containers	160
10.12	FINITE DIFFERENCE SCHEMES FOR UNSTEADY HEAT EQUATION WITH NON-LINEAR BC	160
10.12.1	Cylindrical Geometry, C-N Scheme.....	160
10.12.2	Spherical Geometry, C-N Scheme.....	161
10.13	CODE IMPROVEMENTS	162
10.14	IMPROVING CORE ENERGY CONTENT MODELS.....	163

Tables

Table 1 Lazard 2021 LCOE data [22] for CCNG and Fission, and extrapolation to Fission (CCNG basis) through various assumptions.	23
Table 2 Non-exhaustive table of general parameter choices for a nuclear reactor. Gaseous or colloidal fuels not included.	27
Table 3 Technology and Economic Strategies. Different strategies are enabled or more easily unlocked by particular design characteristics.	29
Table 4 Hazards in nuclear powerplants that can serve as driving force for fission product release.	31
Table 5 Simplified reactor technology assumptions and relative power rating at 3m diameter core. Limited by fuel or cladding temperature above which fission products will be released.	41
Table 6 Design Estimate summary.	52
Table 7 Core conduction and surface heat transfer equations.	56
Table 8 Heat transfer relations for lumped capacitance model.	60
Table 9 Heat transfer correlations for different layers in Lumped Capacitance Model.	60
Table 10 Heat conduction solutions with component from center of the geometry. C – coolant, M – moderator, F – fuel. Radii indicate outer radius of the material. Solved sequentially from the fixed temperature BC. The thermal conductivity is for the material in question. Gap conductance neglected.	67
Table 11 BoP Example Inputs.	68
Table 12 BoP Configurations.	69
Table 13 HX Characteristic performance assumptions.	71
Table 14 Selection of Electrically Driven Centrifugal Helium Circulators with Magnetic Bearings.	72
Table 15 Example Partial Output for BoP.	73
Table 16 Example HTL layer outputs for BoP.	74
Table 17 Example capital cost results for a 14x22 MWth ES NOAK 1 and 2-digit accounts.	78
Table 18 Other Cost Estimates for dollar amounts.	79
Table 19 BoP Cost and Design Options.	80
Table 20 Nuclear Escalation Factors (linear) to match non-nuclear process equipment estimates.	81
Table 21 Learning progress ratios a , with $w = \log_2 1 - a$	82
Table 22 Planetwide Deployment Example for 1x22 MWth ES.	85
Table 23 Uranium cost inputs. The TRISO fuel cost specified here is on the low end of fabrication cost ranges from past reports like [112].	86
Table 24 Uranium compounds for kernel.	86
Table 25 Example TRISO and Fuel Specification Input.	87
Table 26 Core Cost and Refueling Output for 240x22MWth ES.	88
Table 27 NGNP Staffing from [91].	92
Table 28 Staffing Summary from (MMR [115], NuScale [116], NGNP [91]).	92
Table 29 Staffing Paradigms for Low, Medium, and High automation.	93
Table 30 Example Operation Estimate Output for 14x22MWth ES.	93
Table 31 Staff salary estimates (USD 2020) from the literature.	94
Table 32 Cashflow Accounts.	97
Table 33 Example Financial Inputs.	99
Table 34 Worlds Characteristic and Distributions.	100
Table 35 AM Methods applied to nuclear components.	103
Table 36 AM component design opportunities with expected effects on performance and cost factors.	104
Table 37 Potential HM Mass Loading Improvements for TRISO-based Fuel.	105
Table 38 Base set of free parameters and ranges for Random Sampling and GA evaluations.	120
Table 39 Free parameter configurations.	125
Table 40 Design and Cost Solution summaries. Free parameters highlighted. Unless specified, costs are for NOAK.	126
Table 41 Base design and model inputs.	138
Table 42 Parameters used to evaluate AM costs.	152
Table 43 HX Parameters.	158
Table 44 Unsteady Heat Equation and Conditions.	160

Figures

Figure 1 Launch cost to LEO, reproduced from [10], not including Russian or Chinese launch systems.	17
Figure 2 US Nuclear Power Reactors Overnight Construction Cost by Construction Start Date, reproduced from [21].	18
Figure 3 Overnight Construction Costs of Global Nuclear Reactors in USD2010. Costs are adjusted by local GDP deflator and to USD at 2010 market exchange rates, reproduced from [21].	18
Figure 4 Average US Capital Cost of Nuclear reproduced from [17], which does not include France or South Korea projects that showed plateauing capital costs.	19
Figure 5 Space and nuclear parallels.	20
Figure 6 LCOE limiting cases from Lazard 2021 baseline using the same LCOE estimate as Lazard.	21
Figure 7 Accident events and damage reproduced from [25]; death rates per unit energy delivered from [24].	24
Figure 8 TRISO particle and FCM Fuel pellet from USNC, photographed by author.	33
Figure 9 Fuel Enrichment across civil designs of interest. High enrichment designs are historic reactors like Ft. St. Vrain HTGR.	34
Figure 10 Nuclear reactor power ratings over time reproduced from [54]. EPR (1660 MWe) and other reactors not shown.	37
Figure 11 Decay heat power density after shutdown (assuming 6.6% of operating power for fission) for some advanced reactor technologies. USNC MMR (15 MWth) is shown as a representative Class A HTGR. Values are median values of the available data shown in Figure 13.	38
Figure 12 Core Power to Surface Area Ratio for various fission reactor concepts in development in 2023. Lower power to surface area ratio is associated with a safer reactor as heat can be more easily dissipated by passive, solid state heat transfer. USNC MMR (15 MWth) is shown as a representative Class A HTGR. Values are computed using the same used for Figure 13 with available power and core geometry data.	38
Figure 13 Reactor power metrics across designs of interest based on publicly available information and images. Data for each technology architecture obtained from [56][57][58] and author's analysis of industry reports and public information.	39
Figure 14 Kleiber's Law for Earth-based organisms using data from [60].	41
Figure 15 Power rating envelopes for different reactor technologies under LOCA conditions with only outer core boundary passive cooling. Points are estimated values for various existing and planned nuclear reactors. Lines are estimated using Table 5.	42
Figure 16 Core Power density for the same data and model in Figure 15.	42
Figure 17 Relative economies and effect on cost. Left panel shows economies of scale in reactor Production versus physical economies of scale in Unit Volume. Right side plot shows the cost trend for increasing power or core dimension in the corresponding regions of the left side plot. The four points indicate likely regimes for nuclear reactor systems and industrial hardware generally.	44
Figure 18 Power plant Counts by Delivered Power Rating for US Powerplants using 2021 data [61]	45
Figure 19 Total Delivered Energy by Delivered Power Rating for US Powerplants using 2021 data [61].	45
Figure 20 Relative economies affected by safety constraint relating the power and power density. Smaller core diameter is favored in all nuclear relevant economies.	46
Figure 21 Relative economies affected by safety constraint and fuel utilization. Cost scaling for γ of 2 and α of 2/3.	47
Figure 22 Code Architecture.	50
Figure 23 Core Energy Content Model.	53
Figure 24 Core Energy Content ROM for graphite moderator and 10% fuel volume fraction. Column shows the packing fraction.	54
Figure 25 Power rating ROM	55
Figure 26 Power Rating ROM samples for different safety class and aspect ratios. Each column is a Maximum fuel temperature in K.	57
Figure 27 Power rating for equilibrated Lumped Capacitance at 72 hour coping time. Columns are for different max fuel temperature in K, and rows give different design parameters. Maximum fuel temperature has no effect as the limiting component is the civil structure concrete, in this case 550 K. The fuel volume fraction is 0.1.	59
Figure 28 Lumped capacity ROM for a prototypical micro reactor core during passive decay heat cooling.	61
Figure 29 Finite difference example for unsteady heat equation in cylindrical geometry with decay heat power density. Time in hours.	62
Figure 30 Thermal Hydraulic Solutions across core size and for different safety class and aspect ratio. The safety class A and B refer to the heat transfer coefficient at the RPV surface, with Class A having 20x lower HTC than Class B. Coolant channel length is equal to the core diameter for all designs. Core pressure drop and specific pumping power (pumping power divided by thermal power) increases with diameter because of how power rating is determined resulting in reduced core power density for larger diameter cores.	66
Figure 31 Unit channel in different configurations for the same fuel moderator volume ratio.	67
Figure 32 Temperatures across a CFM unit core channel. Radius in m, temperature in K.	68
Figure 33 Example BoP with 3 HTL layers. There are 3 origin sources with 3 independent primary loops and 3 HXs, a shared secondary loop connected by 2 HXs to a shared tertiary loop, and 5 power conversion devices.	70
Figure 34 Example capital cost results for a 14x22 MWth ES NOAK 2-digit accounts.	78
Figure 35 Origen decay output for single cycle w/17x17 LWR UNF at 5% enrichment under various power densities and burnups. Horizontal line shows an estimate for the maximum dry cask fuel power density.	91
Figure 36 RX 60 year timeline for 40x22MWth ES.	95
Figure 37 Cashflow example for a 14x22 MWth ES with 20 year payback schedule. Note that the cashflows continue to the project end and would lead to under utilized fuel.	96
Figure 38 Packing fraction vs Enrichment showing LCOE change from baseline. Circle represents TCR fuel form with LEU+ enrichment, the only available enrichment within the next 5-10 years.	106
Figure 39 Packing fraction vs Enrichment showing refueling interval in years. Circle represents TCR fuel form with LEU+ enrichment, the only available enrichment within the next 5-10 years.	106
Figure 40 Fuel fabrication cost vs packing fraction. Circle represents TCR packing fraction and the potential for significant fuel fab cost reductions as the process is commercialized and fuel is produced at scale.	107
Figure 41 Fuel fabrication cost vs RX power. Circle represents the fuel fab cost reductions that can be expected as TRISO fuels achieve commercial scale production with related learning and automation. Micro reactor designs including MMR and eVinci have are exploring power uprates to reduce LCOE.	108
Figure 42 Fuel compaction cost vs Burnup gain. Circle represents the fuel fab cost reductions that can be expected as fuels achieve commercial scale production with related learning. Improved core designs, larger cores, improved moderators suggest burnups can increase.	108
Figure 43 Core Cartridge Cost vs Burnup gain.	109
Figure 44 Core dimension against various design parameters. Top left: core energy content, top right: RX power, bottom row: LCOE.	111

Figure 45 Power uprate versus primary pressure, showing LCOE.....	112
Figure 46 Core diameter vs maximum fuel temperature showing core power density.	112
Figure 47 Core diameter vs maximum fuel temperature, showing LCOE.	113
Figure 48 Illustrative best performance curves for different core-design and core manufacturing paradigms. New moderators are likely to have more pronounced effects.	114
Figure 49 Pressure Boundary Cost vs Pressure Drop factor.....	117
Figure 50 Pressure Boundary Cost vs RX Power rating.....	118
Figure 51 Distribution of NOAK LCOEs for uniform random sampling of the free parameters on the range [0,.4] \$/kWehr.	120
Figure 52 LCOE against NOAK/FOAK for random sampling suggesting optimal learning possibilities.	120
Figure 53 GA population scatter plots showing LCOE against reactor size parameters.	121
Figure 54 GA population scatter plots showing LCOE against core and fuel design parameters. Refueling Interval in years.	122
Figure 55 GA population scatter plots showing LCOE against thermal hydraulic design parameters.	123
Figure 56 Random sample of the population of designs grouped by Debt Interest Rates, showing LCOE against refueling interval in years and core power density.	124
Figure 57 Random sample of the population of designs grouped by Debt Interest Rates, showing LCOE against reactor power and diameter....	124
Figure 58 GA discovered Energy Systems under various free parameter configurations.	125
Figure 59 GA results for CA-HTGR at different Energy System electrical power.	127
Figure 60 Cost composition of the reference additively manufactured steel HX at 300 cc/hr.	150
Figure 61 Effect of different parameters on cost per kg of product. As processes are finetuned and CAPEX is reduced, power costs dominate the overall cost.	151
Figure 62 Levelized cost at 10% interest with different inflation rates and lifetimes. Alpha determines how OPEX varies with CAPEX.....	154
Figure 63 Example Unit Area.....	157
Figure 64 Showing the characteristic performance limit for periodic pins of UO2 in graphite. Radius in cm.	164
Figure 65 Performance results for grid evaluation of periodic pins of 20% enriched UO2 in graphite. Radius and edge in cm.	164

List of Abbreviations

- AM: Advanced Manufacturing
- BoP: Balance of Plant
- BDBA: Beyond Design Basis Accident
- CA-HTGR: Class A High Temperature Gas-cooled Reactor
- CBA: Core Barrel Assembly
- COA: Code of Accounts
- DFA: Design for Assembly
- DFC: Design for Cost
- DFM: Design for Manufacturing
- ES: Energy System
- FCM: Fully Ceramic Micro-encapsulated (Fuel)
- FOAK: First of a Kind
- F/M: fuel to moderator ratio
- FP: fission product
- HM: heavy metal
- HTGR: High Temperature Gas-cooled Reactor
- HX: Heat Exchanger
- IHX: Intermediate Heat Exchanger
- LCOE: Levelized Cost of Electricity
- LPBR: Laser Powder Bed Fusion
- MHTGR: modular High Temperature Gas-cooled Reactor
- MMR: Micro Modular Reactor
- NOAK: nth of a kind
- PM-HIP: Powder Metallurgy Hot Isostatic Pressing
- QA: Quality Assurance
- QA/I: Quality Assurance and Inspection
- RPV: Reactor Pressure Vessel
- RX: Reactor
- TCR: Transformational Challenge Reactor
- USD: United States Dollars
- USNC: Ultra Safe Nuclear Corporation
- WAAM: Wire Arc Additive Manufacturing

1 Introduction

1.1 Perspectives on a Stalled Industry & Path Forward

A few general philosophies have emerged to explain the stalled nuclear industry in the U.S.: the doomers, the healers, the warriors, and the wizards. The doomers have pathetically accepted that nuclear fission has limited societal acceptance and there is not a cost competitive way to limit nuclear risk. They believe the high cost and poor execution is inherent to fission while other energy generation and storage systems have no such limitations and can be industrially developed. The simple response is to point out fission's 5-6 order of magnitude advantage in energy density and lower material use compared to other energy generating sources, which will necessarily be lower cost in the limit of competent execution and large-scale industrial deployment. Solving the acceptance and regulatory challenge can be worth the effort.

The healer believes nuclear deployments are stalled because the costs are too high, and they try to reform the industry with incremental improvements to lower cost through the usual suspects: modularization, standardization, and factory manufacturing.[1] The healers do not usually consider the idea that costs are high because of accident risk, perceived or real, and the regulatory requirements it has created. They would generally like to build more tried-and-true LWRs, if only the execution could be improved. The current situation in 2023 favors the healer's approach, with many utilities exploring new LWR deployments, both large and small, most of which offers the same construction and operational complexity as existing fleet of LWRs and in some cases such as Rolls-Royce UK-SMR, similar safety systems. Can the interest withstand another construction mismanagement or black swan accident?

The warrior camps blame regulations and the use of unscientific LNT (described in more detail below). They believe a massive regulatory overhaul, something like abandoning LNT and instituting Underwriter Certification would allow nuclear fission to approach its potential and leave behind an inflated cost due to nuclear cost escalation and the burdensome QA and licensing processes etc. No design changes are necessary other than removing the paperwork and excessive backup systems.

Jack Devaney has written most recently on this perspective and joins many nuclear proponents like Ted Rockwell. He views the nuclear predicament as a Gordian Knot - an intractable and potentially ill-framed problem which Alexander the Great solved by the simple and gutsy act of cutting through it with a sword. He describes two lies that make the knot: 1) the negligible probability lie and 2) the catastrophic harm lie.[2] In the first lie, the industry promises that "the probability of a sizable release of radioactive material from a nuclear power plant is so low that we can just assume it won't happen" which is verifiably false based on historical events. He points out that a nuclear-powered humanity with on the order of 25,000 large reactors would have 6 releases every year based on historical data, and a release every couple years if core damage accident rates can be reduced by a factor of 10. [3]

The argument is that ALARA and the pursuit of low probabilities through engineered safety systems has been "suicidally expensive" and "tragically unnecessary" because of the second lie that "any significant release of radioactive material would be so catastrophic that it cannot be allowed to happen." Devaney argues that the "catastrophic" accidents and release can often be considered non-events with the catastrophic label due primarily to the use of the linear no-threshold (LNT) model for cancer risks and cleanup in regulatory response plans. LNT is a model of radiation harm relating the health damage response to the radiation dose with a line and no bottom threshold. The evidence across the literature tends to suggest that a safe background radiation level threshold exists, probably quite a bit higher than typical background radiation, and that harm is non-linear with dose with a dependence on dose-rate. Many have pointed out the serious flaws with LNT including but not limited to: consistently contradicting evidence, disregarding background radiation, the failure to explain a measurable health impact from weapons testing, evidence of hormesis, etc. An LNT approach applied to other cancer-causing substances would destroy any other industry but nuclear scrapes by on its 5-6 order magnitude advantage in energy density. Cardarelli suggests that the scientific and societal support may exist to replace LNT.[4] The idea is to move from no dose is safe as in LNT, to the more scientifically based perspective that no measurable harm results from a low dose and low-dose rate. LNT could be replaced with a threshold model or a sigmoid model. If that were to take place, the historical accidents and radioactivity releases would no longer warrant the evacuations, but mere insurance payouts, with a similar occurrence as hurricanes or wildfires.

The first lie is made to cover for the second lie, and it is all for nothing because they are just two lies. The cost escalation to prop up the first lie has priced nuclear into obsolesce for new deployments in the U.S. And the lies together have challenged public perception, through currently majority of the public and political parties support nuclear energy as a carbon-free energy source. Ending the lies is unlikely, but these are powerful arguments that could well prevail in a future world of energy scarcity with more practical priorities. Devaney's proposed solutions rest on dropping the LNT and in order of preference: 1) underwriter certification, 2) autocratic public utility, the way of the current nuclear leading countries, or 3) total NRC transformation from design outfit to an emissions enforcement agency.[5]

The wizard's perspective is less antagonistic to existing institutions and local people but somewhat resented by the incumbent nuclear industry. Instead of changing the world directly through regulatory overhaul or autocratic deployment, the wizard seeks to transform the industry through technological approaches that unlock widescale deployment. The perspective is that the overregulation, cost escalation, and weak societal reception are the result of a flawed technological approach, courtesy of Admiral Rickover and the US military-industrial complex, with too big to fail reactors built as one-offs and prone to black-swan events. The

problem is the black swan nuclear accidents. Crucially, the problem with the past approach is not related to the fuel cycle, fuel availability, or the production of long-lived waste – where any of the proposed advanced approaches are likely to increase costs and accident rates. To introduce the wizard’s perspective, this work quotes Dr. Ning Li who adds the most recent academic contribution [6] to a perspective built over decades by Alvin Weinberg [7][8] and Freeman Dyson [9].

In responses to nuclear disasters and public demands, nuclear regulatory frameworks become more rigid, highly prescriptive, with strong preference toward established designs of large monolithic nuclear power plants. This ratcheting trend, combined with and enhanced by the industry's singular pursuit of economies of unit scale through increasing reactor power, locked nuclear technologies into a vicious cycle. To improve safety and economics in the same paradigm with already minuscule probabilities of core damages and large releases, more systems and higher costs are necessary, which have led to increasing total power in an attempt to spread and reduce specific costs, but have led to increased construction times and costs, and increased consequences of severe accidents beyond design basis, which in turn demand more safety and emergency response systems and containment, and on and on.

The scaling-up in such development with associated safety risks requires multiple careful steps, from zero power, experimental, prototypic, commercial demonstration reactors to deployment. With each step needing a decade or more time, total cycle times of technologies and system designs became multi-decadal. The safety concern and resultant slowdown have deprived nuclear technologies and systems from very many diverse and rapid innovation opportunities available to other technologies and industries, especially those exponentially growing disruptive innovations made possible by networking effects and combinatorial explosions.

They also led to decades-long stagnation and decline of the first nuclear era. Weinberg pointed out that safety and emergency systems almost dominated the whole nuclear power technology, years before the Three Mile Island incident in 1979... To some visionary pioneers of nuclear power, a second era of nuclear is called for, and inherent safety is key to restarting nuclear energy growth and expansion.

This thesis aligns with and builds on the final perspective, having more explanatory power and offering new solutions in the current world rather than hoping for a fundamental change in the political and societal situation. If we can build systems with negligible accident consequence, within the current societal framework, and at a similar or lower cost– then we should build those systems. A novel technological approach can also better justify the regulatory overhaul suggested by the warriors and in this way the wizard becomes the warrior.

1.2 A Space Launch Parallel for the Nuclear Industry

SpaceX’s Falcon 9 achieved step change reduction in launch costs, from the Space Shuttle’s \$54,500 /kg to Low Earth Orbit, to \$2,720 /kg [10] as shown in Figure 1. While Falcon has established the ability to reliably land and reuse most of the rocket without human intervention, the reuse capability has only recently started to kick-in and substantially reduce the launch cost in a high-cadence launch environment, as worldwide launches number less than a hundred per year. This lifetime extension would give launches a linear cost reduction on most of launch costs except the propellant and operations costs. Even without significant reuse cost reductions and despite the payload sacrifice displaced by significant extra systems and propellant needed to pull off the landing, Falcon has achieved undercutting launch costs.

Falcon’s undercutting of launch costs, if they are not artificially lowered by investor subsidy (i.e. venture predation [11]) and projected reuse financials, are likely due to other factors including vertically integrated supply chains, advanced manufacturing including additive manufacturing techniques, a rapid hardware development and testing campaign, and large-scale manufacturing. Many argue that the cause of Falcon’s success is SpaceX’s “cowboy engineering” culture and urgency that cuts development time, increases the rate of learning, and allows for radical changes in design and manufacturing compared to more typical aerospace engineering that is conservative, process driven, and well planned but slow to change, learn, and take advantage of new technologies. SpaceX’s approach, like many successful hardware companies, has been characterized by its high rate of attempts, ignoring or ignorance of the orthodoxy, failing, but learning very quickly. Such approach was also foundation of the 1960s fission technology development where added regulatory burdens has slowed down the needed iterative process utilized by SpaceX.

SpaceX’s design thesis can be distilled to “simplicity enables both reliability and low cost.”[12] This work appends that simplicity can enable safer designs and processes to make a 4 in 1 bundle of inter supporting characteristics: simplicity, reliability, low cost, and safety. Systems and parts are eliminated or reduced, often radically breaking with tradition. Vehicle configurations are simplified to reduce system counts and mission complexity. Margins are increased to allow early prototype and product success and tuned during later product evolutions. Instrumentation and measurements are reduced to the minimum required, as more data requires more downstream resources often with no or negative benefits. As obvious as it sounds, the design needs to consider manufacturability, mass production, and easy operation. Conventional engineering in aerospace and nuclear have taken the opposite perspective, viewing reliability and safety as expensive features, requiring more systems, more capital and operating expense, better parts, and more quality control.

Elon Musk has described the product realization process in five somewhat parallelized activities: make requirements less dumb, delete the part or process, optimize, iterate, and automate.[12] The first activity acknowledges that requirements are often arbitrary or inherited and that nobody really knows the necessary or minimum requirements. Still, the team must start with some set of requirements, and these should be treated skeptically and loosely. Then, all efforts should be taken to remove the part or process. If the same function can be fulfilled by another system or not at all, the part or process should be eliminated. The team should always be looking for ways to do less work. Finally, after and while improving the requirements and accepting that the part is truly necessary, the design can be optimized ideally in hardware rather than on paper, with sufficient iterations to see design evolution and spark new thoughts and considerations. The team should optimize for minimum cost to achieve minimum performance requirements. Automation is used to accelerate the iteration process and ease the transition to manufacturing. In practical terms, this means using micro controllers and software to automate measurement and reporting, testing, or even automating a simple prototyping step. These are standard and expected R&D skills using a growing library of off the shelf automation tools. Finally, a realized prototype or product is always superior to a perfect design or study.

This mentality and approach to product realization has led to notable spacecraft design decisions compared to past rockets.[13][14] Falcon's overall size is large enough to carry significant and diverse payloads at low-cost, but still small enough that dozens of launches are required per year in current market conditions, allowing for a high production rate and launch cadence. Much larger rockets could risk saturating the nascent space launch market and dousing the cost and experience benefits of high production and launch rates.

Additive manufactured components are used in Falcon's Merlin engine to reduce the number of parts and achieve complex geometries, overall leading to simpler assembly and a record-breaking rocket with 200:1 thrust to weight ratio. Engine failures are the leading cause of launch failure and nailing engine reliability was the focus of Merlin development. Merlin is an unusually small engine, and Falcon requires 9 Merlin engines, compared to 3 or fewer on similar sized rockets. This allows for faster and lower cost engine development, higher engine production rates that lower cost and enhance reliability, more manageable manufacturing, and gives Falcon the ability to withstand multiple engine blackouts. Having many smaller engines proportionally increase the engine time and performance experience, accelerating any finetuning and troubleshooting efforts. Indeed, the Merlin engine and Falcon overall have the highest reliability in launch for any rocket ever developed. Falcon even has higher reliability in landing than any rocket has had in launching.

SpaceX produces essentially one engine for Falcon, with variants tuned for sea-level versus vacuum. The same propulsion systems and propellant are used for both upper and lower stages, greatly reducing the rocket complexity and supply chain needs, with follow on reliability and cost benefits. Other rockets have multiple stages with perhaps three different engines, which may optimize performance, but "to a first-order approximation, you've just tripled your factory costs and all your operational costs," says Musk.[13] A similar approach is taken for the fuel tanks and barrels, with Falcon's upper and lower stage having the same diameter, made of the same alloy, thus making use of the same tooling and manufacturing processes and supply chain. Unlike many other rocket systems, Falcon undergoes system level rocket testing prior to launch, capturing any launch issues prior to a launch setup.

Central to low costs, and deviating from traditional space industry consortiums, SpaceX has taken a lean manufacturing approach, with significant vertical integration producing 80% of Falcon components in-house, under a flat management structure. SpaceX limits subcontracting, producing its own avionics hardware and software, with, perhaps exaggerated, claims that every dollar spent internally saves 3-5 dollars spent externally due to subcontractor overhead, wastage, and profit. With Starlink, SpaceX even aims to be its own customer, driving launch demand and producing an information-based product with profitable cashflows that can leverage its reduced launch costs.[15]

To further reduce costs, targeting US\$1100/kg and under SpaceX began developing Starship in 2016. Starship aims to achieve greater reuse capability than Falcon while leveraging scale economies of larger rockets and launches. Operating costs per launch should be similar for small and large rockets, reducing operating costs per kg of payload. Larger rockets also have better payload efficiency as overhead mass gets diluted by a larger payload. While Falcon has a reusable lower stage, and can recover payload fairings, the upper stage of Falcon is not recovered. Starship has an upper and lower stage, and both are being designed for full reuse, targeting a daily launch cadence similar to long-haul aircraft.

Falcon was the first step into the market with a relatively small but capable technology demonstrator that had a financially palatable development cost in the hundreds of millions, and could outcompete any market alternative, primarily state sponsored launch providers. But Falcon is not a cost-optimized or ideal chemical launch system. Leveraging company cash flows, investor confidence, and NASA cooperation built through Falcon, SpaceX expects to spend 2 to 10 \$B in development costs for Starship, [16] aiming for an even lower cost fully reusable design. In many ways, Falcon will be viewed as the steppingstone to Starship, proving mass-scale rocket reuse capability, the cost reducing power of lean manufacturing and vertical integration, and providing cash-flows with sufficiently low launch prices to drive massive increases in launch demand. Falcon proved the technology, the manufacturing approach, and expanded the market.

To illustrate the magnitude of SpaceX cost reductions, Figure 1 shows launch costs since the beginning of the space age. A marked period of stagnation is evident during and after the Vietnam War which brought the Apollo program to an end. Curiously, this coincides with a period of rapid cost escalation for nuclear capital costs in the US and stagnation worldwide shown in Figure 2 and Figure 3. Even nth-of-a-kind (NOAK) units find increasing costs, as shown in Figure 4. US nuclear cost escalations have usually been attributed to the Three-Mile Island accident and subsequent regulatory and industry changes to address higher than expected

accident probabilities. Mega project cost escalations, US deindustrialization, and construction cost stagnation have further increased costs.[1] [17] [18]

Similar cost stagnation and escalation for both nuclear power and space launch industries suggests the possibility of a shared origin, albeit catalyzed by different events. Nuclear power and space launch industries, fruits of the Cold War, share some characteristics. Both are complex hardware systems that require long development times, unusually high-quality control, and attention to safety due to high consequence accidents. Development costs and timelines are on the same order of magnitude in both industries and execution costs are similar. Space Shuttle launches cost on the order of \$1.5B per launch when considering full program costs. The recent Space Launch System, started in 2011 and not yet complete, has passed \$24B in development costs and expected to cost \$2B per launch.[19] Southern Company's Vogtle Plant Unit 3 and Unit 4 have cost about \$30B over a 14 project.[20] Both industries are heavily incentivized, funded, and regulated by government efforts related to the Cold War and geopolitical strategy with DOD, NASA and DOE serving as arbiters for R&D funding in both industries. Both have some environmental and societal stigma related to weapons, accidents, and pyramid building. Both industries have suffered from US deindustrialization policies that began in the 1980s with wide scale offshoring of heavy industry and labor-intensive work. These are similar industries, sharing many of the same features and challenges, and recent positive developments in the space industry suggest potential paths forward for the nuclear industry.

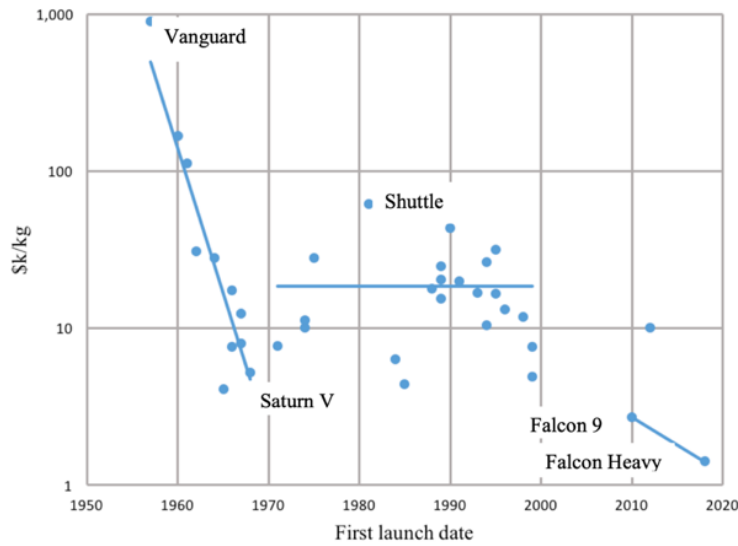


Figure 1 Launch cost to LEO, reproduced from [10], not including Russian or Chinese launch systems.



Figure 2 US Nuclear Power Reactors Overnight Construction Cost by Construction Start Date, reproduced from [21].

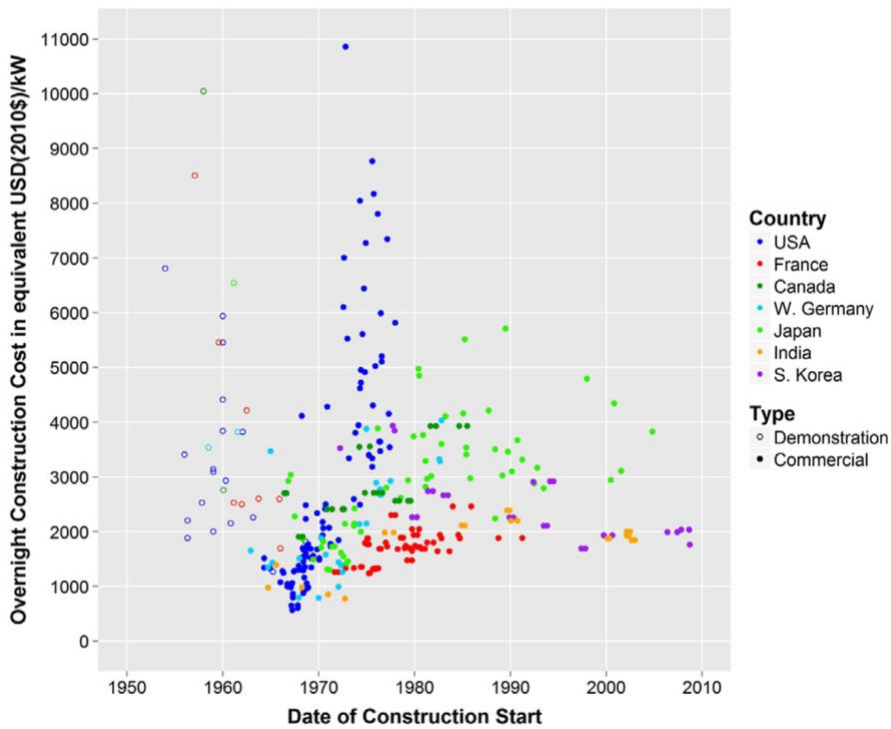


Figure 3 Overnight Construction Costs of Global Nuclear Reactors in USD2010. Costs are adjusted by local GDP deflator and to USD at 2010 market exchange rates, reproduced from [21].

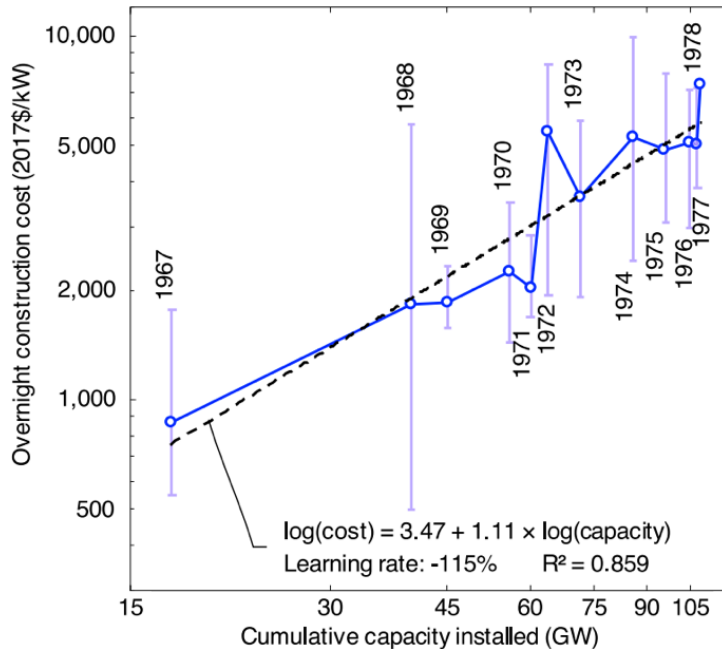


Figure 4 Average US Capital Cost of Nuclear reproduced from [17], which does not include France or South Korea projects that showed plateauing capital costs.

What can the nuclear industry learn from these recent developments in space launch? For starters, new designs should incorporate new manufacturing technologies, make design choices, and create company structures that reduce time and cost for product development and deployment.

New designs should capture economies of scale in the right places. Starship is big to capture scale economies on drag and launch costs, but it uses 35-39 Raptor engines across 2 reusable stages, deviating from the Saturn V which used 11 engines of two types across 3 single use stages. A nuclear Corolla can leverage economies of scale in the balance of plant, and still use many centrally controlled small reactors to gain economies of scale in the manufacturing and operation of reactors.

Another lesson is to start with something financially and practically achievable, not the currently accepted physical ideal. High TRL materials, components, and technologies with a storied history will outshine significantly new technologies and approaches – incremental improvements over foundational changes. Designs that aim for the 4-in-1 bundle (simplicity, reliability, low cost, and safety) will leave ideal designs behind. Nuclear designers should more carefully trade performance and real work costs related to demonstration and manufacturing. This means developing small reactors, with low capital costs, using established or high TRL technologies. The idea, now brandished by many nuclear vendors, is to start small, build cash flow and then slowly go bigger to gain economy of scales. These first reactors do not need to be perfect solutions with the lowest theoretical cost of power from the get-go. To enable manufacturing at scale, the unit size of the reactors must be small and the technology simple enough for rapid development, standard transport, high production rates, and low-cost manufacturing processes. A 10x lower power requires 10x as many units.

Finally, high, or increased capital costs can be reduced with simpler designs, lean manufacturing, and vertical integration and can be discounted by reuse and life extension. For nuclear, this means not only integrating as much hardware manufacturing and supply chain as possible including fuel, pressure vessels, and control systems, but also integration of on-site construction and assembly, site operations and maintenance, power sales, and even decommissioning. Each supply chain and added service related to the nuclear industry exposes nuclear products to excess financial leakage and schedule slip. Crucial vertically integrated components for nuclear systems would be fuels, moderators, and vessels, control, and measurement equipment as well as project development, construction, operations, and decommissioning. The importance of vertical integration diminishes with large markets, weak national boundaries, and many suppliers – a situation that nuclear, like aerospace, may never find itself in. Finally, if the biggest battle is convincing customers, a nuclear vendor should find ways to be its own customer. As Starlink deployments drive demand for Falcon launches, zero-carbon data centers or zero-carbon chemical plants can drive nuclear deployments.

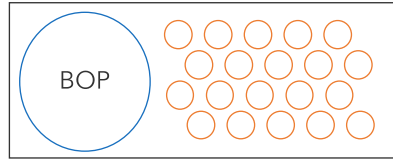
**Built like a Ferrari
Performs like a Corolla**

- Low Performance (just electricity)
- Handmade
- Complex systems
- Operate at the edge
- Overpowered
- Extremely expensive
- Mega Project
- Low demand



**Built like a Corolla
Performs like a Ferrari**

- High volume production
- Small unit size & Coupling
- High Performance
 - Electricity + High Temperature Heat
 - Small and large customers
 - Micro grid
 - Dispatch capable to prop up renewables
- 4 in 1 bundle
 - Simplicity
 - Reliability
 - Low cost
 - Safety



Reactor Fleet

Figure 5 Space and nuclear parallels.

1.3 Possible Limiting Cost for Fission and Fusion

Before examining the nuclear design choices and technology down selection, this exercise is motivated with some bounding cases on the LCOE. Estimating nuclear energy costs compared to other energy generating assets is challenging yet necessary to make financing decisions. We must be aware as to who has their fingers on the spreadsheet. Is it a wind and solar zealot, a fossil profiteer, or one of the hundred nuclear (both fission and fusion) startups? The following is a little exercise to see what the cost limits might be for nuclear energy with 21st century industrial technologies. To bound the problem from point-of-view of the lowest nuclear LCOE, the existing nuclear fission technology is considered.

1.3.1 Fission like CCNG Limiting Cases

The simple comparison is made using Lazard's 2021 data [22] and is based on the idea that there is no good reason for combined cycle natural gas (CCNG) and nuclear plants to be built or operated at significantly different cost. There are roughly the same number of systems and parts in both. If anything, CCNG should have higher operating costs due to its higher temperatures, more corrosive substances, and six orders of magnitude higher fuel mass throughputs. CCNG operating costs should be higher because refueling happens continuously with large volume and mass flows compared to nuclear refueling which occurs every two years in the legacy fleet, and 10 years or longer in some designs. CCNG are also often operated as load following plants with rapid power and thermal cycling which requires higher quality parts that will fail faster. CCNG fuel costs are obviously higher and more volatile than nuclear fuel costs. But it appears regulatory and security requirements have made staffing at nuclear reactors two orders of magnitude larger than CCNG.

To find a theoretical lower bound for fission, I took the cost inputs for CCNG and substituted CCNG's fuel, thermal efficiency, and capacity factors with those from an advanced nuclear powerplant. I used CCNG's 20-year project lifetime as opposed to the 40 years used in Lazard for New nuclear. CAPEX, Fixed O&M, and fuel costs are scaled according to the thermal output of the plant. Both CCNG and nuclear are turbomachinery-based energy harvesting systems, but by using CCNG's inputs, I eliminate "nuclear" penalties like ridiculously large nuclear cost escalation factors, indirect costs, nuclear staffing, and regulatory burden. Compared to CCNG, the fuel costs are reduced, and the thermal efficiency is decreased.

When nuclear powerplants are built and operated like natural gas plants, LCOE in Figure 6 labeled 'Nuclear (CCNG basis)' is achieved. This Nuclear LCOE is 0.7x lower than CCNG and 4.3x lower compared to Lazard's Nuclear LCOE estimates which are based on the realized cost of AP1000 with 20-year financing and high discount rate. Using a CCNG basis, nuclear fission has the potential to provide on-demand energy at the lowest cost.

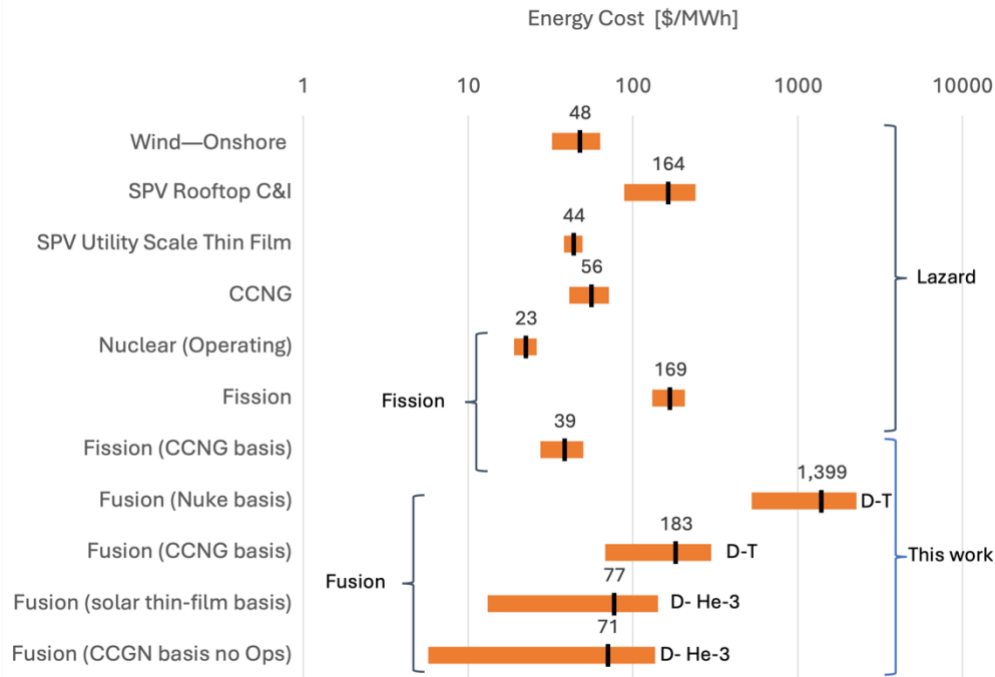


Figure 6 LCOE limiting cases from Lazard 2021 baseline using the same LCOE estimate as Lazard.

Does one have to build and operate a nuclear plant in a completely different way than a natural gas plant to account for the radiation and proliferation risk posed by nuclear fuel? That is probably the case for many reactor designs - systems with high a power density, many interacting components and chemicals, and an annoying proclivity to melt or damage themselves during beyond design basis accidents. These reactors are high-performance systems requiring containment and safety systems to prevent fission products from being released to the environment. It is like a Ferrari racing through tight turns in a long race. It has lots of kinetic energy and chemical energy that must be carefully controlled and dissipated to avoid disaster. Everyone is on edge. The driver is hyper aware of his speeds, turning rates, and the machine's health; the pit crew carefully maintains all the parts before and during the race, praying that the brakes don't give out and that cooling systems remain functional; and when things inevitably fail, the racetrack has massive barriers to contain the speeding car, with ambulances and firetrucks standing-by. A lot of effort goes into preventing the vehicle controls from failing and reducing the damage when they do.

Taking the same approach for a nuclear reactor can be expensive. But nuclear reactors do not have to be built and operated like Ferraris on a racetrack. Instead, they can be built like Corollas and driven in a giant parking lot – slow, simple, reliable, and cheap – the approach taken by the CA-HTGR. In fact, for some designs out there, the Corolla metaphor doesn't go far enough. With extremely low power and high thermal mass, a CA-HTGR lacks the driving energy to damage itself during accidents, and it can more easily dissipate excess heat passively without overreliance on safety systems. In terms of performance and risk, CA-HTGR is more like a golf cart than a Corolla – it is slow and not very exciting. The focus of CA-HTGR is how radiation risk can be decoupled from reactor design, bringing the technology closer to a natural gas plants, where it would incentivize a new regulatory framework to be able to realize CCNG-type capital cost.

Another consideration, in line with the “warrior” perspective, is that nuclear plants have been over-hardened and over-regulated for decades. The cost-benefit of catastrophic nuclear accidents does not indicate that radiation is an important cost factor, even during extreme accidents like Chernobyl or Fukushima. Indeed, most of the damage comes from the government and industry response following the accident rather than any direct or inferred radiation deaths. This damage would occur with or without safety and containment systems or nuclear cost escalations.

1.3.2 Fusion Limiting Cases

Given recent fusion concept investments, it is of interest to repeat the cost exercise for a fusion system in 4 cases that match some of the system attributes advertised by fusion proponents. The first case is the most relevant for current and near-term prototypes like ITER, SPARC, and NIF. ITER and SPARC are tokamak devices using the D-T reaction achieved with magnetic fields to confine plasmas in a torus. NIF is a D-T laser-based inertial confinement fusion experiment taking place a Lawrence Livermore National Laboratory The last 3 cases concern simpler systems that use aneutronic reactions or simplified technologies that are more challenging to achieve but portend a promising fusion future.

1.3.2.1 *Conventional Fusion w/ Conventional Nuke Basis*

First, it is assumed that fusion systems would have similar attributes to current nuclear mega projects, but with low or zero fuel cost, and limited or no long-lived fission product - ostensibly the big benefits for fusion over fission. This is representative of many of the devices under development like ITER, SPARC and ARC, NIF derived systems, and various compression target systems. This may even be unfair to normal fission reactors, as these fusion reactors are bulkier, introduce many new complex and expensive systems to start and sustain fusion reactions, have 1.5x -2x parasitic power losses, and require on-site fuel reprocessing to feed the reactor. Just look at the ITER powerplant layout where most of the area is covered by systems that do not exist for fission systems like fuel reprocessing and cryocooling.

We only penalized the fusion plant with the expected reduced capacity factors, shorter lifetime, and parasitic power losses. Capital costs are, unrealistically the same as a fission powerplant. The operating costs for a fusion system will be far greater because there are more numerous and more complex systems to maintain and because radiation damage will be 32x greater per unit of thermal energy according to the neutronicity of the D-T reaction. The dpa damage is extreme, and this requires better materials, more shielding, more replacements, more inspection and maintenance. And the real kicker is the low capacity because of how often a fusion reactor is likely to be shut down for maintenance and repairs. For example, laser-based inertial confinement devices have target chamber optics that have to be cleaned after each pulse. Decommissioning costs can also be expected to be higher for fusion because they are likely to produce 50-100x the radiological waste volume per net energy produced. I used an operating cost factor of 1 and 5 for the lower and upper bound estimates.

1.3.2.2 *Conventional Fusion with CCNG basis*

Now, what if the fusion reactors turn out to be easy to build and require very few "nuclear" cost escalations? I recalculated using a CCNG cost basis characterized by the low capital and operating costs of a non-nuclear thermal conversion system. It's not a realistic assumption because a fusion powerplant of any kind is far more complex and capital intensive by physical requirement than either CCNG or a normal fission powerplant. There is not a clear path to size and system reduction or overall simplification, as is the case for some fission designs, as discussed earlier. I gave the fusion system the same low operating costs as a CCNG plant, but again, it's difficult to imagine why this would be. I still punished the fusion system with low capacity factor, shorter lifetime, and parasitic power losses.

In this case, fusion systems would produce electrical power that is 3x higher cost than CCNG. The upper and lower bounds represent the upper and lower estimates on the various parameters. I can be more optimistic on the lifetimes, parasitic power losses, but these back-of-the-envelope estimates suggest a challenging LCOE hurdle for the possibility of commercial fusion systems in the next several decades. Something has to change.

1.3.2.3 *Direct Conversion Fusion with Solar or CCNG basis*

The benefits of direct energy conversion may have motivated a half-billion-dollar investment in Helion Energy. Helion is aiming for a low neutronicity D-He3 reactor fed by a D-D reactor to generate He3 which would yield roughly double the net neutronicity of fission in the ideal case. Helion intends to generate electricity without turbines using the charged fusion products. Solid state power conversion is not limited to Helion's flavor of nuclear fusion. Fission systems can also generate power with solid state methods, although less directly. Thermoelectrics [4], thermionics [5], and thermo-photovoltaics [6] all generate electricity from temperature differences with varying efficiencies and challenges. There are also methods to generate power using magneto hydrodynamic generators [7]. There was even a US project for Direct Energy Conversion from Fission Reactors [8] aiming to convert the kinetic energy of fission fragments directly into electrical energy. But for many reasons, including accumulated investment and technology momentum and the sheer difficulty of implementation, the cheapest way to generate electricity from thermal flows is still through a thermal hydraulic cycle with turbines or steam cycles.

Helion's claims portend a simple and elegant system with high efficiencies. For now, let's take them at their word and assume all the theory adds up and the practical and regulatory challenges are resolved - what could the cost of energy eventually be? Helion's claim, provided here for the record, is that "Helion's fusion power will be one of the lowest cost sources of electricity. Helion's cost of electricity production is projected to be \$0.01 per kWh without assuming any economies of scale from mass production, carbon credits, or government incentives. Helion's fusion powerplant is projected to have negligible fuel cost, low operating cost, high up-time and competitive capital cost. Our machines require a much lower cost on capital equipment because we can do fusion so efficiently and do not require large steam turbines, cooling towers, or other plant requirements of traditional fusion approaches." They even have announced first net electrical power of 2024, and a power purchase agreement with Microsoft for 2028.[23]

Without thermal power conversion, Helion's system would be more like a wind turbine or solar panel than a conventional powerplant, but with higher power density, more significant control, thermal, radiation, and corrosion challenges that require more expensive hardware and maintenance. It could be a solar panel or wind turbine running at 100% capacity at all times, or a more conservatively, a half-price CCNG plant with no operation or fuel cost, and these would be in the range of 0.01 to 0.015 \$/kWh. But considering the net neutronicity will still be greater than Uranium fission owing to the D-D reactions needed to produce He-3 and other side reactions, it is not clear that operation and maintenance costs would be negligible.

Table 1 Lazard 2021 LCOE data [22] for CCNG and Fission, and extrapolation to Fission (CCNG basis) through various assumptions.

Value	Unit	CCNG		Fission		Fission (CCNG basis)	
		Low Case	High Case	Low Case	High Case	Low Case	High Case
Case	Low or High						
Net Facility Electrical Output	MWe	550	550	2,200	2,200	550	550
Net Facility Thermal Output	MWth	991	1,112	6,738	6,738	1,338	1,684
EPC Cost	\$/kW	\$650	\$1,175	\$6,100	\$10,025	\$650	\$1,175
Capital Cost During Construction	\$/kW	\$50	\$125	\$1,675	\$2,775	\$50	\$125
Total Capital Cost	\$/kWe	\$700	\$1,300	\$7,800	\$12,800	\$945	\$1,969
Total Capital Cost	\$/kWth	\$388	\$643	\$2,547	\$4,179	\$388	\$643
Fixed O&M	\$/kWe-yr	\$15.00	\$18.00	\$121.00	\$140.50	\$20.24	\$27.26
Fixed O&M	\$/kWth-yr	\$8.32	\$8.90	\$39.51	\$45.88	\$8.32	\$8.90
Variable O&M	\$/MWhe	\$2.75	\$5.00	\$4.00	\$4.50	\$2.75	\$5.00
Heat Rate	Btu/kWh	6,150	6,900	10,450	10,450	8,300	10,450
Heat Rate	kWhth/kWhe	1.8	2.0	3.1	3.1	2.4	3.1
Capacity Factor	%	70%	50%	92%	89%	92%	89%
Fuel Price	\$/MMBtu	\$3.45	\$3.45	\$0.85	\$0.85	\$0.85	\$0.85
Construction Time	Months	24	24	69	69	24	24
Facility Life	Years	20	20	40	40	20	20
CO2 Emissions	lb/MWh	720	807	0	0	0	0
Levelized Cost of Energy (Lazard)	\$/MWh	\$45	\$74	\$130	\$204	-	-
Parasitic Power	%	0%	0%	0%	0%	0%	0%
CRF		0.102	0.102	0.084	0.084	0.102	0.102
Recalculated LCOE	\$/MWh	\$41.21	\$71.36	\$131.18	\$206.51	\$27.51	\$50.09
CAPEX	\$/MWh	\$14.77	\$38.39	\$103.08	\$174.85	\$15.16	\$32.67
Fixed O&M	\$/MWh	\$2.48	\$4.17	\$15.22	\$18.27	\$2.55	\$3.55
Variable O&M	\$/MWh	\$2.75	\$5.00	\$4.00	\$4.50	\$2.75	\$5.00
Fuel	\$/MWh	\$21.22	\$23.81	\$8.88	\$8.88	\$7.06	\$8.88

1.4 Risk Reduction Approach for Widescale Adoption

The risk related to nuclear fission is first described and it is argued that aversion to nuclear at the local level is not as unfounded as the nuclear community would make it out to be, considering the alternatives. It is shown that widescale democratic adoption can only be achieved through a different approach to risk reduction. Instead of reducing risk through reduced probabilities and militaristic operations, risk can be reduced by lowering consequences primarily through the use of passive safety mechanisms and inherently safe design characteristics that consider the hazards surrounding the fission products. This was the predominant approach to nuclear safety in the 1990s and gave rise to passive safe designs such as AP1000. In the 1990s both government and public support were low for nuclear energy. Since only the Vogtle units have come online in the last 30 years, it is still not clear, if such a strategy will be ever commercially viable. Nevertheless, this is the direction for nuclear design behind this thesis and many recent SMR and micro reactor demonstration and commercialization efforts, that push passive and inherent safety to the extreme, considering designs where risk can be evaluated deterministically.

1.4.1 Energetic Driving Force Creates Consequence from Fission Products

Nuclear reactors produce radioactive fission products, roughly a third of the periodic table, and these radioactive isotopes pose a notable financial and health risk during accidents where various hazards can help unleash the fission products outside the fuel clad. A nuclear reactor must address this source term head on. It must protect the powerplant investment and surrounding community from the radioactivity. To do so, it must contain fission products and radiation by remaining at safe temperatures across the condition space including operations, beyond design basis accidents (BDBA), and disposal.

We must not conflate the existence of the fission products with potential consequence. A source term can only have a large consequence if there is a driving force to energize and disperse the fission products. In a nuclear reactor, that energetic driving force is usually the decay heat power, rapid power increases during a reactivity accident, unexpected loss of cooling, or a chemical energy release – but can be any of the hazards shown in Table 4. Removing the driving forces and hazards removes the consequence. This is as far as one can go to reduce consequence while still generating neutrons and fission products. All fission reactors have a source term, but not all reactors have an energetic driving force to turn those fission products into a consequence. A nuclear corolla should aim to reduce energetic driving force and contributing hazards that can create a consequence from fission products. Achieving this in a cost-effective manner, has remained elusive.

1.4.2 Risk = Probabilities • Consequences

Aversion to nuclear deployment is more subtle than just an overreaction or an overinflated risk perception. While deaths per TWh attributed to nuclear power, including those from black swan accidents, are on par with renewables,[24] and while reactor accident event frequency has been reduced from 0.01 in the 1970s to 0.003 events per plant per year worldwide through industry reform and learning, we have simultaneously seen the less frequent but extremely high-cost accidents every ~6,000 reactor-years. There have been 24,000 commercial reactor years and 4 of the commercial ones have undergone meltdowns. These accidents pose a low probability but high consequence financial risk relative to alternative technologies.[25]

The majority of operating nuclear power plants are statistically safe on death per TWh metrics because the death statistics are a shallow way of measuring consequences, and the statistics are theoretically diluted across very large populations. But the local adverse effects of an accident to the utility, asset owners, and customers are concentrated and crushing. Coal and fossil fuels are statistically less safe by the same metric, but any climate change and health effects are diluted worldwide in a real and practical way. The reality is that there are cost competitive alternatives to nuclear energy, and these systems are not able to fail catastrophically like a nuclear reactor because they do not have fission products onsite. Why expose oneself to the even small probabilities of extreme consequences when there are alternatives?

Ordinarily, comparisons are made on the deaths per energy unit delivered. But the public is more concerned with significant hardship than with simple deaths. A better metric than death rates is a death equivalent consequence like displacement or financial loss. It appears likely that excess death rates from accidents like TMI and Fukushima are too low or too difficult to measure over the decades. But the financial cost of a nuclear cleanup and forced population displacements of the region surrounding the power plant can be considered equivalent to deaths. Forced displacement, prolonged financial hardship, loss of land are equivalent to death. Financial losses diluted over large populations can be converted to deaths even without a single actual death.

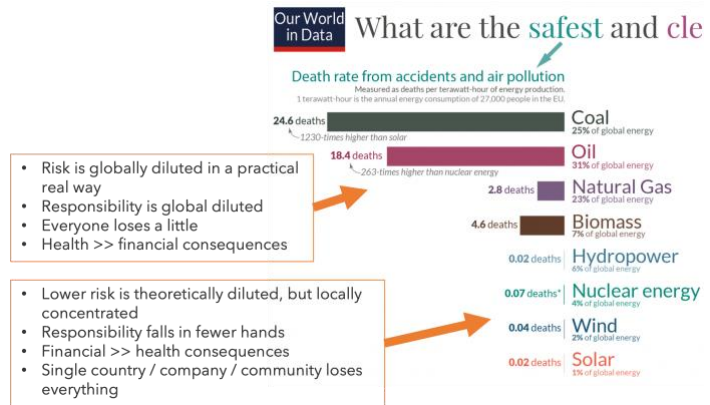
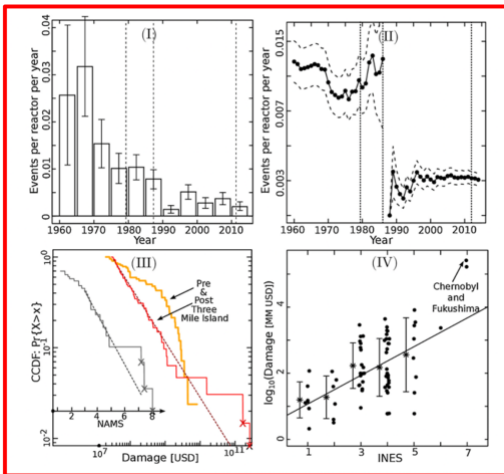


Figure 7 Accident events and damage reproduced from [25]; death rates per unit energy delivered from [24].

The below equation represents the concept of risk as the probability of an event multiplied by its consequence. [26] added a power of α to the consequence to incorporate the idea that perception of consequence does not always match the real consequence. While I can assume perception matches reality with $\alpha = 1$, I suspect that the public is an adherent to Murphy's Law, and α increases to compensate lower theoretical probabilities from engineers, a kind of hedge against the word of those who stand to benefit most and often have no skin in the game. With $P = 1$, risk is often perceived simply as the potential consequence.

$$Risk = PC^\alpha$$

We have seen nuclear accidents play out over the last 60 years, with a reported probability of about 1/100 reactor failures with severe local consequences, perhaps double if including close calls, and extra dangers associated with spent fuel pools. This comes out to about 1/6,000 probability of a severe nuclear accident per reactor year. The consequences of these accidents have proven substantially different from other sources of energy. In particular, the health consequences have been limited or comparable to other sources of energy, while the financial consequences have been immediate and long lasting, staggeringly high and concentrated to the regions around the reactor.

Direct effects of nuclear accidents have historically been geographically constrained to within tens of kilometers and at most a hundred kilometers if the weather is particularly unfavorable. There is little reason to believe nuclear accidents can directly have global effects because radioactivity is massively diluted with distance and travel time, and weather is a comparatively slow phenomenon relative to the most relevant radioisotopes. For nuclear, the risk of serious financial or health disaster is a local matter with local consequence.

Fossil fuels damage at both local and global scales. The pollution around fossil fuel plants reliably increases respiratory diseases and cancers. The production of greenhouse gases is a global effect, but its financial and health impact have not yet managed to justify a full decarbonization at the expense of slower economic development. Financial losses due to changes in climate, should the predictions ever materialize, may be recouped through newly available and useful land at higher latitudes. For fossils, in the worst case of power plant destruction, the utility or insurer will lose the value of the power plant and a new one can be built. There are no century-long cleanup efforts for fossil power plant accidents. There are no bankruptcies at the city, company, or country level. But the group risk is higher because of the health consequences of polluting the atmosphere and perhaps some climate change effects could materialize at some point.

Financial consequences of fossil fuel use are not clearly measurable owing to the great dilution, long time frames, and guesswork involved in its estimation. Fossil fuel health consequences are globally diluted. The probability of death-like consequences from fossil fuel pollutants is $P_F = 1/3000$ in the USA, [24] equally applied to the entire population.

From a global planner perspective, nuclear makes sense if the nuclear risk is less than the fossil risk. The risk is computed for each course of action below. The risk of each choice is the product of the population exposed, the probability of consequence, and the consequence itself which is a death or death equivalent consequence. For nuclear the reactor accident probability multiplied by the local population is considered. For fossils, the probability of death from emissions multiplied by the total population is considered.

$$P_N n_N C_{death,eq} < P_F n_F C_{death,eq}$$

We can drop the $C_{death,eq}$, the consequence, since it's on both sides. Compared to fossils, nuclear doesn't have to have as low an event probability because its accidents can be locally confined. That is $n_N < n_F$. The risk averse global planner chooses nuclear if the following inequality is met.

$$P_N \frac{n_N}{n_F} < P_F$$

But for the local planner and local population, where $n_N = n_F$, nuclear only makes sense if the nuclear event probability is lower than the fossil event probability.

$$P_N < P_F$$

The problem is that P_N and P_F are perceived as roughly equivalent and could well be about the same in reality. Historically, we know that most of existing reactors fail at a rate of about 1/6000 per year, with extreme costs, concentrated on the local populations and countries of operation. With this history and this comparison, a rational, local population sees roughly equivalent risk from either choice. But more likely, the local population perceives $P_N \gg P_F$, in deference to Murphy's Law. Fossil exposures are mostly conventional deaths and not easily traceable to fossils – it's difficult to blame fossil fuels for the premature cancer and respiratory deaths of a 60-80 year old, especially considering that fossil burning has been the norm for three centuries. And one can blame the whole fossil fuel industry, not any single fossil fuel emitter. Nuclear accident consequences have a clear source. It's easy to connect the financial and death equivalent consequences related to a specific nuclear reactor accident.

The local population also has no influence over the fossil fuel emitters. Their exposure to fossil risks is not affected by their local choice of nuclear or fossil energy. For the local population, choosing nuclear only adds to the fossil risk. On the other hand, the global planner is willing to put some populations at elevated risk to achieve lower overall risk. While globalist autocratic societies are on the rise, I hope self-determination by local people remains the way of the west. With this understanding, massive nuclear deployments in democratically run countries requires a new approach to risk reduction – one based on a deterministic approach that better approximates the public's respect for Murphy's Law.

1.4.2.1 Risk Reduction Via Lower Probabilities

The typical design approach for nuclear reactors has been to avoid accidents at all costs because the fuel can fail catastrophically in such events, due to melting or rupture. As a result, nuclear powerplants have become overengineered behemoths with a complex web of safety systems aimed at reducing the probability that accidents occur and trying to contain them when they do occur. Costs balloon rapidly, in large part due to paperwork but also due to quality control, material costs, and inefficient construction.[27] Accidents are yet to happen in GENIII and III+ reactors but GENI and II designs' accidents have resulted in unexpected fission product release and loss of public trust that continues to limit the industry's growth in certain region of the world. To become viable decarbonization tools, nuclear reactors must simultaneously eliminate black-swan risk and reduce costs.

Reducing reactor accident rates is expensive in large and traditional nuclear reactors. For new reactors and new components including passive safety systems, the probabilities are educated guesses that remain to be tested in time. During licensing, reactor designers make a safety case by using Probabilistic Risk Assessment (PRA). They analyze event trees that can lead to catastrophic accidents and assign probabilities to the events to come up with "core-damage frequencies." PRA emerged as a tool to figure out where the engineering design should be focused to reduce risk most efficiently. Worst case high consequence accidents like complete Loss of Coolant Accidents (LOCA) are not likely and somewhat impossible to deal with, so the focus shifted towards dealing with lower consequence but higher probability accidents like partial LOCAs which would have more impact on the overall risk. This is a sensible way to lower the overall risk as economically as possible but still leaves reactors exposed to worst case black swan accidents that could occur despite very low theorized probabilities.[28]

But even very low probabilities lead to reasonably high chances of failure at very high deployments. This is why the operating reactor rely on containment for both predicted low probability events and unknown events, the containment limits the radioactive release and exposure of it to humans. Those failures, rare as they are, despite the ability of containment to reduce off-site dose consequences, still lead to a global slump in financial and political support – the nuclear resets. The black swan risk is always there. Regulators, bankers, and the public are ready to slow down nuclear adoption, throttle financing and approvals, and heap on a few more regulations. Does the public care about these estimated PRAs considering the history of nuclear accidents and prior erroneous claims? No matter how low the estimated probability or how much extra CAPEX and OPEX goes into lowering the probability, the public is likely to continue to respect Murphy’s Law and will pick amongst the many available alternatives.

1.4.2.2 Risk Reduction Via Lower Consequences

Minimizing probabilities is a fool’s game that can only increase costs because the underlying problem is not solved. We should avoid building and operating reactors in such a way that they can melt during inconvenient conditions. The alternative approach to risk reduction is to lower consequences and embrace accidents through passive safety systems as almost all new reactors world-wide have limited to full reliance on passive safety. In CA-HTGR, the probabilities in PRA are generally set to 1 and the safety analysis becomes more deterministic. For CA-HTGR, consequences of accidents are negligible because of the inherent safety mechanisms that can deal with the decay heat. This means that reactor designs should not have to include elaborate systems to lower the theoretical probability of accidents from happening.

This deterministic, Murphy’s Law approach accepts that worst case accidents will happen at some point, commonly refer to as the maximum credible accident, and then designs the reactor and fuel so that the worst-case accident has low and if not zero nuclear related consequences. This is achieved by reducing the hazards and driving forces that can turn fission products into a consequence. More practically, this can be done by designing the reactor to passively remain at safe temperatures in worst case accident conditions including simultaneous Beyond Design Basis Accidents (BDBA). The ability to safely dissipate the reactor’s energy can be relegated to passive physical mechanisms rather than active systems.

No one doubts that a nuclear reactor can be designed this way. But the idea that it can be done at competitive costs remains in question. The reduction in consequence has far reaching implications beyond potential public acceptance. Using passive heat dissipation systems, the reactor can be simplified with fewer safety systems and parts. Rather than trying to avoid accidents through perfect operations and safety systems, these reactors would rely on physical material properties to withstand accidents rather than external or active systems. This means worst case accidents can happen without fission product release – a radical shift from today’s reactors in which mechanical cooling capability is required to avoid meltdown. Without conventional meltdown risk, these reactors may be treated like non-nuclear industrial sites with a corresponding reevaluation of costs and applications. The nuclear corolla takes this approach aiming for a cost profile of CCNG if the nuclear regulation treats it as such.

2 Design Approach and Technology Down Selection

We aim to achieve the lowest cost of energy under various constraints. To ultimately break the nuclear cost escalation absurdities, the design must reduce nuclear risk by reducing the accident consequence in a deterministic fashion, and this is done by carefully addressing each of the hazards in Table 4 through inherent characteristics and passive mechanisms.

What are the principal design choices and trades for a nuclear system? Nuclear systems have many interacting subsystems and there are many choices and trades to consider with a multitude of effects on safety and cost, both subtle and drastic. And many of the choices are not straightforward to understand or predict. For introductory purposes, I can distill the many technology choices to just a couple: fuel, coolant, temperature, size, and power rating as listed in Table 2. Each usually has some partisan zealot, championing a particular choice and design path. As designers, we are forced to down-select technologies and we cannot forever be open to all the thousand combinations of reactor technologies. The diversity of design possibilities suggests many ways to the same end, but the fact is that one architecture can be best for a given set of goals. We shall be lucky indeed, if we manage to wrangle the financial and political backing to demonstrate just one reactor, so we better have some ideas about how to compare them and down select.

I will first define the guiding design principles and the hazards to address. I then down-select technologies for a nuclear Corolla, picking HTGR to address the hazards through passive mechanisms and inherent characteristics with brief comparisons to the alternatives. With the HTGR in play, I describe the remaining free parameters and the path forward using design for cost.

Table 2 Non-exhaustive table of general parameter choices for a nuclear reactor. Gaseous or colloidal fuels not included.

Parameter	Options	HTGR choices for this thesis (discussed in detail later)
Fuel Form	Oxide, carbide, nitride, metallic, molten salt, liquid metal.	U oxy-carbides, U nitrides: established fuel forms.
Fuel Wrapper and Geometry	TRISO-matrix, metallic clad, ceramic clad, no clad, (geometry: cylinders, annuli, pebbles), fuel wrapped moderator	TRISO and SiC or graphite, Prismatic.
Fuel Type and Cycle / Enrichment	LEU converter, Natural U converter, HALEU converter, HEU burner, Pu burner, U-Pu breeder, Th-U breeder	U Burner.
Coolant and pressure	Helium, water, CO ₂ , sodium, sodium heat pipe, molten salt (fluoride or chloride), other liquid metals, organic, other gases (H ₂ , N ₂ , air)	Helium: extreme chemical compatibility and neutron transparent. Pressure is free parameter.
Moderator / Reflector	Graphite, water, heavy water, hydrides, Beryllium (no clad, ceramic, or metallic clad, composite / entrained)	Graphite: readily available, neutronicly efficient, high temperature capabilities and high specific heat. Canned and ceramic encapsulated hydrides are promising.
Size	Physical dimension of the reactor [~1-6m diameter, 1-20m height]	Free parameter. Generally constrained to 3.2x10 m envelope transportability, particularly rail (3.2m). Aim for max surface to volume ratio through high aspect ratio. Vertical orientation.
Power Rating	Power rating per reactor core [0,inf] MWth	Free parameter.
Temperatures	[150-1050 °C], 2000 C+ for Nuclear Thermal Propulsion 1-15 MPa, typically 3-7 MPa for He	Free parameter but constrained by metallic components, fluid phase change for molten salt or water, and fuel temperatures to 630-1050 °C outlet. Each loop must define inlet and outlet temperatures.

2.1 Design Principles

The discussion in Section 1 can be summarized in the following design principles:

1. Identify the X metric so that you can Design for X. Other metrics, requirements or specifications are secondary, intermediate, and flexible.
2. Seek design trends characterized by the 4 in 1 bundle whereby simplicity, reliability, low cost, and safety go hand in hand.
3. Avoid thoughtless design. Design choices must be intentional. When they are not intentional, they must be intentionally so. That said, we are ignorant and time constrained, so we must focus our efforts on the things that we can control, and those that have the largest impact. Design choices should have a physically derived basis, an optimization, or some kind of evolved logic. We might look to nature or other industrial fields for evolved design; things like perimeter minimizing honeycomb structures, surface maximizing geometries, redundancy counts, symmetries, etc.
4. Good enough is good enough. Don't optimize yourself into a pigeonhole.
5. Reduce the accessible state space. This means prioritizing low energies, low interactivities, and low potential gradients. Systems trend towards equilibrium with the surroundings and energy minima, it's just a matter of how much damage and how much change happens from one state to the other. We pick materials and design parameters that maximize the energy and time required for state change. We use and maximize negative feedback mechanisms to limit the energy available

for state change and pick parameters to maximize state change energy thresholds. We pick arrangements that reduce gravitational and chemical potentials and gradients. This is why we seek solid materials with high thermal conductivity, high heat capacity, and high melting point by which it takes more energy to change the state that is available from the potential differences. Limiting state change and state space contributes to point 2.

6. Match the design to the target environment. On Earth, we are dealing with air and water around 250 to 350 K with potential for complete flooding, aircraft impacts, hurricanes, and tornadoes, and 1g seismic loadings. This defines the ultimate heat sink, chemical backdrop, and bounds the most extreme encountered conditions. Conditions of a more extreme nature, such as a nuclear bombing, would be of greater consequence in themselves than the worst-case nuclear accident at the site.
7. Reduce part and system counts by simple elimination or through multi-use parts. Adding systems may address risks and probabilities, but usually introduces new failure mechanisms, new states, and uncertainty. Complexity is often faster than linear. Our understanding of the problem is often sub linear.
8. There are regulatory and political forces as real as physical laws. We must work within them as we aim to unlock CAPEX and OPEX reductions.
9. Materials are constraining, particularly under irradiation, temperature, and chemical degradation. New materials offer step changes in performance, but we are largely limited to the materials currently available, perhaps with some small extrapolation based on the state of the art.
10. Manufacturing capabilities are constraining. We cannot build whatever we dream up. Earth's economy is geared towards the production of a wide variety of sizes and complexities using many different materials, developed over decades and with significant underlying investment. We should strive to utilize existing capabilities and work within the available manufacturing envelopes.
11. A few of Murphy's Laws, in particular: anything that can go wrong, will go wrong.

2.2 Cost Reduction and Revenue Generating Strategies Depend on Risk Reduction

Table 3 summarizes some of the possible cost and revenue strategies pursued in the nuclear industry. The design choices in Table 2 and the local regulatory environment will determine which of these strategies is likely to work. For example, higher RX outlet temperature can offer process heat to more applications while lower temperature reactors are more limited to electrical power generation and desalination. Technology implementations and regulatory landscapes will have to be created in order to achieve particular cost and revenue changes.

A detailed analysis of how choices in Table 2 unlock strategies in Table 3 is beyond the scope of this thesis, but the underlying trend is that technology choices aimed at reduced consequence are needed to access different cost reduction and revenue generating mechanisms. Regulatory and societal safety expectations from nuclear has ballooned costs and limited its applications. Reducing that risk of severe accidents without engineered safety systems is a path to deflate costs and allow wider use.

The following describes a few cost reduction and revenue generating mechanisms and show how they depend on reduced risk. First, reduction in nuclear grade components, reduction in site EPZ, and the elimination of safety systems are only justified if the technology implementation significantly reduces the potential accident consequences. Remote and autonomous operations will only be possible and allowed if the consequence of bad operation and error is negligible. For an example, aircraft and ships still have crews despite how readily these operations could be conducted remotely and even autonomously with existing technologies.

Process heat applications, especially at high temperatures, require RXs to be placed close or adjacent to the point of use, which the end-user may accept only if the worst-case consequence is negligible. Perhaps most important are the economies of RX production, whereby RX and BoP are modularized and produced serially in factories. Only small reactors are amenable to factory production because of tonnage and volume limits for transport and a higher number of units produced per unit power capacity that justifies a dedicated production line. Finally, without consequence reduction, the fleets of smaller reactors will create more risk. If the accident probability rate is unchanged per reactor year, the number of accidents will be proportional to the increased reactor time and could be even higher if less stringent certification and control is adopted when operating a fleet of small reactors. A reduction in the consequence is needed to unleash fleets of reactors without increasing the nuclear risk.

Ultimately, all nuclear deployments are limited by the black swan risk that resets societal acceptance and order books and smothers the possibility for cost or revenue strategies. Eliminating conventional nuclear consequence may be the only way to shatter the black swan risk in the western world. With this in mind, I describe the design choices and constraints to reduce and eliminate conventional accident consequence and enable the strategies in Table 3.

Table 3 Technology and Economic Strategies. Different strategies are enabled or more easily unlocked by particular design characteristics.

Cost and Revenue Strategies	Strategy Basis	Enabling Design Characteristics
Economies of scale for heat production	Size / Power	Larger size
Diseconomies of scale due to size/complexity	Size / Power / Technology	Smaller size and consequence reduction
Economies of scale for reactor production	Size / Power / Technology	Smaller size and consequence reduction
High performance BoP	Size / Technology	Consequence reduction
Modularized RX	Size / Technology	Smaller size and consequence reduction
Modularized BoP	Size / Technology	Smaller size and consequence reduction
Modularized Civil	Size / Technology	Smaller size and consequence reduction
Remote operation from centralized control rooms	Technology / Operations	Consequence reduction
Autonomous operation	Technology / Operations	Consequence reduction
Dispatch capability through stored/sensible heat	Technology / Market	Smaller size and consequence reduction
Reduce defense in depth	Technology	Consequence reduction
Minimize nuclear site boundary	Technology	Consequence reduction
Minimize emergency planning zone	Technology	Consequence reduction
Minimize decommissioning cost	Technology / Execution	Favors low civil impact
Increase capacity/uptime	Technology	-
Reduce safety systems	Technology	Consequence reduction
Reduce use of nuclear grade components	Technology	Consequence reduction
Reduce on-site construction time	Technology / Execution	Smaller size and consequence reduction
Access high price end-users	Technology / Market	Smaller size and consequence reduction
Access wide gamut of end-users [29]	Technology / Market	High temperature reactors, consequence reduction, favors smaller size
Process heat f(T) [1]	Technology / Market	High temperature reactors, consequence reduction
Hydrogen production	Technology / Market	High temperature reactors, favors smaller size for distributed hydrogen production
Capacity markets in price capped markets [30]	Policy	-
Carbon tax [30] [31]	Policy	-
Radionuclide production [32]	-	-
Black start services [32]	Policy	Smaller size
Ancillary services [32]	Policy	-
Secure supply payments	Policy	Thermal storage
Reduce UNF costs	Size / Technology / Policy	High burn-ups, advanced fuel cycles, larger size
Resilience payments (solar and terrestrial weather [33], terrorist attack [34])	Policy	Smaller size and consequence reduction
Distributed power (delayed grid investment, grid decongestion, land use change, deurbanization) [35] [36]	Size / Market	Consequence reduction, smaller size
Land conservation payments	Policy	Larger size
Reduction in licensing and development costs through standardization	Size / Technology / Policy	Smaller size and consequence reduction

2.3 Hazards and Mitigating Design Choices


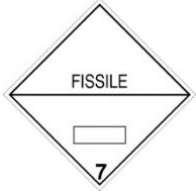


A nuclear reactor contains many hazards that can ultimately lead to a fission product (FP) release including decay heat, excess reactivity, chemical reactions, and high pressure. Hazards can be considered the potential gradients that can or could become accessible and who equilibration can lead to fission product release. The FP source term is the potential gradient, a hazard, underpinning the nuclear hazard, where FP gases are concentrated in the fuel at high pressure and temperature, but nonexistent in the low temperature and low-pressure environment.

Each hazard is listed in Table 4 with the mitigating approach taken in the HTGR architecture. Each in their own, the hazards can be mitigated through passive mechanisms and inherent characteristics. The International Atomic Energy Agency's (IAEA) definition of inherent safety being "safety achieved by the elimination of a specified hazard by means of the choice of material and design concept" and their logic on the various categories of passive systems is followed.[37] Table 4 discusses various design choices, and their effects on the hazards.

According to several studies, a TRISO fueled HTGR reactor is the highest TRL Generation IV technology [38], the most able to mitigate chemical and reactivity insertion hazards, and has sufficient acceptance from regulators and nuclear skeptics [39]. This perspective is becoming mainstream in academic [40] and industrial circles with HTGR being the most heavily invested advanced reactor technology besides LWR SMRs. It is postulated that this class of reactors can be characterized by small unit power systems connected to a large balance of plant, with few or no safety systems or safety grade equipment and lower operating costs. For HTGRs, this risk reduction is principally achieved by limiting power rating and using refractory ceramic materials so that fuel temperatures do not exceed limiting temperatures during simultaneous Beyond Design Basis Accidents (BDBA), assuming an

appropriate degree of security and safeguards is provided to the reactor, and all while using only Class A Passive safety mechanisms. This reactor technology is called the Class A HTGR (CA-HTGR), which more or less mirrors the design architecture of the commercially developed USNC MMR.

Table 4 Hazards in nuclear powerplants that can serve as driving force for fission product release.

HAZARD	Description	HTGR Approach
<p>Chemical Hazard</p> 	<p>Core components can interact with each other, the coolant, or external water and air to release energy or cause corrosion. At a minimum, this exacerbates maintenance and inspection needs during normal operations. During accidents, these features escalate conditions beyond the point of no return such as when Zirconium and water react at elevated temperatures to release energy and hydrogen which can then explode resulting in loss of control functions or LOCA. Similar problems occur with sodium coolant and heat pipes.</p>	<ul style="list-style-type: none"> • Avoid water, sodium, and metals that react with target environment and RX components at high temperatures. Keep the fission products contained and solid to reduce reaction rates and state space. • All core materials chemically compatible across radiation and temperature space • Core materials have high chemical and radiation tolerance. • Minimize use of water, keep it away from the core, provide excess drainage. • Use helium coolant which is totally unreactive with fuel and graphite. • Graphite has some reaction potential with water/air, which can be mitigated by reducing its surface area, reducing water ingress potential using separate steam exchanger or intermediate non-water loop, fuel-moderator inversion concepts
<p>Reactivity Hazard</p> 	<p>Control rod extraction or other mechanisms can cause the reactor to become dangerously supercritical and dramatically increase the power output of the reactor beyond what it is capable of handling. Too much power and the fuel will melt itself, releasing fission products. Most reactors can somewhat tolerate the partial ejection of one or two control rods but will fail catastrophically when more are extracted.</p>	<ul style="list-style-type: none"> • Strong negative temperature feedback in the fuel. As the power or temperature increases, the power is forced backdown by physical characteristics of the materials (no actions or mechanisms) • Minimize voids in and around the RX that can be filled with foreign substances (e.g., water or flowing air) • Control rods are used for startup, core power controlled by coolant flow. • Properly design reactivity margin to withstand water submersion and other reactivity insertions. • Tolerate full extraction of all control rods
<p>Terrorist Hazard</p> 	<p>Bad actors may intentionally sabotage reactor components by explosive or kinetic means. Bad actors could intentionally withdraw all reactor control rods, cause intentional coolant depressurization or flooding.</p>	<ul style="list-style-type: none"> • Other hazards are drastically minimized compared to other reactors, reducing the potential impact of any terrorist action. • Buried cartridges, fully below ground level, with limited access volumes. • TRISO subdividing the nuclear fuel by 4-5 orders of magnitude compared to other fuel eliminates single point failure of fuel claddings and pressure vessel. • Particles small and durable enough that has potential to remain intact during explosive fractures.
<p>Pressure Hazard</p> 	<p>High pressure constitutes a stored potential energy that can be released explosively leading to impacts and damage to reactor components or the release of radioactive coolant. Pressure can escalate accidents.</p>	<ul style="list-style-type: none"> • Other hazards are drastically minimized compared to other reactors, reducing the potential impact of any pressure release. Unlike water or sodium, helium has limited damage potential, especially if clean from fission product gases or dust. • Keep the helium clean using TRISO-based fuels. • Reduce pressure and helium inventory when possible.
<p>Decay Heat Hazard</p> 	<p>When a reactor shuts down, it continues to produce some fraction of the power as decay heat for hours and days. This decay heat is what leads to reactor melting, when the reactor operators are unable to cool the reactor down, such as in the case of pipe clogging, loss of power for pumps, or loss of coolant.</p>	<ul style="list-style-type: none"> • Refractory all-ceramic cores (metals on the periphery) with high 2800 °C melting points. • 1600°C tolerable temperatures in the fuel vs 800°C for UO₂ and 400 °C for Zircaloy in conventional fuel forms. • Materials with high melting temperature, high k, high c which enhance heat transfer and reduce temperature changes. • Passive cooling systems to remove decay heat from the core without coolant, power, or operators and despite changes in the geometry of reactor surroundings. This is achieved by maximizing surface area to power ratio. • Appropriate power rating for Class A passive safety (no moving parts or fluids). That is, reduce the decay heat burden and BDBA power so that the reactor geometry and physical materials can withstand the rise in temperatures.

2.3.1 Fuel

The conventional UO₂/Zircaloy fuel and TRISO based fuels are introduced below on the basis of how they address or exacerbate the hazards. In summary, compared to conventional fuel, TRISO aims to contain and limit the fission product risk at a much smaller scale with higher performance materials thereby limiting the state space and growth of periphery coping systems. TRISO's hazard

reduction goes far beyond that of conventional fuel and its potential to allow for simplified reactor systems may outweigh its higher fabrication costs. Though, for the smaller reactors with already smaller consequences, the benefit of TRISO will be more limited than larger reactors.

2.3.1.1 *Conventional Fuel*

Conventional nuclear fuel is UO_2 oxide pellets inside a Zircaloy tube, called a cladding. As the fuel is used, the UO_2 expands and crumbles into pieces and pressurizes the Zircaloy tube. The fission products, gases, and solids, are released into the tube, creating a high pressure (>40MPa) in the tube. Just beyond the coolant operating conditions of roughly 400 °C, the Zircaloy tube will experience excessive corrosion over its 4-6 year lifetime. By 700-900 °C Zircaloy tube can burst and by 1000 °C it can generate significant amount of hydrogen gas in an exothermic reaction with water. In any of these cases, if the UO_2 fuel operates at greater than 800 °C, fission gases are released into the coolant. The hydrogen generation from Zircaloy, if left unmitigated and its underlying critical safety functions for a reactor will likely lead to a hydrogen explosion or fire. The containment will then hold the pressure of the accident and withstand impacts of hydrogen explosions, fires, and elevated temperatures. If helium is utilized as the coolant, then the limiting temperature for conventional fuel is closer to 800 °C. Even at 1000 °C, very limited fission gas inventory is released from UO_2 pellets.

2.3.1.2 *TRISO/FCM Fuel*

Originally conceived in 1957 [41] during the British Dragon program, TRistructural ISOTropic (TRISO) particle fuel consists of fissile Uranium or Thorium fuel kernels measuring 250 to 600 μm across and coated with layers of Pyrolytic Carbon and Silicon Carbide (sometimes ZrC for NTP applications). TRISO particles are the fuel spheres with ceramic layers, while the matrix is the ceramic material that surrounds the TRISO particles to form a consolidated fuel pellet, usually a cylinder, measuring about 1-2 cm in diameter. The matrix is traditionally graphite, but use of SiC has also been explored.

The driving idea behind TRISO particle fuel is to give each 250 to 600 μm sized piece of nuclear fuel its own containment and pressure vessel to enhance the fuel's ability to contain fission products at very high temperatures and neutron bombardment. The physical basis for miniaturizing the pressure vessel is twofold: fuel subdivision and pressure vessel enhancement.

First, subdividing the nuclear fuel by four to five orders of magnitude significantly reduces the risk of single point failures in the pressure vessel or fuel cladding. Ordinarily, if a single failure in the reactor's main steel pressure vessel or one or few fuel cladding is significant enough, it can lead to a radioactivity release that requires plant shutdown and costly cleanup. With TRISO, particles fail at rates of 10^{-5} during operating conditions, and when they occur, lead to a small radiation release into the fuel matrix where it can be stopped to a degree. With TRISO, fission product retention is achieved at the millimeter scale and by high performance ceramics which limits the accessible state space and the growth of periphery systems at a larger scale. Addressing problems at the smallest feasible scale reduces the required overhead containment effort before they have a chance to grow in size, area, and rate. In fact, U.S. NRC has accepted the idea of a "functional" containment and for HTGRs, it is expected to not require expensive pressure retaining containments. With conventional fuel, much effort must be taken to prevent their escape. Subdivision of fuel into particles is even believed to provide blast resistance as the particle may be small and durable enough to remain intact during explosive fractures like a direct missile hit. Indeed, with this reasoning in mind, the US Department of Defense began funding development of TRISO fueled reactors for forward bases in early 2019.[42]

The second advantage to miniaturizing the pressure vessel is the ability to enhance pressure vessel performance through use of thin layered ceramics in a mass manufactured, seamless, spherical design. Fabrication of millions of particle pressure vessels can be highly standardized and controlled in a mass manufacturing environment with defect rates of 1 in 100,000.[43] Crucially, the millimeter scale vessel allows the use of highly pure brittle ceramics made through CVD techniques that maintain high strength and stability under high temperature and irradiation and have dual use as low reactivity fission product barriers. Normal reactor pressure vessels are made one at a time and have to be cylindrical, with various seaming and joining techniques, multi cm wall thickness, and cannot use brittle materials. As the pressure vessel size is reduced, the more efficient spherical geometry can be adopted, and the required wall thickness drops dramatically to the point that a 35 μm SiC layer can indefinitely contain gas pressures in excess of 200 MPa.[44] This compares to the main reactor steel pressure vessel which may go as high as 15MPa or the Zircaloy cladding which can have pressures up to 50-100 MPa in high temperature conditions. As the nuclear fuel fissions, it continues to accumulate fission product gases and increases the gas pressure that must be contained. If the pressure vessel can handle higher pressures, the fuel can be burned more extensively and safely, which means more efficient use of fuel.

The attractiveness of TRISO-matrix fuel is derived from its ceramics' high thermal conductivity, high fission product retention, and superior irradiation and corrosion resistance across operating, accident, and storage conditions. This translates into better efficiency and safety for current civilian reactors (operation at higher temperatures with higher safety margins) as well as upcoming micro reactors, gas cooled reactors, and molten salt cooled reactors. More extreme performance applications enabled by TRISO-matrix type concepts include nuclear thermal propulsion (NTP) for space, VHTR, Subterrene tunneling, and nuclear ramjets.

2.3.1.3 *TRISO in Graphite*

TRISO is traditionally packaged into graphite pellets. These pellets are formed through a high pressure and high temperature process with various organic binders. The process allows for only simple pellet shapes and can lead to overstressing of the particles, though this can be controlled. Although the TRISO particle is an excellent fission product retention device, some fission products

like Ag and Ce can leak into the coolant. More particles will fail as temperatures are elevated in the core during extreme accident conditions. The graphite pellets or pebbles will tend to undergo irradiation induced swelling and property changes and sometimes crack, impacting the heat transfer from fuel to coolant and complicating spent fuel handling with extra processing steps before permanent storage.



Figure 8 TRISO particle and FCM Fuel pellet from USNC, photographed by author.

2.3.1.4 TRISO in SiC Matrix – FCM Fuel

TRISO particles must be packaged into a fuel form or pellet, and SiC encapsulation, also known as Fully Ceramic Micro-encapsulated Fuel (FCM)[45] or Fuel-in-Fiber [46], offers a series of benefits over graphite including higher fission product retention, greater tolerance to air/steam ingress, and potentially higher burnup capability. The most significant benefit to SiC encapsulation is that the additive process used in its manufacture can achieve around 65% packing fraction with little to no stress on the TRISO particles during manufacturing, although this can ostensibly be accomplished with graphite as well. This process also gives design freedoms for near-arbitrary fuel form factors such as annular fuel and other highly specified shapes that can vary 3-dimensionally across the core.[47] This allows a reactor to operate at higher power and with greater energy content without increasing temperatures in the fuel. Other benefits include reduced dimensional changes of the pellets, reduced thermal property changes of the pellets over time and radiation damage. SiC ends up swelling instead of shrinking and its swelling saturates after 1 DPA.[48] Finally, the SiC or graphite encapsulation creates a ready-for-storage form factor that is simpler to handle than traditional crumbling fuel pellets and a step above simple graphite encapsulated TRISO.

SiC-encapsulation may enhance the resilience of TRISO particles to higher temperatures and irradiations allowing for more extensive burnups, higher power densities, and extreme accident tolerance. Higher burnups allow for a reduction in the long-lived fission products, reducing the spent fuel's radioactivity lifetime to thousands of years rather than hundreds of thousands.

2.3.1.5 Fuel Enrichment

HALEU greater than 5% enrichment does not exist in the US outside the military complex, and significant quantities are unlikely to be available for demonstrations before 2030, let alone commercial rollouts. The capability to use lower enrichment fuel unlocks several benefits with a cascade of knock-on advantages. The lower enrichment fuel improves the risk profile for technology demonstration and deployment. Supply chains do not have to be created from scratch and favorable regulations and facility requirements are allowed for lower enrichment fuel, which will directly impact fuel fabrication and reactor manufacturing costs. Finally, lower fuel enrichment reduces strategic value and proliferation risk because it takes more effort to further enrich to weapons capable grades.[49]

For this thesis, the use of TRISO/FCM fuel with a range of packing fractions and enrichments up to 20% is assumed.

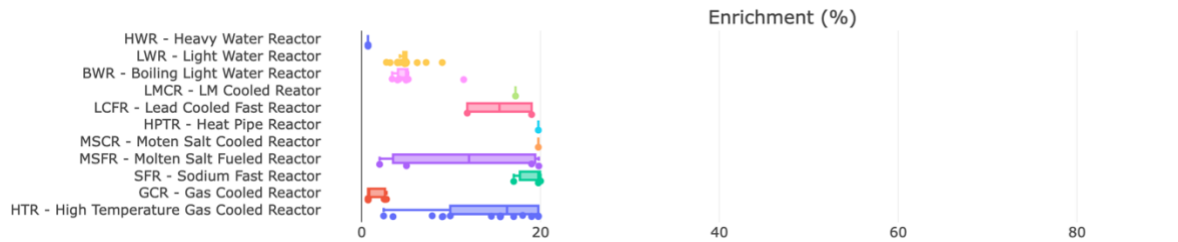


Figure 9 Fuel Enrichment across civil designs of interest. High enrichment designs are historic reactors like Ft. St. Vrain HTGR.

2.3.2 Coolant

2.3.2.1 Water

The role of coolant is to transfer heat from the nuclear core to the thermal application, be it steam generation for an electrical turbine or direct process heat. The main considerations in choosing the coolant have historically been heat transfer effectiveness, neutronic moderation for thermal reactors, and availability. In the case of water, designers have chosen a highly effective and available fluid that also moderates neutrons (allowing for smaller cores or more fuel). Unfortunately, water also introduces significant chemical energy sources (hydrogen generation), material corrosion challenges, and high-pressure requirements.

Are water's excellent heat transfer capabilities worth it? In terms of hazard reduction, the answer is "no" as there are ready alternatives. Water is directly implicated in all three past nuclear accidents, either causing or escalating the accident. At Fukushima, loss of grid and emergency power left operations without cooling ability for the reactors during decay heat shutdown. Without flowing water to cool the fuel, temperatures increased, and water reacted with Zircaloy cladding to produce hydrogen gas, increasing pressures, and leaked out of the containment and eventually exploding violently in the reactor building.

In terms of cost, one would expect water to offer clear benefits, but the fact is that heat transfer in the primary loop is a small component of the LCOE. A 10x reduction in heat transfer related costs could be negligible. And unfortunately for water, lifecycle heat transfer costs related to OPEX and extra CAPEX to deal with activated water and water related accidents could be higher. The higher corrosion and pressure necessitate a more involved maintenance and inspection burden, and more numerous and more expensive subsystems and components. Water cooling components and systems may be cheaper up-front today only because of their ubiquity in other manufactured systems including engines, air conditioners, and conventional power plants.

2.3.2.2 Helium

Using Helium, a designer sacrifices significant volume in the core for coolant channels and has to use larger pumps and heat exchangers to accomplish the heat transfer task. But the advantages are an incredibly simplified system and access to higher temperatures. It is wasted volume because helium as a gas, has very poor heat transfer properties and is also neutronically transparent and does not moderate the neutrons as water does. The coolant is clean and totally non-corrosive thereby reducing the maintenance, inspection, and radioactivity problem in the reactor peripherals. The helium has very little chemical reaction potential to produce other compounds or release chemical energy. It can basically leak out at any time with minor effects, though it may become costly to replace it if wide deployment of helium cooled reactors take place. Combined with all-ceramic cores, using helium coolant is like using an underpowered electric motor while massively, upgrading the brakes and traction control. Since helium is a poor heat transfer fluid, it has to be pressurized and combined with its large volume, HTGRs feature enormous reactor pressure vessels per power generated. However, if the core inlet temperature is kept low enough (not using salt storage or SCO₂ power cycle), the use of helium allows the pressure vessel to be manufactured with low alloy steel and last 40-60 years with minimal corrosion.

Another consideration is phase change. Helium is already a gas at all encountered conditions, while other coolants (sodium, molten salt, water) will have phase changes at different temperatures and pressures. Having only a single phase in a typical nuclear reactor operating space limits the design and system burden of dealing with multiple phases and limits the possibility of some accidents. Under HTGR conditions, a gas cannot phase change into a more chaotic phase. This is especially a concern during accident conditions when liquid coolants begin to boil, providing a dispersive energy source and increasing pressure and corrosion and can result in loss of coolant or rapid degradation of components as in the case of water, sodium, or molten salt boiling.

Compared to water or molten salts, helium is less effective at heat transfer at the relevant temperatures and pressures. Greater electrical power must be used to pump the coolant and the heat exchangers are larger. As mentioned before, while the heat transfer fluid is small cost component of the LCOE, the heat transfer equipment can be a significant part depending on the design LCOE target. Nevertheless, the heat transfer equipment with helium should reduce the maintenance and inspection burden and not complicate the chemistry and neutronics of the core. The helium poor heat transfer properties are actually leveraged in HTGRs as it allows them to operate with such low power densities that most rare postulated accidents can be passively overcome.

2.3.3 Moderator

Moderators are judged based on safety considerations and the volume they require to moderate (or thermalize or slow down) the neutrons. I briefly compare moderator options for thermal reactors, showing that graphite or other high temperature moderators more effectively address the hazards.

2.3.3.1 Safety Aspects

What chemical reaction potential does the moderator material introduce into the core and how does the moderator change with temperature changes, both neutronic and structurally. Ideally, the moderator has little to no reaction capability with other core materials as well as water or air that might enter the core during extreme accidents. Furthermore, the moderator should not be able to phase change at the encountered accident temperatures as phase change can exacerbate the accident through expanded state space, pressure changes, and higher reaction potential. The moderator should be chemically stable at the operating and accident temperatures. For example, as water temperature increase, pressures will increase in the loop, perhaps leading to pressure boundary failure. The upper bound on water reactor temperatures is roughly 350 °C, and anything beyond will require new materials, particularly improved cladding materials. Graphite's upper bound is on the order of 3500 °C. Graphite does not limit absolute temperatures in the core. Compared to water, graphite reduces the chemical reaction considerations, eliminates hydrogen generation potential, and improves the thermal properties of the core as it provides a large thermal heat sink that can absorb heat with modest temperature increases. Still, liquid moderators do not suffer graphite's radiation damage or dimensional changes and do not significantly add to the decommissioning waste stream.

2.3.3.2 Neutronic and Dimensional Aspects

Moderators should use as little volume as possible in their moderation function. This reduces the cost of the moderator component and reduces the size of the Reactor Pressure Vessel or allows for more fuel to be packed into the reactor. These can be significant cost effects. Hydrogen bearing compounds like H₂O, ZrH, YH are the most efficient using the least amount of volume compared to Beryllium and Graphite but introduce hydrogen chemical reaction potential and related material degradation. Graphite can more than double the core volume for the same fuel load compared to other hydrogen bearing moderators but with a safety benefit of higher heat capacity and not introducing explosive hydrogen in the core. Composite moderators and Fuel Moderator Inversion Blocks are methods to overcome temperature and radiation limitations and reduce the compatibility issues of hydrogen bearing compounds with air or water.

Most moderators have good negative feedback mechanisms. That is, they have less moderation at higher temperatures, thus slowing down the nuclear reactions. The main mechanism is thermal volume expansion which reduces the density and collision rates.

Because moderators tend to make up the bulk of the core volume, their thermal properties often define both responsiveness of the core to temperature changes and ultimate power rating safety considerations. For this reason, solid moderators with high thermal conductivity and specific heat are favored for their ability to transfer heat during accident conditions.

2.3.4 Coolant and Reactor Temperatures

There are two main benefits to increasing the coolant temperatures as much as possible, particularly using all-ceramic cores and helium cooling: 1) passive cooling and 2) power conversion efficiency. The main drawbacks include the need for higher performing materials for core internals and the pressure boundary, and a larger stored energy during accidents.

LWRs are the lowest temperature commercial reactors, operating at less than 400 °C outlet conditions, sodium and lead cooled reactors can operate up to 520°C, Molten Salt cooled reactors can be slightly higher, up to 700°C. These reactors use coolants that will boil at extreme temperatures. HTGR variants may be able to operate with core outlet temperatures of up to 1050 °C, with core components that can withstand accident temperatures of 1600°C. The only way to achieve high temperatures approaching natural gas temperatures is to use refractory ceramics, extreme performance fuel, and helium coolant. No other fission technologies can achieve these temperatures as their coolants are not inert, like Helium.

2.3.4.1 Enhanced Power Conversion Efficiency

Combined Cycle natural gas turbines are the most efficient turbomachinery heat engines devised by humans to date. They achieve this efficiency by operating at very high temperatures and using multiple thermodynamic cycles to extract as much useful mechanical work from the hot gases as possible. High temperature unlocks higher thermal cycle efficiencies, reduces the reject heat burden, and allows for higher reject heat temperatures.

HTGR can achieve these high efficiencies by virtue of its high temperatures and ability to couple to modern power conversion systems. Over time and as the EPC capabilities develop, HTGR may use a variety of power conversion cycles starting with Rankine cycles and moving into Brayton, combined cycles, and sCO₂ cycles (Section 3.5.1). In this thesis, I evaluated only a BoP with helium primary, a molten salt secondary, and subcritical Rankine tertiary loop – mimicking the MMR-1.

Future nuclear reactors may also be well suited for solid-state power conversion systems that may become cost-effective in the next decade and benefit from higher temperatures. These include thermo-photovoltaics and thermionics which could eliminate turbomachinery and reduce the operating and maintenance costs of the BoP.

Another benefit of higher temperatures is reducing the total coolant mass flow rate for the same heat removed, allowing for smaller pumps and heat exchangers and reduced coolant channel volumes in the core.

2.3.4.2 Larger Stored Energy Raises Afterheat Temperatures

Operating at higher temperatures means the core will have a larger stored energy. During accidents, this stored energy dissipates to the surroundings, raising temperatures.

2.3.4.3 Enhanced Passive Cooling

The key to an HTGR's safety is the ability to dissipate heat through passive means. During accidents, heat is transferred from the core to the core barrel through conduction, and then to the RPV through convection and radiative heat transfer, and finally to the concrete reactor building or reactor cavity cooling system primarily through radiation and natural convection. Heat transfer is affected by the difference in temperatures between the heat source and the heat sink. The heat sink is the outside world, either bedrock or atmosphere, and this is roughly fixed at 25 °C. If I increase the temperature difference between the heat source and the heat sink, heat transfer rates will also increase. For conductive and convective heat transfer, this is a roughly linear benefit. Increasing the heat source temperature allows for linearly more heat transfer. For radiative heat transfer, which is more passive and reliable, heat transfer scales to the 4th power of temperature. Passive heat transfer is simpler, more effective, and reliable at higher temperatures.

2.3.5 HTGR Type and RX Geometry

There are various ways to concoct an HTGR core and BoP. HTGR can be characterized principally by the use of a TRISO fuel, helium coolant, and a moderator. In terms of moderators, there are HTGR designs intending to use graphite, beryllium [50], water ([51] and BWXT Pele), or various hydrides [50] both canned or ceramic encapsulated. Besides choice of moderators, designs vary by the fuel form shape, the reactor shape and orientation, and the primary heat transfer system. There are pebble bed and prismatic cores, vertical and horizontal cylindrical cores like AGR or more recent concepts [52][53], spherical and pancake cores. And finally there are designs with direct or indirect Brayton cycles, or coupled to a separate steam generator, integrated steam exchanger, molten salt heat exchangers, and CO₂ or other gas heat exchangers.

The thesis chose the established avenue of vertically oriented cylindrical, prismatic HTGR, again mirroring MMR. Consideration should also be on the activation of the vessel, air, concrete, and bedrock which have regulatory limits and decommissioning effects. Design knobs to control the activation include spacing of equipment and components, shields of lead, water, concrete, or borate, and ultimately reducing the leakage from the core through larger reflectors and diameters and lower surface area cores.

2.3.6 Power and Size – General Considerations and Metrics

A nuclear reactor can be operated at any desired power provided that the heat can be carried out of the core. In practice, the power is limited by industrial ability to make and deliver large components and the limiting temperatures of the fuel and materials in a given cooling architecture during operating and accident conditions. If cooling does not match the heat generation, temperatures increase, and the reactor will essentially turn off beyond certain temperatures. It will similarly shut down if it melts into a non-critical configuration – but the battle is lost with large remediation costs and leakage concerns even with a functional containment.

Traditionally, reactor power density has been determined by the maximum heat transfer that can be achieved with the given geometry and cooling fluid during operating conditions and favorably defined accident conditions. And power rating is determined by simply applying the power density to the entire core volume adjusting for power rating. This means designers have favored very high powers and high-power densities, irrespective of the size, even though the reactor will probably melt itself when conditions deviate from the carefully defined accident conditions. In Figure 10, we see how nuclear reactor power ratings have increased since inception, logistically approaching the size and complexity limits of practical turbomachinery and mega projects. Size and power are decoupled. Why seek the highest power? To reduce cost because it means the reactor materials are being maximally utilized per unit time.

Nuclear Reactors In the Past

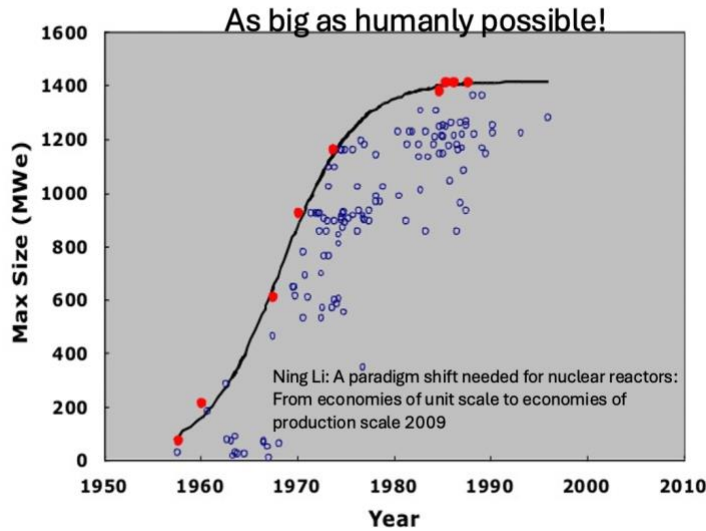


Figure 10 Nuclear reactor power ratings over time reproduced from [54]. EPR (1660 MWe) and other reactors not shown.

The alternative is 100s of reactors producing the same total power as a few very large units. Nuclear utilities and operators often believe that reactor count is an important part of the operating cost and complexity. The count of micro reactors to achieve a power level is neither here nor there. It's like trying to scare people by quoting the number of LiPo cells in a battery pack, or the number of transistors in a chip, or the number of car engines on the road. It is a very large number! For one, the reactors will probably all be coupled to one large BoP, achieving similar economies of scale on the power plant and turbine island side. Each reactor may require its own control system and could suffer from less efficient RPVs, HXs, and tubing – but the mere number of units may well have only a small effect on the total cost that is outweighed by economies of factory production. Similar production economies occur with large aircraft or automobiles which are produced at rates of ~2000 and ~100M per year, respectively.

2.3.6.1 Decay Heat Hazard

The principal way reactors fail is when operators are unable to sustain reactor cooling. When a reactor is turned off, it still produces roughly 7% of its full power as decay heat falling off with a power law of roughly -0.2 over the course of hours and weeks. But if cooling cannot be sustained continuously for any reason, this decay heat can be sufficient to cause fuel failures and fission product release. To make sure this does not happen, the reactor needs to run at sufficiently low power ratings, so that even if the operators cannot provide cooling, the reactor can cool itself or can manage to remain at safe temperatures. I first discuss power density, and surface area to power ratio (SAPR) metrics, and then consider a preliminary approach to define safety: limited power levels.

2.3.6.2 Power Density

Power rating and size determine the power density of the reactor. Higher power densities are more difficult to passively cool down. Higher power densities also lead to Xenon poisoning of the reactor core, which can prevent the reactor, depending on the concept from changing power quickly. PWRs in development have too high a power density to quickly change power to match demand because of Xenon poisoning. To overcome Xenon poisoning, they use excessive control rods or other neutron control systems. For some reactors, it takes hours and sometimes days to be restarted once it has been shut down.

HTGR tend to have sufficiently low power rating for their size to limit the worst-case accident temperatures from exceeding fuel failure temperatures. In extreme cases like MMR, low power density also means it has negligible xenon poisoning and can change power very quickly without inordinate amounts of reactivity insertion potential though temperature gradients in the ceramic components must be carefully accounted for.

MMR in particular has a lower decay heat power density than fusion systems like SPARC, DEMO, or ITER and orders of magnitude lower than other prototypical advanced reactors as shown in Figure 11. A lower decay heat is more manageable by passive cooling systems, allowing the reactor to dissipate heat more easily and without damaging the reactor. The other aspect to consider is the maximum temperatures that can be safely maintained in the reactor. HTGR cores can withstand much higher temperatures than a fusion's reactors metals, molten salts, and magnets. UNSC's 15 MWth MMR has a lower initial decay heat power density of 0.075 W/cm³, less than DEMO's 0.083 W/cm³ in the blanket and divertor.[55] The comparison would be less favorable for fusion 1 hour after shutdown when fusion's decay heat is almost equal to fission's decay heat.

Low enough power density also eliminates the need for water pool storage of used nuclear fuel. Current reactors produce used nuclear fuel that must be stored in large 12 m deep water pools for 2-5 years before being put into dry-storage casks. Reducing power density and decay heat can eliminate the wet storage and the related accident risk that was first experienced at Fukushima.

Decay Heat Core Power Density (W/mL)

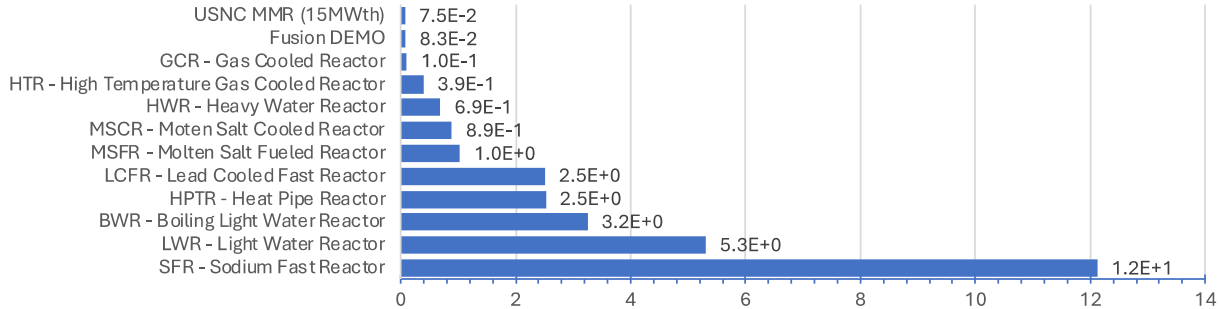


Figure 11 Decay heat power density after shutdown (assuming 6.6% of operating power for fission) for some advanced reactor technologies. USNC MMR (15 MWth) is shown as a representative Class A HTGR. Values are median values of the available data shown in Figure 13.

2.3.6.3 Surface Area to Power Ratio

Another safety metric is the surface area to power ratio. SAPR is an indication of how much surface area the reactor has to dissipate excess heat during accidents. With sufficiently high SAPR, the reactor can dissipate all excess heat through conduction and radiation – totally passive and intrinsic heat transfer mechanisms that are basically guaranteed to work. Passive physical heat dissipation is based on physical laws and material properties and can occur through natural convection, conduction, or radiative heat transfer. The more intrinsic the heat dissipation mechanism, the stronger the argument for reduced safety systems. This makes radiative cooling and thermal conduction from an external surface superior to natural convection of liquid with internal flows. Natural convection can be mechanically obstructed and coolant pools can leak or become displaced, whereas conduction and radiation are intrinsic solid state physical mechanisms. In the context of IAEA’s passive system categories, [37] a Class A system requires no intelligent signals, no external power or force, has no moving parts, and has no working fluid. A Class B Safety system requires moving parts or fluids, but fundamentally relies on natural and passive mechanisms. An Active Safety system requires functional moving parts like pumps, may require operator action, and requires functional control systems.

If the power produced in the core is too high for the given surface area, the reactor temperatures can increase to the point where core components or structural components outside the core are damaged. Higher surface area to power ratio translates into a safer reactor as heat can be more easily dissipated by passive, solid state heat transfer. To summarize, there are a few knobs to improve resilience to decay heat: reduce power rating, increase surface area, or improve the thermal capabilities and temperature tolerance of the core materials. The last point can also include the use of a large heat sink in the reactor core, such as graphite blocks that can absorb heat and reduce temperature increases, as previously discussed.

Core Power to Surface Area [MWth/m²]

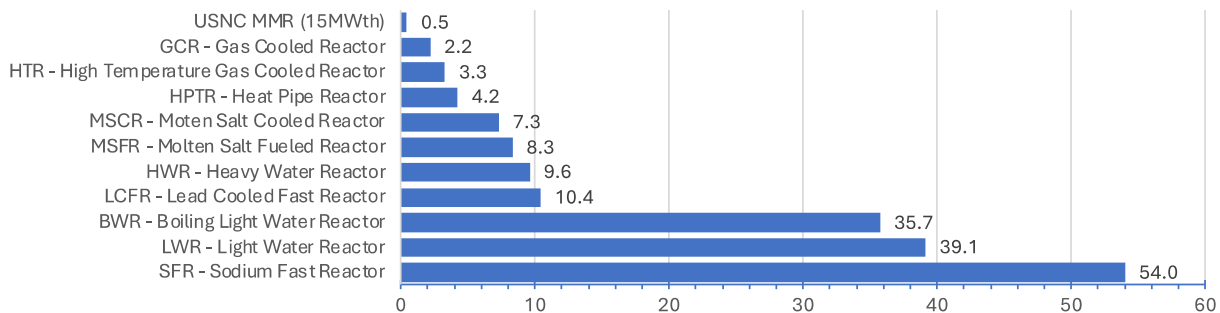


Figure 12 Core Power to Surface Area Ratio for various fission reactor concepts in development in 2023. Lower power to surface area ratio is associated with a safer reactor as heat can be more easily dissipated by passive, solid state heat transfer. USNC MMR (15 MWth) is shown as a representative Class A HTGR. Values are computed using the same used for Figure 13 with available power and core geometry data.

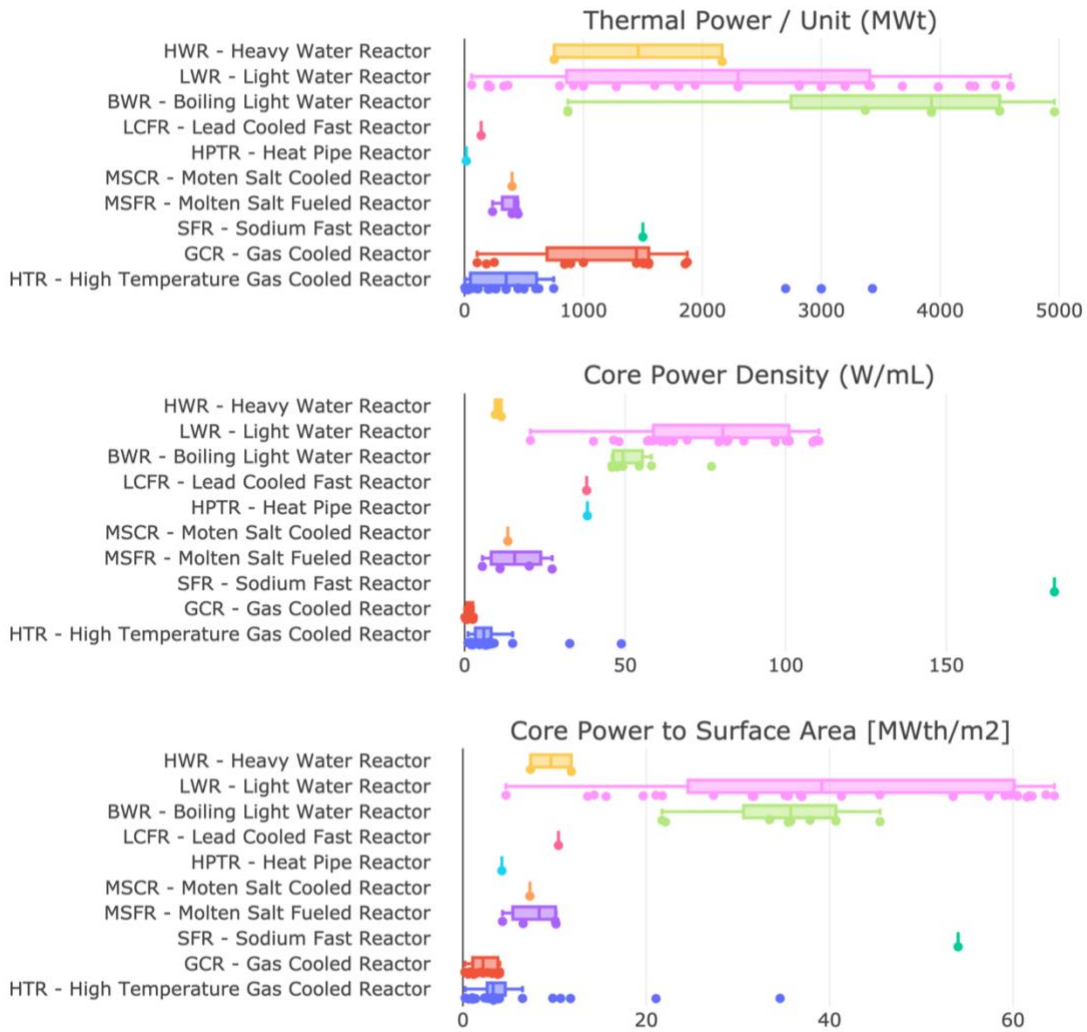


Figure 13 Reactor power metrics across designs of interest based on publicly available information and images. Data for each technology architecture obtained from [56][57][58] and author's analysis of industry reports and public information.

2.3.6.4 First Order Power Rating Constraints

Power density and power can be related by considering the heat transfer and limiting the temperatures in the fuel and RPV. A simple analytic solution is found for either temperature or heat flux boundary conditions. I solve for the steady power as a function of volume or power density. Equation 2-1 gives the solution for a maximum heat flux, and Equation 2-2 gives the solution for temperature boundary conditions.

Definitions:

Sphere radius, r
 Sphere volume, V
 Decay heat power, \dot{Q}
 Decay heat power density, \dot{Q}_V
 Maximum surface heat flux, $\dot{Q}_{S,Max}$
 Core centerline temperature, T_{max}
 RPV temperature, T_{wall}
 Thermal conductivity, k

Constant Heat Flux B.C.

$$\begin{aligned}\dot{Q} &= \dot{Q}_V * V = \dot{Q}_V \frac{4}{3} \pi r^3 \\ \dot{Q}_V &= \frac{4\pi r^2 \dot{Q}_{S,Max}}{\frac{4}{3} \pi r^3} = \frac{3\dot{Q}_{S,Max}}{r} \\ \dot{Q} &= 4\pi r^2 \dot{Q}_{S,Max} = 3V^{2/3} \propto r^2 \propto V^{2/3} \\ \dot{Q} &= \frac{36\pi \dot{Q}_{S,Max}^3}{\dot{Q}_V^2} \propto \frac{1}{\dot{Q}_V^2}\end{aligned}\tag{2-1}$$

Constant Temperature B.C.

$$\begin{aligned}\frac{\dot{Q}}{V} &= \dot{Q}_V = (T_{max} - T_{wall}) \frac{6k}{r^2} \\ \dot{Q} &= V (T_{max} - T_{wall}) \frac{6k}{r^2} = 8\pi k (T_{max} - T_{wall}) r \propto r \propto V^{1/3} \\ \dot{Q} &= \frac{1}{\dot{Q}_V^{1/2}} 8\pi k^{3/2} 6^{1/2} (T_{max} - T_{wall})^{3/2} \propto \frac{1}{\dot{Q}_V^{1/2}}\end{aligned}\tag{2-2}$$

The scaling is $\dot{Q} \propto V^{1/3}$ for temperature BC compared to $\dot{Q} \propto V^{2/3}$ for heat flux BC. More generally, I can write the scaling for a given power to volume scaling exponent α .

$$\dot{Q} \propto \dot{Q}_V^{\frac{\alpha}{\alpha-1}}\tag{2-3}$$

We will describe other methods to estimate the power rating for different safety classes in Section 3.3 that combine both estimates. The approach taken and shown in Table 7 is to define the heat flux boundary conditions with an HTC and radiation-based heat transfer to the environment based on the geometry and passive cooling assumption. This total heat transfer then depends on the outer wall temperature, and I can couple the models to iteratively solve for the max power rating constrained by the maximum temperatures of the materials. This steady state power is assumed to be the decay heat power.

2.3.6.5 Biological Parallel

In the biological realm, there are various empirical relations associating an organism's dimensional parameters and other characteristics. The general form is shown in Equation 2-4. For example, if bone strength is limited in biological structures, I would expect the cross-sectional area of bones to scale with the mass or volume to the 2/3rd power. Other relations include heart rate $t = M^{-1/4}$ and cruising flight speed $v = M^{1/6}$, each with their own underlying physical explanations.

$$y = bx^\alpha\tag{2-4}$$

Kleiber's law [59] relates the mass or volume of an organism with its power rating. Figure 14 shows how organism power rating is constrained in a fashion consistent with a maximum surface heat flux boundary condition. Organisms must dissipate heat and remain at safe temperatures, and they are constrained by their surface area and the temperature limits of Earth-based biological processes. The power law varies somewhat between insects, mammals, birds, and trees, but the overall trend in Figure 14 has α between .6 and .85, meaning that specific power decreases with mass. This is slightly better than the heat flux boundary condition in Equation 2-1 ($\alpha = 2/3$) showing organisms can only give off so much energy per unit area without overheating. Solving for the maximum heat flux for spherical plants and animals yields 22 and 83 W/m², and HTC between 1-20 W/m²K. The greater cooling capabilities of animals and birds could be due to evaporative cooling, higher flow rates, and higher thermal conductivity.

Why might evolved structures have developed this relation between power and volume? I can speculate that it is the most survivable and successful way to design a power system, regardless of the materials at hand because it more or less retires the risk of overheating. The existence of Kleiber's Law in evolved systems inspires its application to man-made thermal power systems that aim for passive safety and reduced risk through reduced consequence. How might these heat flux boundary conditions apply to mechanical systems? The temperature limits of typical biological processes are about 40 °C – much lower than metal and ceramic based systems. The bodily flows homogenize temperature across the body so that the maximum temperature gradients are at most a few degrees. Low surface heat flux is likely due to low temperature difference between the outer wall and the ambient. A mechanical system using metals and ceramics will be able to achieve far higher centerline temperatures and wall temperatures and a larger heat flux boundary condition.

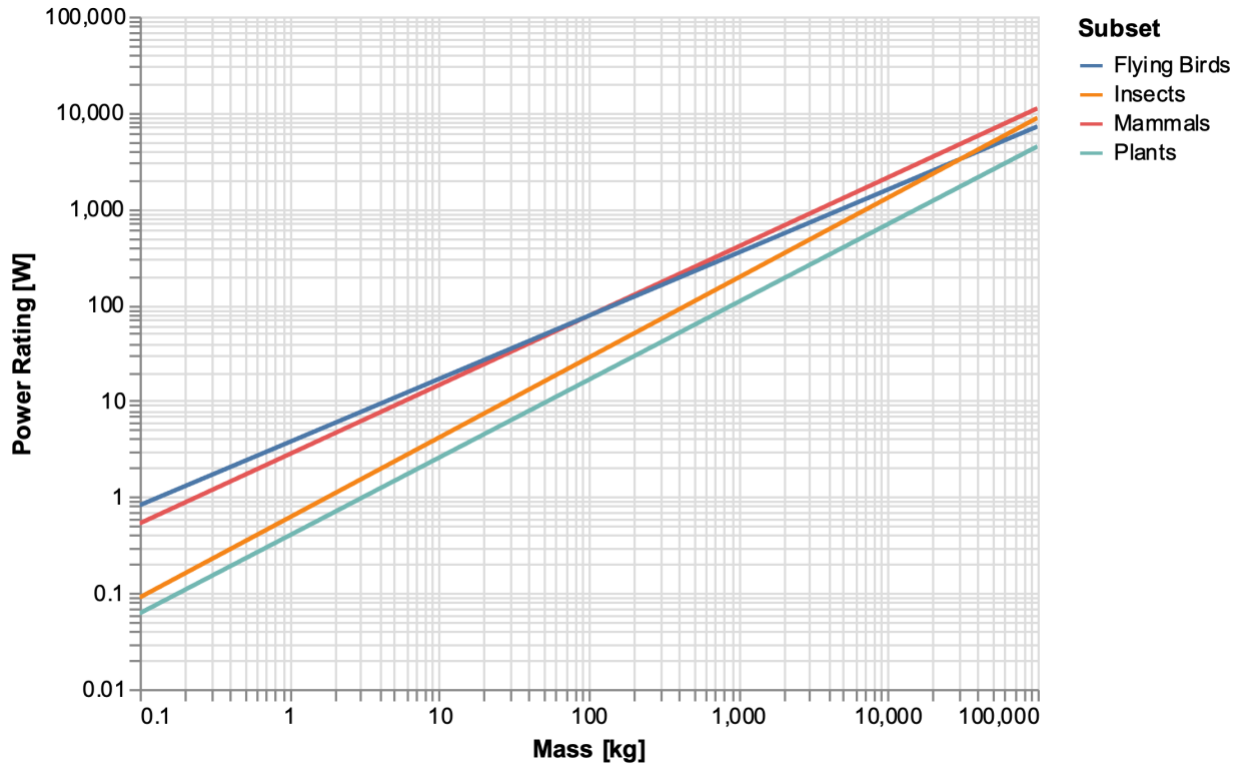


Figure 14 Kleiber's Law for Earth-based organisms using data from [60]

2.3.6.6 Different Reactor Architectures under Passive Cooling Constraint

I applied the power rating constraints similar to Kleiber's Law, and elaborated in Table 7, to a few nuclear technology architectures. The architectures are defined by the parameters listed in Table 5. I varied the radius for a spherical core in each case and computed the decay power limited by maximum fuel and wall temperatures. This would constitute a Class A Passive Safety design capable of withstanding multiple BDBA without moving parts or fluids. The results are shown in Figure 15 together with estimated values from existing designs.

I find that temperature BC is the most limiting for reasonable values of reasonably sized cores. Heat flux BC is more important for smaller cores or boundary heat transfer limited cores. From Figure 15 and Figure 16, I find that HTGR is the only viable architecture to achieve useful power densities. The comparison as formulated is clear, and the competition is nonexistent. HTGR and GCR designs are the only designs that are close to being appropriately sized under this power constraint. This is the primary reason for HTGR down selection. Stunningly, HTGR can and has been designed to follow an approximation of Kleiber's Law. This is not typically done by choice, but from the limited achievable power densities in cores built using graphite and TRISO.

Table 5 Simplified reactor technology assumptions and relative power rating at 3m diameter core. Limited by fuel or cladding temperature above which fission products will be released.

Reactor Technology	Max Core T [°C]	Max Vessel T [°C]	k [W/mK]	Power Rating 3m [MWth]	Relative to Max
HTR - High temperature gas cooled reactor	1600	450	35	15.5	1.00
LWR - Light Water Reactor	450	450	10	2.0	0.13
MSCR - Moten Salt cooled Reactor	800	600	20	6.3	0.41
SFR - Sodium Fast Reactor	800	600	10	3.6	0.23

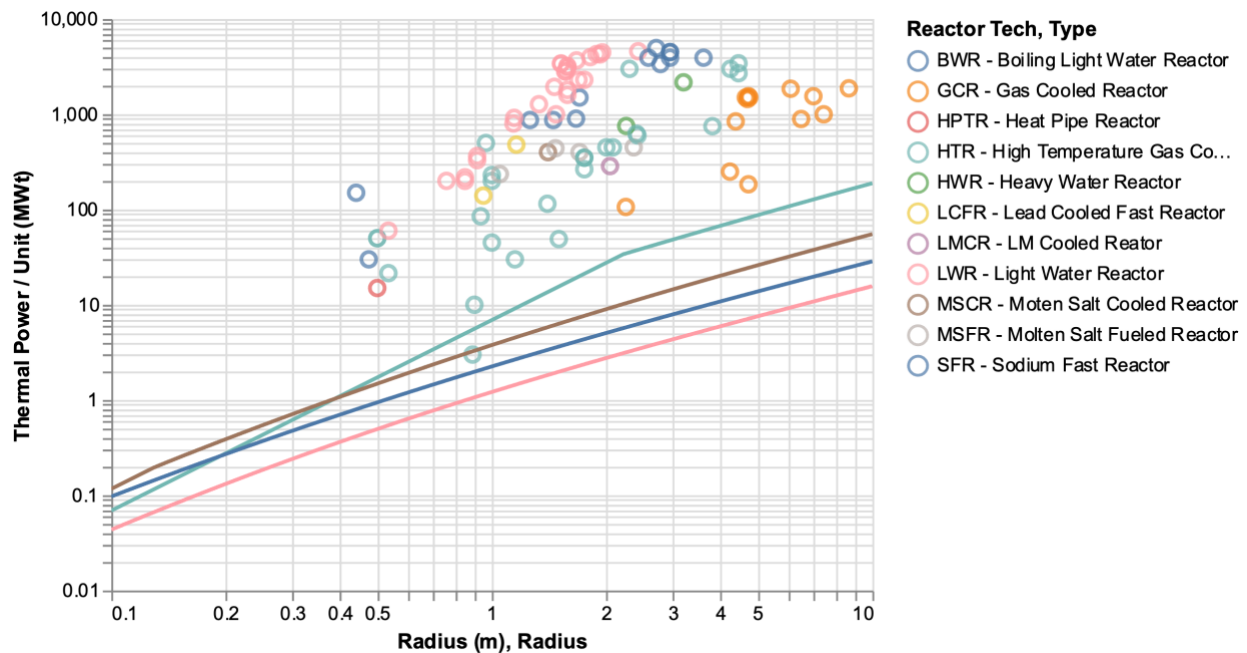


Figure 15 Power rating envelopes for different reactor technologies under LOCA conditions with only outer core boundary passive cooling. Points are estimated values for various existing and planned nuclear reactors. Lines are estimated using Table 5.

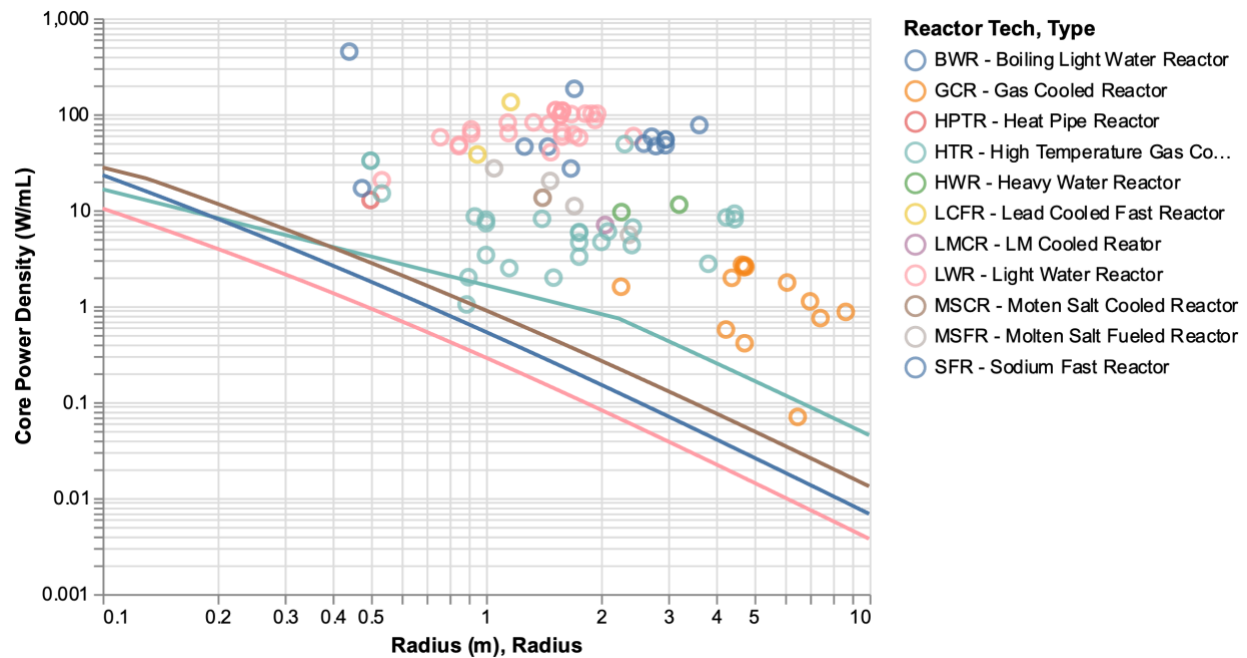


Figure 16 Core Power density for the same data and model in Figure 15.

2.3.7 Power and Size – Economies

We can assemble a toy model to understand the trades associated with reactor size expanding on the approach in [6]. In brief, higher power rating gains economies of scale in the production of heat but loses economies of multiples in the production of reactors. In turns and in altogether, the LCOE effects of economies of heat production with larger reactors, serving diverse end-users, economies of scale in RX production with smaller reactors, safety constraints that link power and size, and constraints between size and burnup are considered. The overall formulation suggests a non-obvious approach for performative designs, moving away from the historical approach of bigger is better.

2.3.7.1 Economies of Heat Production in Larger Reactors

If we want economies of scale on the reactor itself, that is in the production of heat, we aim for large reactor: 4+ meters across, producing gigawatts of power in one reactor core. The advantage of economies of scale on the reactor is that larger components are more efficient. A larger reactor will tend to use less steel, concrete, and raw material per unit of power delivered. A larger reactor loses fewer neutrons, can use more efficient pumps and containment structures. Refueling would occur continuously or at 1-to-2-year intervals. These neutronic and thermal hydraulic advantages have been steadily decreasing over time, with disadvantages associated with megaproject complications and construction inefficiencies in countries with constrained labor.

The cost effect of physical economies of scale is typically approximated with a power law. The cost of the first unit is proportional to the volume with $s = [0.5, 0.9]$. An exponent less than one indicates costs are reduced per unit volume with larger volumes.

$$c_1 = c_0 V^s \quad 2-5$$

2.3.7.2 Economies of RX Production

A large reactor sacrifices the opportunity to achieve economies of mass production - the fundamental driver of productivity and technological progress in the last fifty years. Reactors and BoP systems can be too big to be produced in factories due to size and transport limitations. Instead, they must be manufactured and assembled at the site by separate teams on decade long time scales. There is limited opportunity to learn and improve and there is little opportunity to automate and share manufacturing costs across hundreds or thousands of units. It is tackling manufacturing with hands tied, unable to reap the benefits of 50 years of factory manufacturing technology and automation. Larger units can be like hand-built Ferraris versus factory manufactured Corollas.

We approximate economies of production using wright's law with $w \approx [0.15, 0.25]$, though learning does not always take place in Western nuclear gigawatt scale builds.

$$c_{unit} = c_1 N^{-w} = c_0 V^s N^{-w} \quad 2-6$$

Now I can relate the number of units produced by requiring a certain total produced power capacity, P_{total} .

$$N_{total} = \frac{P_{total}}{P_{unit}} \quad 2-7$$

Relating the power of each unit to the volume using the power density,

$$V = \frac{P_{unit}}{P_{density}} \quad 2-8$$

The total cost is approximated as the cost per unit multiplied by the total number of units produced.

$$c_{total} = c_{unit} N_{total} \quad 2-9$$

Then the cost of each unit from learning and volume scaling is substituted.

$$c_{total} = c_0 V^s N_{total}^{1-w} \quad 2-10$$

$$c_{total} = c_0 \left(\frac{P_{unit}}{P_{density}} \right)^s \left(\frac{P_{total}}{P_{unit}} \right)^{1-w} \quad 2-11$$

The relations above are substituted to find how total cost is related to the power density and the power per unit, the same result as [6].

$$c_{total} = c_0 P_{density}^{-s} P_{total}^{1-w} P_{unit}^{-1+w+s} \quad 2-12$$

As expected, the total cost increases for larger P_{total} but with the learning effect. The negative exponent on $P_{density}$ shows we want the highest power density. But the chosen unit power is sensitive to the values of w and s . Figure 17 shows the different possibilities for w and s and the regions that favor economies of production (green) versus regimes that favor economies of physical scale (red) like volume economies. The diagonal line is the equivalence line. If w and s add up to 1, there is equivalence between production and volume economies such that the chosen power rating has no effect on cost. In the case of little learning (low w) and large physical economies (lower s), cost is lowered by choosing higher power ratings. This is what nuclear designers have long believed. Over the last two decades, the SMR push is driven by the belief that there are stronger learning effects and weaker physical economies designs (green dot).

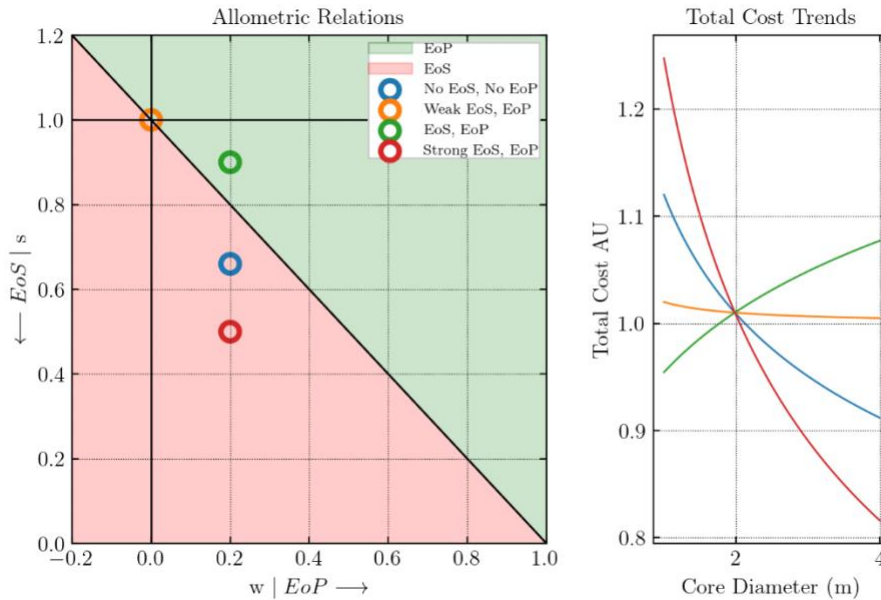


Figure 17 Relative economies and effect on cost. Left panel shows economies of scale in reactor Production versus physical economies of scale in Unit Volume. Right side plot shows the cost trend for increasing power or core dimension in the corresponding regions of the left side plot. The four points indicate likely regimes for nuclear reactor systems and industrial hardware generally.

2.3.7.3 Serving Diverse End-Users

A single 1GWth reactor cannot supply heat to 10 dispersed 100MWth users, but a 100MWth reactor can be replicated to serve a gigawatt user. From a business perspective, large reactors sacrifice the ability to serve a wide range of geographically distributed and smaller end-users. The average electrical powerplant in the US has a name plate capacity of 120 MWe and delivered capacity of 46 MWe. The average US process heat facility in petroleum, chemical, paper, and food industries has a heat demand of 77 MWth (using data from [29]). Figure 18 and Figure 19 show the distribution of electrical power plants according to their delivered power rating. Over half the power supplied comes from power plants less than 500 MWe. Lower power ratings are even greater contributors when we consider other energy generation devices like automobiles, ships, and aircraft. One should also consider transmission and distribution costs which can vary widely depending on the degree of centralization and the specific location, but generally can be on the order of half the delivered cost of power and in the range 1-15 cents per kWhe.

It has been proposed that nuclear continue to try multi-gigawatt scale deployments in the form of nuclear hubs - megaproject facilities where massive power plants are collocated with large power users. [Nuclear tech hub: Co-siting cutting-edge nuclear facilities with waste management sites] This can often make sense if there is already an industrial zone, ready to receive a large central power plant. But the reality is that much of our power generation is at a much smaller scale and geographically distributed, by physical requirement of the end-user or the sheer impracticality of centralized power projects. We have existing infrastructure that has evolved over centuries with influence from waterways, roads, cities, and the resources at hand. We should consider matching new solutions to the existing infrastructure. Creating new gigawatt scale hubs could devolve into the usual predicament of the central planner: underutilized and unwanted infrastructure.

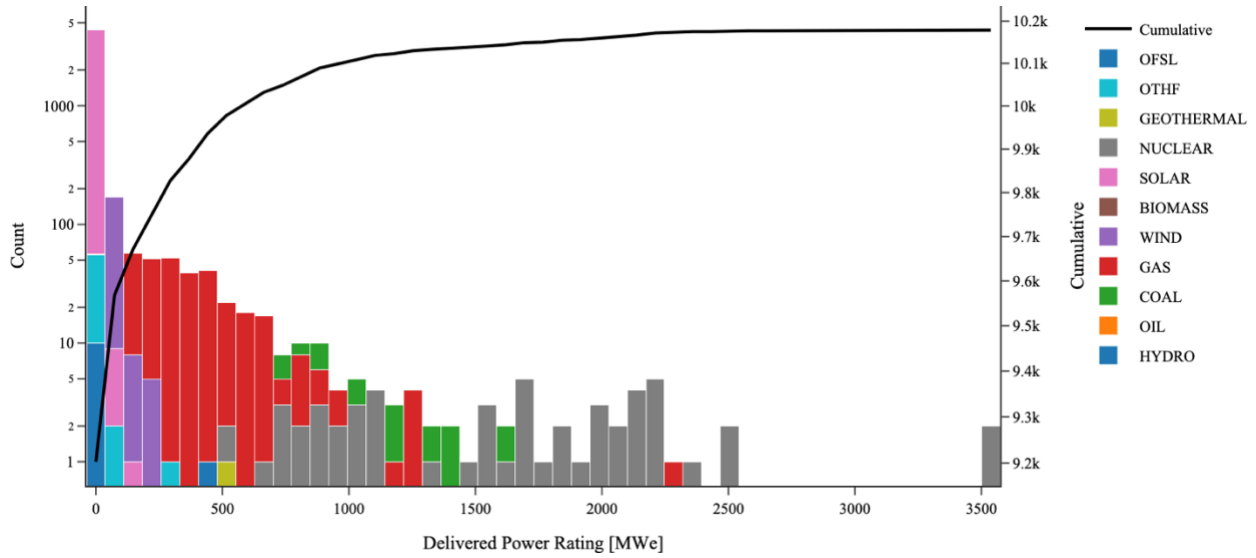


Figure 18 Power plant Counts by Delivered Power Rating for US Powerplants using 2021 data [61]

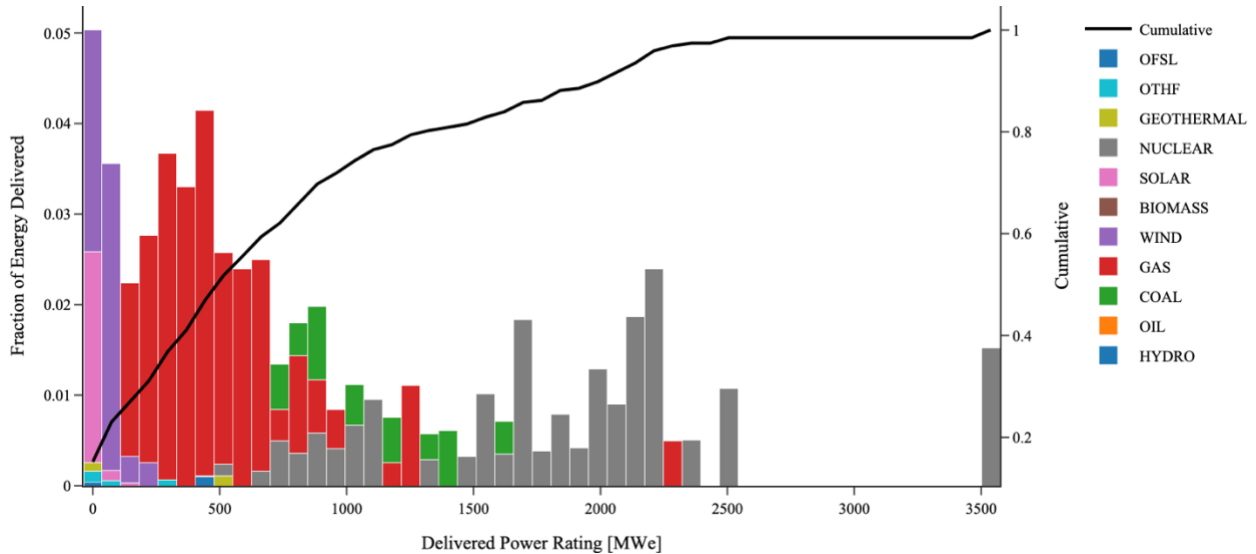


Figure 19 Total Delivered Energy by Delivered Power Rating for US Powerplants using 2021 data [61].

2.3.7.4 Transport and Manufacturability Constraint

Other considerations for reactor size are manufacturability and transportability. The latter limits RPV diameters to a little over 3 meters (rail limited, which could be relaxed), lengths to 10-15 meters, and module mass under 100 tons. Most vendors of SMRs and MMRs have picked the maximum road and rail transportable size and weight for the reactor RPV, but this is not always the case.

2.3.7.5 Safety Constraints

The limit on how high of the power rating and power density can be chosen is related to safety constraints, in particular the ability to dissipate decay heat passively while ensuring fuel integrity. Historically, power density and reactor physical dimension have been decoupled. Power ratings were set merely on the basis of peak fuel temperatures during operating conditions with active cooling. In this way, power rating was maximized regardless of the size and shape of the reactor by using a maximum power density allowed by the fuel and coolant. But, for the same reason that a large reactor is more neutron efficient than a small reactor due to low surface to volume ratio, large reactors are also less capable of dissipating excess heat during most severe conditions and as such have to rely on complex safety systems that require costly decommissioning in the aftermath.

A central idea of this thesis is that power and reactor size should be related by a passive safety constraint like that evolved by biological organisms. Power rating and power density should not be picked arbitrarily. They are constrained by safety considerations, most importantly the decay heat cooling during Beyond Design Basis Accidents. To date, LWR power density has been primarily constrained by coolant capability at operating power and a limited period during Design Basis Accident Conditions. One can relate the power and power density by solving the heat conduction equation with temperature BC, as in Equation 2-2,

$$P_{density} = \frac{k^3(T_{max} - T_{wall})^3}{P_{unit}^2} \quad 2-13$$

and substitute the relation into Equation 2-12,

$$c_{total} = \frac{c_0 P_{total}^{1-w} P_{unit}^{-1+w+s(1+2)}}{(k(T_{max} - T_{wall}))^{3s}} \quad 2-14$$

Finally, Equation 2-14 is simplified using $\beta = -1 + w + 3s$,

$$c_{total} = \frac{c_0 P_{total}^{1-w} P_{unit}^{\beta}}{(k(T_{max} - T_{wall}))^{3s}} \quad 2-15$$

We adjust Figure 17 with the safety constraint to produce Figure 20. If $\beta > 0$ (green), smaller cores and power ratings will reduce the total cost. β defines which economies dominate: economies of mass production (learning) or economies of physical scale, limited by a safety constraint. $\beta > 0$ occurs in all but the most extreme economies of unit volume. Most of the w - s space favors economies of reactor production and therefore smaller cores and power ratings will reduce the total cost. Equation 2-15 also reveals that total cost is reduced by higher thermal conductivity or higher maximum fuel temperature.

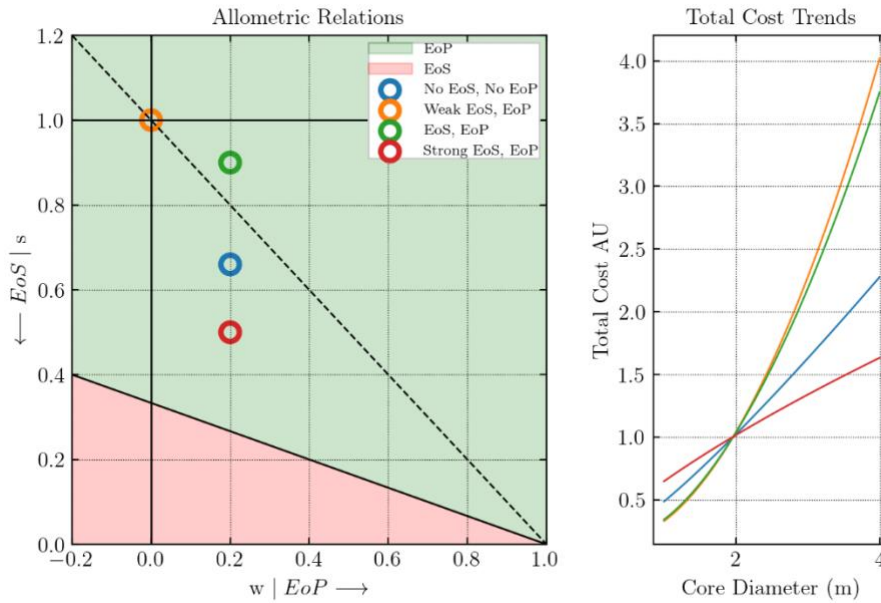


Figure 20 Relative economies affected by safety constraint relating the power and power density. Smaller core diameter is favored in all nuclear relevant economies.

The more general form of Equation 2-15, without material properties or temperature limits is given below. In this case, $\beta = -1 + w + s/\alpha$ where α is the exponent relating volume and power per unit and should be in the range 1/3 to 1.

$$c_{total} = c_0 P_{total}^{(1-w)} P_{unit}^{\beta} \quad 2-16$$

2.3.7.6 Burnup, fuel loading, enrichment

The toy model has so far addressed only the Capital costs, without considering the fuel burnup tradeoffs of smaller reactor cores. Our interest lies in the LCOE, and we now add a fuel cost component, using a simplified definition of LCOE. The reference point

is a 4m diameter core, with the CAPEX/FUEL levelized cost ratio of γ . Burnup scales with radius to some exponent ϕ , peaking at 2m. Fuel costs can be modeled as inverse of the burnup.

$$C_{FUEL} = c_F (r/r_0)^{-\phi} \quad 2-17$$

For simplicity of the model, it is optimistically assumed that there is no added or reduced cost to different refueling cycles and that OPEX per unit power is the same regardless of size. LCOE is simplified by lumping together the constants for a given financial setting and technology choice.

$$LCOE = c_0 C_{CAPEX} + c_1 C_{FUEL} + O \quad 2-18$$

Using the 2m radius reference point, and ignoring constants, we find the constants of proportionality.

$$\gamma = \frac{LCOE_{CAPEX}}{LCOE_{FUEL}} \propto \frac{c_0 P_{unit}^{(-1+w+3s)}}{c_1 (r/r_0)^{-\phi}} \rightarrow c_1 = \frac{c_0 r_0^{(-1+w+3s)}}{\gamma} \quad 2-19$$

Substituting into 2-18, we have the LCOE as function of radius,

$$LCOE(r) = c_0 \left(r^{(-1+w+3s)} + \frac{r_0^{(-1+w+3s)}}{\gamma} (r/r_0)^{-\phi} \right) + O \quad 2-20$$

which is minimized at each location in the w, s diagram as,

$$r_{min} = \phi \left(\frac{r_0^{\phi-1+w+3s}}{\gamma(-1+w+3s)} \right)^{\frac{1}{-1+w+3s+\phi}} = \phi \frac{r_0}{(\gamma\beta)^{\frac{1}{\phi+\beta}}} \quad 2-21$$

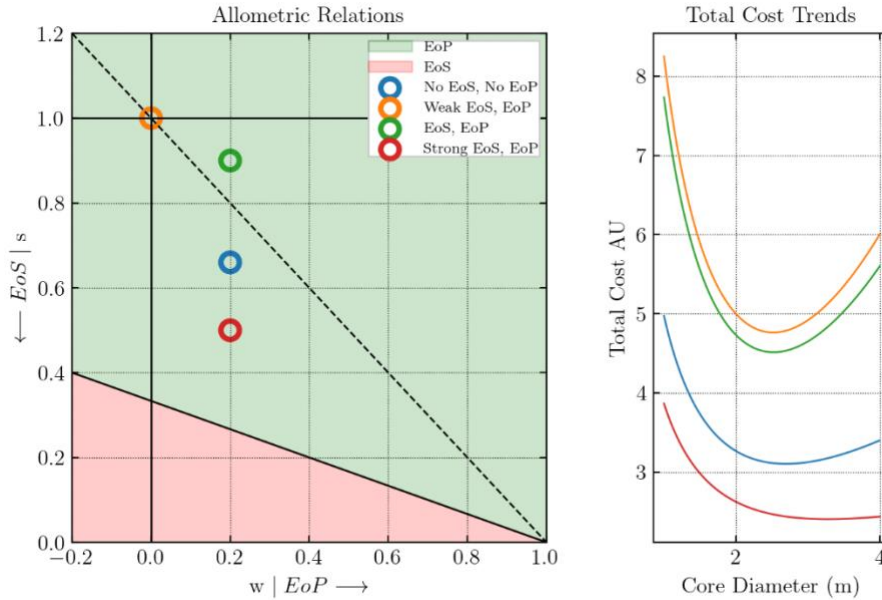


Figure 21 Relative economies affected by safety constraint and fuel utilization. Cost scaling for γ of 2 and α of 2/3.

The toy model hints at some of the design parameters' effects on cost due to economies of scale and economies of production and existence of cost minimizing designs. Because of the power density safety constraint, the radius also determines the power rating per RX. We can then generalize for all the LCOE components and utilize many more design and financial parameters. Analytical minima are no longer available. The rest of the thesis concerns more carefully determining the terms and variables for the below equation to find optimal designs.

$$LCOE(x_i) = \sum c_j(x) C_j(x) \quad 2-22$$

2.3.8 Technology down selection: Class A HTGR

Perhaps the most significant hazard in Table 4 is decay heat because the other hazards will usually lead to fission product release through decay heat – depressurization and LOCA are decay heat problems. Solving the decay heat hazard lowers the burden of solving the other problems. While the other reactor hazards are still a concern, they are secondary concerns compared to decay heat and are guarded against through other inherent mechanisms. HTGRs with passively safe power ratings can have sufficient negative temperature reactivity to deal with excess reactivity and decay heat accidents.

The remaining hazards are mitigated by the inherent characteristics of TRISO-based fuel forms, and various design choices like below grade RX and decoupled steam generators. The most distinguishing feature of the HTGR is that the RX materials allow for solid-state conduction and fission product retention, sustained to very high temperatures and with limited or no chemical reaction potential. The strategy is to avoid state change and state space expansion, keeping in mind the local environmental conditions of air, water, ambient temperature, and pressure. Alternative gases and liquids occupy a higher energy state with an enlarged thermophysical property space and potential for corrosive and energetic chemical interaction. In simpler words, non-solids tend to corrode, leak, and escape and energetically react with other core materials. The major hazards are address, but a few new accidents will have to be considered and guarded against (Appendix 10.9)

I have down selected to a Class A or Class B passively safe HTGR (CA-HTGR) and now have to decide on the remaining free parameters as the search for nuclear Corollas are performed. The free parameters include core diameter, fuel enrichment, and primary pressure. I described some of the benefits and drawbacks and discussed constraints such as the temperature, size, and material options. This defines the technology architecture within which we can design an Energy System. Fortunately, there are not that many free parameters left and many are interdependent by physical laws, engineering codes, and regulatory requirements as described in Section 3. Setting one will affect others and so we are left with an even smaller set of undetermined free parameters.

2.4 Design for Cost Opportunities

Design for Cost (DFC) encompasses all Design for X approaches such as Design for assembly (DFA), design for manufacturing (DFM), and Design for Inspection. DFC is a systems problem that considers the entire product lifecycle and the interactions of design choices with costs arising from feedstock, manufacturing, assembly, inspection, delivery, operations, and decommissioning. DFC can even include the design and qualification costs associated with the product lifecycle, though these should be ignored for sufficiently large deployments. DFC is closely tied to the overall company strategy and product execution and is especially relevant to companies aiming for significant vertical integration and supply chain management. For a commercial nuclear design, the DFC approach should aim to minimize the levelized cost of electricity (LCOE). An even more general and customer relevant metric for energy DFC would be system levelized cost of electricity (S-LCOE) or heat such as in a nuclear-wind-solar-storage hybrid grid for target geographies and customers with particular demand profiles, but that is beyond the scope of this report.

2.4.1 Motivation and Prior Work

Reactor design can take decades and combines several disciplines from nuclear core design, fuel and materials development, heat transfer, civil structures, manufacturing and construction, power generation, and grid integration as well politics and regulation. The wide-ranging disciplines, the timelines and development costs involved, and the barriers to change, combine to form a complex design process that often leads to siloed subsystem teams, and leaving little room for optimization, iteration, or integrated design, and more easily favors design by regulation, tradition, and sunk cost. Some aspects of this tortuous design approach are discussed in [62]. One-off estimates for a concept design can pigeonhole a design after just a few 2-d trade studies, usually without even considering the primary or secondary cost effects of the trades. This must change if nuclear is to address its cost and safety challenges. Many engineered products use DFC methods to lower costs, integrating manufacturing and supply chain costs with design codes.

DFA, DFM, and any Design for X approach usually requires detailed process and component design information, followed by a laborious analysis and constrained search for improved designs that reduce manufacturing cost, assembly cost, or whatever other costs can be measured and predicted. In a full DFC, all these Design for X optimizations might take place for each subsystem and component. Such a detailed analysis is beyond the scope of this project and would be the responsibility of a supplier or subsystem team. Instead, I consider a high level, low-resolution form of DFC from the system designer's perspective to calculate what LCOEs can be achieved under different cost and performance regimes. This is done through a coupled design and cost model that yields LCOEs and discussed in the next section.

Past work in cost optimization for Nuclear Power Plants exists. Any nuclear designer will attempt simple point estimates and trades from a reference design to try to improve cost or performance. This has a tendency to be a limited optimization, a painfully slow 1-dimensional hill climber that can work in sufficiently constrained design spaces.

[63] builds a bottom-up cost model for a heat pipe fast reactor concept. The study is filled with too simple assumptions on the qualitative effects of design choices on cost, without considering the possibilities of mass manufacturing, and does not attempt to explore the design space through optimization. The work is similar in intention to this thesis.

[64] adapted NGNP design concepts and EEDB benchmarked cost models to a 4-meter diameter transport constrained horizontal RPV configuration targeting lower civil works volumes to reduce capital costs by 20%. This work is highly promising in its conclusion that simply changing the reactor orientation may lead to significant capital cost reductions.

[65] optimizes systems, structures, and component (SST) fragilities of a generic NPP with and without the option of seismic isolation to reduce the capital cost. Seismic isolation allows for greater fragility and lower cost systems, which is not typically used in conservatively designed NPP. For fair comparison, the cost minimization is performed under a constrained seismic risk, computed using PRA from MASTODON. Genetic algorithms are used to explore the design space. Fragility vs cost functions are somewhat generalized functional relationships based on past data and reports from EPRI, and seismic isolation is assumed to be 10% of the nominal cost. The study finds the capital cost reduction potential of 16%, when optimizing fragilities, a further 5% when allowing for seismic isolation, and potentially more for NOAK standardization. A follow-on study [66] using industry cost estimates (which appear to largely scale with component mass) for pressure vessel, steam generator, and control rod drive mechanism under different seismic isolation requirements showed a potential factor of four to five for NOAK isolation design relative to FOAK traditional design. A simpler comparison shows that cost of an RPV with seismic capacity associated with PGA = 0.1g was 50% smaller than a 0.5 g non-isolated RPV, suggesting significant potential for NOAK cost reductions via seismic isolation. Overall, the study is a useful example of design for cost using approximate engineering calculations and cost functions. For micro reactors, seismic isolation is a lesser cost concern due to smaller masses and dimensions.

[17] analyzes the sources of cost overrun in past nuclear power plant projects, managing to identify particularly egregious cost items related to construction management. This work is limited to realized LWR designs on mega project scales, a product that is believed cannot be improved in countries like U.S. due to the inherent construction requirements and lack of scaling of the safety case to microreactors. [67] is a simple cost estimation and sensitivity analysis on micro reactors with little basis in realized designs, regulation, or design capabilities.

[62] creates a multi-objective design optimization approach using a type of genetic algorithm to find design parameters for the flash-Rankine power conversion system of the I²S-LWR and Passive Endothermic reaction Cooling System (PERCS) in a PWR. The optimization considers cost, core temperatures, and cooling longevity. The paper includes several past studies where nuclear subsystems were optimized using similar approaches and sensitivity analysis.

[68] uses genetic algorithms to optimize a multi objective function for a fast gas reactor. Objectives include power conversion efficiency, breeding efficiency, peaking factors, and fuel burn up, with somewhat arbitrary weights. To tackle the computing scale issues associated with the neutronic calculations, the authors execute MCNP runs on a limited set of parameters, then compute multivariate regressions, and then use the fit to compute results for new parameter sets determined by the genetic algorithm. Presumably, this can be iterated. The paper is like many of the system optimization work previously reported except they also include thermohydraulic and power conversion cycle objective functions. In computing the multivariate regression, the authors are trying to find the cost derivatives and searching for improved solutions. The model's knobs are limited, and the arbitrarily weighted objective function is not particularly useful and clearly related to leveled costs.

In [69], HX designs were cost-optimized using lifetime cost using various capital and operating cost estimates based on the power and mass. Operating costs were treated as pumping power multiplied by electrical energy costs. Not included are system costs associated with larger HX (PV, support, transport) and or larger pressure drops (circulator knock-ons, etc.) and how these costs may be dwarfed or amplified in a full system.

Overall, many researchers have considered the importance of cost metrics in design, but have typically modeled cost in simplistic ways, without accounting for knock-on effects and design parameter interactions or considering the final LCOE. While this work is far from complete in its simplistic handling of various design parameters, it does provide a step towards a sufficiently complete design and cost model coupling with useful LCOE trends for design choices.

2.4.2 Code Architecture

The DFC approach shown in Figure 22 couples design and cost models to minimize an overall cost metric or at least observe the general design trades and how they affect the cost metric, in this case LCOE. In the design model, a minimal set of input parameters, for example Table 38, is used to estimate a broader set of design parameters using engineering codes, scaling laws, conservation laws, and reduced order models listed in Table 6. To the maximum extent, design calculations are simplified, linearized, and reduced. The full design parameter set is then used by a cost model to determine LCOEs. In this way, I can observe the effect on LCOE of simple changes in design parameters or conditions. I order the solutions to first find the design parameters and then solve for cost parameters. The order of calculations is determined by availability of intermediate variables needed for each calculation. For example, design calculations occur before cost estimates because the cost estimates use design parameters. Similarly, some design estimates can only be computed using other intermediate design parameters.

Model inputs define a world's financial and physical framework. This includes interest rates, inflation, material costs, reference design and base cost data, performance factors, and others. Cost parameters have an associated reference date and inflation type so that they can be inflated to other dates. Model inputs should not change when evaluating multiple designs so that comparisons can be more easily made within a given world. Model inputs can be changed to study the sensitivity of a design in different worlds such as higher interest rates or reduced wages.

2.4.3 Use Modes

The code can be used for single evaluations of specific design or to explore the search space through 1D and 2D sensitivity, grid evaluation, or constrained optimization.

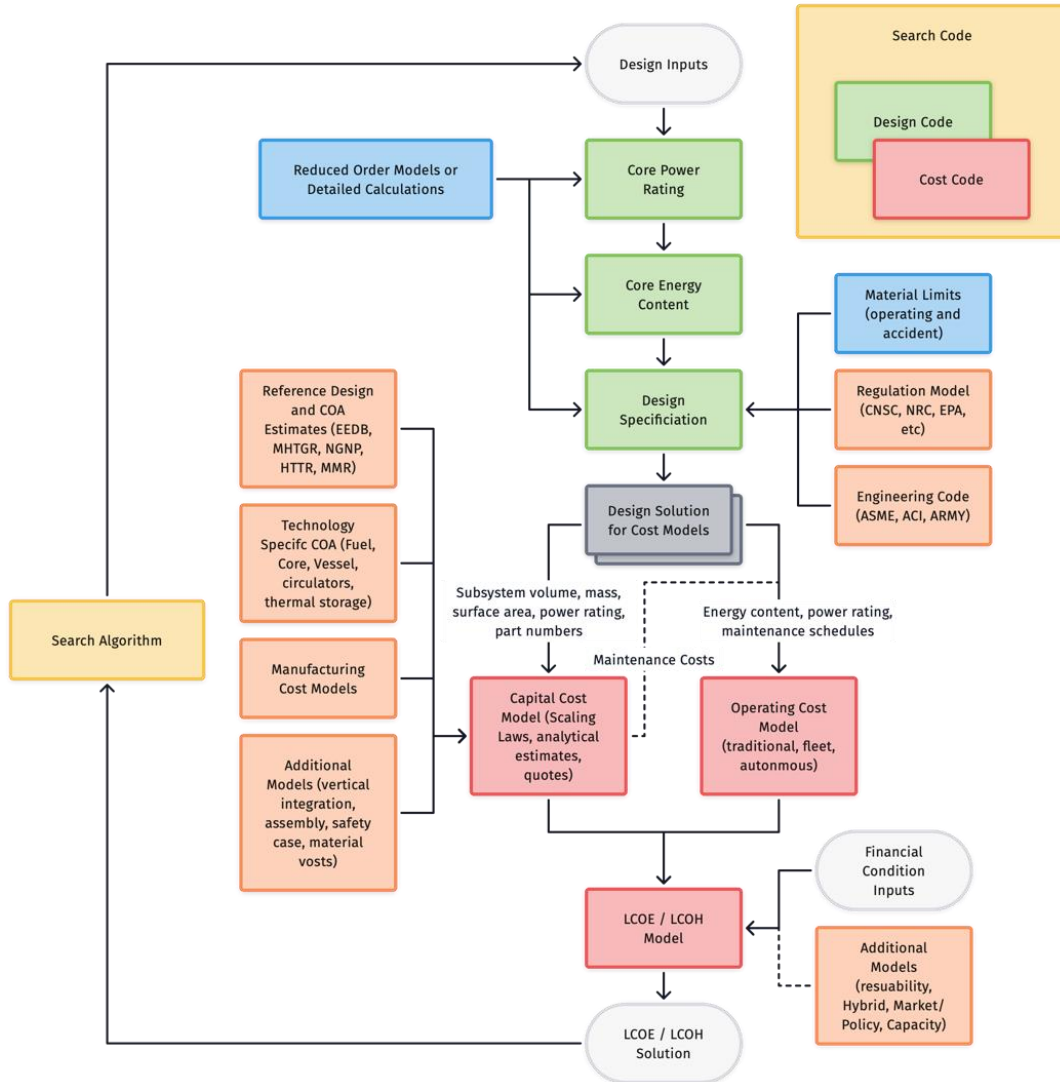


Figure 22 Code Architecture

3 Design Code

The reactor Energy System (ES) or powerplant typically consists of a below-grade nuclear reactor vessel with a number of reactors (RXs), coupled to a Balance of Plant which may consist of a number of intermediate loops, thermal storage systems, coolant purification systems, pressurizers, and ultimately a number of turbines and heat rejection systems. These are all housed in buildings on a plot of land. The following methods specify the design parameters.

3.1 Approach

With the goal of quick comparison of hundreds of thousands of designs in the HTGR architecture without significant compute resources in mind, it is recognized that many reactor subsystems require significant design and optimization studies to achieve high performance characteristics for given reactor conditions. For example, what is the optimal HX definition for two fluids and temperature drops and for a particular manufacturing capability and material? Do you seek the lowest mass, or the lowest pumping power? What heat exchanger technologies are available for the given fluids, temperatures, and pressures in question? What alloy or materials are available? Or, what is the “best” core design for a given core volume and shape, fuel enrichment, and moderator? Is it the core design that maximizes energy content or average burnup or peak burnup? How thick should the reflector be to balance leakage (and vessel/cavity activation) and active core volume? These are computationally intensive studies usually done by experts of one sort or another.

The code architecture has room to allow both computationally intensive estimates and reduced order estimates. The generalizability sought in the design methods. In the near term, performance is estimated using reduced order models. The same architecture can incorporate external thermo-physical computational tools like Serpent to better estimate the performance capabilities. Maintaining a large design space and aiming for low computation prevented the use of higher fidelity models.

The design code must sufficiently specify the energy system design so that I can estimate costs. An example input is provided in Appendix 10.1 while Table 6 summarizes the design methods which are described in the rest of this section. Material data is crucial to many of the estimates, and thermal property data were added to Alexandria, a material library from USNC (see Appendix 10.4) to accommodate a wide range of possible fuels, moderators, fuels, and relevant RX materials.

3.1.1 Reduced order models with parameter specific adjustments

Building detailed calculations to design and size various components proved to be an exceedingly laborious endeavor with too high uncertainty. For some estimates, insufficient fidelity was adopted to match supplier estimates or match existing designs and performance. Design parameters for components like a HX require significant and detailed optimization to approach reasonably adequate results with wide variation between the HX technologies, the design methodologies, and the manufacturer.

As such, several simple approximations and scaling laws for design parameters were adopted. These scaling laws can eventually be replaced with more detailed and reliable design calculations. The general form of the scaling law is shown below. Where needed, publicly available reference design data from MMR or HTTR, the most relevant designs for this study were utilized. The exponent of the scaling law can have a physical basis or comes from a fit of available data.

$$x_1 = x_0 \left(\frac{y_{1,i}}{y_0} \right)^{c_i} \quad 3-1$$

In other cases, physical models were used to estimate physical parameters of the design. Heat transfer and thermal hydraulic solutions were used to solve the power rating and pressure drop. Similarly, engineering codes were applied to estimate component dimensions such as a pressure vessels parameters or vessel support structures.

3.1.2 Incorporating external tools

If desired, each design parameter can be computed by calling an external code from python. For example, a core could be defined with particular neutronic and thermal hydraulic definitions, and the power profiles and burnups could be evaluated externally. Similarly, more detailed time-dependent thermal solutions could be computed to determine the maximum allowable power rating. Or one might replace the HX design approximation with a detailed heat exchanger design solver for different types of fluids and heat exchanger technologies.

3.1.3 Applicable Codes

Where possible, the ASME and ACI sections or the regulations from NRC, CNSNC, and EPA were referenced, though they have certainly fallen short of the intended detail in this report.

Table 6 Design Estimate summary.

Group	Design Parameter	Inputs	Estimate Method
Thermal hydraulics	Mass Flow Rates	RX Power, Temperatures, fluid properties as f(T, P)	Energy Conservation
Thermal hydraulics	Pressure Drops and coolant volume fraction	Pressure, mass flow, reactor dimensions, minimum channel size, performance factor	Correlations, velocity limited, conservation of flow area
BoP	Electrical power, reject heat, number of reactors	Thermal power, efficiency, RX Power	Energy Conservation
BoP	Loop Nodes and Connections	Branching parameters	Energy Conservation
BoP	Power Conversion Enclosures and Footprint	Equipment dimensions and clearance	Geometric considerations
BoP	Cycle efficiencies and energy available	Fluid temperatures and turbomachinery efficiencies.	Reference estimates and TD considerations
BoP	HX/Circ Enclosure and Footprint	Equipment dimensions and clearance	Geometric considerations
UNF	UNF Wet Storage Pool Volume and Area	Power density, burnup (not incl)	Decay heat and Geometric considerations
UNF	UNF Dry Storage Pool Volume and Area	Rate of production	Decay heat and Geometric considerations
RX	# of Control Rods or Drums	Cross sectional area of core, neutron path length (not incl)	Geometric considerations
RX	Enclosure and Footprint	Equipment dimensions and clearance	Geometric considerations
RPV	RPV Parameters (volume, thickness, mass)	Pressure, core diameter, aspect ratio	ASME S3 D5, D8
RPV	RPV Lifetime	Internal energy generation limit from baseline	Linear.
RPV	Core Barrel Volume, thickness, mass	Core dimensions, cross sectional flow area (not incl)	Structural and geometric considerations
HX	HX Size and Mass	Primary and secondary flow rates, temps, and v, HX type and material	Correlations
HX	Pressure Drop	Geometry and fluid conditions	Correlations
Circulator	Pumping Power	Pressure drop, pressure, temperatures, fluid properties as f(T, P)	Pumping Power
Circulator	Size and Mass	Pumping power, pressure, velocity	Correlations
Moderator	Moderator Lifetime	Not incl	Not incl
Fuel	Burnup	Baseline design point from MMR, enrichment, gain	Linear w/ enrichment and diameter, w/ max threshold.
Fuel	Core Energy Content	Baseline design point from MMR.	Linear w/ burnup and fuel loading.
Fuel	Fuel Loading	Burnup and core energy content	Energy Conservation
Fuel	Refueling Cadence	Core energy content, RX power rating, capacity factor	Energy Conservation
Fuel	Core Mass	Fuel moderator ratio, fuel mass	Volume and mass conservation
System	Capacity factor	Refueling interval, outage	Time Conservation

3.2 Core Energy Content

The Core Energy Content model shown in Figure 23 determines the extractable energy of a given core. The inputs define what and how much material are available, and the model determines how much energy can be extracted from the fuel.

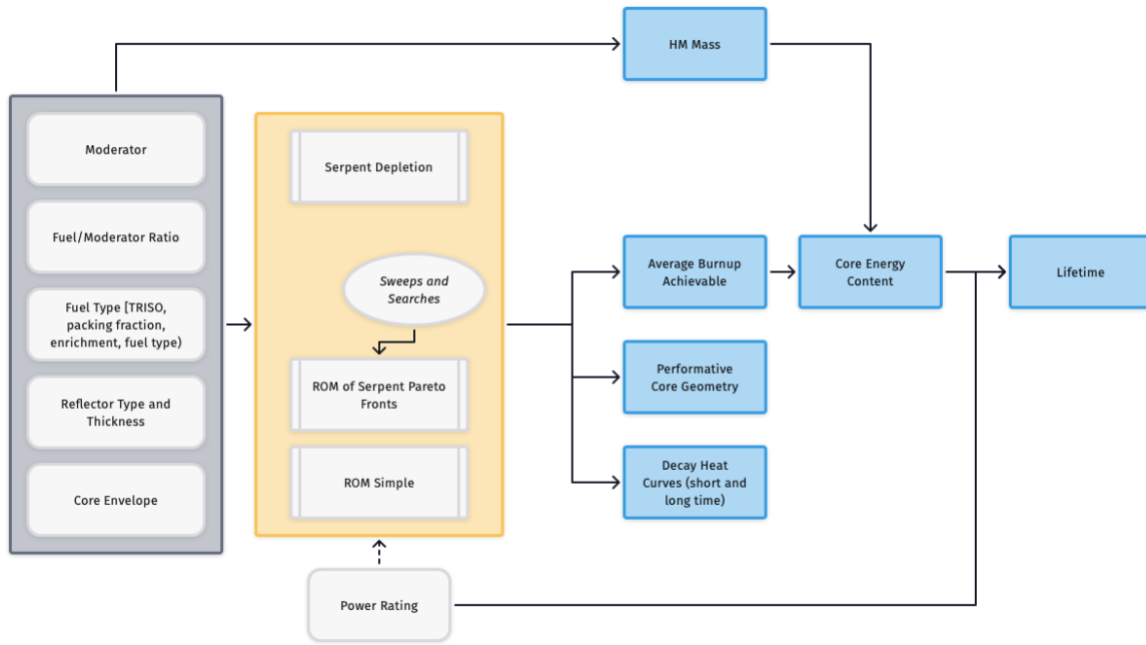


Figure 23 Core Energy Content Model

The core is defined by the fuel and moderator choices, the core dimensions, the reflector thickness, and the fuel loading in terms of the fuel specification and fuel moderator ratio. These inputs bound the core design space in which the designer can tune the heterogenous geometry made up of coolant channels, pin shapes and dimensions, moderator shapes and dimensions. A core energy content model should produce the average burnup of the fuel. The initial inputs determine the HM mass loading, and I can then find the core energy content. Because the burnup is affected by fuel operating temperatures, a neutronic and thermal hydraulic coupling is needed to accurately estimate burnup. The power rating is also needed to estimate the lifetime of the core in years.

With a given set of inputs, the core design tuning can result in a wide range of performance attributes with various trades and effects on downstream costs. It is assumed here that the arrangement of core materials has no effect on the core cost – in other words, that 1000 fuel pins will cost the same as 10000 fuel pins if they are made of the same amount of fuel. In this way, the model only has to produce the maximum burnup achievable for the given materials. Some of the knobs at a designer’s disposal include radially varying fuel enrichments, pin shapes and arrangements, moderator path lengths, and the placement of burnable poisons. This is on top of the given inputs of fuel and moderator choice, core shape, etc. And the fuel choice can include variable packing fraction and different TRISO particle kernels and layers. Ideally, I would have a robust core design optimization and burnup estimator to build a model that can handle a wide variety of inputs and produce the maximum burnups, even accounting for the chosen power rating. The first steps along this path are given in Appendix 10.14, but this was not achieved in this thesis.

Instead, this work defined a ROM for burnup approximated as linear with enrichment and diameter up to a maximum burnup allowed by the fuel and at a fixed fuel moderator volume ratio. The reference burnup value was for the USNC MMR. Obviously, this does not capture temperature effects, fuel-moderator ratio effects, and non-linear effects at low diameter cores. A sample of ROM outputs for different fuel kernels, enrichments, and core diameters is shown in Figure 24.

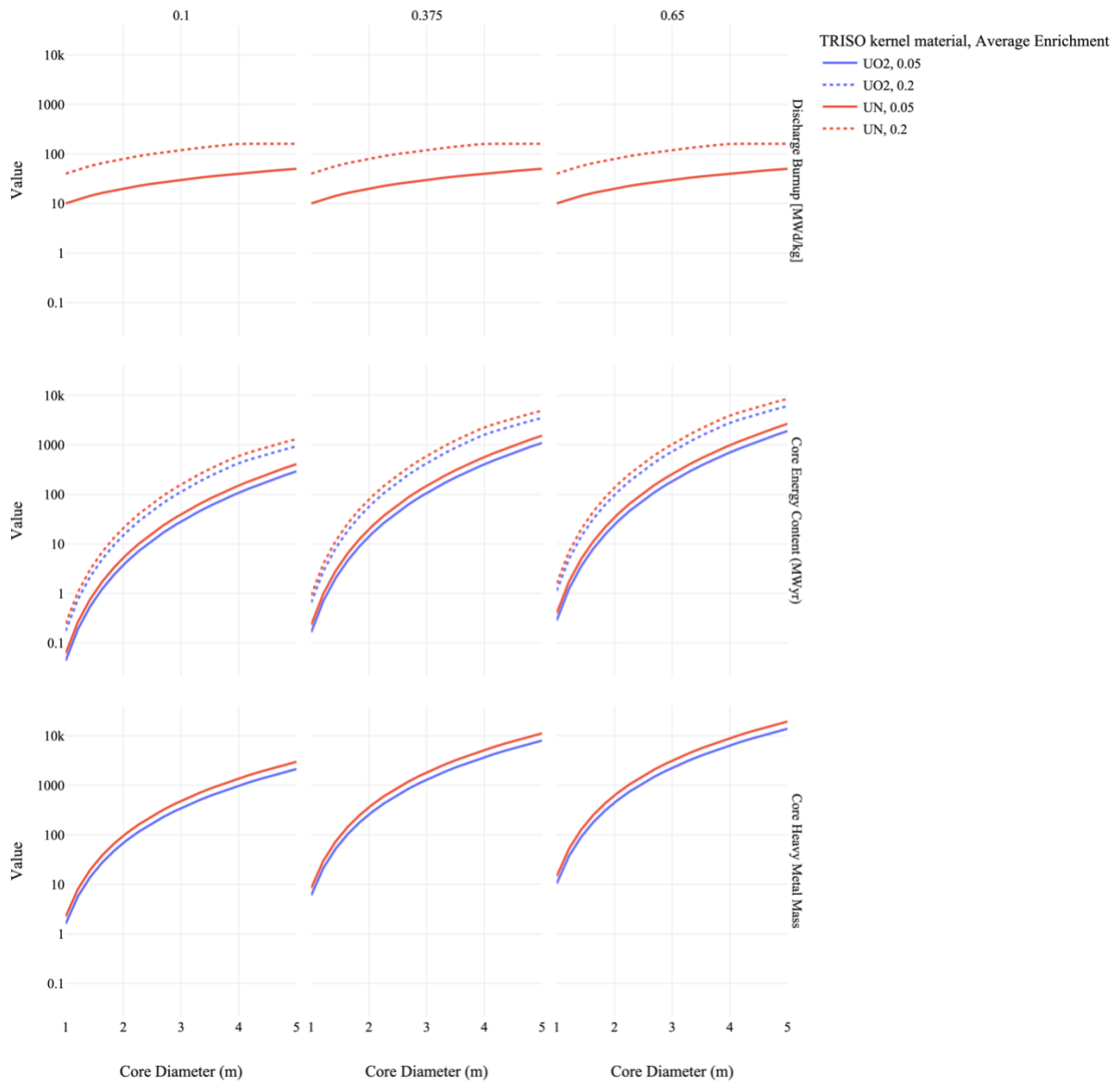


Figure 24 Core Energy Content ROM for graphite moderator and 10% fuel volume fraction. Column shows the packing fraction.

3.3 Power Rating

The power rating is selected based on safety system configuration. For an active safety design, the power rating is set to a maximum fuel power density, and it is assumed that an emergency core cooling system, RCCS, or active cooling system will be used. In passive safety designs, power rating is selected so that maximum temperatures are not exceeded in the core. In the simplest case, I make no assumption on the engineered solution for passive cooling and simply use a heat transfer from the surface using radiation and natural convection and assume the environment remains at constant ambient conditions. Power density is still limited by the maximum fuel power density. The power rating can be set to a user defined power rating. While GRSAC [70] can provide an alternative solution with higher fidelity and more accident scenarios prismatic cores, I wanted something simple, fast, and customizable.

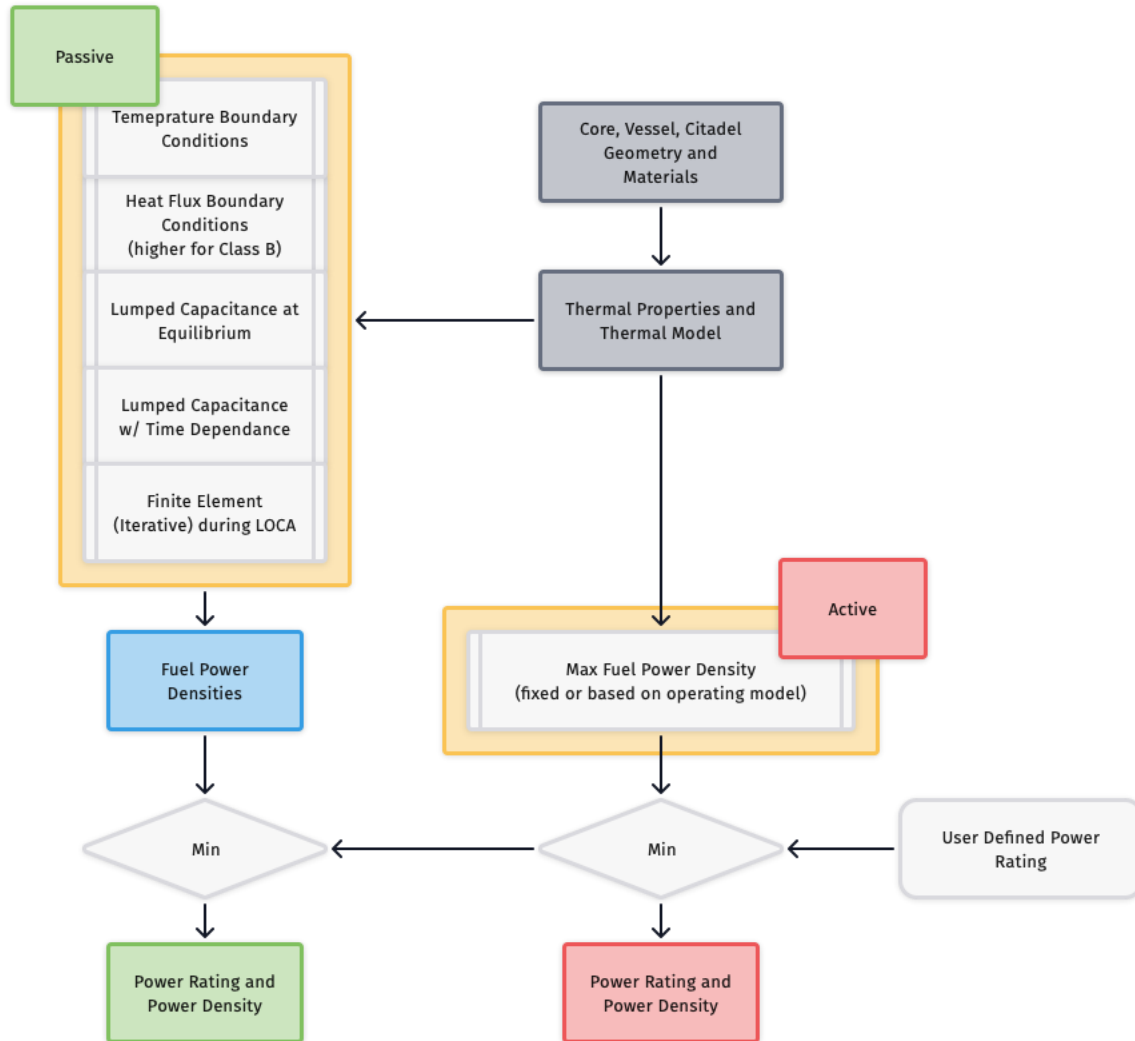


Figure 25 Power rating ROM

3.3.1 Maximum Fuel Power Density

Depending on the fuel, moderator, and coolant configuration, the fuel can be run at different power densities while avoiding maximum thermally induced stresses and absolute temperatures. The maximum absolute temperature can be limited by the fuel's failure temperatures. Higher temperatures will tend to reduce the fuel's achievable burnup. In the Passive Safety designs discussed in this report, maximum fuel power density is never reached and is not of immediate concern. Thermally induced stresses and absolute temperatures can be reduced by fuel and TH design, for example by reducing the thermal resistance between the fuel and coolant.

Very small cores and cores built with active safety systems may seek to operate at a fuel's performance limit. To capture this intention with a stress model or iterative TH model, a maximum allowable fuel power density of 100 W/cc is set as constraint (similar to PWR fuel but ~20 times greater than conventional HTGRs). In a more useful model, the fuel power density would be increased until any of the following are reached: maximum fuel temperature gradient or thermal stress, maximum fuel or fuel layer temperatures, or performance limits of any other component temperatures like the moderator or moderator clads. The design could be iterated with changing component dimensions and TH characteristics.

3.3.2 Passive Safety Power Rating

Ordinarily, and as outlined in the previous section, the power rating is a coupled thermal-neutronic problem that affects the core energy content and power rating simultaneously. However, the passive cooling power constraint severely limits the core and fuel power density well below the performance limits, such that I can, at least for exploration purposes, ignore the possibility of exceeding thermal stress limits and temperatures in the fuel during operations. This can change if the fuel volume fraction is particularly high, thereby increasing the fuel power density for the same core power density.

In general, the power rating will be picked so that materials do not exceed their maximum tolerable temperature during the most extreme accident using only passive means. The most extreme accident considered is LOCA in which the decay heat is transferred radially out of the core through the core barrel and RPV into the reactor chamber which is fixed at a certain environment heat sink temperature. The maximum tolerable temperature can be defined in various ways, but I take some prototypical values for the various materials such that the systems are likely to be reusable after the accident rather than fail permanently during the accident, even if it does not lead to fuel melting.

For either spheres or infinite cylinders, there is high degree of symmetry allowing for a 1-d estimate of the heat transfer. The core conduction and the heat flux are coupled at the boundary condition that depends on the RPV wall temperature and heat sink temperature. Natural convection heat transfer coefficients are defined below. Radiative heat transfer is assumed to take place from the RPV to a fixed ambient environment. To differentiate between passive Class A and Class B, a different heat transfer coefficient h based on an engineering judgment of available natural convection coefficients in the literature is assumed. Table 7 reports the functions and assumptions. The RPV wall temperature is the free parameter used to determine the power and core centerline temperature. I maximize power, constrained by the peak material temperatures. This decay heat power is then converted to the operating power level.

This approach will tend to be conservative estimate of the max power, lacking time and heat capacity dependence and assuming a constant decay heat load of 6.6% of operating power, but is favored by a fixed environment condition. Overall, it provides a quick estimate with reasonable behavior, consistent with the power rating of a 15-30 MWth MMR.

Figure 26 reports the power rating estimate for each safety class and two aspect ratios. For passive systems, we see that power density is the maximum power density at small diameters, but otherwise decreases with diameter. For Class A reactors in the diagram, power is limited first by the heat flux BC and then by the maximum temperatures. The transition depends on the max fuel temperature. For Class B, power is limited only by the maximum temperatures. Total core power increases despite falling power density across all safety classes. We see that high and low aspect ratio cores have the same power densities and surface area to power ratios, but high aspect ratios pack more total power. Increased fuel temperature capability, as shown by each column, increases the transition diameter between and active and passive power density. Note that core power density increases for the active safety case because increasing diameter for constant thickness reflector results in a larger active core relative to the total core.

Table 7 Core conduction and surface heat transfer equations.

	Sphere	Cylinder (inf)
Core Conduction to RPV	$\dot{Q} = V (T_{core} - T_{wall}) \frac{6k}{r^2}$	$\dot{Q} = V (T_{core} - T_{wall}) \frac{4k}{r^2}$
RPV Surface Heat Flux BC	$\dot{Q} = 8\pi k(T_{core} - T_{wall}) r$	$\dot{Q} = 4\pi k(T_{core} - T_{wall}) rL$
	$\dot{Q} = A_s \left(h(T_{wall} - T_{inf}) + \sigma \varepsilon (T_{wall}^4 - T_{inf}^4) \right)$	
	Class A: $h = 5 W/m^2K$	
	Class B: $h = 100 W/m^2K$	
	$T_{inf} = 300K$	
	General Limiting Temperatures	
	- Core: 1600 °C	
	- RPV: 643 °C	
	- Concrete: 100 °C	

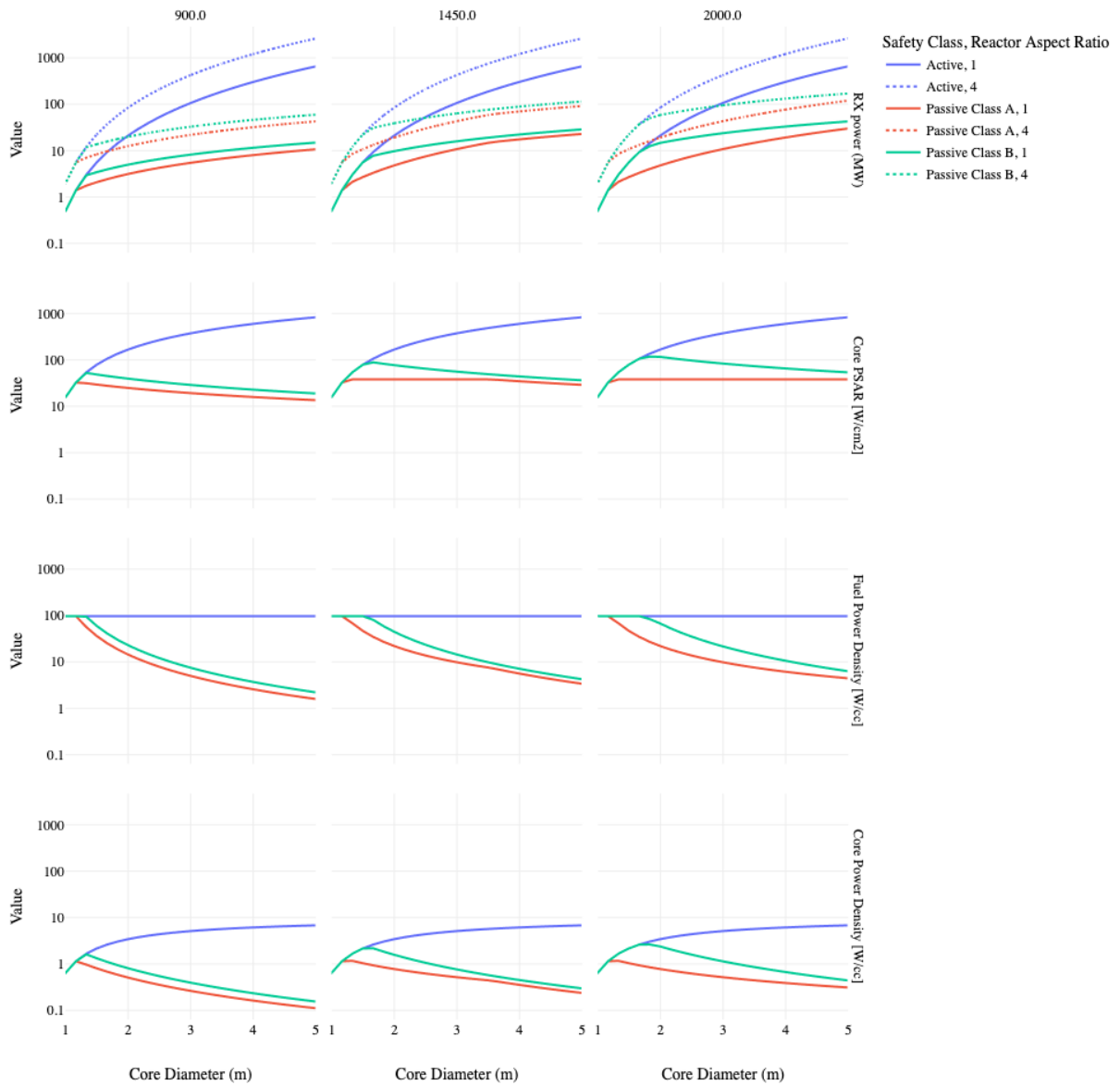


Figure 26 Power Rating ROM samples for different safety class and aspect ratios. Each column is a Maximum fuel temperature in K.

3.3.3 Other Power Rating Estimates

Other power rating estimates for maximum allowable power rating are described below and modeled but generally not used in the used in the evaluations unless specified.

3.3.3.1 Equilibrated Lumped Capacitance

Adiabatic conditions for the citadel and 1 meter layer of bedrock with initial condition defined by the operating conditions are assumed; namely operating core and RPV temperatures and ambient temperatures for the air, concrete, and bedrock. The decay heat is then distributed for the first 20 days across the entire lumped capacitance.

$$T_2 = \frac{\int_{t_1}^{t_2} P_{decay}(t) dt}{\sum m_i c_i} + T_1 \quad 3-2$$

with T_1 as the mass averaged temperature of the system at operating conditions. The bedrock and concrete would be at ambient temperatures, while the vessel and core components are at operating temperatures. Substituting the decay power with a simple decay heat curve,

$$\int_{t_1=0}^{t_2} 0.0622 P_0 (t^{-2} - (t_0 + t)^{-2}) dt = 0.0622 P_0 \left(\frac{5t_2^{\frac{4}{5}}}{4} - \frac{5(t_0 + t_2)^{\frac{4}{5}}}{4} \right) \approx 0.0622 P_0 \left(\frac{5t_2^{\frac{4}{5}}}{4} \right) \text{ for large } t_0$$

$$T_2 = \frac{0.0622 P_0 \left(\frac{5t_2^{\frac{4}{5}}}{4} \right)}{\sum m_i c_i} + T_1 \quad 3-3$$

$T_2 = \min (T_{max,i})$ is assumed, which is the lowest of the set of max tolerable temperature of the i materials, and then solve for P_0 to get the power rating determination shown in Equation 3-4. t_2 is set to the desired coping time. In this isometric scaling, there is no advantage to greater thermal conductivity. It is a lower bound on the power rating as it assumes homogenized temperatures and no thermal losses to the environment. The model is most relevant for cases where the failures occur at long times, such as a well-insulated concrete enclosure with minimal decay heat cooling capability. Figure 27 shows the power ratings for the case of 72-hour coping time. Comparing Figure 27 and Figure 26 suggests that the thermal capacity can be less limiting than conduction and heat transfer, at least for the geometries and materials evaluated and the specific thermal mass included with adiabatic BC. It is noted that the adiabatic boundary condition is overly conservative and not realistic. The power constraint is defined by the limiting temperatures in non-core materials and defines a non-nuclear accident.

$$\dot{Q} = \frac{(T_{max} - T_1) \sum m_i c_i}{0.0622 \left(\frac{5t_2^{\frac{4}{5}}}{4} \right)} \propto (T_{max} - T_1) \sum m_i c_i \propto r^3 \quad 3-4$$

The designer can increase the coping time by enlarging the mass of equilibrated material with heat transfer expanders in the bedrock or surrounding the core with cheap and high heat capacity materials like graphite. This equilibrated model shows a steep penalty for larger cores that are essentially thermal storage in the form of materials at elevated temperature. When cooling is lost, that stored energy spreads to the rest of the reactor cavity. Larger cores and higher operating temperatures increase the energy stored relative to the total RX system mass including the concrete and surrounding bedrock as illustrated in Figure 27.

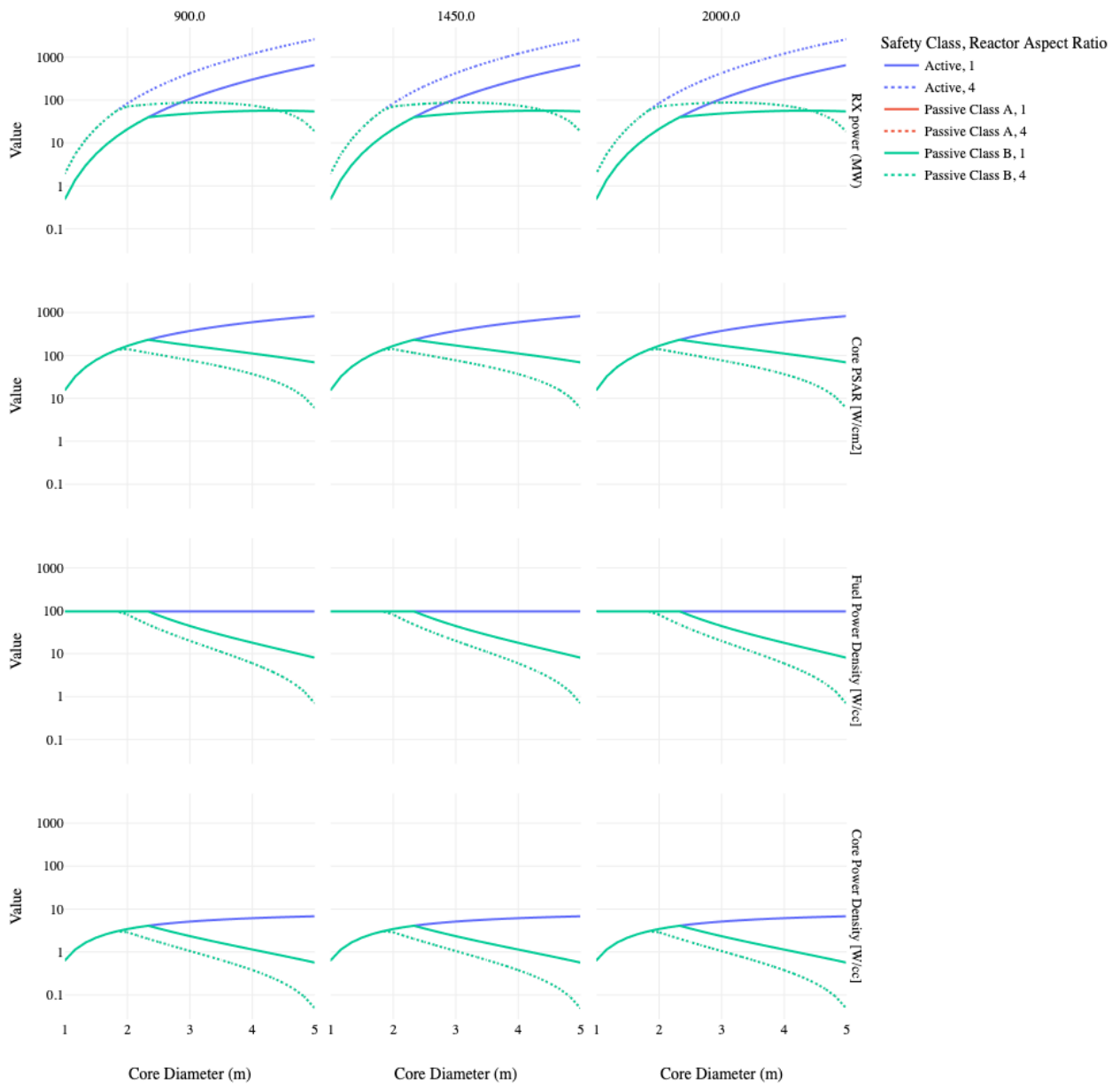


Figure 27 Power rating for equilibrated Lumped Capacitance at 72 hour coping time. Columns are for different max fuel temperature in K, and rows give different design parameters. Maximum fuel temperature has no effect as the limiting component is the civil structure concrete, in this case 550 K. The fuel volume fraction is 0.1.

3.3.3.2 Lumped Capacitance w/ Time Dependence

Core, CBA, RPV, and concrete are configured as lumps of different materials at different initial temperatures connected by heat transfer interfaces, stepping through time. The heat transferred between adjacent lumps using energy conservation with the heat capacity is calculated to find the new temperature at each node as in Equation 3-5. An adiabatic boundary condition is used on the outside node and a standard decay heat power source on the internal core node. I do this for each time step. For either spheres and cylinders, the heat transfer between layers for radiation, conduction, or convection are assessed. All heat transfer relations are from [71]: radiation on p.833, conduction on p.136 Table 3.3. Solid to solid interfaces experience conduction only. Gas separated surfaces have convective and radiative heat transfer. Each layer can be subdivided to improve the model fidelity. The energy balance is computed as below with a sample result in Figure 28. The solver I developed was slow compared to the previous methods, and not reliably stable across the different core configurations.

$$\Delta E = (\text{mean}(Q_{\text{out},t}, Q_{\text{out},t-dt}) - \text{mean}(Q_{\text{in},t}, Q_{\text{in},t-dt})) * dt = -m * c_p * (T_t - T_{t-dt})$$

3-5

Table 8 Heat transfer ratios for lumped capacitance model.

Mode	Cylinder Vertical	Sphere
Radiation	$q_{12} = \frac{\sigma A_1 (T_1^4 - T_2^4)}{\frac{1}{\varepsilon_1} + \frac{1 - \varepsilon_2}{\varepsilon_2} \left(\frac{r_1}{r_2}\right)}$	$q_{12} = \frac{\sigma A_1 (T_1^4 - T_2^4)}{\frac{1}{\varepsilon_1} + \frac{1 - \varepsilon_2}{\varepsilon_2} \left(\frac{r_1}{r_2}\right)^2}$
Conduction	$\frac{2\pi L k \Delta T}{\ln\left(\frac{r_2}{r_1}\right)}$	$\frac{4\pi k \Delta T}{\left(\frac{1}{r_1}\right) - \left(\frac{1}{r_2}\right)}$
Convection	$\dot{Q} = h A_s (T_1 - T_2) = k \text{Nu} A_s \frac{T_1 - T_2}{L_c}$	

Table 9 Heat transfer correlations for different layers in Lumped Capacitance Model

Geometry and conditions	Nusselt	Conditions
Vertical Rectangular Cavities Low Aspect ratio	$\overline{Nu}_L = 0.22 \left(\frac{Pr}{0.2 + Pr} Ra_L \right)^{0.28} \left(\frac{H}{L} \right)^{-1/4}$	$\left[\begin{array}{l} 2 \lesssim \frac{H}{L} \lesssim 10 \\ Pr \lesssim 10^5 \\ 10^3 \lesssim Ra_L \lesssim 10^{10} \end{array} \right]$
	$\overline{Nu}_L = 0.18 \left(\frac{Pr}{0.2 + Pr} Ra_L \right)^{0.29}$	
Vertical Rectangular Cavities Larger aspect ratio, low Ra	$\overline{Nu}_L = 0.42 Ra_L^{1/4} Pr^{0.012} \left(\frac{H}{L} \right)^{-0.3}$	$\left[\begin{array}{l} 1 \lesssim \frac{H}{L} \lesssim 2 \\ 10^{-3} \lesssim Pr \lesssim 10^5 \\ 10^3 \lesssim \frac{Ra_L Pr}{0.2 + Pr} \end{array} \right]$
	$\overline{Nu}_L = 0.046 Ra_L^{1/3}$	
Vertical Rectangular Cavities Large aspect ratio, high Ra		$\left[\begin{array}{l} 10 \lesssim \frac{H}{L} \lesssim 40 \\ 1 \lesssim Pr \lesssim 2 \times 10^4 \\ 10^4 \lesssim Ra_L \lesssim 10^7 \end{array} \right]$
Concentric Horizontal Cylinders	$q = \frac{2\pi L k_{\text{eff}} (T_i - T_o)}{\ln(r_o/r_i)}$ $\frac{k_{\text{eff}}}{k} = 0.386 \left(\frac{Pr}{0.861 + Pr} \right)^{1/4} Ra_c^{1/4}$ $L_c = \frac{2[\ln(r_o/r_i)]^{4/3}}{(r_i^{-3/5} + r_o^{-3/5})^{5/3}}$	$Pr = \frac{\mu c_p}{k}$ $Ra_L = \frac{g \beta (T_1 - T_2) L_c^3}{\nu^2} Pr$ μ [kg/m-s] Dynamic Viscosity k [W/m] Specific Conductivity of fluid c_p [J/kg-K] Specific Heat Capacity of Fluid L_c [m] = Characteristic Length = Distance between hot and cold surfaces T and T [C] = Temperatures of hot and cold surfaces respectively ν [m ² /s] = Kinematic viscosity of fluid β [1/K] = Coefficient of thermal Expansion of fluid (1/Temp [K] in ideal gas) $\alpha = k$ [m ² /s] = Thermal diffusivity
Concentric Spheres	$q = \frac{4\pi k_{\text{eff}} (T_i - T_o)}{\left(\frac{1}{r_i}\right) - \left(\frac{1}{r_o}\right)}$ $\frac{k_{\text{eff}}}{k} = 0.74 \left(\frac{Pr}{0.861 + Pr} \right)^{1/4} Ra_s^{1/4}$ $L_s = \frac{\left(\frac{1}{r_i} - \frac{1}{r_o}\right)^{4/3}}{2^{1/3} (r_i^{-7/5} + r_o^{-7/5})^{5/3}}$	

Decay Heat

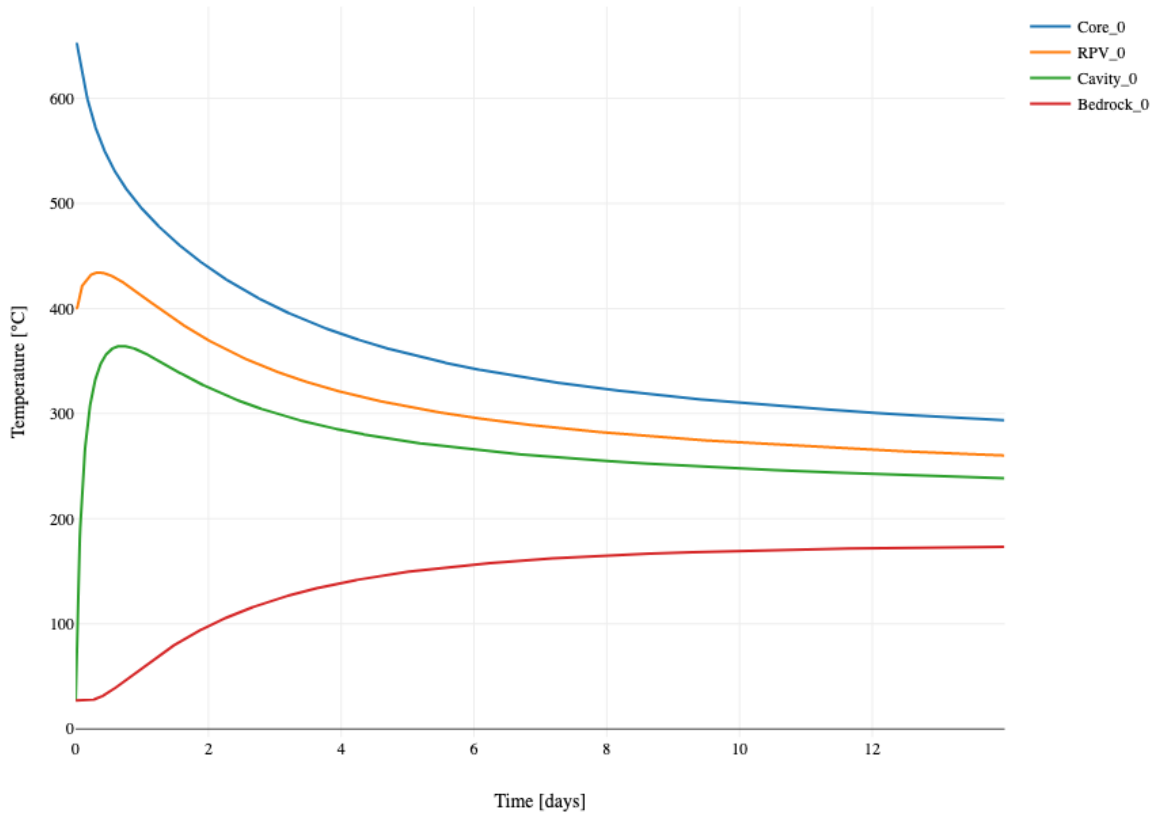


Figure 28 Lumped capacity ROM for a prototypical micro reactor core during passive decay heat cooling.

3.3.3.3 Finite Difference

A final approach to the power rating estimate was to iterate on the results of a finite difference scheme that considers only the core, core barrel and pressure vessel while fixing the ambient temperatures and heat sink in a similar approach as [72]. This ignores the concrete enclosure and volumes and assumes a constant temperature heat sink around the reactor. I solved unsteady 1-d heat equation by finite differences within the reactor with a non-linear boundary condition at the reactor to cavity interface. This was done for a cylindrical and spherical geometry and a sample result is shown in Figure 29. Details on the scheme's implementation are given in Appendix 10.12.

The solution involves an initial estimate of the power rating using a faster method from the previous sections. I then iterate on the finite difference result until I achieve the maximum allowable temperature in any component. The solver was significantly slower than the simpler approaches previously described and was generally not used to determine the power rating.

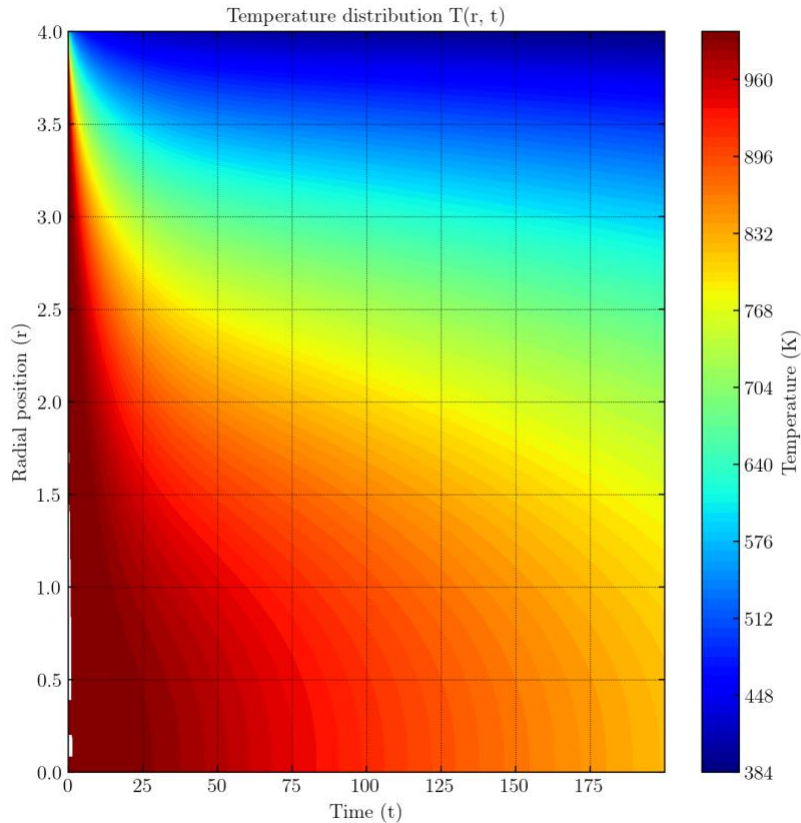


Figure 29 Finite difference example for unsteady heat equation in cylindrical geometry with decay heat power density. Time in hours.

3.3.4 Note on Reactivity Insertion

The power rating estimate used in this code (Section 3.3.2) was based on staying within temperature limits with assuming a constant decay heat power at $t=0$, which is conservative, to a fixed environmental heat sink, which is optimistic. The constant decay heat power is not as conservative as one would expect. During a BDBA with LOCA and full reactivity insertion such as by cavity flooding and full control rod withdrawals, a properly designed HTGR with negative temperature coefficients in all these configurations should equilibrate with a critical non-zero fission power that is well below the operating power. Finding that steady state critical power in the full reactivity insertion and LOCA BDBA requires a more detailed evaluation of the reactivity coefficients and heat transfer considering the flooding and control worth available. In short, the power will stabilize rather than decay to zero as in a simple LOCA with controlled shutdown. If this becomes the power limiting factor, decay heat removal mechanisms can be limited such that the worst-case reactivity state does not lead to fuel failure or other damage to structural components in and out of core. There is also a case to reduce or eliminate the reactor cavity empty volume so that flooding and increased reflection is not possible. Greater use of burnable poisons and temperature feedback control over control rods can also reduce the fission power in this sort BDBA. These considerations are not addressed in the presented model.

3.4 Reactor

3.4.1 RPV

The RPV is dimensioned to fit the core and barrel, with some plenum volume fraction and contain the pressures at the design temperatures. For RPVs, more detailed design outside the of ASME is possible [73] but not clearly beneficial. Increasing vessel thickness beyond that required by the pressure vessel design code would increase costs but could increase the vessel lifetime. It is assumed that the core and reflector are designed to limit radiation damage on the vessel, which requires more detailed core neutronics analysis than included in this thesis.

3.4.1.1 PV Sizing

The ASME Section III Division 5 or 8 is followed to specify the pressure vessels with corrosion allowance and safety margin factors. Only a few materials were used from Table 1 and 2 of ASME, particularly SA-533 Type B, Class 1 plate and SA-508 Grade 3, Class 1 forging – the most readily applicable for nuclear pressure vessels. In most cases, this simplifies to Equation 3-6, the vessel thickness t at design temperature T , design pressure P and vessel diameter D with S_M the design stress intensity at T . A Division 8 Class B vessel uses the allowable stress intensity and different coefficient in the denominator.

$$t = \frac{P \frac{D}{2}}{S_M(T) - 0.5P} \quad 3-6$$

3.4.1.2 PV Support

The PV support is not included in the estimates or different seismic isolation needs that could apply to the RPV and primary heat transport system are accounted. These would have significant variation, depending on the expected ground accelerations, seismic isolation, and the reactor orientation, aspect ratio, and loaded mass.[65]

3.4.1.3 RX Enclosure

The RX enclosure consists of the civil structure surrounding the RX. This must be sized with sufficient room for access and control rods. The particular dimensions have significant effects on the activation of the soil outside of the enclosure, activation of the air of materials inside in the enclosure, the overall system's response during passive or active decay heat cooling conditions. It is assumed RX enclosures would be fully below grade and allowed a 1-meter gap between the vessel and the concrete. It could well be that the system requires flooding considerations, shielding, passive cooling heat sinks, or thermal capacity blocks to address activation and decay heat requirements. These are not addressed in this implementation of the model.

3.4.2 TH Design and Pressure Drops

We must specify a representative RX TH design consisting of channel radius R_{CH} , fuel thickness for each channel t_F , and channel lengths L , ensuring that maximum operating temperatures and fuel thermal stresses are not surpassed while minimizing the coolant channel volume and pumping power. In the case of constant channel diameter across the core, the geometry can be defined after fixing the velocity, diameter, and length. The coolant velocity v and pressure are input parameters. R_{CH} and t_F are free parameters chosen to achieve a target channel length and stay within fuel operation performance limits. Existing HTGR TH codes exist including [74]

Constraints are provided by a minimum channel diameter, a maximum coolant volume fraction, fuel maximum operating temperature, maximum fuel thermal stress (important for TRISO) driven by the temperature gradient, and the maximum coolant velocity. Coolant channel diameter or radius is limited by the manufacturing processes considered and the maintainability of the channel. Channels less than 2.5mm are challenging to manufacture reliably in graphite or most ceramics and metals and can pose clogging issues if there is chance of debris or dust. The coolant channels cannot occupy more volume than the core. I set the maximum coolant volume fraction, α_{cc} , to 0.35 of the active core volume, as occurs in a pebble bed. Solutions that required greater volume fraction were thrown out as too high-power density. Because helium is neutronically transparent, coolant volume proportionally reduces the originally estimated core energy content (the code does account for moderating coolants at this time). The operating temperature of the fuel should remain below recommended fuel operating temperatures needed to reach high burnups. Considerations on the maximum flow velocity are given in Section 3.5.5. Channel geometry options are varied but the most relevant are shown in Figure 31.

- Coolant radius manufacturing and maintenance limits: $R_{CH} \geq R_{CH,min}$
- Coolant volume fraction: $A_c L \leq \alpha_{cc} V \rightarrow L \leq \frac{\alpha_{cc} V \rho v_{max}}{\dot{m}}$
- Fuel performance limits: $T_F \leq T_{F,max,op}$, $\Delta T_{F,max} \leq \Delta T_{F,max,op}$, $\sigma_F \leq \sigma_{F,max}$
- Flow velocity: $v \leq v_{max}$

Traditionally, channel length has been the core length due to manufacturing practicalities, to simplify analysis, to reduce pressure drops in twists and bends, to avoid unforeseen hot spots, and to avoid in-core flow distribution plenums that displace core volume. This need not be the case and is not how heat exchangers are usually designed. Many branching alternatives are possible. For example, a cylindrical core could have a central inlet plenum that distributes flows to the two halves of the core which results in a half-height channel length. Increased branching has the effect of homogenizing core temperatures. One could also imagine a spherical or cylindrical core with nested plenums at the center of the core that distribute flows outwards and back to a central outlet, constituting a channel length of 2 radii and still preserving the benefits of an insulated hot outlet. In an additive manufacturing paradigm and for small cores especially, many types of branching and counterflows are possible.

There are multiple approaches to design the coolant channel geometry for different cores, fuel volume fractions, and power levels. At first, I thought defining a geometry to achieve the same maximum fuel centerline temperature would level the playing field, but

this leads to non-useful coolant geometries and too high temperature gradients in the fuel when trying to design very low power densities with low coolant outlet temperatures.

An alternative approach is to define the geometry for the same maximum temperature gradient or thermally induced stress in the fuel. This would ensure fuel performance does not go underutilized. For example, a core with lower fuel power density can reduce the flow velocity, pressure, or coolant channel volume up to the fuel performance limits in order to reduce pumping power and void fraction. I leave this option to the next version of the code as I have not yet included a mechanical property database or accurate methods for determining stresses of the different geometries. It is well known that fuel temperatures can be homogenized by varying channel diameter, roughness, and shape along the path or around the core to compensate for power peaking and inlet conditions but that is not addressed here and would be part of a coupled thermal-neutronic model.

For future reference, I recommend starting with a maximum temperature difference across the fuel element and then attempting more detailed stress estimates. Fuel blocks will experience thermal stresses and absorb the compressive stress from the core weight and shear stresses from the flows and temperature gradients across the core. Fuel pellets are inserted into fuel blocks. With sufficient extra space to accommodate differential swelling between the pellet and block, so that compressive stresses on the fuel pellets are negligible. Thermal stress are given below from [75, p. 171] with outer and inner temperatures, α the CTE, E the modulus of elasticity, and ν Poisson's ratio.

For a thin-walled cylinder:

$$\sigma_{max} = \frac{\alpha E (T_o - T_i)}{2(1 - \nu)} \quad 3-7$$

For a heat generating cylinder:

$$\sigma_{max} = \frac{\alpha E q''' R^2}{8k(1 - \nu)} = \frac{\alpha E \Delta T_{max}}{2(1 - \nu)} \quad 3-8$$

In the current TH design estimate, I fixed L to the active core diameter and t_F to 1 cm, and I numerically solved for R_{CH} . Alternatively, I could have fixed the coolant channel volume fraction to find a fixed L , and then solve for R_{CH} . Most approaches gave similar trends for the pressure drops and volume fraction. But using L fixed to the core diameter gave well-balanced results across the core population close to the estimates available for other helium cooled designs on pumping power per thermal power metrics.

Starting with the total core thermal power and the inlet and outlet conditions, I compute the mass flow rates using an energy balance.

$$\dot{m} = \frac{\dot{Q}}{h_{out} - h_{in}} \quad 3-9$$

We determine the coolant's cross-sectional flow area using the input flow velocity at the average temperature of coolant in the core.

$$A_c = \frac{\dot{m}}{\rho v_{max}} \quad 3-10$$

The number of channels is found using the channel radius.

$$n_{ch} = \frac{A_c}{\pi R_{CH}^2} \quad 3-11$$

Each channel handles a portion of the core allowing us to analyze a unit thermal channel with cross sectional area $A_{CH,CORE}$. Traditional HTGR blocks have 2 fuel pins for every cooling channel in the hexagonal lattice, with less than 1 coolant channel per pin channel overall because the core block perimeter is itself a cooling channel. Note that multiple coolant channels can service the same fuel thickness which means this initial scoping does not freeze the neutronicly relevant fuel thickness, pitch, or moderating path length.

For an input R_{CH} , I determine the geometric parameters depending on the given coolant, moderator, and fuel configuration such as those shown in Figure 31. R_{CH} , fuel moderator ratio, and fuel thickness determine $A_{CH,CORE}$, which is used to find the core cross sectional area along the flow line and the channel length.

$$A_{CH,CORE} = A_{CH} + A_F + A_M \quad 3-12$$

A_{core} is the effective core cross-sectional area along the flow path,

$$A_{core} = A_{CH,CORE} n_{ch} \quad 3-13$$

And I find the channel length by volume conservation,

$$L = V_{core}/A_{core}$$

3-14

The fuel thickness was fixed and numerically solved for R_{CH} to achieve a particular L . This is sufficient information to estimate the pressure drop and total coolant volume fraction. Pressure drop was estimated according to the relations in Table 10, with K_{entr} and K_{exit} the entrance and exit loss coefficients taken as 0.5 and 1. Future improvements could include estimating form losses at node interfaces and bends, pressure drops in plenums and developing flow sections [76, Figs. 9–5], and parasitic losses in the core, etc.[75, p. 116] This avenue of estimation was used for Figure 30 with reasonable channel diameter, pressure drops, and specific pumping powers across the design space for a fixed inlet and outlet temperatures. Examples of prototypical pressure drops in the primary helium loop for HTGRs are given in Section 3.5.9.

The fuel peak temperature can be solved starting with the coolant temperature at the outlet. Coolant temperatures, wall temperatures, and pressure drops were approximated using energy conservation, Dittus-Boelter Nusselt correlation for enclosed heated flow, Newton’s law, and McAdams friction factor for fully developed turbulent flow in smooth circular pipes.

Using the wall temperature at the coolant outlet and the core averaged fuel power density, the fuel kernel maximum temperature is evaluated. The temperature profile is calculated using 1D steady heat conduction equation for solutions for coolant wall to the fuel centerline (Figure 32) and TRISO kernel centerline, though the temperature rise across a TRISO particle is negligible given its small radius. The coolant wall serves as a heat transfer boundary condition with a fixed temperature and the fuel centerline or opposite boundary is considered adiabatic. The four cylindrical geometries in Figure 31 were considered with external cooling or internal cooling and with internal or external moderator. FMC (fuel-moderator-coolant) is the standard configuration for HTGR, but CFM (coolant-fuel-moderator) has been used at HTTR, although without sealing the moderator and additional moderator coolant channels. TCR fuel forms may be expected to take any of the shapes described here. The analytic solutions are listed in Table 10.

The fuel thickness was fixed to 1 cm, which, combined with the low power densities of the passive designs and a CFM geometry, usually guarantees that fuel temperatures and gradients are within performance limits. If limits are surpassed, I would have to reduce the fuel thickness serviced by each coolant channel. To that end, I can solve a function like 3-15 subject to the constraints on the inputs and the outputs. With fixed L and v , I solve for R_{CH}, t_F that satisfy the constraints which gives a pressure drop and coolant volume fraction without any value optimization. Optimization occurs in the initial selection of L and v and the other conditions that define the problem like the inlet and outlet temperatures, power, and pressure.

$$[T_{F,CL}, \Delta T_F, \sigma_F] = f(R_{CH}, t_F, L, v, O) \quad 3-15$$

It is noted that the higher coolant volume fraction will increase the fuel power density because for a given core, the core power density and power are fixed. The higher coolant volume also displaces fuel and moderator which will reduce core energy content linearly because of lower fuel loading resulting in reduced achievable burnup.

With the chosen geometries, I can estimate the temperature profiles and pressured drops across the core for a more realistic power peaking scenario. For the core power density, a chopped cosine power distributions with peaking are assumed. Pressure drop and wall temperatures in the highest peaking coolant channel using the relations in Table 10 are numerically solved. However, the results of the calculation were not used to adjust the coolant geometry since the channel length was set equal to the core length. To generalize the approach, I would need to specify coolant channel trajectories across the core for any given channel length.

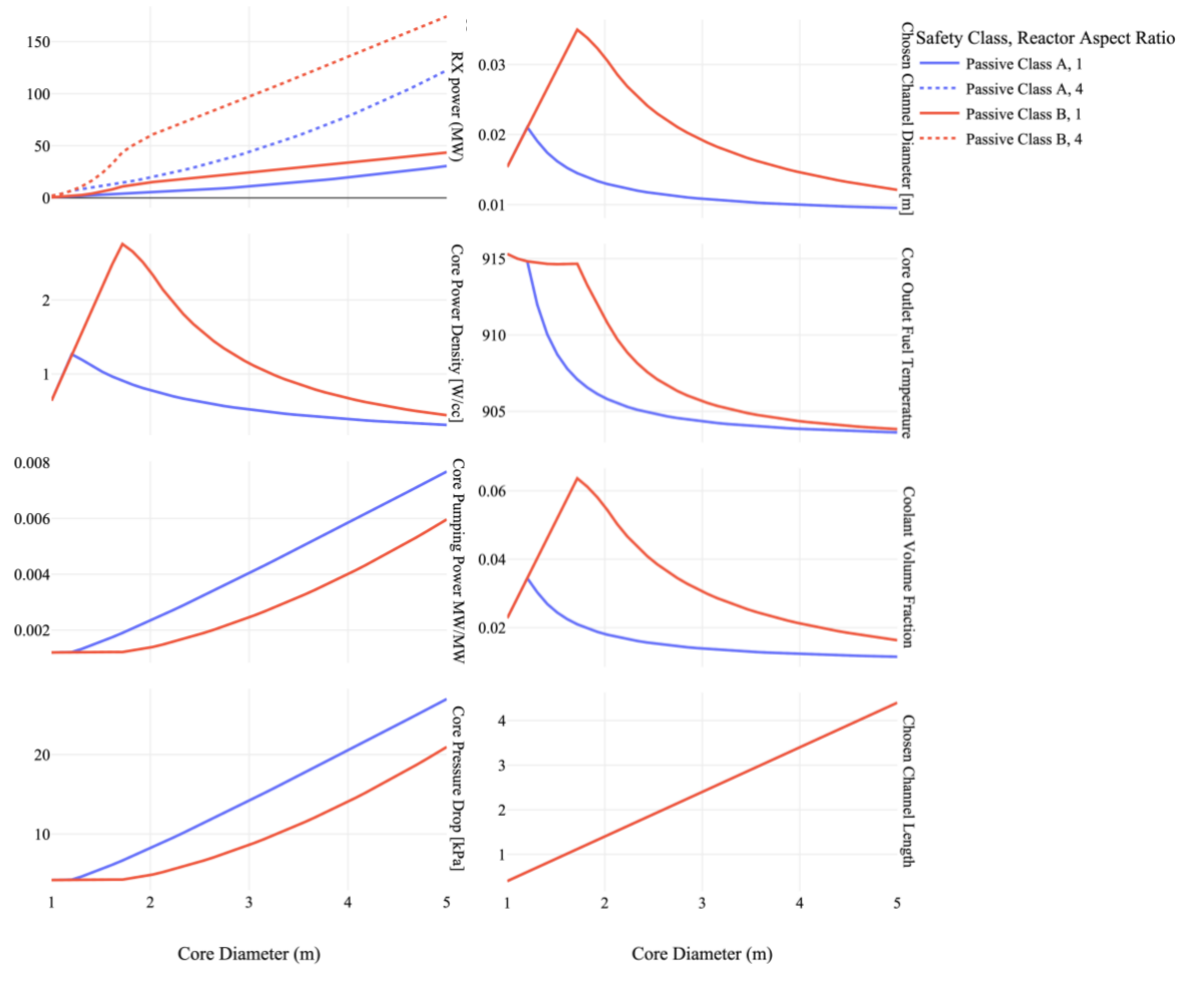


Figure 30 Thermal Hydraulic Solutions across core size and for different safety class and aspect ratio. The safety class A and B refer to the heat transfer coefficient at the RPV surface, with Class A having 20x lower HTC than Class B. Coolant channel length is equal to the core diameter for all designs. Core pressure drop and specific pumping power (pumping power divided by thermal power) increases with diameter because of how power rating is determined resulting in reduced core power density for larger diameter cores.

Fuel to Moderator Ratio: 0.05

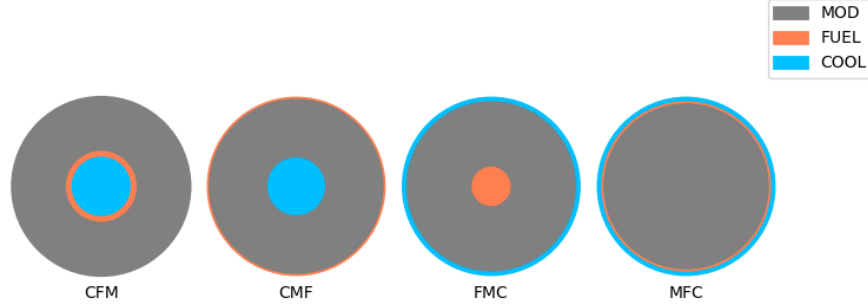


Figure 31 Unit channel in different configurations for the same fuel moderator volume ratio.

Table 10 Heat conduction solutions with component from center of the geometry. C – coolant, M – moderator, F – fuel. Radii indicate outer radii of the material. Solved sequentially from the fixed temperature BC. The thermal conductivity is for the material in question. Gap conductance neglected.

	CFM	CMF	FMC	MFC
BC	$T(r_c) = T_w$ $\left. \frac{dT}{dr} \right _{r=r_F} = 0$	$T(r_c) = T_w$ $\left. \frac{dT}{dr} \right _{r=r_F} = 0$	$T(r_M) = T_w$ $\left. \frac{dT}{dr} \right _{r=0} = 0$	$T(r_F) = T_w$ $\left. \frac{dT}{dr} \right _{r=r_M} = 0$
Fuel Centerline (Peak)	$T_F = -\frac{\dot{q}}{4k}r^2 + C_1 \ln r + C_2$ $C_1 = \frac{\dot{q}}{2k}r_F^2$ $C_2 = T_w + \frac{\dot{q}}{4k}r_c^2 - \frac{\dot{q}}{2k}r_F^2 \ln(r_c)$	$T_F = -\frac{\dot{q}}{4k}r^2 + C_1 \ln r + C_2$ $C_1 = \frac{\dot{q}}{2k}r_F^2$ $C_2 = T_M(r_M) + \frac{\dot{q}}{4k}r_M^2 - \frac{\dot{q}}{2k}r_F^2 \ln(r_M)$	$T_F = T_M(r_F) + \frac{\dot{q}}{4k}(r_F^2 - r^2)$ $C_1 = 0$ $C_2 = T_M(r_F) + \frac{\dot{q}}{4k}r_F^2$	$T_F = -\frac{\dot{q}}{4k}r^2 + C_1 \ln r + C_2$ $C_1 = \frac{\dot{q}}{2k}r_M^2$ $C_2 = T_w + \frac{\dot{q}}{4k}r_F^2 - \frac{\dot{q}}{2k}r_M^2 \ln(r_F)$
Moderator (infinite cylinder)	$T_M(r) = T_F(r_F)$	$T_M = T_w + \frac{\dot{q}}{2k}(r_F^2 - r_M^2) \ln(r/r_c)$	$T_M = T_w + \frac{\dot{q}}{2k}r_F^2 \ln(r_M/r)$	$T_M(r) = T_F(r_M)$
BC	$T_n = T_F(r_F)$ $\left. \frac{dT}{dr} \right _{r=0} = 0$	$T_n = T_F(r_F)$	$T_n = T_F(0)$	$T_n = T_F(r_M)$
TRISO Kernel of arbitrary layers. (sphere)		$T_r(R) = \begin{cases} T_1 + \frac{\dot{q}}{6k_1}(R_1^2 - R^2), & r \leq R_1 \\ T_2 + \frac{\dot{q}R_1^3}{3k_2}\left(\frac{1}{R} - \frac{1}{R_2}\right), & R_1 < R \leq R_2 \\ T_n + \frac{\dot{q}R_1^3}{3k_n}\left(\frac{1}{R} - \frac{1}{R_n}\right), & R_{n-1} < R \leq R_n \end{cases}$		
Power density \dot{q} only in the central kernel. $T(0) \equiv$ Kernel Peak				
Bulk Fluid Temperature Along Channel		$\frac{dT_f}{dx} = \frac{\dot{q}_l}{\dot{m}c_p}$		$\Delta P = (K_{entr} + K_{exit} + fL/D_i) \frac{1}{2} \rho v x^2$
Wall Temperature	$\dot{q}_l = P_w h (T_w - T_f)$ $h = \frac{Nu_D k}{D_h}$ $Pr = \frac{\mu c_p}{k}, Re = \frac{\rho v D_h}{\mu}$		Laminar $f = \frac{64}{Re_D}, Nu_D = 4.023$ Turbulent $Re_D \geq 10^4$ $Nu_D = 0.023 Re^0.8 Pr^{0.4}$ $f = 0.184 Re_D^{-0.5}$ $h = \frac{Nu_D k}{D_h}$	

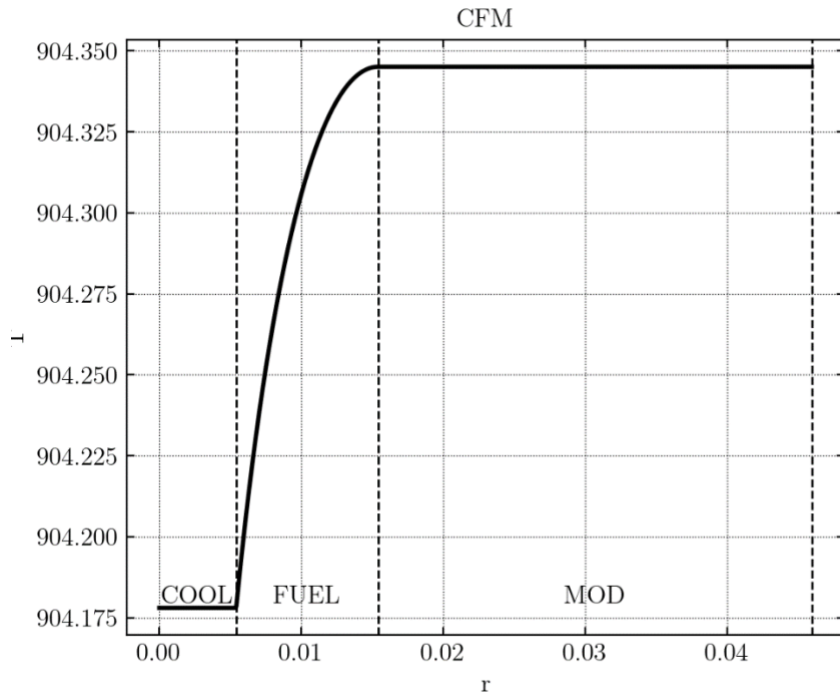


Figure 32 Temperatures across a CFM unit core channel. Radius in m, temperature in K.

3.5 Balance of Plant

Using the inputs in Table 10, BoP components can be specified with dimensions, masses, and performance so that it can 1) estimate the cost by both bottom up and scaling approaches with available data and 2) estimate enclosure dimensions and structural requirements. Example outputs are reported in Table 15 and Table 16.

Table 11 BoP Example Inputs

Parameter	Value	Unit
BoP Type	3-loop sub critical Rankine	from dict
BoP Config	Shared Secondary	from dict
Heat Rejection Type	Air Cooling	from dict
Heat Rejection LMTD	128.42	K
Ambient Temperature	300	K
Turbine Max Size [MWth]	3000	MWth
Primary Fluid Type	He	from dict
Primary Inlet Temperature	573	K
Primary Outlet Temperature	903	K
Primary Operating Pressure	3	MPa
Primary Maximum Fluid Velocity	50	m/s
Secondary Fluid Type	Solar Salt	from dict
Secondary Inlet Temperature	548	K
Secondary Maximum Fluid Velocity	10	m/s
Secondary Outlet Temperature	838	K
Steam Inlet Temperature	423	K
Steam Outlet Temperature	793	K
Secondary Operating Pressure	0.1	Mpa
Steam Operating Pressure	12.5	Mpa

3.5.1 BoP Types

Gas cooled reactors have been envisioned and built with a variety of Balance of Plants [77][78] as shown in Table 12. To date, HTGR's are predominantly built with indirect subcritical Rankine cycles with plans for direct and indirect cycles. This work allowed for two different BoP costing approaches shown in Table 19 but evaluated only the Indirect subcritical Rankine used in EEDB.

Table 12 BoP Configurations

Type	Primary	Secondary	Tertiary	Power Conversion	Efficiency Range	Examples
Direct Brayton	He	-	-	Brayton Cycle	30-55%	GT-HTR, MMR-3, Pylon
Indirect Brayton	He	-/Molten Salt	He, He/Ar, N	Brayton	30-55%	U-Battery, Pylon
He-sCO ₂	He	-/Molten Salt	sCO ₂	sCO ₂ Cycle	15-55%	Radiant
Indirect subcritical Rankine	He	-/Molten Salt	Steam	subcritical Rankine	30-35%	Conventional Nuclear BoP, Ft St Vrain, MMR-1, Xe-100, NGNP
Indirect supercritical Rankine	He	-/Molten Salt	Steam	supercritical Rankine	-	Some coal fired precedents
Combined Cycle Gas Turbine	He	-/Molten Salt	Steam	Brayton in Primary, Rankine in Tertiary	50-55%	VHTR NGTCC, JAEA

3.5.2 Power Conversion and Thermal Cycle Efficiency

Ideally, I would be able to conceptually design the thermal cycle stages and node temperatures for a given set of inlet and outlet conditions and the specified thermal cycle technology. This would allow us to more accurately estimate and optimize the turbomachinery dimensions, sizes, and costs and thermal cycle efficiency. For example, [79] provides concept design and thermal cycle efficiency estimates for a helium Brayton cycle and other design results and techniques are available in the literature [77][80][78][81]. In this work, only simple Rankine and Brayton cycles according to [76, Ch. 6] with power conversion efficiency estimates for a given set of pressures and temperatures were considered.

3.5.3 Heat Transfer Loops

A Heat Transfer Layer (HTL) is defined by the fluid, temperatures, pressure, and maximum flow velocity. An HTL can have multiple loops that carry heat from sources of the lower layer to the loop's sinks. Each layer has a total mass flow rate to accommodate the thermal load.

Each loop carries a portion of the heat load. Each loop has a circulator and piping, pressure relief, a fluid inventory with the option of extra storage, optional pressurizer, fluid purification, and HXs to interface to the next loop or a power conversion system. HX is estimated for the given thermal hydraulic configuration: for example, a steam generator or a micro channel heat exchanger. Nuclear loop also includes radioactive purification systems. Each loop has cylindrical cross sectional areas on hot and cold sides, etc. The Loop Count for a HTL is the number of loops present in the system.

There are many options on the loop configurations and branching. Loop Counts are determined using the number of sources and the number of sinks. For example, 10 sources could be linked in parallel to a single loop with one sink. Or 10 sources could have 5 loops with 2 sources and 1 sink per loop. Or 10 RX could be serviced by a single helium loop with a single direct Brayton cycle. The number of HX between HTLs, essentially the interface between adjacent HTLs, is the maximum of the number of loops in the adjacent HTLs. The IHXs must collectively handle the total heat transfer with some layer-to-layer heat losses.

The specification of heat transfer loops can accept a range of inputs to accommodate different configurations and component limitations. I wanted to be able to easily change the power throughout, node throughput ranges, loop types, and loop branching. Nodes are specified to be within a range of acceptable limits such as a minimum and maximum turbine power load. A few general configuration types can handle most of the design types. While the code can accommodate all these configurations, I limited evaluations to the shared secondary.

1. Fully Independent: each source has its own separate set of loops all the way to the power generation.
2. Shared Primary Separate Circs: sources are connected in parallel with one circulator per source.
3. Shared Primary and Circs: sources are connected in parallel with a single circulator.
4. Shared Secondary: each source has its own separate primary loop that connects to a shared secondary loop.

The cost scaling rules usually guarantee that a shared primary is the lowest cost BoP. But I was more interested in the shared secondary configuration as it balances the cost scaling in a large balance of plant with independence of the RX loops, reducing the risk that problems in one RX cascade to other RXs.

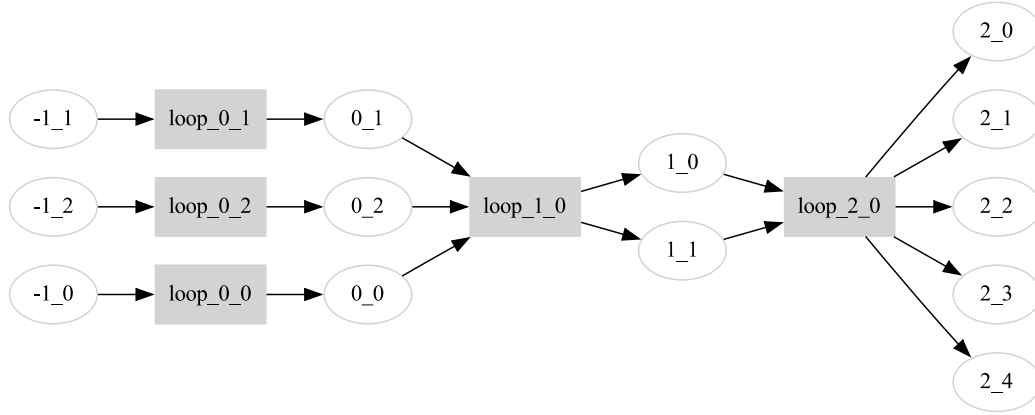


Figure 33 Example BoP with 3 HTL layers. There are 3 origin sources with 3 independent primary loops and 3 HXs, a shared secondary loop connected by 2 HXs to a shared tertiary loop, and 5 power conversion devices.

3.5.4 Net Electric Power

We design the Energy System to deliver a target electrical power. With a particular power rating per RX, I was forced to pick an integer number of RX units, I cannot be assured the desired Energy System MWe will be achieved. So, I find the number of RXs to at least match the requested electrical power, and then define the balance of plant layers. The final MWe produced by each system will be slightly different. $P_{e,total,0}$ is the total electric power requested while $P_{e,total,1}$ is the electric power delivered. There are N_{HTL} heat transfer layers, each with a heat transfer efficiency of η_i . Heat transfer efficiencies are assumed to be 99% between loops, but this can be calculated in the future based on pipe lengths and insulation.

$$\begin{aligned} \eta_{tot} &= \eta_{turbine} \prod_i^{N_{HTL}} \eta_i \\ P_{th,total,0} &= \frac{P_{e,total,0}}{\eta_{tot}} \\ N_{RX} &= \text{ceil} \left(\frac{P_{th,total,0}}{P_{th,RX}} \right) \\ P_{th,total,1} &= N_{RX} P_{th,RX} \end{aligned} \tag{3-16}$$

Net electrical power *delivered* is calculated with accounting for heat transfer efficiencies, cycle efficiencies, and circulator electrical powers. An additional overhead electrical power could be added based on the enclosed building volumes or the site area.

$$P_{e,total,2} = P_{e,total,1} - \sum_i^{N_L} P_{e,circ} \tag{3-17}$$

3.5.5 Piping

3.5.5.1 Pipe Dimensions

Pipe diameter is determined by the area of the pipe that will carry the required mass flow at a chosen flow velocity. Low flow velocities require larger pipes and can lead to sediment deposition but have lower erosion rates and pressure drops. High flow velocities lead to higher erosion and pitting rates, greater friction losses (and so pressure drops), vibrations, and higher hydraulic shocks. The velocity is kept constant throughout the loop to reduce pressure losses from area changes. Typically, a core designer will want to reduce the coolant volume in the core to maximize the moderator or fuel content of the core. This tends to push the design toward higher pressures and flow velocities. HTGRs have had velocities in the range of 30-80 m/s. Sodium coolant is typically run at 3-6 m/s. Water coolant is run at 2-5 m/s. Steam runs at 25-80 m/s. [82][75, Para. Table 10-11]

Pipe thickness is determined using the pressure of the fluid and ASME PG-27.2.1 with a specified material. Pipe lengths are fixed at 10m per loop edge but could be determined based on the distance between adjacent components if a packing and layout estimate

is made. Future estimates could include insulation and thermal loss trades, with the option to enclose hot pipes with cold pipes. Finally, future estimates should specify pipe material based on the temperature requirements of the pipe edge.

3.5.5.2 Piping Pressure Drop

Piping pressure drops were approximated using the Dittus-Boelter Nusselt correlation for enclosed flow and McAdams friction factor for fully developed turbulent flow in smooth circular pipes. Future improvements could include estimating form losses at node interfaces and bends.

3.5.6 Fluid Inventory

The total fluid inventory volume is the sum of pipe volumes, coolant channel volumes in the core and HXs, plenum volumes in the RXs, HXs and pumps, and extra thermal storage as in the case of a molten salt.

3.5.7 Fluid Purification

For primary reactor cooling, I assume 5% of the coolant inventory must be purified each hour, which defines the fluid purification system mass flow rate.

3.5.8 Heat Exchangers

The single-phase gas-gas PCHX (Appendix 10.9) was modeled, but the results produced heat exchanger mass and volumes significantly exceeding known heat exchangers solving for the same conditions. Other types of heat exchangers like compact steam generators, shell in tube etc., were not analyzed in detail. Future work may look at the implications of design decisions like pressure, plate thickness and branching, and fluid temperatures on the HX parameters and the overall LCOE.

For now, I used a few generalized characteristics from the literature for performative HXs (low pumping power and low HX mass) summarized in Table 13. For 15MTh MMR, vendor design estimates suggest a helium to solar salt HX with specific thermal load of 12 MW/m³, or 2 MW/mT of HX material. For helium-steam generator [83] suggests 36 MW/m³, or 7.6 MW/mT. For a compact liquid to steam generator, [84] suggests 86 MW/m³, or 18.8 MW/mT. Pressure drop was approximated as a fixed percentage of the pressure, a particularly crude approach.

Table 13 HX Characteristic performance assumptions.

HX Type	MW/m ³	MW/1000 kg	ΔP fraction of pressure
Liquid-Steam Generator	86	18.8	0.015
Gas – Gas HX	12	2	0.015
Gas-Liquid HX	36	7.6	0.015

3.5.9 Pumping Power and Pump

Each loop has its own pump or circulator that must produce the necessary mass flow and compensate the pressure drops in the loop coming from the RX, HX, and piping. The isentropic efficiency was assumed to be 0.8 to supply the required hydraulic pumping power. The estimated pressure drops did not include a gravitational pressure drop.

$$\dot{W} = \frac{\Delta P \dot{m}}{\rho \eta_{pump}} \quad 3-18$$

Multiple HTGR circulators have been developed, and the information for the MMR and HTR-PM were obtained and partially listed in Table 14. The MMR helium circulator transmits 320 kW with 75% efficiency to an 8.8 kg/s Helium flow, countering an 87 kPa pressure drop. The pump weighs a total of 4.8 tons without vessel coverings. I can perhaps simplify this to 15 tons / MW of pumping power. Tip speed is kept below Mach number of about 0.2, so increasing diameter leads to roughly proportional reduction in rotation speed. The circulator impeller diameter varied very approximately with a power law on the electric pumping power, with units of meters and MW. The circulator housing outer diameter has a roughly four times larger outer diameter. The circulator diameter and pumping were related with the following power law, which is hardly adequate to even begin specifying a circulator design.

$$D = 0.655 \dot{W}^{.33} \quad 3-19$$

Table 14 Selection of Electrically Driven Centrifugal Helium Circulators with Magnetic Bearings

Reference	\dot{m} [kg/s]	ΔP [kPa]	Inlet T [°C]	Pressure [MPa]	\dot{W} [MW]	Pump Efficiency	Pump power/ Thermal power	Rotation Speed (rpm)	Tip Speed [m/s]	Dimension [m] (diameter, height, impeller diameter)
MMR	8.8	57	300	3	0.320	.748	2.1%	15000	244	[1.2 OD x 2.5, 0.311 impeller]
HTR-PM[85] [86]	96	200	243	7.0	4.5	NA	1%	4000	251	[4 OD x 5, 1.2 impeller]

3.5.10 Heat Rejection

There are various ways to reject heat from a thermal cycle. These can take the form of dry or wet cooling in direct or indirect systems, once-through cooling systems, cooling ponds, spray ponds and canals, radiators etc. For HTGRs, higher outlet temperatures make for economical direct air-cooled condensers.

The heat rejection burden is reduced for greater thermal cycle efficiencies. Similarly, the size and cost of a heat rejection system is reduced for higher average temperature differences between the BoP reject coolant temperature and the ambient or ultimate heat sink temperatures. For the same overall heat transfer coefficient, the heat exchanger area will be proportional to thermal duty and inversely proportional to the log mean temperature difference ΔT_m as shown in the below general equation for heat transfer at a surface. For a given heat rejection system, I can scale costs according to $Q / \Delta T_m$. More accurate estimates require estimating U . I did not include heat rejection design or cost estimation in the current model, instead relying on the available heat rejection cost data in the reference design and cost data, scaled with the total reject heat amount. Heat rejection is a significant component powerplant CAPEX and should be subject of design to cost optimization. Some previous work is available [87].

$$Q = UA\Delta T_{lm}, \Delta T_{lm} = \frac{(T_1 - t_2) - (T_2 - t_1)}{\ln \frac{(T_1 - t_2)}{(T_2 - t_1)}} \quad 3-20$$

Table 15 Example Partial Output for BoP

Parameter	Value	Unit
BoP Thermal Efficiency	0.3328	fraction
Cycle Thermal Efficiency	0.3396	fraction
He purification flow rate (kg/s)	0.0004509	kg/s
Heat Rejected (MWt)	199.8	MWt
Heat Rejection LMTD	145.5	
HT Thermal Efficiency	0.9801	fraction
Loop Layers	3	n
Net Electrical Power (MWe)	102.7	MWe
Net Electrical Power Delivered (MWe)	96.6	MWe
Net System Efficiency	0.313	fraction
Number of RXs	14	n
Number of Turbines	2	n
T/B Bldg - Cooling source distance (m)	100	m
Total Plant Thermal Power (MWt)	308.6	MW
Total TH Circulator Power (MWe)	6.115	MWe
Turbine Count	2	n
Turbine Power [MWe/unit]	51.36	MWt
Turbine Power [MWt/unit]	151.3	MWt
Chosen Channel Diameter [m]	0.01083	m
Chosen Channel Length	2.4	m
Coolant Channel Count	1,364	count
Coolant Channel Volume Estimate	0.3013	m ³
Coolant Volume Fraction	0.01388	frac
Core Coolant Velocity	50	m/s
Core Outlet Fuel Temperature	904.4	K
Core Outlet HTC	1,681	W/m ² K
Core Outlet Wall Temperature	904.2	K
Core Pressure Drop [kPa]	14.19	kPa
Core Pumping Power MW	0.08908	MW
Core Pumping Power MW/MW	0.004041	ratio
Core Specific Pressure Drop [kPa/MW]	0.6438	kPa/MW
Maximum Viable Channel Length	8.649	m
Mean Channel Heat Flux [MW/m ²]	0.1981	MW/m ²

Table 16 Example HTL layer outputs for BoP

Loop 1	Value	Loop 1	Value	Loop 2	Value
Loop 0: He to Solar Salt, HX Count	14	Loop 1: Solar Salt to Steam, HX Count	2	Loop 2: Steam, Steam	
Loop 0: He to Solar Salt, HX Mass	11,023	Loop 1: Solar Salt to Steam, HX Mass	8,127	Loop 2: Steam, A_c in	0.001359
Loop 0: He to Solar Salt, HX Volume	1.837	Loop 1: Solar Salt to Steam, HX Volume	1.777	Loop 2: Steam, A_c out	0.03599
Loop 0: He, He	He	Loop 1: Solar Salt, Solar Salt	Solar Salt	Loop 2: Steam, Circ Count	1
Loop 0: He, A_c in	0.1027	Loop 1: Solar Salt, A_c in	0.03085	Loop 2: Steam, Circ Mass	8,496
Loop 0: He, A_c out	0.1614	Loop 1: Solar Salt, A_c out	0.03085	Loop 2: Steam, Circ Volume	
Loop 0: He, Circ Count	14	Loop 1: Solar Salt, Circ Count	1	Loop 2: Steam, Cold Storage Volume	0
Loop 0: He, Circ Mass	5,900	Loop 1: Solar Salt, Circ Mass	1,145	Loop 2: Steam, data	
Loop 0: He, Circ Volume		Loop 1: Solar Salt, Circ Volume		Loop 2: Steam, delP [kPa]	5,164
Loop 0: He, Cold Storage Volume	0	Loop 1: Solar Salt, Cold Storage Volume	0	Loop 2: Steam, Electrical Pumping Power for Layer	0.6142
Loop 0: He, data		Loop 1: Solar Salt, data		Loop 2: Steam, Electrical Pumping Power per Loop	0.6142
Loop 0: He, delP [kPa]	60.66	Loop 1: Solar Salt, delP [kPa]	130.1	Loop 2: Steam, Fluid Inventory Mass	32.47
Loop 0: He, Electrical Pumping Power for Layer	5.451	Loop 1: Solar Salt, Electrical Pumping Power for Layer	0.05018	Loop 2: Steam, Hot Storage Volume	0
Loop 0: He, Electrical Pumping Power per Loop	0.3893	Loop 1: Solar Salt, Electrical Pumping Power per Loop	0.05018	Loop 2: Steam, k average	0.3614
Loop 0: He, Fluid Inventory Mass	259	Loop 1: Solar Salt, Fluid Inventory Mass	1,547	Loop 2: Steam, Layer Piping Length	10
Loop 0: He, Hot Storage Volume	0	Loop 1: Solar Salt, Hot Storage Volume	0	Loop 2: Steam, Layer Piping Mass	1,284
Loop 0: He, k average	0.2915	Loop 1: Solar Salt, k average	0.5	Loop 2: Steam, Mass Flow	94.7
Loop 0: He, Layer Piping Length	10	Loop 1: Solar Salt, Layer Piping Length	10	Loop 2: Steam, Mass Flow per loop	94.7
Loop 0: He, Layer Piping Mass	35,269	Loop 1: Solar Salt, Layer Piping Mass	115.5	Loop 2: Steam, Mass Flow per sink	47.35
Loop 0: He, Mass Flow	180	Loop 1: Solar Salt, Mass Flow	644.7	Loop 2: Steam, Mass Flow per source	47.35
Loop 0: He, Mass Flow per loop	12.86	Loop 1: Solar Salt, Mass Flow per loop	644.7	Loop 2: Steam, mu average	0.0003098
Loop 0: He, Mass Flow per sink	12.86	Loop 1: Solar Salt, Mass Flow per sink	322.3	Loop 2: Steam, Nodes delP [kPa]	187.5
Loop 0: He, Mass Flow per source	12.86	Loop 1: Solar Salt, Mass Flow per source	46.05	Loop 2: Steam, Pipe delP [kPa]	4,976
Loop 0: He, mu average	0.0003719	Loop 1: Solar Salt, mu average	0.005	Loop 2: Steam, Piping Wet Volume	0.3735
Loop 0: He, Nodes delP [kPa]	59.19	Loop 1: Solar Salt, Nodes delP [kPa]	3	Loop 2: Steam, Pumping Power per Loop	0.4913
Loop 0: He, Pipe delP [kPa]	1.462	Loop 1: Solar Salt, Pipe delP [kPa]	127.1	Loop 2: Steam, Re average	11,848,000
Loop 0: He, Piping Wet Volume	36.98	Loop 1: Solar Salt, Piping Wet Volume	0.6169	Loop 2: Steam, rho average	516.4
Loop 0: He, Pumping Power per Loop	0.3115	Loop 1: Solar Salt, Pumping Power per Loop	0.04014	Loop 2: Steam, Storage Mass	0
Loop 0: He, Re average	1,142,100	Loop 1: Solar Salt, Re average	828,390	Loop 2: Steam, v	70
Loop 0: He, rho average	2.049	Loop 1: Solar Salt, rho average	2,090		
Loop 0: He, Storage Mass	0	Loop 1: Solar Salt, Storage Mass	0		
Loop 0: He, v	50	Loop 1: Solar Salt, v	10		

3.6 Civil

3.6.1 Building Specification

Where available, an estimate was made on the civil enclosure required to house the equipment with sufficient clearance and maneuverability aiming to find the site area required, rock and earth excavation volumes, and concrete thicknesses. Building Types must match the standard buildings available in the cost reference such as the Reactor Building, Turbine Building, Primary Auxiliary Building, Admin Building, etc. Different shapes and the options to place buildings fractionally below grade was allowed in the computational framework. The building surface areas, material volumes, and internal volumes were then used for cost scaling purposes. In most cases, there was insufficient component specification of dimensions and mass to accurately estimate the enclosure parameters. In these cases, building costs were scaled with thermal power laws.

I have to decide whether components are above or below ground which would usually include considerations on safety class of the system and presence of radioactivity concerns as well as proximity and seismic functional requirements. For example, a primary loop which may be activated or could become activated would be best located underground. In line with the original down selection, RX and primary HTL are all low grade. One also needs to consider which components can share enclosures and how large enclosures can become. Shared housing will lower building wall and volume estimates. A single enclosure could house multiple reactor units. I assumed distinct low grade RX enclosures.

3.6.2 Site Area

The site area is the sum of all the building areas. Future improvements could include a building packing algorithm to carefully pack buildings with shapes and ensure certain access requirements. When a building was insufficiently specified, the area was not included.

4 Cost Code

4.1 Past Models

There are many cost estimation tools for nuclear power plants ranging from detailed cost estimates from an experienced EPC using supplier quotes to simple power scaling approaches. There are also many commercial tools for cost estimation of industrial equipment like CostLink/CM, Cost Track™, Aspen Process Economic Analyzer, PRISM Project Estimator, Success Estimator, Visual Estimator.[88, Ch. 7] These require significant detail and labor to extract cost estimates.

The approach taken here is the same as the cost scaling approach developed in [89] which offers a simple and programmable way to estimate costs in the nuclear industrial design space for a given set of design parameters. In terms of usefulness and accuracy, this approach lies somewhere between simple power scaling approach and a detailed cost estimation using commercial tools. It is less accurate than a detailed cost estimate from an EPC. Supplier and buyer data is simply missing but is derived from empirical data. The main additions to the original cost estimation model are abstracted and vectorized approach, configurability for new reference designs and costs, inflating capabilities, bottom-up estimates for some accounts, capability for new power plant definitions, balance of plant options, and estimates for operating and project costs.

4.2 Capital Cost

I produce CAPEX estimates with the same accounts as the reference COA and any additional accounts creating in the design code, such as loop dependent accounts. A sample of the CAPEX results are shown in Table 17 and Figure 34 at 2-digit resolution.

4.2.1 Approach

The Cost Estimation codes aims to use a reference or base cost estimate and its associated design parameters to find cost estimates for new designs. To find the costs associated with the new design, various cost estimation functions are used. Besides the EEDB data which includes the COA and basic design parameters, new data from more recent nuclear builds or advanced reactors may soon become available. The code is designed to accommodate new reference data. To the greatest extent possible, reference design data should be as detailed as the design code's outputs so that cost estimation methods can make full use of the available design data. That is, the design details like RPV mass and thermal power rating of the reference design must be sufficiently specified.

Some accounts or components are more easily estimated using a bottom-up approach rather than scaling and these are listed in Table 18. For example, fuel and core component costs are estimated using input material and enrichment costs and assumptions about the manufacturing methods.

4.2.1.1 List of accounts and rules

Every cost account's total cost is split into categories for labor, material, and factor costs, and an additional count and labor hour data. Each account receives its own labor and material inflation indices for properly inflating the accounts to a target year. Root accounts are the bottom level of the accounts and have not subaccounts. Only root accounts contain the base data. Parent accounts are sums of root accounts.

To adjust the cost accounts, I have a list of rules that affect the specified category costs for each account that is a subaccount of the specific account. In this way, I have a systematic approach to add new rules with whatever needed calculation, be it a scaling law that uses design parameters and specific exponents, a learning law, or a modularization function.

4.2.1.2 Arbitrarily specific account toggles and cost estimation functions

While most cost scaling rules are specified at the 3 to 6-digit account level, there are some rules specified for the 9-digit root accounts and with the different cost categories treated differently. Even though I do not use all the available account and category resolution, I maintain the data resolution to simplify the code and more easily allow for future additions of rules at the highest resolution available in the reference cost.

4.2.1.3 Accommodating new reference designs and cost bases

The code needs to seamlessly accommodate new reference designs and their associated cost data. This requires that new cost bases be formatted using the same code of accounts structure used for the EEDB, or at least that the cost scaling rules are written to match the new cost reference cost data. Each reference design and cost base must have an associated origin year from which I can inflate costs.

Each special case or cost estimation rule should reference a reference design parameter to ensure rules are not mistakenly applied and to allow inversion of a scaling approach. As an example, let's consider a reference design that uses E-beam welding for the RPV and its associated cost account is for an E-beam welded vessel. Now, I want to find the cost for a new design that also uses E-beam welding, but I should not reapply an E-beam welding discount (see 6.8.6 for discussion of cost savings on vessels) because the reference cost already reflects the use of E-beam welding. But if the new design does not use E-beam welding, I scaled the

reference cost up by the inverse of the E-beam welding discount. This simple example shows why every cost scaling rule needs to utilize a reference design parameter. In this way, I can adjust costs based on the change from the reference to the new design and can account for many different reference designs. Crucially, a cost rule should not assume the state of the reference design and should explicitly use a reference design or cost parameter when the cost rule is applied. The inversion logic is shown below.

	$\gamma_{new}: \text{No}, 0$	$\gamma_{new}: \text{Yes}, 1$
$\gamma_{old}, 0$	1	β
$\gamma_{old}, 1$	β^{-1}	1

For a toggle rule, the resulting factor is α .

$$\gamma = 0 \text{ or } 1$$

$$\alpha = \beta^{\gamma_{new} - \gamma_{ref}} \quad 4-1$$

This can get complicated for modularized accounts. For example, what happens if the reference design is partially modularized, and its cost data also reflects the modularization? How do I account for a different modularization in the new design? I must scale the costs according to the relative modularization between the new and old designs.

Consider the case where the modularization for a cost account is 50% for the reference and 100% for the new design. The site material cost in the reference would be twice as large if the account were not modularized. The computation is then to find the non-modularized costs for the reference, and then modularize for the new design. A fully modularized reference design will not contain the 0% modularization data.

4.2.1.4 Boundary Cases

4.2.1.4.1 Over specification or incorrect scaling

We account for users supplying too many rules that would over scale an account. This could be the case if a user specifies a parameter scaling law for both a root account and its parent account. A user may also accidentally specify a special rule that affects a parent account without affecting its root accounts. In this case, the cost adjustment would not be reflected in final sums because only root accounts are summed. Various checks are made on the inputs to prevent over specification or incorrect scaling.

4.2.1.4.2 Too much or too little cost data

The code will only compute costs for accounts that exist in the reference cost data. For designs with more systems or accounts than the reference, new accounts must be added. This could include additional heat transfer loops, circulators instead of pumps, reactor cavity cooling, etc. Depending on design parameters, accounts may be removed like containments or spent fuel wet storage. I deal with adding or removing accounts for a given architecture by specifying a toggle on each account. Some accounts are generated based on the design inputs. There might be three heat transfer loop levels, with different counts for each loop. For example, if a powerplant has 10 reactors, each with its own primary heat exchanger and circulator, but a shared secondary loop, the COA are generated to reflect that.

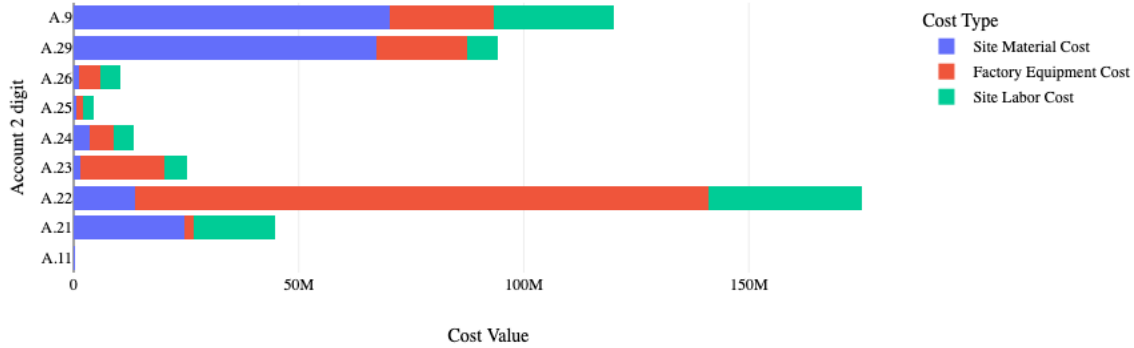


Figure 34 Example capital cost results for a 14x22 MWth ES NOAK 2-digit accounts.

Table 17 Example capital cost results for a 14x22 MWth ES NOAK 1 and 2-digit accounts.

CAPEX	\$M	\$/kWe
Capital Cost Total (\$M)	487.6	5,047
A.1	0.16	1.7
A.2 Total Direct Costs	367.39	3,803
A.9 Total Indirect Costs	120.00	1,242
A.11 Land costs	0.16	1.7
A.21 Structures and Improvements	44.78	463.5
A.22 Reactor Plant Equipment	175.09	1,812
A.23_Turbine Plant Equipment	25.11	260
A.24 Electric Plant Equipment	13.43	139
A.25 Miscellaneous Plant Equipment	4.40	45.51
A.26 Main Condenser Heat Reject System	10.35	107.1
A.29 Loop BoP equipment	94.24	975.5
Total Construction Labor (million hours)	1.07	
Construction Duration (months)	16.2	

4.2.2 Baseline Design and Cost Data

The reference data in prior cost estimation work [89] was the Economic Energy Data Base (EEDB), created in 1987 to estimate the cost of a 1200 MWe Westinghouse PWR. EEDB contains the cost breakdown for 1400 accounts with associated factory, labor, material quantity, and material costs. While useful, EEDB is not an ideal costing reference for reactors in this study, which are up to 250 times lower power using different fuels, moderators, and coolants, and thirty-five years after the original catalogue was developed. Still, EEDB is the most detailed publicly available code of accounts for nuclear energy systems and was used as the cost baseline. Cost accounts specific to HTGR reactors were added and approximated with cost scaling laws from [64] and new estimates. Design parameters used in the cost scaling were already available from the prior work.

Below is a procedure to prepare a reference design and cost data set for use with the code:

1. Define the design parameters for the reference design in a uniquely named column in the “design” sheet of OMEGA14_variables.xlsx. The column should be named “X Value”, with X the unique reactor designation also referenced in the below `basis_meta` dictionary.
2. Add additional cost rules directly in the code ‘omicon_estimator’
3. Format the reference cost data to match the columns and account codes in the prior reference cost databases.
4. Add the new reference as new entry to the `basis_meta`, indicating the cost data file and the reference year

```
basis_meta = {"EEDB": {"file": "PWR12_ME_inflated_reduced.csv", "year": 2018}}
```

MMR Direct Cost	Count Scaling Variable	Count Scaling Exp Var	Cost Scaling Variable	Cost Scaling Exp Var	Toggle Base LWR	Toggle Base BWR	Toggle Base HTGR
-----------------	------------------------	-----------------------	-----------------------	----------------------	-----------------	-----------------	------------------

4.2.3 Direct Costs Rules

All the rules discussed below are Appendix 10.2 including the scaling, modularization, safety class, toggle, and learning rules.

4.2.3.1 Inflation

Following the inflation scaling approach of [89], I give each cost account 2 inflation indices: one for labor and the other for materials and factories. I can then inflate from the data's origin year to the desired year. I added functionality to inflate into the future using a three-year average of the most recent inflation data updated from the BLS and FRED. This also makes it relatively straightforward to add a new cost basis into the same code of accounts and use the same inflating process.

4.2.3.2 Parameter or Count Scaling Rules

Following the cost scaling approach of [89], Scaling relations to estimate cost for a new design scaled from the baseline design and cost estimate with rules reported in Appendix 10.2.1 was used. The generic scaling of each cost account consists of a baseline cost scaled by a normalized design parameter, such as mass or thermal power, with an exponent. The choice of design parameter and the exponent applied is determined from the literature and intuition regarding the manufacturing and construction for a given cost account. The previous assumptions from [89] was used whenever possible.

$$\left(\frac{P_{D,j,i}}{P_{B,i}}\right)^{p_i} \quad 4-2$$

Each cost account also has a scaling law for quantity to adjust for the number of reactors or any other available design variable the number of control rods, or number of HX of a particular type. This makes scaling quantities for multi-unit plants more generalized and less prone to input mistakes. The scaling is linear unless otherwise specified.

$$\left(\frac{N_{D,j,i}}{N_{B,i}}\right)^{n_i} \quad 4-3$$

4.2.3.3 Other Cost Estimates

[88, Ch. 7.5.2] provides multiple cost scaling equations for industrial process equipment of the form provided in Equation 4-4, where C_e is purchased equipment cost, a, b are cost constants, S is a design parameter, and c exponent for that type of equipment. [89] found linear nuclear escalation factors, d , for the same equipment, which are often embarrassingly high. I used the same approach where applicable. Other cost estimates are bottom-up approaches where the feedstock and manufacturing costs are estimated with available information. The underlying data is often of the form of a cost per unit of feedstock and manufacturing cost per unit product or per unit subtracted or added material with varying degree of detail to account for process steps when the data is available. The cost estimate method used for each group is shown below. Except for the core costs and the RPV costs which are considered annualized OPEX, the estimates are contained in the CAPEX COA.

$$C_e = (a + bS^c)d \quad 4-4$$

Table 18 Other Cost Estimates for dollar amounts.

Cost Component	Estimate Method	Inputs [a,b,c,d,S]
Fuel Cost	Bottom-Up	Enrichment, Feedstock prices, SWUs, fabrication cost estimates.
Moderator Cost	Bottom-Up	Feedstock prices and machining cost.
He Circulator	Cost scaling	[580000, 20000, HTGR circulator - exponent, HTGR circulator - nuclear escalation, volumetric flow rate]
He Purification	Cost scaling	[0, 145101229, HTGR He purification - exponent, 1, He purification volume flow rate]
Pressure Vessel	Cost scaling	Bottom-up for sheet/weld, forging and carbon or stainless steel.[90]
Pumps	Cost scaling	[9054, 247, RCP - exponent, RCP - nuclear escalation]
Steam Generator	Cost scaling	[31688, 61, Heat exchanger - exponent, Steam generator - nuclear escalation]
Heat Exchanger	Bottom-Up	Feedstock prices and manufacturing cost. HX design parameters like mass and volume.

4.2.3.4 Balance of Plant Accounts

In a simple approach to compare just Brayton and Rankine cycles for HTGRs, there is an option to use the correlations from [91] for the FOAK capital cost of the balance of plant as a function of reactor outlet temperature, power rating, and number of cycles. This approach assumes a shared balance of plant for the energy system and removes pressure drop and loop branching effects.

Alternatively, this work built custom BoP COA by adding accounts for each HTL considering the HX, pumps, piping, purification systems, fluid inventory and their respective counts. Arbitrary number of HTL of different types and counts for loop specific components can then be added to the COA with an accounting of the pressure drops and temperature effects.

The power conversion turbines still posed a challenge as it lacked reliable data for power conversion devices other than the indirect subcritical Rankine available in the EEDB COA. As such, the analysis was limited to the EEDB balance of plant.

Table 19 BoP Cost and Design Options

	Gandrick BoP	Custom BoP w/ subRankine EEDB
Accounts removed from reference COA	A.221.12, Vessel Structure A.221.3, Vessel Internals A.222.1, Main heat transport system, A.23, Turbine plant equipment A.24, Electrical plant equipment A.262.1, Heat rejection system A.226.3, Reactor Makeup Water System A.229., A.229. A.213., Turbine Room & Heater Bay A.215., Primary Auxiliary Building & Tunnels A.228., Reactor Plant Miscellaneous	A.221.12, Vessel Structure A.221.3, Vessel Internals, A.222.1, Main heat transport system, A.226.3, Reactor Makeup Water System A.229., Special Design Specific A.228., Reactor Plant Miscellaneous
Accounts added	A.29, BoP Aggregate Estimate	A.29, BoP Custom HX, pumps, piping, purification systems, fluid inventory)
Power conversion cost Accounts	Built into A.29	Carried from EEDB (A.23 and A.24)

4.2.3.5 Special Rules

4.2.3.5.1 Special Rules from Prior Work

Part of [89]’s contribution was to rank different SMR concepts based on overnight capital cost using stated or inferred design parameters. Most of these rules were carried over with some changes or exceptions as listed in Appendix 10.2.2. [89] includes various special rules to address the effects of different technologies used in each SMR design relative to the EEDB. For example, there is a 40% discount applied to the RPV for E-Beam welding when the RPV thickness is less than 11 cm.[92] Special discounts or multipliers are applied to various accounts for other special cases like passive safety systems, design simplifications, steel composite, and different containment types.

4.2.3.5.2 Vertical Integration

Vertical integration is commonly pursued among selected nuclear startups despite a limited literature on the cost benefits. As in the discussion on Space X, the idea is that integrating upstream and downstream businesses under a single economic entity allows for tighter control on margins and delivery, achieving closer alignment of economic entities. Owning or operating a supplier allows the integrator company to absorb profit margins, reduce taxable events, more closely align the supplier with the core business objectives, and improve the delivery model. For example, in-house manufacturing of subsystems can lower costs by reducing supplier overhead, eliminating tax and customs events, eliminating supply chain profits and supplier stock purchases, and control schedule delays and inefficiencies such as transport costs or non-customized designs.

In the US, corporate net margins can range from 0 to 30% depending on industry and company. Effective profit margins can be higher as businesses individually try to reduce their declared profit margin and reduce tax burdens. A given component may have several middlemen from the supplier to the end use. Each transfer of goods or services will add transaction fees and margins. There are low value reports of 20% to 80% savings depending on the component and case study, but this may simply reflect uncompetitive markets. [15] Supplier alignment can also reduce costs by eliminating non-central activities relating to other customers and distilling the supplier’s business activities to only those necessary for the integrator business.

On the other hand, there is 28-year-old evidence that disparate profit seeking entities have better performance because there are more self-motivated business owners.[93] One study finds vertically integrated businesses reduce costs in general and administrative, advertising, and R&D but have higher production costs compared to nonintegrated lines of business in the same industry. In nonintegrated lines, each owner is exposed to market pressures and more directly incentivized to reduce costs.[93] Vertical integration strategies may be favored in the planning phase because of the clear and widely advertised advantages accrued by strategy’s biggest winners. It remains unclear how performance varies across the population of commercial attempts and what might explain the variance other than execution.

4.2.3.5.3 Country of Manufacture

Since the 1970s, the advanced economies of USA, Canada, Japan, and Western Europe have lost large portions of their manufacturing capabilities with resulting domestic manufacture cost escalations. The world’s most competitive manufacturing hubs are now in India, China, Vietnam, South Korea, Mexico, Indonesia, Russia, Poland, and Singapore. These countries have the most competitive manufacturing costs, large engineering and manufacturing labor pools, advanced technical and delivery

capabilities, and high growth markets.[94] Manufacturing in the advanced economies is largely limited to advanced R&D methods, massively subsidized products, or export control products.

Recent public information about TSMC’s Arizona chip factory indicates a projected 50% higher manufacturing cost compared to the same factory in Taiwan, primarily due to 3-4x higher factor capital costs and high operating costs overall.[95] US chipmaking subsidies are sufficient to justify the higher costs for now.

Reactor pressure vessels manufactured in the legacy economies of USA, western Europe, or Japan are 2-3x higher cost than those manufactured in the world’s leading manufacturing hubs. Poland’s recent selection of the Westinghouse AP-1000 was made despite a roughly 50% higher specific capital cost and a history of project delivery problems in the US, compared to the Korean APR-1400 which was delivered on time and mostly on budget in the United Arab Emirates (though the first APR1400 underwent similar schedule and cost overruns in ROK).[96] Anecdotally, graphite billets from Chinese vendors are 3-5x lower cost compared to other vendors. There is no North American supply chain option for graphite billets.

Even additive manufacturing costs, which should be country agnostic because machines are sourced internationally, are currently 1-5x lower cost from Chinese suppliers compared to North America or western Europe. This is the case across materials and additive methods as sourced for small to medium size order from an online sourcing service.[97]

Similar to the vertical integration opportunity, no effort was made to model the country of manufacture or operation beyond the US centric costs engrained in the EEDB and other cost sources. One might consider global sourcing to be part of learning experience curves. Even though most modularized reactor systems could be manufactured anywhere and shipped to site, the ability to harness the most competitive global manufacturing capabilities is likely to be forever thwarted by national interests.

4.2.3.5.4 Nuclear Quality

The escalation multipliers used in [89] and shown Table 20, were used to reconcile non-nuclear and nuclear components of precisely the same physical dimension and purpose. Any nuclear cost reference will already be escalated with similar nuclear escalation factors. Achieving non-nuclear balance of plant or Class A safety Case reactors may allow many of these escalations to go to 1. These are not modeled in the cost code, though are the ultimate target of a nuclear Corolla. Future work might attempt a bottom-up nuclear power plant estimate using industrial estimates for a non-nuclear power plant. Like vertical integration and country of manufacture, reductions in the nuclear cost escalation could be considered part of learning curves.

Table 20 Nuclear Escalation Factors (linear) to match non-nuclear process equipment estimates

Component	Factor
RPV - nuclear escalation	34.4
RCP - nuclear escalation	39.7
Steam generator - nuclear escalation	17
Pressurizer - nuclear escalation	12.98

4.2.3.5.5 Standard Licensing

Licensing costs are not included in the cost estimation as they are one time development costs, perhaps the same for any design, making up a tiny fraction of the total deployed capital costs in a global deployment.

4.2.3.6 Modularization

Modularization is the shift of labor and costs from the reactor site to the reactor factory. Equipment and structures that were stick-built or constructed on site are bundled into modules that are fabricated in factories. In this way, labor and material productivity is improved and factory manufacturing methods can be used effectively. There can be added material cost to modularized design because of less efficient packaging infrastructure, size and shape constraints, and other modularization requirements.

The extent of modularization potential is constrained by the size and weight limitations of module transport.[98] For example, NuScale cannot modularize its Giga-pool, and reinforced concrete containments of any size are not amenable to modularization. Smaller reactors and powerplants can be more extensively modularized. Reducing the number of modules also improves the impact of modularization with fewer on-site connections and assembly steps. A car is fully modularized into a single self-contained unit. The advantage of car’s modularization would be greatly reduced if the car were split into 6 or 7 modules or subsystems that had to be assembled at the showroom before the sale.

On-site manufacturing will require local labor and one-off infrastructure, often spanning a decade or more. Where local labor does not exist, it must be brought in, often at great expense to the reactor vendor and reducing the exportability of the reactor design. Countries without manufacturing capabilities, let alone nuclear infrastructure, have little hope for near term nuclear deployments if nuclear vendors continue to market large nuclear powerplants. For these non-modularized designs, there is little opportunity to learn or improve the manufacturing. As more of the plant becomes modularized and more of the value add occurs in factories, learning begins to take place. Imagine a factory workforce that produces 10-100 reactor and powerplant modules per year, with a

local manufacturing culture that grows and maintains the workforce. Compare that to a temporary, imported or ad-hoc work force for typical nuclear mega-projects that may produce one reactor every ten years. Most of the workers will never see the project completion. There is little workforce continuity and no opportunity or incentive to learn or reduce the manufacturing costs for non-modularized nuclear power plants.

The code includes no advantage for designs that are more amenable to modularization. The factor improvement in labor productivity is taken as 50%, the same as [89]. In short, all designs have been equally modularized according to these modularization discounts relative to the baseline, unless otherwise specified.

4.2.3.6.1 Factory Costs

Modularization requires a significant factory capital cost depending on the rate of production, the degree of modularization, and the type of factory technologies used. I am aware of factory costs for SMRs ranging from 100M to 2B for production rates from less than 1 reactor per year to 100 reactors per year. The factory production rate is characterized by unit throughputs like number of parts, tonnage, or volumes as opposed to power ratings. Factory costs can be estimated, but it was assumed the production is high enough to ignore the factory CAPEX.

4.2.3.7 Capital Costs Learning

Learning will take place both within a project and across projects. Within a project, there will be repeated component production like the number of reactors $N_{RX \text{ per } ES}$, the number of turbines, or the number of heat exchangers of a certain type. Over Z repeated Energy Systems (ES) or powerplant projects, there will be $ZN_{RX \text{ per } ES}$ reactors produced, and the learning will scale with the total produced.

Comparing energy systems based on the initial overnight capital costs per unit power is like comparing the cost of the first as manufactured Boeing 777 with the 1000th Boeing 777. It is similarly insufficient to use the LCOE for the first project ($Z = 1$). Instead, I should look at LCOEs across very large deployments and make comparisons for either 1) the LCOE of the last powerplant to achieve a total deployed electrical power capacity Q_{Planet} , or 2) the LCOE of the total deployed power capacity. In the first case, I would compare the LCOE of the last project after having deployed a given installed capacity. This is a deviation from the typical nth of a kind comparison which might look at the 10th unit. I can also observe LCOE curves against the installed power or energy capacity.

Z is defined in Equation 4-5. What total installed capacity should I consider for the planetwide deployment? I am interested in large nuclear deployment systems, such as producing 1% of the planet's electrical generating supply in the 20th year, which would be about 30 GWe at 100% capacity factor.

$$Z = \frac{Q_{e,planet}}{Q_{e,ES}} \quad 4-5$$

[89] uses different learning rates for labor, material, and factory costs applied for the first and 10th unit, and without including learning for the first 100 units. Each cost account i has a count per project N_i . I find the cumulative units produced, ZN_i , and apply Wright's Law [99], with learning rates for each cost category j and optionally for each cost account i . Equation 4-7 is the cost for each account for the last deployment.

$$c_n = c_1 n^{-w} \quad 4-6$$

$$c_{ZN_i,i,j} = c_{1,i,j} (ZN_i)^{-w_{i,j}} \quad 4-7$$

In the second case, I compare the LCOE of the total deployed electrical capacity. In Equation 4-8, I find the average capital cost for each account over the deployment by integrating the cost over the cumulative quantity produced from the 0th to ZN_i .

$$\bar{c}_{i,j} = c_{1,i,j} \frac{(ZN_i)^{-w_{i,j}}}{1 - w_{i,j}} \quad 4-8$$

Table 21 Learning progress ratios a , with $w = \log_2(1 - a)$

Account	Labor Costs	Labor Hours	Material Costs	Factory Equipment Costs
Nuclear Plant A.22	0.131	0.131	0.071	0.16
Buildings A.21	0	0	0	0
Adjacent Plant A.23, A.24, A.25, A.26	0.131	0.131	0.071	0.16
Fuel Fabrication	0.131	0.131	0.0	0.16

4.2.3.7.1 Base Unit Choice

What quantity should be used for learning law base units? I could apply learning at various levels of the system. I could use the Energy System count, the RX count, the number of cores, the number of pellets, or even the number of TRISO particles. I could use cumulative capacity, or cumulative capital expenditures. I should pick a base unit similar to other industries. It should represent a significant quantum of delivery that can practically experience learning and design improvements. Instead of learning based on the number of fuel pellets or fuel blocks delivered, I should use the number of cores delivered. This would constitute design batches for which there are design and production feedback mechanisms. In general, this work uses quanta like, RX count, core count, and control rod count. The learning factors are all equivalent for sufficiently large starting N.

4.2.3.7.2 Comments on Learning Rates

Learning rates for different electric production technologies [100] and different components [101] show a wide range of possibilities. For solar, learning rates in the range of 30-40% have been observed. Tesla's recent emergence has shown the impact of purpose-built factories, vertical integration, and learning with manufacturing costs per vehicle decreasing by 2.33 times from 2017 to 2022, which does not include Tesla's recent battery cell innovations. I speculate that learning related cost reductions are most prominent with high production rates, novel product architectures, and vertically integrated companies.

Nuclear has experienced negative learning in the production of very large reactors since the 1970s, at least in the USA, and this is generally attributed to lack of new builds, long time frames between repeat builds, and increased regulation, paperwork, and system requirements after TMI. [17] Rapid and high numbers of new builds are not possible due to the massive capital and time requirements for traditional nuclear. France and South Korea showed learning is possible for 20 and 12 units produced in the 1980s and 1990s.

It has further been proposed [89] that there is little, or no learning left for nuclear, who identified a 16%, 13%, and 7% learning rate for factory costs, labor costs, and material costs, respectively. In their model, learning for standard equipment starts at N=100 to account for the fact that these equipment accounts have been produced many times in other industries. Newly modularized equipment like RPVs, core internals, control rods, instrumentation, and the turbine plant start at N=1.

As the argument goes, high learning rates found in other energy industries like CCNG or solar do not translate to nuclear because nuclear industries are not able to incorporate new technologies or iterate designs. The nuclear industry's R&D expenditures do not lead to changed designs because of "regulation." Furthermore, the argument goes, much of the learning in thermal hydraulic components and power conversion has already taken place.

Yet, highly regulated industries like aviation, automotive, and aerospace have achieved significant learning by one means or another, be it vertical integration, high volume and competitive sourcing, global supply sourcing, advanced manufacturing, new materials and technologies, purpose-built factories, very high R&D (design and production) expenditures, or simply sheer volume of production and scale economies.

In general, learning rates are predictions, where bias can exist [102]. U.S has not benefited from production economies, R&D expenditures, vertical integration, or any other learning and cost reduction conditions that other industries benefit from. This is likely because there are too few reactors in production at too slow a production rate to learn anything at all. The learning is too expensive in time, money, and risk to justify trying.

First, I point to the limiting case of CCNG plants running on nuclear fuel, presenting a simple example of nuclear potential, as outlined in the limiting cases of 1.3. Second, a significant fraction of nuclear costs and cost escalations are bureaucratic in nature. Take, for example, the escalation multipliers used in [89] used to reconcile non-nuclear and nuclear components of precisely the same physical dimension and purpose. These are not physical hardware limits. They are quality assurance requirements and organizational inefficiencies that affect timelines, productive use of labor and factory equipment. Data and paper costs are far easier to tackle than physical barriers or technological limits. These do not require technology R&D or breakthroughs but learning from doing through continuous execution.

4.2.4 Construction Duration

The construction duration is used for project deployment timelines and for applying scaling factors to the indirect costs. Previous work from [89] used genetic algorithms to estimate the construction duration. The results also gave simple linear and power law relations between the total site labor hours (millions of hours) and the total construction duration (in months). A power law is used for fitting the results. The model should intersect the origin because a project with zero site labor hours would have 0 construction duration. This is the expectation for transportable micro-reactors developed under the DOD Project PELE. These reactors aim for less than 72-hour deployment capability. The construction sequence could be as simple as site preparation by digging a ditch and placing concrete barriers and shielding. I note that the power law fit as below, ignores the opportunity for parallelized work and will be wide off the mark for any project with a higher degree of parallelization compared to single unit plant like EEDB. This has notable CAPEX implications, as construction duration is used to compute the indirect costs in this model.

$$[\text{construction duration months}] = 15.65 * [\text{Site labor hours millions}]^{0.51}$$

4-9

4.2.5 Indirect Costs

Indirect costs vary from reference design to reference design. EEDB's indirect costs include construction services, engineering services, home office services, field supervision, and field offices, temporary roads, parking, laydown area, quality assurance, security, insurance, payroll taxes, startup costs, and construction tools. It excludes owner's land costs, property taxes, financial management costs, and owner's project management costs.

Even though indirect costs make up 53% of the PWR-12ME overnight capital cost, the lack of detail and justification behind indirect costs has forced previous approaches to take a simplified estimation approach. In [89] the summed indirect costs for each category (labor, material, factory) are compared to specific direct costs to come up with linear factors. The same approach is taken here. For a given reference dataset, the coefficients are computed using the same relation where all the direct and indirect sums are known.

4.2.6 Transmission and Delivery

Accounting for transmission and delivery was added using data from [103] but not used in any of the evaluations.

4.3 Operating Cost

4.3.1 Reactor Expendables: Fuel, Moderator, Vessel

Fuel and RPV are treated as expendable components distinct from the maintenance and spares in the operating costs described below. In terms of architecture, future versions of the code should utilize CAPEX accounts with recurring cost schedules, but this version of the code treats these recurring CAPEX as cashflow accounts. Fuel cartridge replacement constitutes a large lump sum payment made on a variable refueling cadence. Similarly, the RPV must be replaced or annealed [104][105] as radiation damage accumulates, which is particularly pertinent for micro reactor systems that have minimized reflectors and high surface to volume ratio resulting in more neutron leakage than conventional reactors and therefore higher dpa/MWth on the RPV materials. For MMR, RPV lifetimes have been estimated at the equivalent of three core cartridge refueling. At that point, the RPV must be replaced, recycled, or thermally annealed to recover its strength.

Both the fuel and RPV charge are lump sum charges that occur at intervals depending on the power rating and core energy content. As a result, the core and RPV lifetimes may not coincide with the project lifetime, which could lead to underutilized cores and RPVs at the end of a project and so artificially higher LCOEs. To avoid this, I treated the fuel and RPV as expendables with a yearly charge based on the discounted value of the component at the project interest rate d , over the component's lifetime N as in Equation 4-10 with CRF the capital recovery factor.

$$c_{\text{year}} = c_{\text{total}} \text{CRF} = c_{\text{total}} \left(\frac{d}{1 - (1 + d)^{-N}} \right) \quad 4-10$$

Core load and RPV learning occurs faster than powerplant learning because fuel and RPVs are produced for each new RX and to supply operating energy systems. The planet wide deployment over t_{planet} years requires production rates as defined below. That said, I kept the core and RPV costs fixed at FOAK prices.

Below are the straightforward relations for planetwide deployments and requisite production rates.

$$\dot{n}_{\text{ES}} \left[\frac{\text{Energy systems}}{\text{yr}} \right] = \frac{Z[\text{ES orders}]}{t_{\text{planet}}}, \text{ energy systems deployed per year} \quad 4-11$$

$$\dot{n}_{\text{RX}} \left[\frac{\text{RX}}{\text{yr}} \right] = \dot{n}_{\text{ES}} n_{\text{RX per ES}}, \text{ reactor production} \quad 4-12$$

$$\dot{n}_{\text{core}} \left[\frac{\text{cores}}{\text{yr}} \right] = \dot{n}_{\text{RX}} \left(1 + \frac{t}{t_{\text{core}}} \right), \text{ core production to feed new RX and refuel} \quad 4-13$$

$$n_{\text{core}} = \dot{n}_{\text{RX}} \left(t + \frac{t^2}{2t_{\text{core}}} \right), \text{ cumulative cores produced during growth stage} \quad 4-14$$

$$\dot{n}_{\text{core}} \left[\frac{\text{cores}}{\text{yr}} \right] = \frac{Z[\text{ES orders}]n_{\text{RX per ES}}}{t_{\text{core}}}, \text{ steady state core production} \quad 4-15$$

$$\dot{n}_{\text{RPV}} \left[\frac{\text{RPVs}}{\text{yr}} \right] = \dot{n}_{\text{RX}} \left(1 + \frac{t}{t_{\text{RPV}}} \right), \text{ reactor pressure vessel production to feed new RXs and replace RPVs} \quad 4-16$$

$$E_{\text{planet}} = \frac{t_{\text{planet}} Z Q_{\text{th}}}{2}, \text{ energy delivered} \quad 4-17$$

Table 22 Planetwide Deployment Example for 1x22 MWth ES

Parameter	Value
Orders	4,509
Planet Scale Deployment (GWth)	98.42
Orders per year	225.4
Planet Scale Energy Extracted [GWth yr]	984.1
Planet Scale Energy Extracted [core eq]	4,396
Planet Scale RX Production [RX/yr]	225.4
Planet Scale Cores produced	4,592
Planet Scale RPVs produced	1,531
Planet Scale Steady State [cores/yr]	439.6
Planet Scale Steady State [RPV/yr]	145.8
New Core Production Rate [core/year]	225.4
Peak Core Production Rate [core/year]	665.1
Planet Scale RX Population	4,509

4.3.2 Fuel Costs

Fuel Cost estimation follows the same line as [106, Pt. Appendix C-9]. The parameters used for the fuel cost model are listed in Table 6. Fuel cost inputs are used to estimate the fuel cost per kg of heavy metal (HM) at different enrichments, packing fractions, and fuel loadings. In addition to fuel cost per kg HM, I estimate the fuel volume and density. Spot prices are from June 30th, 2022. [107]

Conversion and enrichment costs are defined per unit of HM mass. Enrichment costs are found using the Separative Work Unit (SWU) approximation and value function (V) [108] with enrichments (x) and mass feeds (M) specified for feed (f), product (p), and tailings (t). The SWUs per kg of HM are calculated as below to find the enrichment cost.

Definitions:

- M_{HM} , the heavy metal loading in the core
- γ_{TRISO} the TRISO packing fraction which ranges from .35 to .7;
- ρ_{HM} the heavy metal mass density per volume of fuel as in Table 24;
- ρ_K the mass density of the fuel kernel as in Table 24.
- ρ_{MATRIX} the mass density of the inter-particle matrix which can be graphite or SiC.
- $\alpha_{c\&e}$ the cost of conversion and enrichment per kg HM
- $\alpha_{TRISO Fab}$ the cost of TRISO fabrication per TRISO particle
- $\alpha_{compaction}$ the cost of compaction per cc fuel pellet
- α_{matrix} the cost of matrix per kg of matrix material
- $\gamma_{recycle}$ the fraction of the core that is recycled from previous core
- $D_{i=K,1,2,3,4}$, $V_{i=K,1,2,3,4}$, $\rho_{i=K,1,2,3,4}$ TRISO kernel layer thicknesses and layer volumes

$$\frac{M_f}{M_p} = \frac{x_p - x_t}{x_f - x_t} \quad 4-18$$

$$V(x) = (1 - 2x_p) \ln \left(\frac{1 - x_p}{x_p} \right) \quad 4-19$$

$$SWU \left[\frac{SWU}{kgHM} \right] = M_p V(x_p) + M_t V(x_t) - M_f V(x_f) \quad 4-20$$

The TRISO fuel form costs are assembled from conversion and enrichment costs per unit HM, TRISO coating costs per TRISO particle, compaction costs per unit fuel volume, and matrix costs per unit of matrix mass. The intermediate calculations are shown in the below equations. In this way, the advantages of higher HM density fuel types is accounted for. The uranium inside a TRISO particle can be packaged as uranium dioxide (UO₂) or uranium nitride (UN). UO₂ is the standard off-the-shelf option, but UN offers a higher uranium (heavy metal) density than UO₂ or UCO (two phase mixture of UO₂ and UC_x. [109] Kernel cost is assumed to be only a function of the U content. While UN is included in the estimates, no effort was taken to model ¹⁵N enrichment costs which can be on the order of 1000 \$/kg ¹⁵N (USD 2012) [110] or 60 \$/kg HM. The various intermediate calculations for finding the core cost are listed below. The code also accepts different fuel types and dimensions for the TRISO particle kernel and layers but this was left as an unused input as no effort was made to model fuel performance in a manner like Parfume [111] or TP3 that considers stress, fission product diffusion and heat transfer for the individual TRISO particles and surrounding matrix.

Fabrication costs are consistent with low to median estimates from past TRISO fuel fabrication reports like [112]. TRISO fuel fabrication costs may significantly be reduced from current estimates if production scales up.

$$V_K = \frac{M_{HM}}{\rho_{HM}}, \text{ total fuel kernel volume per core} \quad 4-21$$

$$M_K = V_K \rho_F, \text{ total mass of fuel kernels per core} \quad 4-22$$

$$n_{TRISO} = \frac{1}{\rho_{HM} V_K}, \text{ number of TRISO per kg HM} \quad 4-23$$

$$V_{TRISO} = \sum V_i, \text{ volume of TRISO particle} \quad 4-24$$

$$\rho_{TRISO} = \frac{\sum V_i \rho_i}{V_{TRISO}}, \text{ smeared density of TRISO particle} \quad 4-24$$

$$V_{FP} = \frac{V_{TRISO} n_{TRISO}}{\gamma_{TRISO}}, \text{ fuel pellet volume per kg HM} \quad 4-25$$

$$M_{MATRIX} = \rho_{MATRIX} V_{FP} (1 - \gamma_{TRISO}), \text{ inter particle matrix mass per kg HM} \quad 4-26$$

$$\rho_{FP} = \rho_{TRISO} \gamma_{TRISO} + \rho_{MATRIX} (1 - \gamma_{TRISO}), \text{ smeared density of fuel pellets} \quad 4-27$$

$$C_{core} = M_{HM} (1 - \gamma_{recycle}) [\alpha_{C\&E} + n_{TRISO} \alpha_{TRISO Fab} + V_{FP} \alpha_{compaction} + M_{MATRIX} \alpha_{matrix}], \text{ fuel cost/core} \quad 4-28$$

Table 23 Uranium cost inputs. The TRISO fuel cost specified here is on the low end of fabrication cost ranges from past reports like [112].

Fuel Cost Inputs	Value	Unit
Natural Uranium enrichment	0.71	%
Tailing enrichment	0.27	%
Cost of disposal	0	\$/MWe
Cost of Uranium	49	\$/lb of U308
Cost of Uranium conversion	32	\$/kg HM
Cost of Uranium enrichment	87	\$/SWU
TRISO Fabrication Cost [\$/particle]	0.0045	\$/particle
TRISO matrix Material Cost (\$/kg)	1	\$/kg
Fuel Compaction Cost [\$/cc Fuel]	1.5	\$/cc Fuel
Cost of Fuel Fab Total	9,000	\$/kg HM
U3O8 cost	5,661	\$/kg HM
Conversion cost	1,422	\$/kg HM
Enrichment cost	3,513	\$/kg HM
Total Fuel Cost	19,597	\$/kg HM

Table 24 Uranium compounds for kernel.

Compound	Heavy metal density (g/cc)	Compound density (g/cc)
UN	13.53	14.33
UO ₂	9.17	10.4
UO ₂ +UC _{1.1} (UCO)	9.85	10.92
UC ₂	10.64	11.72
UC	12.96	13.61
U ₃ Si	14.98	15.57

Table 25 Example TRISO and Fuel Specification Input

Fuel Parameter	Value	Unit
TRISO Volume Packing Fraction	0.4	fraction
TRISO kernel radius [um]	255	um
TRISO 1 radius [um]	355	um
TRISO 2 radius [um]	390	um
TRISO 3 radius [um]	425	um
TRISO 4 radius [um]	465	um
TRISO kernel material	UO2	material
TRISO 1 material	BuC	material
TRISO 2 material	PyC	material
TRISO 3 material	SiC	material
TRISO 4 material	PyC	material
TRISO Matrix Material	SiC	material
Fuel Block Reuse (fraction old)	0	fraction
Max Fuel Temp [K]	1600	K
Max Fuel Power Density [W/cc]	100	W/cc
Average Enrichment	0.0999	fraction

Table 26 Core Cost and Refueling Output for 240x22MWh ES.

Parameter	Value
Core Cartridge Lifetime (year)	10.26
Refueling Interval	10.31
Number of Refueling Systems	6
Number of Refuelings per year	91.67
Feed uranium kg feed / kg product	22.04
SWU [\$/kgHM]	18.16
Total feed U / core	30,044
UF6 [\$/kgHM]	32.6
U3O8 [\$/kgHM]	25.93
U3O8 Cost [\$/kgHM]	2,287
Conversion Cost [\$/kgHM]	132.2
Enrichment Cost [\$/kgHM]	2,906
Matrix Material Cost [\$/kgHM]	3.026
Fuel Compaction Cost [\$/kgHM]	2,357
TRISO Fabrication Cost [\$/kgHM]	6,715
Fuel Fabrication Cost [\$/kgHM]	9,072
Total fuel cost [\$/kgHM]	14,400
TRISO [kWhr/particle]	0.9508
Moderator Cost [\$/core]	1.113
Fresh Core Fuel Cost [\$/core]	19.63
Fresh Core Cost [\$/core]	20.74
Reshuffled Core Cost [\$/core]	20.74
UNF Average Yearly [m3/RX]	0.2117
UNF Average Yearly [m3/ES]	58.23
Dry-Cask Max Power Density [W/cc]	0.1
Time in Wet Storage (year)	0
Wet Storage Needed?	FALSE
UNF Equilibrium Volume Wet Storage [m3]	0
Fuel storage building - Spent fuel pool volume	0
Fuel storage building Side length [m]	0
Fuel storage building - Spent fuel pool surface area	0
Fuel Storage building dims [m]	
Dry Cask Cost [\$/yr]	43,052,000
Dry Cask Cost [\$/core]	1,605,600
UNF Loading in Dry Cask [kg]	6,766
UNF Dry Casks per year	28.69
UNF Dry Casks ES Lifetime	1,607
Footprint UNF Dry Casks ES Lifetime [m2]	40,175
UNF Dry Casks Area ES dims [m]	
Fuel crane capacity (tons)	2
Fuel cask capacity	116.8
UNF disposal cost (\$/core)	1,960,900
Refueling Cost / Core (\$M)	24.31
RPV Lifetime at Power Design (year)	41.23
RPV Lifetime at Power (year)	30.93

4.3.3 RPV Cost and Lifetime

There are various RPV cost estimates. [90] estimate plate-built cost of 76,800 \$/ton. Rolled plate construction can be utilized also for thicknesses larger than 6 inches. For forged vessels, they find 120,000 \$/ton for carbon steel, 310,000 \$/ton for SS+ 12,800 \$/ton for site labor, +1280 \$/ton for site materials. Forging is not well suited for wall thicknesses smaller than 6 inches. EPRI's work on E-beam welding suggest that vessels less than 3m in diameter and 110 mm thick can be delivered at a 40% lower cost. [89] produced an RPV cost fit with coefficients in Table 18. The cost of a refurbished RPV would be the cost of thermal annealing or other refurbishment which could be some factor <1 of the original RPV cost.

$$C_{RPV} = (c_1 + c_2 \alpha^{c_3})(c_n) \quad 4-29$$

The RPV must be replaced or refurbished when its properties can no longer support the operating requirements of the vessel, for example via radiation induced embrittlement. [Uncertainty assessment for the displacement damage of a pressurized water reactor vessel] This service lifetime could be a simple scaling based on a reference data design. As an example, $[\dot{Q}_0, t_{RPV0}] = [30,30]$.

$$t_{RPV} = \left(\frac{\dot{Q}_0}{\dot{Q}}\right) t_{RPV0} \quad 4-30$$

I round down the RPV life to the nearest core refueling.

$$t_{RPV} = t_{RPV,0} - t_{RPV,0} \% t_{core}$$

But I know that the vessel lifetime will be greatly affected by how it is damaged by the neutron flux. This lifetime is primarily determined by a DPA buildup which will accrue at rates that depend on the reactor geometry, neutron spectrum and fluence, irradiation temperature, and power rating of the core. DPA rates are typically modeled with neutronics codes and used to model the material degradation to specify a lifetime. Smaller reflectors, faster spectrums, lower temperatures, and higher power rating will shorten the lifetime of the RPV. RPV lifetime is also affected by the activation and how long the developers are willing to wait as the RPV changes waste classification.

The lifetime of the vessel for a given reactor can be increased by increasing the vessel margins, using steels or materials that can withstand higher doses or stabilize at acceptable levels [113], enhancing the reflector, or increasing the operating temperature of the vessels. Ordinarily, the vessel will be designed according to ASME S5 D5, but it can be specified using material properties at the desired dpa. For example, to increase the lifetime, the vessel could be designed with Design Stress Intensities and Allowable stresses of the degraded material at a future point in the project life.

4.3.4 NRC Fees

Previous NGNP operating cost estimates used NRC costs “based on fees presented in 10 CFR 171.15 (b) (1), INPO fees, NEI fees, outage costs, and the administration and general cost overhead were estimated based on values in the Dominion report (2004).” [91] This summed up to \$4.78M per reactor. However, this should not apply to micro reactors as the various fees are based on the cost of inspection which should scale with the capital cost, part count, or site area. Furthermore, balance of plant inspections may not even be a part of NRC jurisdiction for reactors having separate and distinct balance of plants with few or no safety implications on the nuclear reactor. This would further reduce the inspection burden to only the nuclear site. Licensing fees per reactor may also be reduced for multi-unit plants by some scaling factor. In this report, a fee of 1% of the CAPEX per reactor was assumed and made no effort to model regulatory whims, however justified by passive safety systems or a decoupled balance of plant.

4.3.5 Cost of Land

A cost of \$100,000 per acre was assumed but would be site-specific and could very well be dropped from the considerations.

4.3.6 Insurance and Property Tax

The safety case for a micro reactor possessing infinite coping time, with refractory fuels and non-interacting core components, would suggest the possibility of a steep insurance discounts. Still, used a yearly total insurance fee of and 1% of capital costs.

4.3.7 Spares and Maintenance Cost

For yearly spares and maintenance, 2.5% of capital costs were assumed with a 40-year replacement cycle. For comparison, [91] uses the equivalent of 1% of the NOAK capital cost and 0.5% of FOAK.

4.3.8 Refueling Activity Cost

Refueling activity costs are accounted by the reduction in power delivered and crane costs. Refueling can range from continuous refueling (pebble-beds and CANDUs) to 20 year refueling (some micro reactors). Continuous refueling requires dedicated infrastructure and operations cost for each reactor.

There are two advantages for long fuel life. First a group of reactors can share the same refueling hardware, diluting its capital and operating costs. The refueling team can be employed continuously and efficiently service a large fleet of reactors rather than serving as deadweight labor between refueling events. Second, there are fewer refueling outages and so higher capacity factor. Long fuel life has the disadvantage of increasing the frozen capital of the powerplant.

I estimated the crane capacities for fuel blocks and UNF casks based on the mass of the fuel blocks and the mass of a filled UNF cask with the particular fuel form mentioned at the indicated volume packing fraction.

There need to be enough cranes to handle all the refueling events. Assuming the operator has fully staggered the refueling events and all the reactors at a site go online within the first t_{deploy} years I can find the maximum number of cranes needed at the site.

$$n_{cranes} = \max \left(\frac{\max \left(\frac{n_{RX}}{t_{deploy}}, \frac{n_{RX}}{t_{core}} \right) \left[\frac{refueling}{yr} \right]}{\left(\frac{1}{t_{outage}} \right) \left[\frac{refueling}{crane yr} \right]}, 1 \right) [t \text{ in years}] \quad 4-32$$

4.3.9 Used Nuclear Fuel Costs

The current fleet of light water reactors produces high activity used nuclear fuel (UNF) that must be placed in wet-storage for a number of years, transferred to dry storage, and ultimately placed into permanent repositories. The low power density designs analyzed in this thesis produce similar waste volume per unit energy delivered, in more robust waste forms (TRISO and ceramic encapsulation rather than pressurized clads), and lower decay power. For example, the fuel kernel makes about 16% of a TRISO particle volume and 10% of a fuel pellet volume (at 62% packing fraction). For a 3x higher burnup compared to conventional UNF, the UNF volume of separated TRISO particles will be 2.1x greater per unit of energy extracted. With the matrix, the UNF volume will be 3.3x greater. In terms of UNF mass, TRISO with matrix typically carries about 0.37 kg HM/kg of fuel. With 3x burnup, a TRISO based fuel can have equivalent or lower total UNF mass compared to conventional UNF. These fuels do not typically require wet-storage and could be ready for geologic storage with limited handling or repackaging needs.

Current nuclear waste fees for long term geologic waste are paid by most utilities to the US government at a rate of 1 \$/MWh according to the Nuclear Waste Policy Act. Because there is not yet a permanent geologic repository, the US government has been forced to cover user expenses associated with storing UNF on site. In future, mechanisms may exist to reward reduced UNF volumes, more robust waste forms, and reductions or elimination of wet storage.

4.3.9.1 Pool Dimension and Wet Storage

Wet storage has to be built and operated with sufficient capacity to sustain the steady state UNF stream at the site. UNF must be kept in wet storage until the decay heat is sufficiently low that it can be safely placed into dry-cask storage. The current LWR fleet stores UNF in wet storage for 2-10 years depending on the burnup, enrichment, and power density. The fuel remains in wet storage until its power density is low enough for dry cask storage. LWR and HTGR fuels will have to be treated differently. HTGR are likely to produce UNF with higher burnups, lower volumetric decay heat, and higher temperature tolerance. Dry-casks with TRISO-based UNF could potentially handle higher decay heats and UNF volume loadings. Careful evaluation of the decay power density, fuel pellet performance capability, and dry cask heat transfer are needed. It is assumed that HTGR UNF can forgo wet storage and go directly into dry casks.

Finding the time in wet storage requires a detailed Origen evaluation like those shown in Figure 35. Generating the Origen cross section libraries for each core and evaluating the UNF decays was not completed for this thesis and not needed with dry cask-only storage option.

If I had wet storage time estimates, I could find the steady state wet storage UNF volume and mass using \dot{V}_{UNF} , the average yearly spent fuel discharge of the powerplant and the time in storage. I then assume the fuel is arranged in the same manner and density as an LWR fuel assembly in terms of fuel volume per assembly volume (26 cm pitch for 21.5 cm assembly pitch) to estimate the wet-storage pool dimensions which are 12m in depth, 8m of which are top water. The UNF pellets make up about 8% of the pool's volume.

$$V_{wet} = \dot{V}_{UNF} \left[\frac{m^3}{yr} \right] t_{wet} [yr], \text{ wet storage UNF volume} \quad 4-33$$

$$V_{pool} = \frac{V_{wet}}{0.08}, L_{pool} = \sqrt{V_{pool}/12}, \text{ wet storage UNF volume and side length} \quad 4-34$$

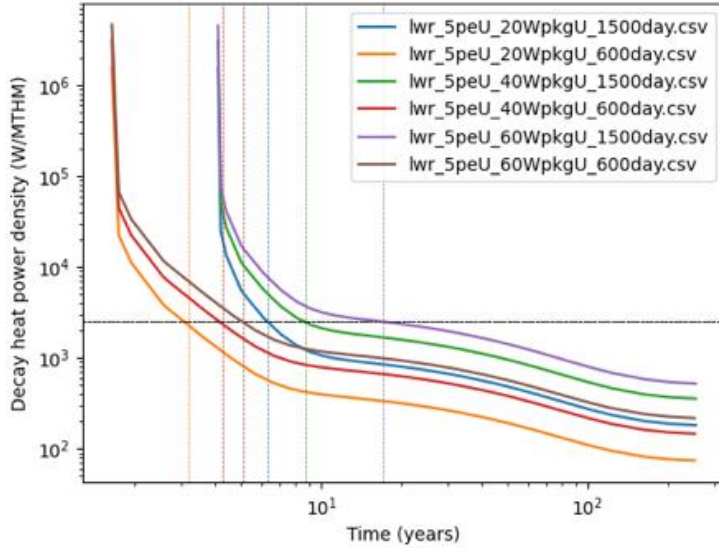


Figure 35 Origen decay output for single cycle w17x17 LWR UNF at 5% enrichment under various power densities and burnups. Horizontal line shows an estimate for the maximum dry cask fuel power density.

4.3.9.2 Dry Cask Costs

NRC licenses dry-casks for LWR fuel can handle between 20 and 50 kW of decay heat without damaging the UNF depending on the dry-cask and the pattern of fuel assemblies which corresponds to roughly 0.025 W/cc LWR fuel. The decay heat in the cask depends on the number of fuel assemblies (usually standard 37x 17x17 LWR FA), the time since discharge, the discharge burnup, and the operating power density of the fuel.

Dry-cask storage costs for LWRs are in the range of 100 to 300 \$/kg HM, and the lower bound value without inflating is used for this work.[114] This corresponds to \$88/kgUO₂ and roughly \$0.74/cm³ of LWR UNF or \$0.244 \$/cm³ of cask volume. Each cask holds 32 LWR fuel assemblies corresponding to 10-15 MT of UNF and 6.15 m³ of cask volume, with 5x5 m pad footprint.

Volumetric cost is the most relevant metric because a dry-cask's cost is defined by its volume. I assume that higher performing fuel forms could reduce dry-cask storage costs by 1-5x by better utilizing a cask's volume and reducing fuel handling costs. Currently, dry casks are filled with fuel assemblies which include the zircalloy claddings and are ~28% UNF by volume. High performance fuel forms could be unloaded from fuel blocks or fuel assemblies and, without metallic parts, would be able to withstand higher temperatures. The fuel could be repackaged from graphite blocks into closely packed cylinders to achieve a volume packing of up to 90.1%, a 2.7 times more efficient use of the dry cask space per unit of UNF volume compared to conventional UNF. Fuels with lower decay heat and greater temperature tolerance can be packaged closer together. Because the HTGR fuel is of limited HM volume fraction, the mass of the UNF casks would be around 2.7x less for the same volume packing fraction.

$$c_{UNF} = \frac{0.244}{\gamma_{packing}} \left[\frac{\$}{cm^3} \right], \text{ cost per volume of UNF} \quad 4-35$$

4.3.10 Staff Scaling

I looked at past operating estimates and upcoming micro reactor operating plans to formulate operating paradigms and scaling methods for HTGR micro reactor operations. INL produced operating estimates based on Dominion reports and Entergy feedback including staffing requirements for the first unit and additional units [91] as shown in Table 27, showing 382 staff for the first unit and an additional 71 staff for each additional unit. On a per unit and per MWth basis, this is similar though somewhat lower, compared to currently operating large LWRs and represents a traditional staffing model. USNC and NuScale reports have suggested low staffing counts according to Table 28.

Table 27 NGNP Staffing from [91].

Labor Group	Single Unit	Additional per Unit
Maintenance	56	12
Operations	38	15
Security	89	20
Other	199	24
Total	382	71

Table 28 Staffing Summary from (MMR [115], NuScale [116], NGNP [91]).

	Unit power [MWth]	RX Units	System Power [MWth]	Staff Count	Specific Staff [Staff / MWth]
Micro Reactor (dual)	30	2	60	7	0.117
Micro Reactor (multiple)	30	8	240	20	0.0833
NuScale	231	12	2772	200	0.0722
NGNP	350	1	350	382	1.0914

Given the wide disparity in estimates between NGNP, micro reactor, and possible aspirational operating schemes using few if any active operators and automated security measures, the work created a generalized staffing model with parameters for three different operating paradigms for low, medium, and high automation corresponding to NGNP-like staffing, micro-like staffing, and aspirational high automation staffing. Table 29 summarizes each staff grouping and how it may scale in each operating paradigm, culminating in a generalized scaling law in Equation 4-37 with paradigm specific coefficients.

While a greater number of reactors may require more maintenance, the same staff could support multiple units as such the cost per MW will be reduced.

In addition, smaller reactors tend to have simpler systems that are easier to handle, access, and maintain, potentially allowing for reduced O&M scope. This means I need a size scaling and a reactor count scaling as below.

$$n_{maintenance,RX} = n_{0,RX} \alpha^s \frac{N^{1-w}}{1-w} \quad 4-36$$

If $s = 0$, size scaling has no effect, but if $s > 1$ there are diseconomies of scale. α could be the surface area of the system normalized to the baseline design's surface area, or accessibility or maintainability metric such as the reactor chamber free volume or the number of control rods. A smaller surface area or greater free volume is more maintainable because there is easier access with less motion. Each component is smaller and lower cost so that manual replacement without cranes or heavy machinery might be favored over repair. Another consideration for economies of scale in maintenance is that individual reactors can be worked on without shutting down the entire powerplant. The quantity scaling with exponent w is similar to a learning model, except I integrate the maintenance staffing over the N units at the site (integral of a learning curve). The exponent for MMR is assumed to be $w = 0.27$, and an aspirational paradigm could have $w = 0.35$.

A starting point for balance of plant maintenance staff estimates is to assume a coupled balance of plant that scales with thermal power regardless of the number of reactor units, and utilizing a scale economies exponent of 0.9. This levels the playing field for different BoP designs, which can be considered commoditized systems.

Security staff is assumed to scale with the site perimeter or site area. In general, the site perimeter is more relevant than site area. Reductions in security may be achieved by high perimeter/area ratio for the nuclear island, automated security and threat identification, reactor burial, and other design features.

In a low automation or traditional operating paradigm, reactor operators should scale with the number of reactors as in $n_{ops} = A + B * N$. One more reactor constitutes B more operators. But in a high automation CA-HTGR paradigm, fleets of reactors could be centrally controlled by a fixed or reduced number of operators. Automation for nuclear reactor operations can be relatively simple with PID feedback and straightforward control logic – much like a CCNG peaker plant which may have no human operators at the site. In medium and high automation paradigms with CA-HTGR reactors, there is little for extra operators to do.

The generalized staff scaling law is shown in Equation 4-37 for n staff with a base quantity ($c1$), an additional per unit quantity ($c2$) scaled by a normalized design parameter (α) with power (s), and quantity scaling (N) such as the number of reactors or power plant with a scaling exponent (w). This scaling law and the coefficients in Table 29 accommodate all the staffing groups and different operating paradigms, allowing for fixed base staff and additional staff that scale based on different design parameters such as the number of reactors, total thermal output, RX size, or site area with specifically defined scaling exponents.

$$n = c_1 + c_2 \alpha_1^s \frac{N^{1-w}}{1-w}$$

4-37

Table 29 Staffing Paradigms for Low, Medium, and High automation.

	Group	c1	c2	N	w	alpha	Reference Value	s
Low automation [NGNP-like] <ul style="list-style-type: none"> Standard operating assumptions from established estimates and operating reactors. Lots of support personnel for powerplant specific engineering planning and implementation Custom BoP High cadence refueling operations 	Reactor Maintenance	23	6	# RX	0	RPV Surface Area	1	0
	BoP Maintenance	23	6	Constant	0	System Power	350	0.9
	Reactor Operation	38	15	# RX	0	Constant	1	0
	Security	89	20	# RX	0	Constant	1	1
	Other	199	20	Constant	0	Constant	1	0
Medium automation [micro reactor claims] <ul style="list-style-type: none"> Uses off-shelf EPC powerplants, serviced and improved by the EPC, not tailor made for the nuclear plant in question. Operating fleets of reactors Do not locally employ engineering teams, supply chain, human resources, training etc. 2 operators base + operator rate per RX 2 maintainers base + maintainer rate per RX Scaling law for security based on plant area Scaling law for BoP maintenance Scaling law for reactor maintenance 	Reactor Maintenance	2	0.2	# RX	0.27	RPV Surface Area	38.17	1.1
	BoP Maintenance	1	0.2	Constant	0	System Power	60	0.9
	Reactor Operation	2	0.05	# RX	0.1	Constant	1	0
	Security	2	0.2	Constant	0	Site Area	1	1
	Other	0	0	Constant	0	Constant	1	0
High Automation [aspirational] <ul style="list-style-type: none"> 2 operators can control arbitrarily many reactors Scaling law for security based on plant area Scaling law for BoP maintenance, power level Scaling law for reactor maintenance, power level 	Reactor Maintenance	2	0.05	# RX	0.5	RPV Surface Area	38.17	1.2
	BoP Maintenance	1	0.05	Constant	0	System Power	60	0.9
	Reactor Operation	2	0	# RX	0.1	Constant	1	0
	Security	2	0	Constant	0	Site Area	1	1
	Other	0	0	Constant	0	Constant	1	0

Table 30 Example Operation Estimate Output for 14x22MWth ES.

Parameter	Value	Unit
BoP Maintenance Staff	2	n
Other Staff	0	n
Reactor Maintenance Staff	8	n
Reactor Operation Staff	3	n
Security Staff	3	n
Labor Staff Total	16	n
Reactor Operation Staff / reactor	0.214	n/RX
Reactor Maintenance Staff / reactor	0.571	n/RX
Staff per MWth	0.0518	n/MWth
Total Staff per Reactor	1.143	n/RX
Operating Labor Cost Energy System (\$M/yr)	2.4	\$M/yr

4.3.11 Staff Salary

Staff salary was taken as an average 150,000 \$/FTE/yr, a rough approximation of the various estimates available from North American sources, listed in Table 11. This approximate value is 25% and 8% lower than inflation adjusted United States estimates

for NGNP [91] and LWR [117]. Still, these are conservative FTE costs given that the first major deployments of micro reactors and SMRs will be in more favorable labor markets such as China, Russia, and perhaps eastern Europe and Canada.

Table 31 Staff salary estimates (USD 2020) from the literature

Staff Standard Plant	INL: with overheads	INL: adjusted : salary + 60% fringe benefits	Exelon: adjusted : hourly rate + 60% fringe benefits
<i>Country</i>	<i>USA</i>	<i>USA</i>	<i>USA</i>
Nuclear plant operators	\$299,750	\$235,004	\$199,680
Security	\$240,377	\$188,456	\$103,168
Planner	\$239,583	\$187,833	\$173,056
General Worker	\$239,583	\$187,833	\$173,056
Average	\$254,823	\$199,781	\$162,240

Salaries can vary drastically worldwide when comparing North America to Europe, Russia, South Korea, China, and India. Software engineer salaries can be 15x lower in India and Southeast Asia compared to the US. In Eastern Europe, software engineers earn 2-5x less than in the US.

4.3.12 Operations Learning

Operations activities like core refueling, RPV replacement or annealing costs, and maintenance costs will reduce over time and potentially across the fleet of Energy Systems. Labor costs will be reduced through labor automation and improved design that requires fewer operators and maintainers or security personnel. This would be expected to improve on a base unit of cumulative reactor years across the fleet. I did not include OPEX learning in the model.

4.4 Project

The project is composed of the construction, startup, operation, refueling, and decommissioning events of the Energy System. A corresponding timeline of the power generation and cashflows is developed.

4.4.1 Timelines

After the construction duration, RXs begin to go online. If needed, different CAPEX accounts can be deployed sequentially with a specified installation duration after the main construction period is completed. This is useful for looking at the effect of sequential RX and turbine deployments at the same site.

Reactor startup times are staggered to minimize the overlap of refueling and RPV replacement events. Outages can include refueling, inspection, and major refurbishment activities. For LWRs, outage varies from 9 to 35 days depending on country and the outage's activities. For a typical LWR, the refueling activities associated with fuel assembly shuffling or replacement can be completed in less than 5 days. The rest of the outage is occupied by various shutdown, disassembly, assembly, and startup procedures.[118] While smaller reactors may have fewer and lighter components, similar checklists and procedures will have to be followed during the outage. A fixed average outage of 20 days per refueling event is assumed. The RXs continue to generate power until they exhaust their current core after the project lifetime. Labor costs match the number of reactors online.

Rounding effects occurred when reactor refueling intervals did not match up with the end of the project lifetime. This is a real effect and should be considered in the concept design, but I allowed all reactors to continue power operations until the end of lifetime without considering that the final fuel load would be only partially consumed.

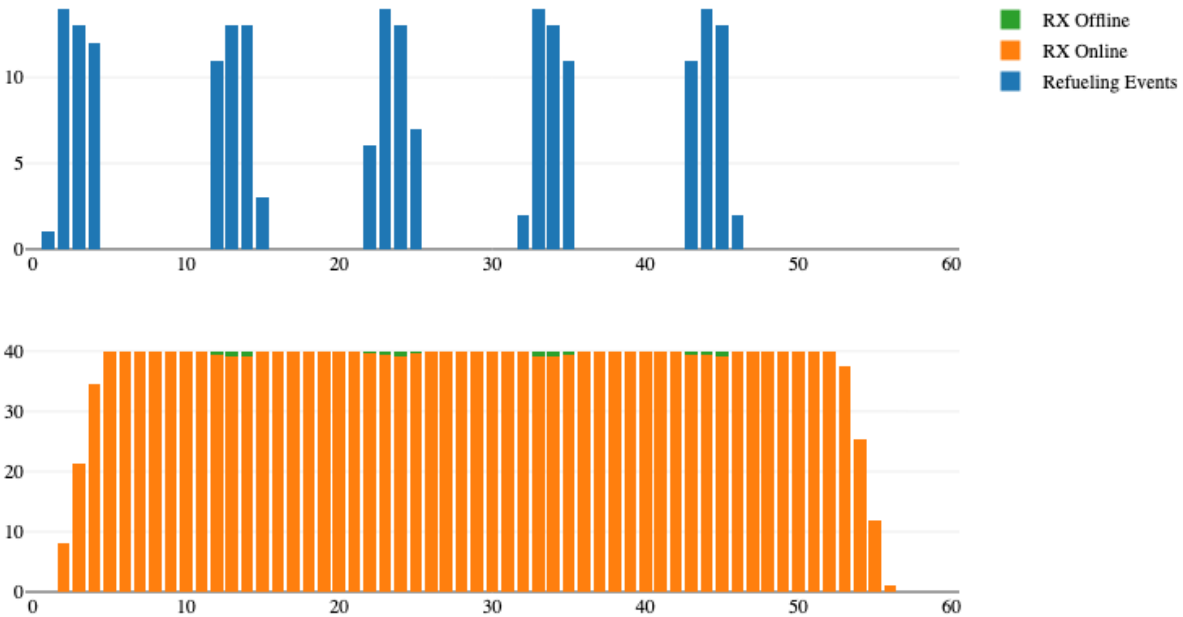


Figure 36 RX 60 year timeline for 40x22MWth ES.

4.4.2 Decommissioning Cost

Decommissioning costs for US reactors over 1100 MWe has ranged from 460 to 730 per \$/kWe. The specific cost are higher for units half the size, ranging from 1,070 to 1,200 per \$/kWe [119], roughly corresponding to between 5 and 15% of initial CAPEX of current nuclear builds. In the US, powerplant licensees must report the decommissioning funding according USC 10 CFR 50.75(c)(1), which provides the required minimum decommissioning amounts for LWRs and BWRs at powers above and below 3400 MWth. For example, LWRs above 3400 MWth require \$293M (2023 USD) or 244 \$/kWe, without including energy and labor escalation, while reactors less than 3400 MWth require $293 + .0231 P$ (2023 \$M), P the thermal power, which is consistent with higher specific CAPEX of smaller unit sizes. BWR have 28.6% higher required fund size. HTGRs are not included in the current law, although there are decommissioning precedents for both Magnox and HTGR.[120]

In this cost model, I assumed a decommissioning fund with a future value at the end of the project equal to 15% of starting CAPEX, which is conservative compared to the required amounts for US nuclear new builds. For example, assuming an optimistic overnight CAPEX of 3000 \$/kWe, US law requires a fund of only 10% of CAPEX. Scaling the decommissioning cost with CAPEX is preferable to a fixed cost per unit power as CAPEX is a good indicator of the effort required to dismantle, disassemble, and decommission a site. With this approach, decommissioning indirectly benefits from learning experience in the CAPEX. The fund grows at the reinvestment rate of return and contributions are made on an annualized basis. The annual decommissioning fund cost is shown below. It is likely that decommissioning funds are highly over budgeted and have created a community of profitable companies that prey on the difference between regulated decommissioning funds and the actual low cost of the activities such as waiting for radioactive material to decay by simply storing it in place (if feasible).

$$c_{DECOM}[yearly] = C_{CAPEX}(0.15) \frac{i_r}{(1 + i_r)^N - 1} \quad 4-38$$

4.4.3 Tax Credits and Expense

Taxes are paid on net profits. Net profits are the gross profits minus the tax credits and depreciation expense on the capital costs. Interest paid on debt is tax deductible while interest paid on equity is not tax deductible. The effect of tax rates is represented by an adjustment on the debt discount rate in WACC. Further considerations of tax credits and expense require a revenue model to estimate gross profits. Depreciation would be applied to CAPEX costs using a Modified Accelerated Cost Recovery System (MACRS) on 15 years. I did not consider tax effects in the analysis.

4.4.4 Financing

Project capital costs are financed through debt, equity, or internal financing. Debt is repaid annually at the CRF so that principal and interest is returned by some date. An equity investor is paid a fixed yearly return and the lump sum at the end. Debt arrangements can have payback periods on the order 10-30 years and interest rates from 2 to 25% depending on the perceived risk, competition,

and financial environment. Equity arrangements can be arranged on similar timelines but higher interest rates. The equity rate may vary depending on the debt-equity ratio. Larger debt-equity ratios may require higher equity rate of return as debt obligations are higher ranked in the liquidation hierarchy.

Each financing scheme creates its own cashflows to support the required capital cost expenditure. For the debt financing, Equation 4-10 gives the CRF yearly payment on the debt defined by payback period and debt interest rate, i_d . The debt payments begin at the start of construction. Debt amounts can be matched to the RX and core deployment times. Interest rates will usually be different before and after power generation begins but are not considered here.

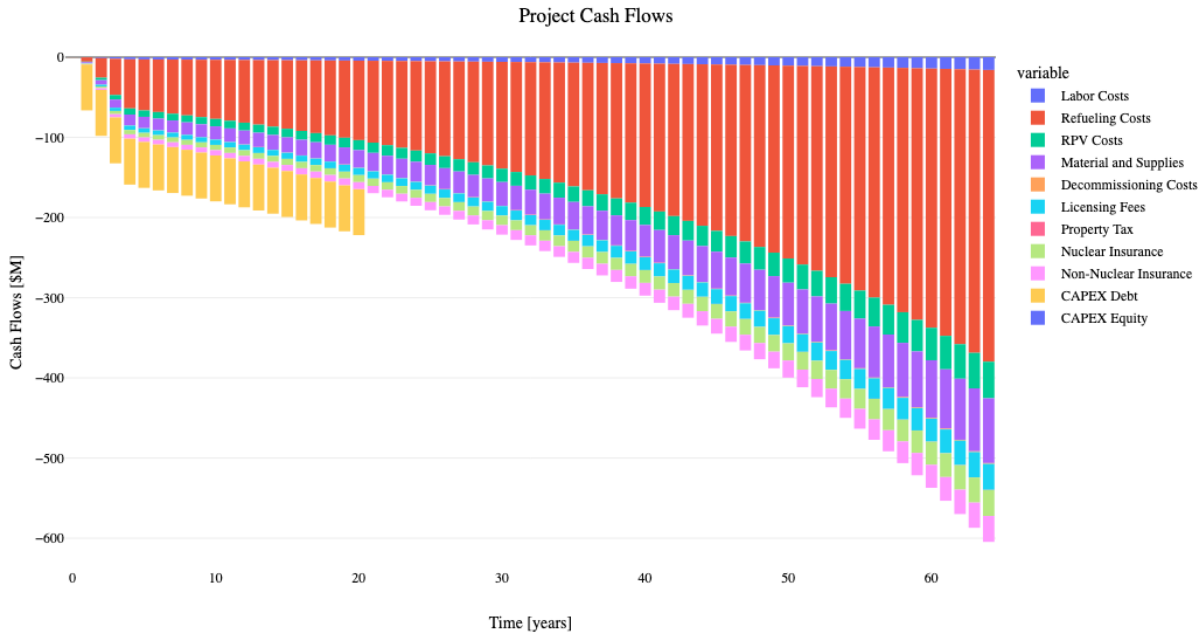


Figure 37 Cashflow example for a 14x22 MWh ES with 20 year payback schedule. Note that the cashflows continue to the project end and would lead to lead to under utilized fuel.

In the case of equity financing, the yearly return to equity investors is the capital times the equity interest rate i_e . The equity investor is also paid back the original sum at the end of the payback period which means the project company is collecting revenues over the years for the final repayment. The assumption is that excess revenues in the project are held and grow at the same discount rate applied to the rest of the project to eventually match what must be paid to the equity investor. This is not necessarily true, and excess revenues are more likely to be reinvested at lower rates than the project discount rate, although the opposite has been true for the last few years. The project company must save sufficient capital for the equity payback in a similar fashion as the decommissioning fund payments which is an annuity growing at a reinvestment interest rate to match a future value. This suggest that in standard financial environments, the cost of equity financing is often higher than the cost of debt financing even at the same interest rate.

Table 32 Cashflow Accounts

Cashflow Account	Timeline	Inflation	Discount Rate	Base Amount
CAPEX Debt Financing	CRF at interest rate i_d over payback period N_F	None	i_d	CAPEX
CAPEX Equity Financing	Yearly Equity Return at i_e and lump sum at the payback period as annuity for future value with reinvestment interest i_r	None	i_e	CAPEX
O&M (labor, licensing fees, insurance, property tax, material and supplies)	Yearly according to the number of reactors on-line	Labor and Standard	Financing discount rate	Annual O&M
Refueling and RPV replacement	Refueling and RPV replacement events	Standard	Financing discount rate	Core and RPV Annualized Cost
DEPRECIATION	MACRS15 on the reactor CAPEX	Standard	Financing discount rate	CAPEX
TAX Credit and Expense	None	None	None	None
DECOM Annual Cost	Starts at RX startup. Annuity for future value with reinvestment interest i_r	None	Financing discount rate	Standard inflation and 15% of CAPEX at $t=0$

4.4.5 Nominal LCOE

Although LCOE does not account for capacity and dispatch benefits of nuclear, it is an appropriate metric to minimize within a technology group. The LCOE is defined so that net present value of revenues and costs are equal. It is calculated using Equation 4-39, which gives the net present value of costs over the net present value of the lifetime energy produced, with N the project lifetime, not to be confused with the N_F , the financing payback time. [121] shows that Equation 4-39 is valid for any of the three financing schemes with discount rate d set to the financing scheme's interest rate.

$$LCOE = \frac{\text{NPV of Total Costs}}{\text{NPV of Delivered Energy}} = \frac{\sum_{n=1}^N \frac{\sum c_{i,n}}{(1+d)^n}}{\sum_{n=1}^N \frac{E_n}{(1+d)^n}} \quad 4-39$$

The equation assigns the present value weights for each cost component. Inflation rate and discount rate assumptions will strongly affect the relative weight of recurring costs compared to one-time costs. I estimate nominal LCOE in which nominal interests are used and cashflows are appropriately inflated. Nominal LCOE cannot be used to compare projects of different lifetimes. Instead, analysts use the real LCOE, which lacks an inflation assumption and will inaccurately weigh the cost components.

To compare projects with different lifetimes, the literature suggests forcing different projects to have the same lifetime by adding projects back-to-back. This accounts for the repeated and inflated CAPEX expenses along the timeline. But it becomes difficult to compare projects with non-multiple lifetimes and the baseline lifetime is a free parameter. The repeated CAPEX also overestimates the required CAPEX because the cashflows contain a CAPEX spare and maintenance account.

Our approach was to inflate the energy revenue flows (d_{inf}) as in Equation 4-40. The estimated LCOE can then be considered the base or starting cost of energy required to break even, which is then inflated over the project lifetime. This approach of inflating the revenues misses the fact that power must be delivered over the longest project lifetime in the comparison or even in perpetuity. Shorter lifetime projects will have to be redone multiple times to reach the longest project lifetime, building up large, inflated CAPEX expenditures along the timeline. However, the cashflows include a spare and maintenance account as a percentage of the original CAPEX, which can be considered a CAPEX replacement over a certain amount of time, a design result by itself as the replacement cycles will vary depending on the how the system is designed and used.

$$LCOE = \frac{\text{NPV of Total Costs}}{\text{NPV of Delivered Energy}} = \frac{\sum_{n=1}^N \frac{\sum c_{i,n}(1+d_{inf})^n}{(1+d)^n}}{\sum_{n=1}^N \frac{E_n(1+d_{inf})^n}{(1+d)^n}} \quad 4-40$$

Extensive thermal cycling, low margins, etc. will require higher replacement and inspection cadence. This is the ongoing cost of CAPEX and tends to be small relative to other annual cashflows. An Active Safety Class system with high performance heat transfer will probably have a higher cost of CAPEX than a passive system. It is not clear how starting CAPEX will relate to the annual or replacement cost of CAPEX. In other words, if CAPEX is increased 50% to improve margins or component lifetime, will the cost of CAPEX just increase proportionally or be reduced because the extra margins allow for longer lifetime of the part? See Appendix 10.7 for brief discussion on CAPEX and ongoing OPEX.

We can compare projects at the same lifetime; but, as in the back-to-back approach, changing the overall lifetime will change the relative weights of each cost component. What lifetime is acceptable and useful in LCOE comparisons? The civil works of the energy system could easily last several hundred years, perhaps perpetually if supported by sustained energy cashflows. There is precedent for 1000-year-old civil structures like Rome's Pantheon (126 AD), the Great Wall of China (220 BC), Venice since the 9th century, Istanbul's Hagia Sophie (527 AD), and England's Windsor Castle (1070 AD) to name just a few. Most of Europe's historic city centers were built before 1919. 25% of Europe's housing stock was built before 1919 with some countries having almost 40% [122], despite the bombings and massive rebuild after WWII. These historic structures have survived due to excellence in construction, sustained maintenance, some preservation laws, and continued value typically originating in religious, political, or aesthetic function.[123] The structures often have built-in resilience, natural equilibration with the environment, self-healing characteristics [124], and low energy geometries in compression (e.g. pyramids and barrows). 100-year power systems exist all over the world, including 60- to 80-year-old nuclear powerplants and hydroelectric plants. Are these systems overbuilt or overly conservative? These sites are often extremely valuable, having been fully developed and accepted into the community. All this to say, that I chose a 60-year lifetime, a somewhat standard value across nuclear power plant LCOE estimates.

Is there any difference in the designs evaluated in this thesis that justifies a different lifetime for one design compared to another? With non-nuclear power systems, the civil works are often reutilized, and portions of the power cycle can be upgraded to utilize the most competitive technologies available at the time of replacement. A nuclear system is more often stuck with the original technology selection and design because the balance of plant is deeply linked to the overall safety of the system and changes to are expensive multi-year license processes. Decoupled balance of plant, passive safety, and modular civil works are some of the avenues to reduce the upgrade limitations in nuclear powerplants.

I generate the cashflows and NPVs directly, but most readers will be more familiar with Equation 4-41 which separates the capital cost term C_0 with the financing costs over the financing payback period N_f . C_0 is the net present value of the CAPEX cashflows including the financing costs which reduces to just the CAPEX on day 0 regardless of the financing scheme because the financing interest rate and project discount rate are the same.

$$LCOE = \frac{C_0 + \sum_{n=1}^N \frac{\sum c_{j,n}}{(1+d)^n}}{\sum_{n=1}^N \frac{E_n}{(1+d)^n}} \quad 4-41$$

Estimating LCOE for mixed debt and equity financing is usually accomplished with the weighted average cost of capital (WACC) in Equation 4-42, with a tax rate T , according to the debt ratio f_d .

$$d = WACC = f_d i_d (1 - T) + (1 - f_d) i_e \quad 4-42$$

Because CRF varies nonlinearly with the rate of return, WACC introduces a model error. Instead, I separately compute the LCOEs for 100% equity and 100% debt with their associated interest rate and combine with a weighted average.

$$LCOE = f_d LCOE_d + (1 - f_d) LCOE_e \quad 4-43$$

Special consideration can also be made regarding the rate of return on reinvested revenues needed to cover an equity payback as previously mentioned. This is simply done by adding an annuity at the reinvestment return rate to cover the equity payback. A lower reinvestment return rate requires a higher LCOE. Failure to account for lower or higher reinvestment returns can yield large errors, for example 8% in the case of a 20-year payback with equity rate of 5% and reinvestment rate of 2%. [121] provides the LCOE* formulation shown in Equation 4-44 for an equity financed project, with $f(x) = ((1+x)^N - 1)/x$, $i_r \neq d$ the reinvestment rate of return which I compared to the LCOE directly computed from the cashflows.

$$LCOE^* = \left(LCOE \sum_{n=1}^N E_n (1+d)^{N-n} - \sum_{n=1}^N \sum c_{j,n} (1+d)^{N-n} - dC_0 f(d) + \sum_{n=1}^N \sum c_{j,n} (1+i_r)^{N-n} + dC_0 f(i_r) \right) / \sum_{n=1}^N E_n (1+i_r)^{N-n} \quad 4-44$$

The comparative nature of this study should be somewhat resistant to the particular LCOE definition used as this work is not concerned with the absolute magnitude of the LCOE but rather the relative estimates and trends under different cost and performance conditions. Table 33 reports the baseline interest rates, inflation rates, payback period, and project lifetime which will dramatically change the relative contribution of each cost component.

Table 33 Example Financial Inputs

Parameter	Value	Unit
Inflation Labor	0.03	fraction
Inflation Standard	0.03	fraction
Debt Interest Rate	0.1	fraction
Equity Interest Rate	0.1	fraction
Capital Cost Financing Repayment Period	20	years
Revenue Surplus Reinvestment Rate	0.03	fraction
Debt Ratio	1	fraction
<i>Depreciation Rate</i>	NA	
<i>Tax Rate</i>	NA	
<i>Cost of Electricity (CPI adj)</i>	NA	
<i>Cost of Heat (CPI adj)</i>	NA	
Startup duration (months)	36	months
Planet Scale Deployment (GWe)	30	Gwe
Planet Scale Deployment Time (Years)	20	years

5 Model Uncertainty vs Design Rankings

I seek the lowest LCOE designs for a given world. I might also seek the lowest LCOE designs in the most probable population of worlds. A world is defined by the model parameters, design methods, learning rates, etc. – essentially the model. Proposed distributions to support the model uncertainty analysis are given in Table 34, where it has conservatively simplified the uncertainties reported in [125] to a single lognormal with $\sigma = 0.15, \mu = \ln(\mu^*)$, μ^* the median value. For a given design, Monte Carlo uncertainty techniques can be used to estimate a portion of the overall model uncertainty. In a Monte Carlo uncertainty estimate, model parameters are sampled from a distribution, for example a normal or uniform distribution with a given mean and standard deviation or from a weighted sack of discrete choices. These distributions could have basis in historical data or some theoretical expectation. This produces a population of estimates which may resemble a normal distribution with a mean value, and I might define the uncertainty as its standard deviation. Previous work defined uncertainty distributions for various model and design parameters as well as a construction duration uncertainty estimate using probabilities of delays.[125] Similar approach could be used here. These uncertainties can be useful as a partial estimate of the overall model uncertainty in a metric of interest for a given design.

However, these uncertainty estimates may not be particularly helpful in picking optimal designs. Consider two designs with the same mean value metric but different model uncertainties as measured by sampling the worlds. One might be tempted to favor the design with the lower uncertainty. But if I were to rank the two designs evaluated in each world in a sample from the population of worlds, I may find the higher uncertainty design beats the other more often than not. Or the mean and uncertainty could be the same, yet the rankings in each world may favor one over the other.

For our design purposes, all designs will be realized in the same manner. Depending on the market, I might want the best design in a high interest and low inflation world with no learning. Or I might want the design with the highest average rank across a distribution of expected worlds. The approach would then be to sample worlds and rank designs in each world, but this was not done in this thesis.

Comparing world uncertainty for a set of designs versus comparing design rankings across worlds or the target worlds could lead to different conclusions depending on the model and designs in question. For a model where designs are highly correlated across worlds and a design's value distribution is symmetric about the mean, optimizing to the mean LCOE across worlds or even the LCOE in one world can be sufficient. Analysts can be fortunate that model results tend to be highly correlated across worlds, especially for small variations in the designs. That is, the best design in one world is the best design in most worlds. But for a model where designs are not highly correlated across worlds, the former straightforward comparison will lead one astray. This is the case here where the world can significantly change the LCOE, particularly through interest-rate, inflation rate, project lifetime, learning rate, and the cost scaling rules.

Table 34 Worlds Characteristic and Distributions

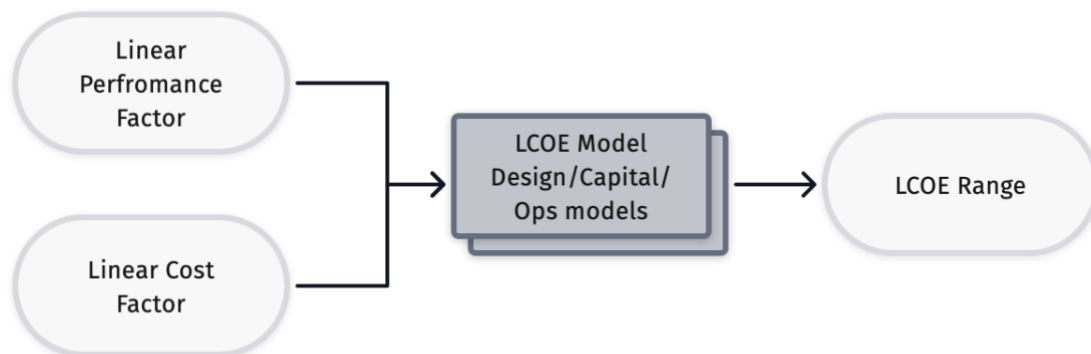
World Characteristic	Proposed Distribution
CAPEX Rule coefficients	Lognormal
Cost reference (COA and manuf costs, labor costs)	
Labor Staffing	
CAPEX and OPEX fractional cashflows	
Design parameters estimates	$\sigma = 0.15, \mu = \ln(\mu^*)$
Design inputs	$\mu^* = e^\mu$
Financial Parameters	$E[X] = e^{\mu + \frac{1}{2}\sigma^2}$
	$\text{Mod } e[X] = e^{\mu - \sigma^2}$
	$\text{Va r}[X] = (e^{\sigma^2} - 1)e^{2\mu + \sigma^2}$

6 2D-Trades to Explore AM Opportunities

Advanced manufacturing (AM) processes, primarily additive methods, are currently being used for high value, high complexity parts including for aerospace and automotive applications and are being developed for nuclear deployment in both operating and advanced reactors. [126][127] In operating reactors, AM may be used to replace components with better characteristics in terms of performance, manufacturability, and cost. AM may also be used for specialized tooling used in servicing and maintaining operating reactors, many of which are one-of-a-kind systems serviced by in-house engineering teams. Advanced reactors may take more drastic advantage of AM techniques to completely replace certain components, broadening the design and cost space.

Specific AM components under development include large vessels, vessel internals, fuel assembly components, and piping components of varying sizes. Several vendors, university groups and industry groups are developing AM components most predominately in the Transformational Reactor Program. NuScale is exploring Powder Metallurgy Hot Isostatic Pressing (PM-HIP) for vessel heads and other large vessel components and e-beam welding of vessels. Framatome and GE-Hitachi are looking at AM-enabled fuel bundle assemblies, repair equipment, and vessels. Ultra-Safe Nuclear Corporation (USNC) is exploring FCM fuel made through the TCR AM method, LPBF HXs, and composite moderators.

In some cases, an AM method may prove more expensive on a manufacturing and QA cost basis compared to a traditional method, but may provide sufficient assembly, inspection, and operating cost savings to justify its use. A performance advantage of an AM-enabled design may justify a higher manufacturing cost. On the other hand, AM methods may have both lower manufacturing, assembly, and QA costs as well as better performance. Even if an AM method shows higher manufacturing costs today, many of the techniques are at the beginning of their development curves with potential cost reductions in the future. I provided some costing guidelines for AM parts in the Appendix but recognize there is too high uncertainty to use expected AM component costs in system cost models. The uncertainty arises because of too large uncertainty in inputs, large variability/margin in OEM and supplier quotes, uncertainty in emerging tech with downward trends, unclear regulatory acceptance, and the fact that I can only guess at the cost changes from part integration and reduced inspections. And to be clear, AM performance characteristics are also uncertain and subject to change, particularly the inferior structural and thermal properties relative to bulk materials. The realizable costs and performance attributes of AM methods and parts is an active area of research and development.



6.1 General AM Opportunities

Table 35 identifies AM methods that can be applied to nuclear fuel, moderators, heat exchangers (HX), and pressure vessels or large steel components. These methods were identified through a literature review of AM methods currently under investigation for nuclear components [126][128][129] as well further research into AM methods and success stories from other industries, particularly aerospace. Whether a method can be used for a nuclear component depends on the method's capabilities in terms of materials, purity, as-built properties, build volumes, feature size, and cost. I mainly considered existing work for nuclear AM components but also anticipated method/component pairings that could work where capabilities match needs.

The general opportunities of introducing an AM method and component are listed below. Each opportunity will manifest itself in the cost of feedstock, manufacturing, assembly, capital side QA/I, operating-side QA/I, or performance attributes like fuel burnup and or reactor power rating.

- **Favorable cost and time metrics.** For example, a manufacturing method that produces the same component using less energy, feedstock, labor, time, or equipment costs.

- **Material flexibility and tunability.** AM may offer different and sometimes improved material properties particularly in radiation environments.[130] Other material opportunities are the high degree of tunability regarding porosity and grain structure, as well as use of unconventional feedstocks that are perhaps more performative or cost effective.
- **Part integration.** AM offers the ability to create complex geometries that combine multiple components into single parts. This applies to additive techniques but also PM-HIP and others. Reducing part counts will reduce failure modes, improve reliability, lower maintenance, and operations cost. Lower part counts also reduce assembly, QA, and inspection costs and can help eliminate supplier dependence.
- **AM-enabled designs** that change a component's performance attributes or enable a different system performance and ultimately lower specific capital or operating costs of the system. See Table 3 for design opportunities. For example, a higher performance fuel or moderator increases fuel loading, burnup, or allowable power rating. Similar topological designs for structure, flow, thermals, or neutronics can improve some performance metric.
- **Strategic Objectives** include reduced lead times and development cycles (additive specific); design invariant manufacturing process and tooling, vertical integration due to lower required expertise and staffing, relatively low-cost tooling (additive specific); one roof design, manufacturing, inspection, and integration (Additive specific); and supply chain onshoring.
- **QA/I simplification** through digitized, high-resolution inspection or testing of final part allowing for a reduced QA and traceability burden. This is crucial for reducing nuclear part costs which have a large paperwork component devoted to QA/I and traceability.

The nuclear industry overall has difficulty achieving significant hardware milestones for new demonstrations due to financing and megaproject risks. From a deployment and demonstration perspective, AM will almost surely lower product prototyping costs, but qualification and licensing of AM prototypes will not easily translate to traditionally manufactured products. As such, it is likely that AM used for prototyping and demonstrations will also be used for full scale production, even if the AM part is higher cost or lower performance. This is especially the case if it takes many years for large production runs to materialize and if frequent design evolution is expected. AM costs are on a solid downward trend as technologies mature and scale, while traditional manufacturing costs are more stable.

The performance attributes achievable by an AM-enabled design can only be determined by relatively detailed design and optimization studies. Furthermore, the performance metric used for optimization may or may not be well correlated to an LCOE metric. For example, criticality or burnup optimizations for core design may not necessarily lead to LCOE minima. But with existing design work on some of these AM components and design optimizations, I can envision some of the possible trends and ranges in performance metrics. For example, I expect that AM fuels will allow a wider range of packing fraction, temperatures, and burnups with effects on the core energy content and power rating. I can expect heat exchangers to be of reduced mass and pressure drop. AM-enabled vessels and large steel components can similarly lead to reduced mass and pressure drops but may also aid in accident scenario heat dissipation thereby allowing for power uprates.

Table 35 AM Methods applied to nuclear components.

Manufacture Method	Fuel Kernels	Fuel Matrix	Moderator	Pressure Vessel or Large Metal Components	HX
Binder Jet and CVI	-	TCR Fuel [131] [132]	Possible (composite moderators or cans)	-	Micro channel HX
LPBF DED	-	Replace Binder Jet for TCR Fuel	Possible	Integrated vessels and intrusions, Orthogrid, optimized vessels	Micro channel HX
Laser CVD	Fuel in Fiber	Fuel in Fiber [46]	Possible (moderator in fiber)	-	-
EBM DED [133]	-	-	-	Integrated vessels and intrusions, Orthogrid, optimized vessels	Micro channel HX
Wire + Tig	-	-	-	Possible	-
Wire Arc Additive Manufacturing (WAAM)	-	-	Possible (canning)	Integrated vessels and intrusions, Orthogrid, optimized vessels	-
SLA Beads	-	Possible	Possible	-	-
Cold Spray	-	Possible, clad coating [134][135]	Possible	Possible	-
Forging	-	-	-	Established [136]	-
Sheet and Weld	-	-	-	Established	-
Seamless	-	-	-	Established	Established
Sol Gel	UCO, UN, and other kernels	-	Possible	-	-
CVD	TRISO (FCVD)	TRC FCM (CVI)	x	-	-
Tape casting	Possible	FCM attempt [137]	Possible	-	Possible
Sintering or SPS	Possible	Possible	Established [138], composite moderators [139] [140] [141]	-	-
Powder Metallurgy-Hot Isostatic Pressing	x	x	x	[142]	-
Machining	x	x (post)	Established	Established	Established
Diffusion Bonding or other advanced joining	-	-	-	EPRI Vessel [92]	Micro channel HX [143]

6.2 Baseline Design

The multi-unit micro reactor baseline design parameters were obtained by the design model and is a CA-HTGRs with rough approximation to the USNC MMR-1. MMR characteristics were publicly available like baseline design burnup, pressure drops, core energy content, and vessel damage limits which were used as point estimates for design scaling. Any other design details were inferred, estimated, or extrapolated from public images and reports. The design model was compared to an MMR-1 design and performance parameters [115] and were shown to be roughly equivalent. The baseline input is reported in Table 41 and a portion of the computed results is given in Table 40.

6.3 Parameter Sensitivity Results

For each component, I establish the motivation for expanded cost and performance ranges and observe the resulting LCOE scenarios under changes from the point design in the two variables. These trades serve to improve the credibility of the results rather than find optimal design choices which are easily determined in 1- or 2-dimensional trades. Each figure presents the relative change in LCOE from the baseline design when changing two variables along rows and columns. The baseline design is a 100 MWe Energy System with 3m diameter cores. Only the two inputs are changed. All other design inputs are kept at the baseline design. But note that changing diameter will change the power because power is a computed design parameter. In Figure 38, packing fraction and

enrichment are varied and all other design inputs like diameter and operating paradigm are held constant. The means the analysis is only meaningful for these departures from the baseline design.

The baseline design point is starred (0.0 fractional difference). I also include a circle representing expectations of cost and performance ranges. Table 36 summarizes the various AM design opportunities and expected effects on performance and cost factors. Each row in the table is discussed in the following analysis. In general, I expect AM components to offer beneficial trends in both performance metrics and cost. Performance and cost trades give a view of the LCOE possibilities without firm estimates and poorly informed judgments on these emerging techniques.

Table 36 AM component design opportunities with expected effects on performance and cost factors.

AM Component	Design Opportunity	Fuel Loading	Burnup	Core Dimension	Power Rating	Pressure Drops	Waste Volume	Waste Activity	Capital Cost	Operating Cost	Thermal Efficiency
Sensitivity (LCOE factor / parameter factor)		-	-	-	-	-	-	-	-	-	-
Fuel	Fuel Loading	↑	↓			↓	↓				
Fuel	Topological Core Design	↑	↑	↓	↑	↓	↓				↑
Fuel	Temperature and Rad Capability		↑		↑	↓	↓	↓			↑
Fuel	Fuel Shuffling / Recycling		↑				↓	↓			
Moderator	Canned / Composite moderators	↑	↑	↓		↓	↓	↓			
HX	Topological Design					↓			↓	↓	↑
HX	Part integration					↓			↓	↓	
HX	Alloy freedom				↑				↓		↑
RPV	Heat Transfer Features				↑						
RPV	On-site Manufacturing	↑	↑	↑	↑				↓		
RPV	Topological opt for mass reduction				↑				↓		
RPV	Topological opt for flows		↓	↓		↓				↓	
RPV	Part Integration and Weld Removal					↓			↓	↓	
RPV	Replacement / Annealing						↓		↓		
System	Pressure				↑	↑					
System	Scale Economies										Aggregate Effects
System	Operating Paradigms										Aggregate Effects

6.4 Fuel

6.4.1 Fuel Loading through Higher packing fraction, UN Kernels, Larger Kernels, Multi-Size Kernels

HTGR fuels have aimed to enhance fuel particle packing fraction and enhance fission product retention under high burnups and temperatures. Various approaches are being taken to use additive methods for fuel.[144] The most readily available AM fuel opportunity is the TCR Fuel form (commercial USNC FCM fuel) which uses binder jet printing and CVI of SiC to achieve high packing fraction of TRISO particle without particle rupture.[145] Alternative manufacturing techniques including tape casting and spark plasma sintering have been explored but overall suffer from limited packing fraction and particle damage effects. Higher packing fraction expands the design space and allows for a wider range of trades between fuel loading, burnup, enrichment, and core size. The higher packing fraction also comes with a SiC matrix. Replacing the graphite matrix with a SiC matrix achieves many of the fission product retention and burnup goals which could have knock-on effects to improve fuel utilization, reduce

helium contamination, and ultimately could lead to non-safety classification for the helium pressure boundary.[146][45] Both TCR [131] and Fuel-in-Fiber [46] fuel forms are strategies to increase the fuel packing fraction and use a SiC matrix.

The evolutionary TRISO-based fuel improvements listed in Table 37 could allow TRISO-based fuels to achieve an effective HM loading that is up to 3 times greater than standard TRISO in graphite. This means a reactor could have 3 times the energy content with the same fuel pellet volume, without changing the smeared fuel to moderator volume ratio appreciably. Alternatively, the designer could choose 3x lower enrichment, getting into LEU territory of 5%. Increasing the HM loading per unit volume of fuel can also reduce fuel fabrication costs as compaction and matrix costs are per unit fuel volume. Similarly UN kernels aim to increase the heavy metal loading owing to a 13.53 g/cc heavy metal density compared to 9.85 for UCO.[109] For AM fuels, the packing fraction could be extended to up to 65% as in the CVI FCM Fuel. When using multiple size TRISO particles, large diameter TRISO particles, and/or UN kernels, fuel loading can be further increased by a factor of between 1.3 to 1.5 without displacing moderator.

Table 37 Potential HM Mass Loading Improvements for TRISO-based Fuel

TRISO Fuel Loading Pathways	Effective HM Loading Factor
Packing fraction: currently TRISO-graphite compacts have 35-40%. CVI/FCM aiming for 60-65% with a single particle size.	1.5
Multiple Particle sizes like at Ft. St Vrain use two or three TRISO particle sizes to achieve 65-70% packing fraction.	1.15
Fuel kernel: transitioning from UCO kernels to UN kernels allows for 38% more heavy metal packing.	1.38
Larger kernels: larger fuel kernels are possible in FCM because of the SiC compressive interface on the TRISO particle and allow for increasing the ratio of uranium to ceramic coatings, ultimately increasing the heavy metal content of the fuel by 20-30%.	1.25
Total Potential Factor	2.98

As of 2023, there is no HALEU available for US vendors. Figure 38 shows the trade between packing fraction and enrichment with a baseline design started at 10% enrichment and 40% packing. The same trade is shown in Figure 39 but with contours of estimated refueling interval instead of relative LCOE. Reducing enrichment from 20% to 10% results in similar LCOE and a reduction in refueling interval from 20 years to 10 years. Increasing packing fraction to 60% with an AM-enabled fuel, allows the system to recoup the refueling interval to 15 years but with an increase in LCOE of about 5% from the baseline. This is due to increasing stagnant fuel costs and limited modeled benefits of reduced refueling.

Figure 40 reiterates these results by showing that there is no benefit to higher packing fraction for the same or greater fuel fabrication cost. The “fuel fab cost factor” only changes the fabrication cost including both TRISO fabrication and compact fabrication. Enrichment costs are unchanged.

These results should be considered in the context of the model’s deficiencies stemming from fixed financial parameters and low penalties for high cadence refueling. The financial parameters include low inflation and high interest rate, which favors reducing the capital locked in fuel purchases. In a low interest regime, these trends are reduced and even reversed so that longer refueling is favored. High cadence refueling will require more refueling and spent fuel infrastructure and a larger staffing requirement. The extra staffing is not included in the model. Even low cadence refueling will require refueling infrastructure, though it is expected that a mobile refueling system can be used across reactor and perhaps sites with a specialized team. Many potential micro reactor customers prefer low cadence or no-refueling options as features and would like to avoid on-site spent fuel storage. It should also be noted that stagnant fuel costs occur even for large reactors where fuel supplies are secured in times of low prices and high expected inflation, sometimes with several years’ fuel supply on site.

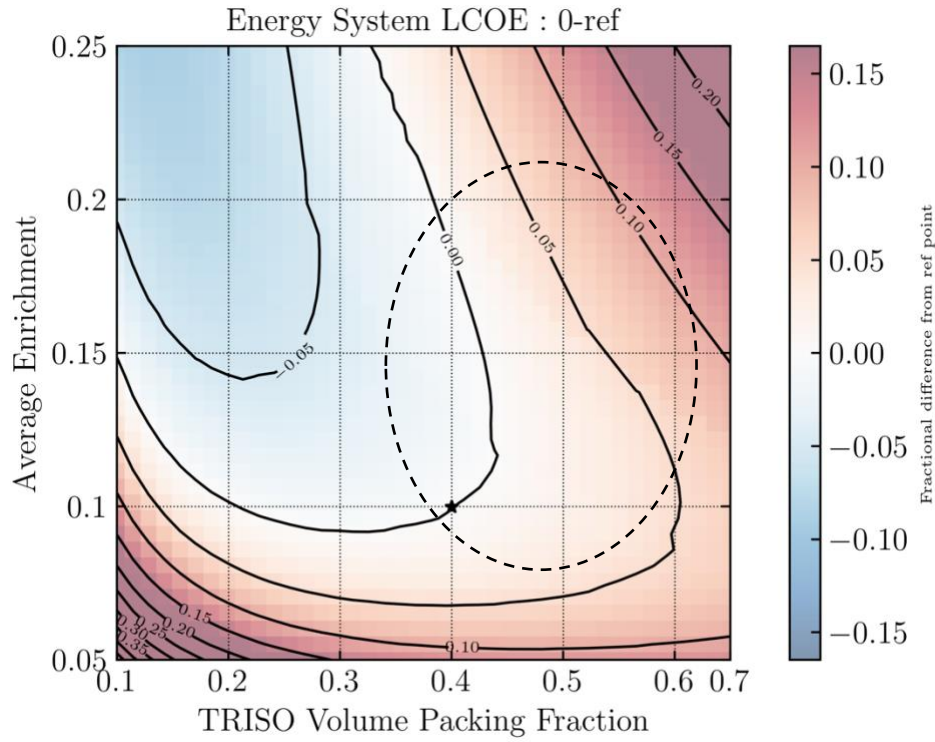


Figure 38 Packing fraction vs Enrichment showing LCOE change from baseline. Circle represents TCR fuel form with LEU+ enrichment, the only available enrichment within the next 5-10 years.

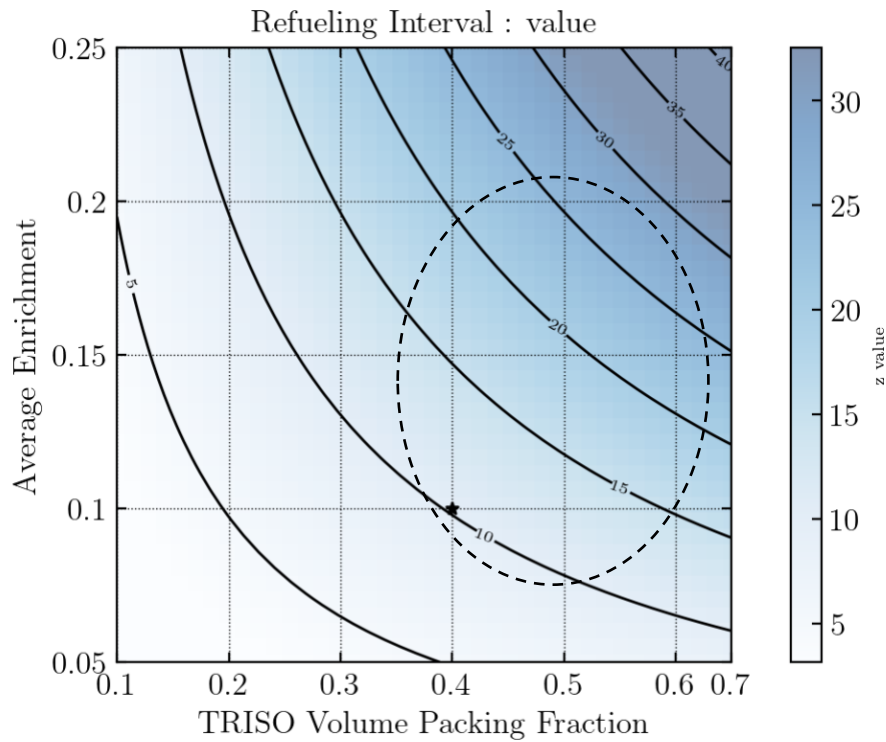


Figure 39 Packing fraction vs Enrichment showing refueling interval in years. Circle represents TCR fuel form with LEU+ enrichment, the only available enrichment within the next 5-10 years.

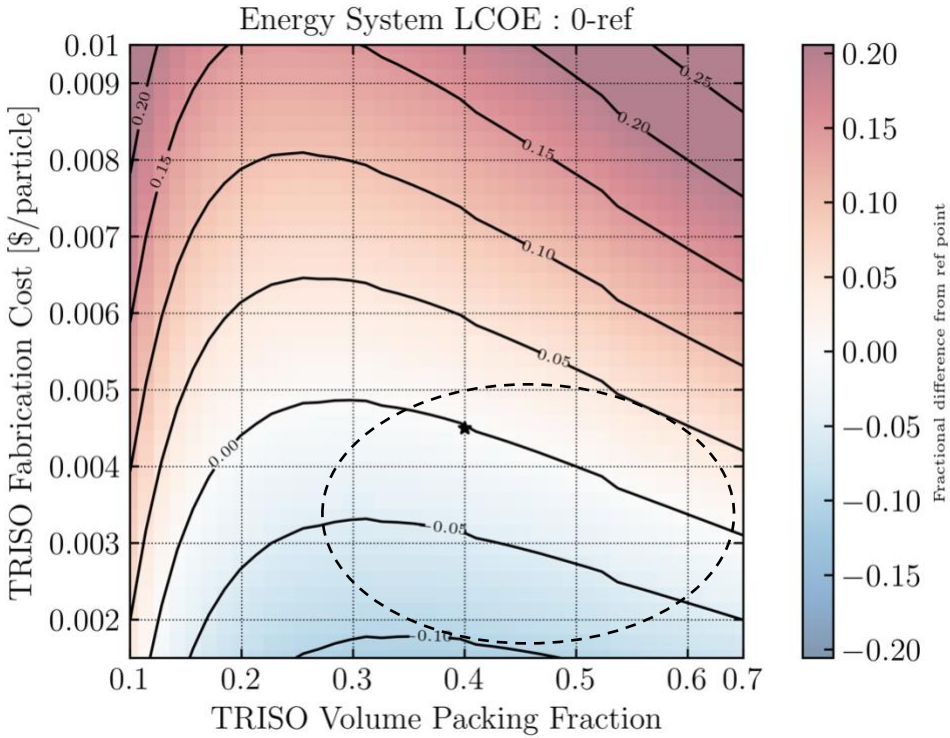


Figure 40 Fuel fabrication cost vs packing fraction. Circle represents TCR packing fraction and the potential for significant fuel fab cost reductions as the process is commercialized and fuel is produced at scale.

6.4.2 Fuel Capability: Higher Temperature Fuels w/ Enhanced Radiation Tolerance

AM fuels may offer enhanced temperature and radiation tolerance to achieve higher burnups, power ratings, and power densities. TRISO fuel is survivable to 1600 °C in benign chemical atmospheres. AM fuels may push the temperature limits a few hundred degrees higher with better chemical tolerance to water and air. Higher temperature limits or greater thermal conductivity of the fuel could increase the allowable power rating of a reactor, often limited by fuel temperatures during accidents. More relevant to operations, improving the maximum thermal gradients and thermally induced stress can reduce TH costs by reducing coolant volume and pumping powers.

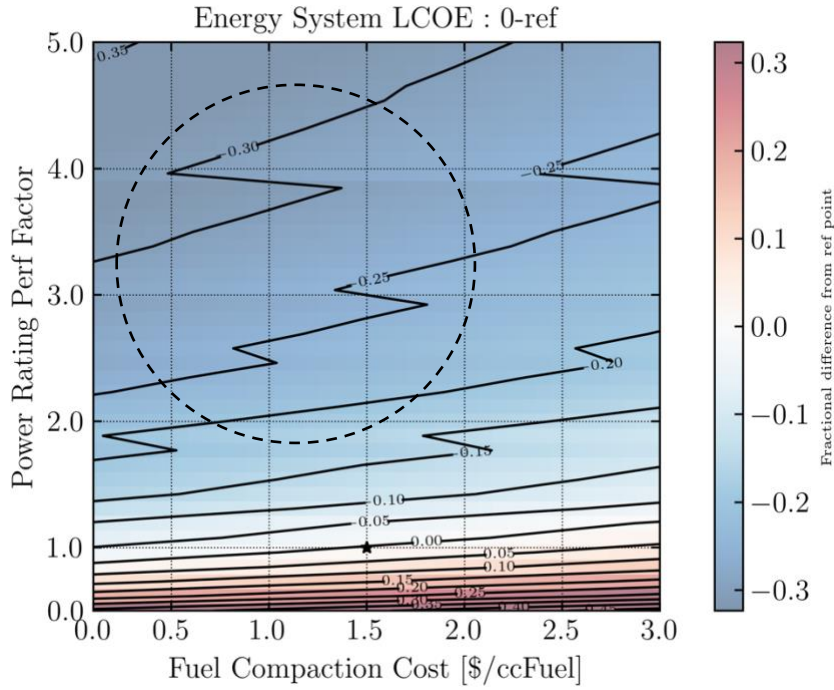


Figure 41 Fuel fabrication cost vs RX power. Circle represents the fuel fab cost reductions that can be expected as TRISO fuels achieve commercial scale production with related learning and automation. Micro reactor designs including MMR and eVinci have are exploring power uprates to reduce LCOE.

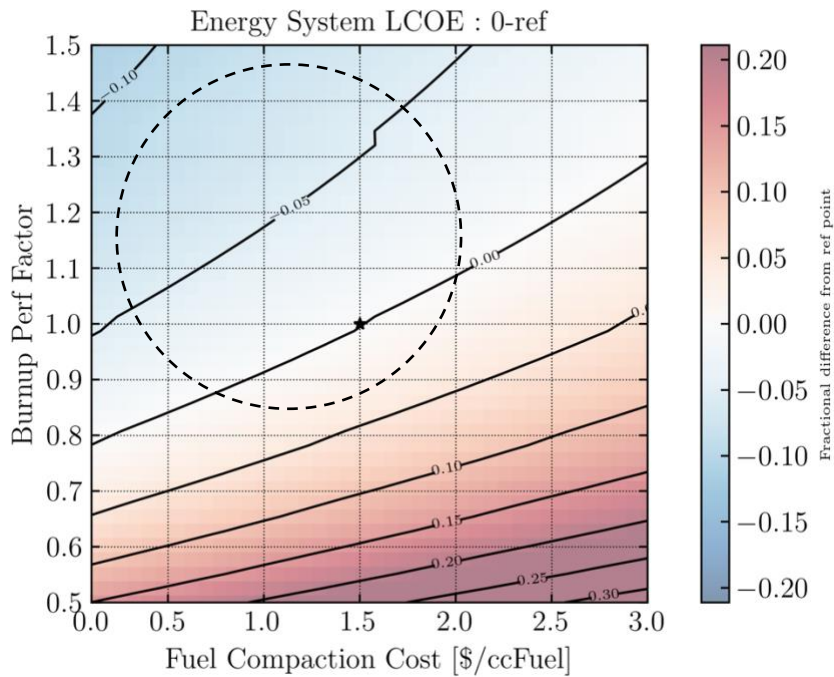


Figure 42 Fuel compaction cost vs Burnup gain. Circle represents the fuel fab cost reductions that can be expected as fuels achieve commercial scale production with related learning. Improved core designs, larger cores, improved moderators suggest burnups can increase.

6.4.3 Fuel Shuffling

Most plans for micro reactors are for once through fuel cycles. Shuffling or recycling fuel blocks may offer reductions in fuel needs by achieving higher burnups, though I could expect lower energy content per core refueling. The trade in Figure 43 reveals steep LCOE reductions for lower fuel cartridge cost. Burnup gains are more important at higher core cost. Perhaps one to two-thirds of a used core can be reshuffled, similar to other HTGR fuel shuffling schemes.[147] The powerplant site could have a fuel block shuffling system where fueled graphite blocks are shuffled. Or, if avoiding on-site fuel handling and storage, used core cartridges could be shipped back to a cartridge assembly center, rearranged with new fuel blocks, and sent out as a fresh cartridge. For particularly robust fuel forms, there could be opportunity for pellet level shuffling schemes where fresh and used fuel pellets are intermingled. This is not considered an option in other reactor types, and I do not yet speculate at the potential burnup effects.

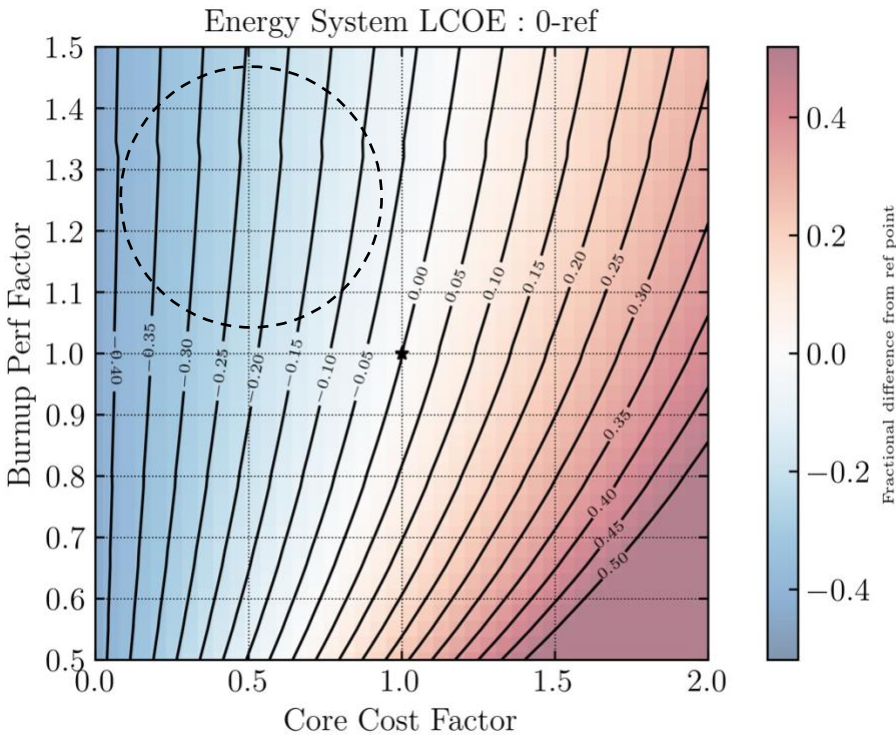


Figure 43 Core Cartridge Cost vs Burnup gain.

6.5 Moderator

Graphite is the established HTGR moderator due to its high availability, long operational history since the first Chicago-Pile, ease of forming and machining, high melting temperature and heat capacity, and overall excellent performance as a high temperature moderator up to about 30 dpa. The main drawbacks for graphite are non-uniform expansion and contraction and radiation induced changes in thermal and structural properties. There are more mass efficient moderators like Beryllium metal, but these are prohibitively expensive as of 2022, except for the space systems for which transportation cost, relative to Earth, is on the order of 300 times higher for Low Earth Orbit and 2000 times for a Mars deployment. Beryllium metal has some temperature, dpa, and swelling limitations.

AM moderators under development include canned metal hydrides, both Zirconium and Yttrium Hydride, and composite moderators which can include entrained hydrides or beryllium compounds. Canned metal hydrides consist of a metal hydride placed in a cladding that can withstand the partial pressure of the hydride at the design temperatures.[148] Composite moderators are multiphase composites, having a moderating entrained phase, like ZrH or BeO, encapsulated within a stable matrix like SiC or MgO.[139] [149] [140] The matrix has low neutron cross section, low gas permeability, low chemical reactivity, good radiation stability, good strength, and thermal conductivity.

[141] provides a good history of neutron moderators for gas-reactors and describes methods for manufacturing composite moderators such as MgO-ZrH and MgO-Be. The impetus for developing new moderators is to reduce core volumes, improve burnups, reduce enrichment requirements, and improve damage thresholds.[140] This is very similar to the fuel and core design goals mentioned in the previous section, and the LCOE effects of these developments can be observed in the same trade studies shown in Figure 43. Note that for MMR-like designs, the moderator makes up about a quarter of the core internal capital cost and can therefore experience proportionally greater cost factors for the burnup gains than those shown in Figure 43 to achieve the same LCOE effect.

To find the potential savings of composite moderators for MHTGR, [140] attempted a three-batch fuel cycle estimate limited to criticality optimized fuel to moderator ratio (F/M), which would not account for a more complete LCOE consideration and the secondary effects due to changed refueling intervals, reactor dimensions, or power rating. The relation between criticality, burnup, and core energy content is not straightforward, which makes criticality optimized F/M ratio not a DFC optimized choice. By using criticality optimized F/M ratio, the study changes the fuel loading, burnup, and refueling interval with unaccounted LCOE effects. In their analysis, they find composite moderators could reduce electricity costs by 12-23% at the same system and moderator cost. In terms of burnup, they find composite moderators can increase burnup from 132 MWd/kg to 171 MWd/kg, a factor of 1.3. In this analysis, Figure 43 can be used to assess the effects of improved burnup at the same system cost. I observe 3% LCOE reduction for a 1.25x higher burnup value at the same system cost.

Compared to nuclear grade graphite, it is not clear how composite moderators would fare in cost per kg, let alone cost per slowing down power or cost per MWh as they are still early in development. The fabrication process for a composite moderator includes more feedstocks and process steps compared to forming a graphite billet and machining it. And a composite moderator would probably have to undergo a heated inspection test beyond the operating and accident temperatures to ensure gas entrapment at the design pressure. But there are several capital cost advantages for composite moderators. First, there is no machining step to place fuel and coolant channels as in a graphite block. Advanced moderators may be formed in simple cylindrical shapes contained within a TCR-fuel element, or even in other arbitrary shapes amenable to pressurized sintering processes and dies. Composite moderators might even be formed in a similar binder jet and CVI method as a TCR fuel form. Second, advanced moderators will have greatly reduced volumes and mass per core, thereby reducing the inspection and assembly burden. The critical core volume for different moderators is shown in their report with optimized fuel moderator ratios from [141]. The composite moderators could reduce core volumes by 30 to 60%, thought this is not at the same core energy content or power rating but is at least suggestive of moderator volume reductions. Third, the forming process for a composite moderator requires lower sintering temperatures of roughly 1000 °C, compared to graphite's 2800 °C. Lower process temperatures will lead to lower energy costs for forming, though one would need to account for the lower mass and higher heat capacity of the composite moderator.

A final potential capital cost advantage for composite moderators is QA reduction of the feedstocks. The concept of entraining a highly efficient moderator within a gas-tight, structurally, and thermally stable, radiation tolerant, and chemically inactive matrix reduces the purity and quality control requirements of the moderator material. For graphite, much attention is paid to radiation induced effects to its strength, volume, and thermal conductivity requiring extensive lifecycle modeling and testing of the component and strict control of the composition, grain size, porosity, and dimensional tolerances. A composite moderator's matrix will be radiation stable in terms of thermal and structural properties. The matrix will cushion property changes and contain gases. In essence, a composite moderator is like an FCM moderator, and can, to some extent, contain property and isotopic changes occurring in a moderator that can be made from materials with reduced QA. This could reduce coolant contamination and avoid graphite dust complications, though potentially introduce SiC or MgO dust issues. In terms of safety, the composite moderator eliminates air and water interactions that affect graphite, reducing the safety significance of the pressure boundary.

A significant advantage of graphite is its high specific heat capacity and thermal conductivity which buffers thermal transients during accidents. Many of the advanced moderators proposed will have higher specific heat, but lower thermal conductivity and lower moderator to fuel volume ratios. This will affect allowable power ratings. [140] looked at pressured and depressurized loss of forced coolant accidents in a fixed geometry and power of MHTGR and found maximum fuel and moderator temperatures for composite moderates that were comparable to graphite.

6.6 Core

6.6.1 Core Dimensions

Not entirely related to AM techniques, a few figures are provided to show 2D trades relating to the core dimensions. In Figure 44, The top row shows the core energy content and RX power, confirming the expected behavior of a CA-HTGR. The bottom row gives the LCOE and shows the baseline design is close to a LCOE local minima. With other input design parameters held constant, there is minimal benefit no benefit to increasing the core diameter unless there is also an increase in operating pressure, aspect ratio, or fluid temperature gain. For this CA-HTGR, Figure 46 shows how fuel temperature becomes limiting for lower maximum fuel temperature and reduced radius. Otherwise, the power density scales with the surface area. The baseline design has significant margin on the fuel temperature. Figure 47 shows LCOE for the same trade.

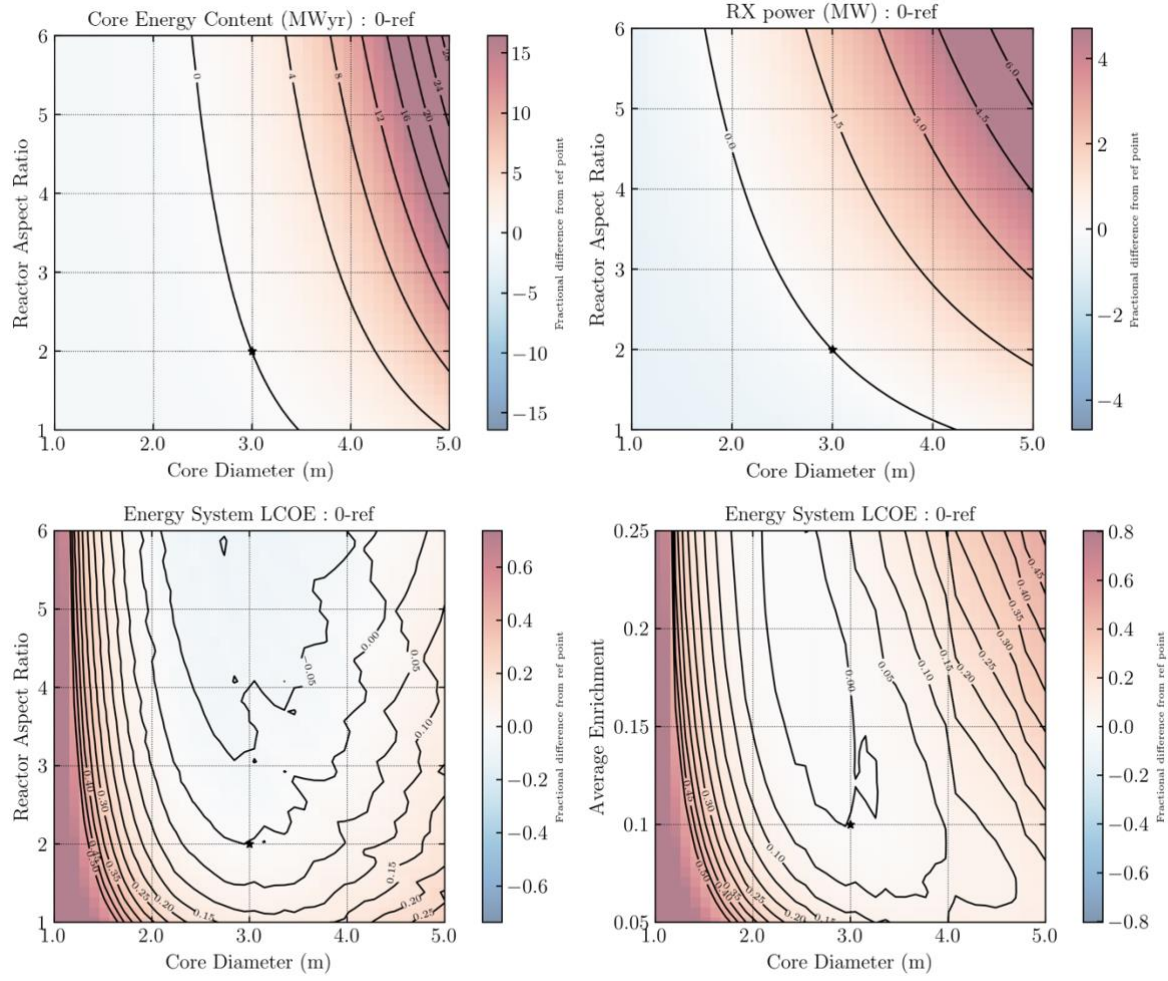


Figure 44 Core dimension against various design parameters. Top left: core energy content, top right: RX power, bottom row: LCOE.

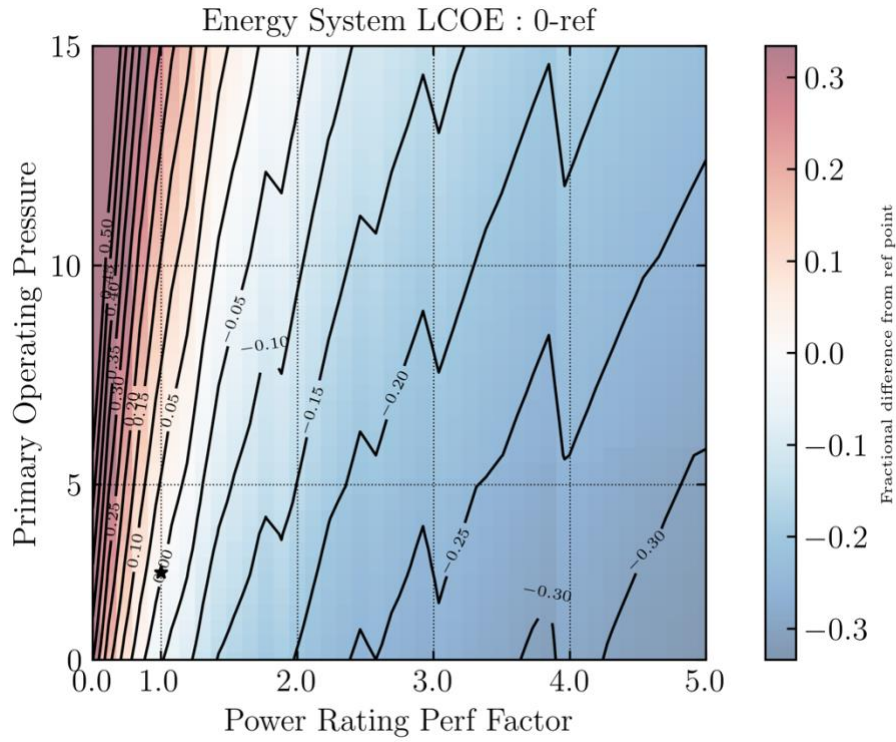


Figure 45 Power uprate versus primary pressure, showing LCOE.

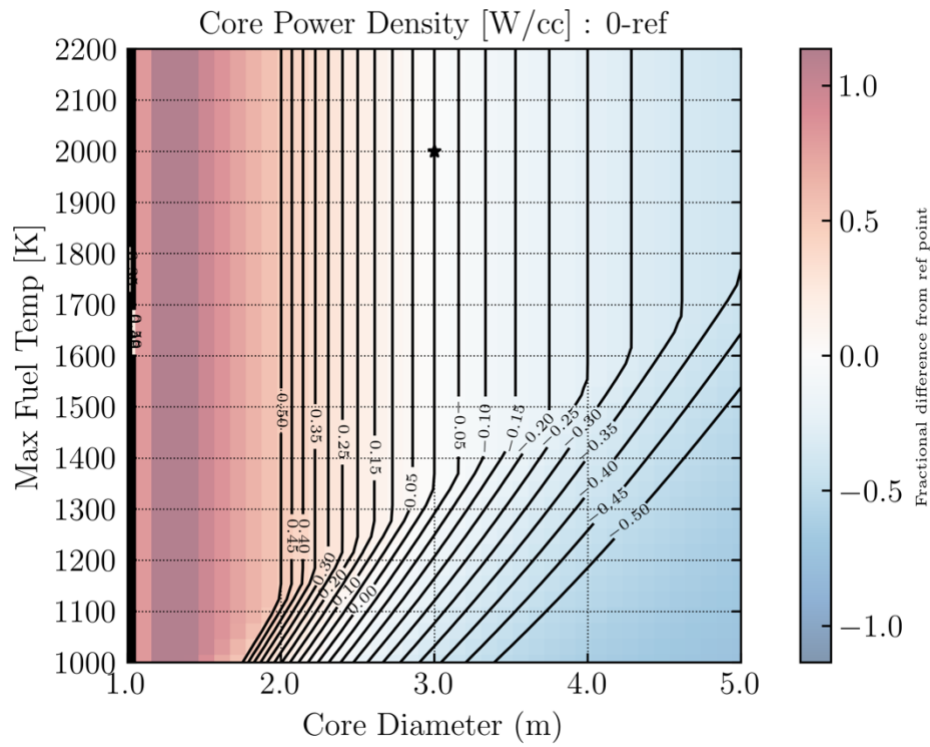


Figure 46 Core diameter vs maximum fuel temperature showing core power density.

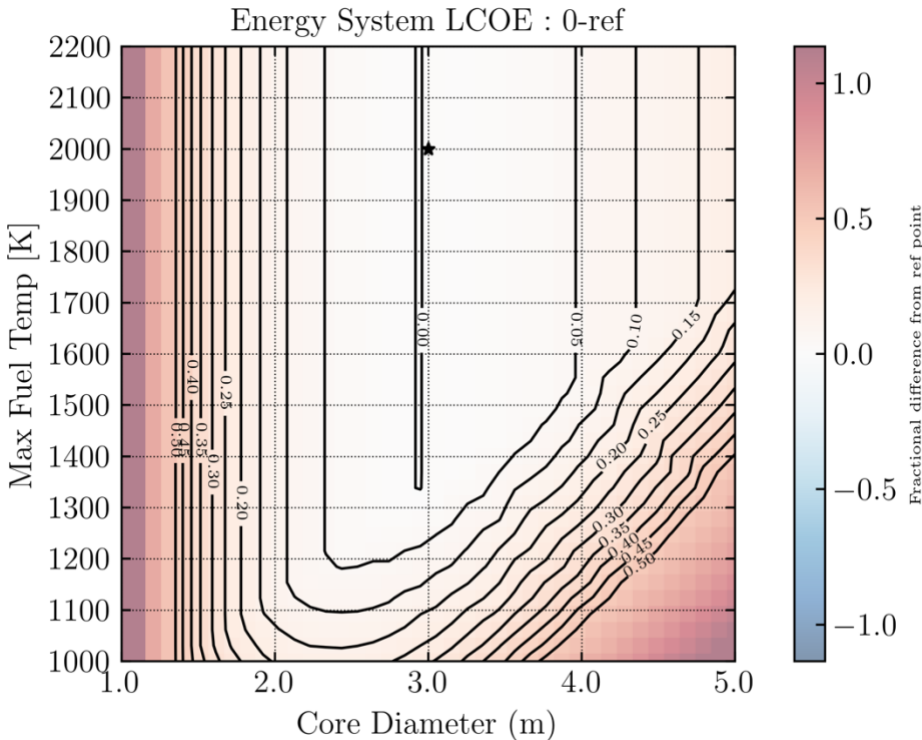


Figure 47 Core diameter vs maximum fuel temperature, showing LCOE.

6.6.2 AM-Enabled Core Design

AM fuels like the TCR fuel form may allow for arbitrary core configurations with fuel, coolant channels, moderator, and poisons placed in topologically optimal formations that consider thermal and neutronic coupling to achieve more favorable average burnups, fuel loadings, and power ratings. A core might be segmented into voxels at the millimeter scale, with each voxel containing either fuel, moderator, coolant, or poison. Similarly, enrichment or porosity might be varied precisely in each voxel. AM-enabled core designs might utilize topology optimization [150] [151], gap conductivity features, improved heat removal, uncertainty reductions by virtue of greater dimensional control, core heterogeneities, and feedback.[152]

Beyond the TCR binder jet fuel form, an enabling AM technology is laser powder bed fusion (LPBF) with individual machines currently able to deposit on the order of 30 kg per hour with sub millimeter resolution. Such systems are available from various developers including GE Additive, Desktop Metal, and Seurat Technologies. Combined with precision powder deposition and on-the-fly pattern modulation, laser powder bed fusion may eventually allow fully specifying materials and processing conditions for each millimeter-sized voxel of a component. LPBF can be adapted to deposit many different materials including metals and ceramics.[153] Multi-material structures with compositional grading and property modification have already been demonstrated.[154]

Manufacturing arbitrarily defined cores appears to be a likely possibility in the near future, but core designs and methods have not yet been developed to exploit these future capabilities. As a result, I do not know what performance gains can be expected. But performance gains may become increasingly important for nuclear core design as civilian nuclear reactors trend towards smaller and safer cores that improve passive safety capabilities and economies of reactor production but suffer from increased neutron leakage and reduced burnup.

Figure 6 shows the possible pareto fronts for different core design paradigms suggesting the performance improvements of an AM-enabled core design through topology optimization. The pareto front represents the outer boundary for the performance metrics selected. For nuclear cores, the pareto front might be defined in more than 2 performance dimensions, but two useful dimensions are core dimension and burnup or core dimension and core energy content. Core energy content is the total energy that can be extracted from the core. Successive design paradigms expand the pareto front into previously unobtainable performance spaces. An important shift in the last decade has been the emergence of parametric design in space reactors including nuclear thermal propulsion and transportable reactors that have allowed increasingly smaller cores using HALEU instead HEU. [155] Topologically optimized cores may further expand the pareto fronts for nuclear cores allowing for cores of reduced size, greater energy content, or lower enrichment – important trends for implementing cost-effective infinite coping time reactors.[151]

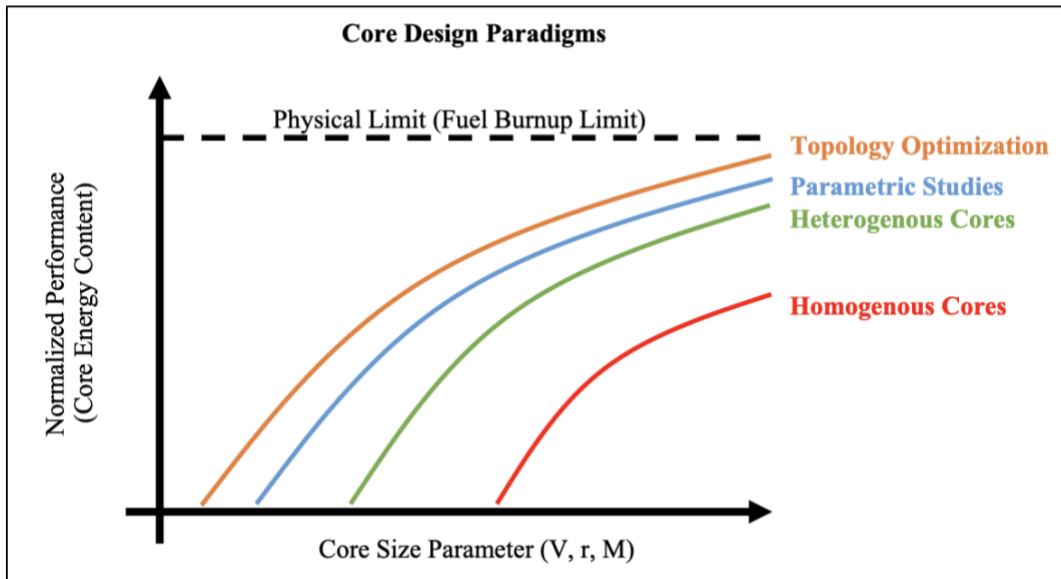


Figure 48 Illustrative best performance curves for different core-design and core manufacturing paradigms. New moderators are likely to have more pronounced effects.

Topological design for thermal considerations and AM fuel's shorter thermal paths can reduce fuel temperatures and peaking in the fuel across the core. TCR fuel element cooling channel design has been studied without topological optimizing techniques [156], but has undergone a conceptual optimization for reduced temperatures and pressure drops. Specifically, TCR fuel form uses a Y-shaped block with internal and external cooling channels to reduce the thermal path between fuel matrix and coolant, which is ordinarily some thickness of graphite, to a direct contact with the coolant, not unlike annular fuel forms in HTTR. The binder jetting of SiC could allow for small and even micro channels to be shaped into the fuel element enlarging the cooling design space. This also allows for axial and radial core channel tuning to reduce peaking factors and maximize the core energy content for the a given fuel loading.[157] Fuel temperature and peaking reductions can improve burnup and power rating. While micro reactors like MMR operate at sufficiently low power densities that fuel temperature effects do not significantly reduce burnup, the TCR fuel form could allow for shorter path lengths from heat generating regions to coolant flows, reducing temperatures, and allowing for higher fuel power densities or burnups. With improving cooling options, a designer will choose between lowering temperatures, reducing pressure drops, or increasing power rating or some DFC mix of the options.

The possibilities of topologically optimized cores can be seen in Figure 41 and Figure 43. Figure 41 shows the fuel fabrication cost against RX power rating, the most effective way to make use of a more capable fuel and core design. A 50% greater fuel fabrication cost will achieve cost-parity if power rating can be increased by 10-20%. Burnup changes by any method are shown in Figure 43 where a burnup gain is applied at a given fuel fabrication cost. Core design improvements would improve burnup opportunities, but the LCOE reductions are not breathtaking.

6.7 Heat Exchanger

There is interest in a variety of HX types for HTGR systems to support both single phase to single phase heat transfer as well as single phase to two phase heat transfer. In particular, designs exist for heat exchange systems from Helium to Molten Salt, Helium to Helium, Helium to Nitrogen, Helium to Steam, and Molten Salt to Steam. Different applications require different configurations. For example, a process heat application would probably require an intermediate loop between the primary coolant and the steam generator. In the case of NGNP, this was a second Helium loop, while for MMR, this is a molten salt loop. Both have steam generators for electrical power conversion though some other designs employ Brayton cycles. The current state of the art is Compact Heat Exchangers (CHX) which offer high heat transfer density, small size, and thin pressure boundary sections compared to Tubular Heat Exchangers (THX). Printed circuit diffusion bonded heat exchangers are an available technology, for example from Heatric in the UK.

Heat exchanger design considerations include the inlet and outlet conditions for the hot and cold fluids, effectiveness, pressure drops, total volume, total mass, and transient performance. The HX must carry the full thermal load and accomplishes this at a maximized delivery temperature and minimized reactor outlet temperature. Various previous work for micro channel HX optimization exists from [69] and [158].

6.7.1 Topological Optimization for Mass and Pressure Drop

From the manufacturing side, there are a few reasons to expect that AM-enabled HXs will be lower in capital cost. First, topologically optimized HX designs may reduce feedstock use by removing unneeded structural or corrosion allowance material, making better use of a given mass in terms of increased specific heat transfer and specific pressure drop. Topological HX design is a growing field.[159] [160] Current HXs are significantly manufacturing constrained, with channels and plates shaped to what is readily manufacturable with large margins on structural supports. Beyond reducing the feedstock quantity, AM-enabled HX may use lower quality and less costly feedstocks.

In terms of operations, Topologically Optimized AM-HXs may reduce pressure drops, in turn reducing the parasitic power used by the circulators as well as the capital costs associated with a larger circulator being the circulator itself, power management, circulator cooling. Pressure boundary components should be unchanged at the same pressure.

6.7.2 Part Integration

AM-HX may integrate surrounding components to reduce part counts, reduce assembly time, eliminate manual welds, and reduce QA and inspection costs – considered here as the capital costs of the HX. Specifically, an AM HX could integrate plenums, inlet/outlets, insulation layers, pressure boundaries, and mounting brackets. This can reduce capital costs by reducing the assembly, QA, and inspection steps during fabrication. AM-enabled part integration in the HX and circulator system can reduce the operating costs through reduced maintenance and outage costs.

6.7.3 Alloy freedom

HX for nuclear applications are usually made in SA 316, but high temperature alloys can also be used such as Inconel617, Alloy 230, HastelloyX, and Alloy 800H.[161] Very high temperature applications may require silicon carbide or other ceramics. [143] Many AM additive methods have greater versatility in terms of which candidate alloys and materials can be used. Additive methods also tend to accelerate alloy development times. This will be helpful for a HX aiming to achieve higher temperatures and power cycle efficiencies and better reliability for lifetime operations or thermal cycling. Thermal cycling capability can reduce maintenance costs for dispatch micro reactors in which power level may be varied relatively frequently compared to traditional reactors.

6.8 Vessels and Large Metal Components

HTGR have multiple large steel components serving as pressure vessels, pipes, and structural components. Reactor Pressure Vessel (RPV) holds the Core Barrel Assembly (CBA) which holds the graphite fuel elements. The CBA is usually used to create an insulating inlet cold leg on the RPV that rises along the inside of the RPV. The same approach is taken in the primary Heat Exchanger which holds a HX and helium circulator on the cold leg to reduce the circulator temperatures. Together, these components can make up roughly 15-25% of a micro reactor's nuclear plant capital costs.

Nuclear pressure vessels are currently manufactured using plate and weld techniques with a range of costs depending on the dimensions and suppliers. Post-processing steps include heat treatment, welding, machining, and inspection. Large vessels greater than 4 meters present extra difficulties for transport from factory to site. To expedite first deployments, Reactor Pressure Vessels are currently constructed using materials and designs governed by current ASME code, limiting the selection of materials and operating temperatures to SA-508 and an upper temperature of 450°C. The lead time for a small or medium-sized RPV is one to two years. Once operating, vessel welds require frequent inspection with related operating costs and physical access requirements built into the reactor cavity design.

Like AM-enabled HXs, AM-enabled vessels and large metal components can reasonably be expected to experience capital cost reductions. Recent developments at EPRI with e-beam welding may lower RPV costs for large vessels by up to 40% for vessels less than 3 meters in diameter and 110 mm thick based on a 90% reduction in welding time.[92] Beyond E-Beam welding, other AM methods like PM-HIP, WAAM, and LPBR could be used for vessels and large steel components making up the pressure boundary for micro reactors. Relativity Space's WAAM machines can achieve print dimensions 6 meters in diameter and 12 meters in height, with thickness of 3 cm, and smallest feature size <.5 cm. These capabilities put micro reactor vessels well within the building constraints of WAAM.

Even traditional techniques like seamless extrusions or plate and weld could achieve significant scale economies for very large deployments. Natural gas pipelines use .2 to 1.2 m inner diameter with pressures ranging from 3 to 22 MPa, compared to a prototypical micro reactor like MMR's 3.2 m diameter and 6 MPa. To illustrate the massive scale of production, I note the Nord Stream Pipeline is made up of 200,000 sections of 1.2 m pipe made by plate and weld methods, each weighing 24 tons and up to 3.4 cm thickness, comparable to MMR's 34 tons and 3 cm thickness. Full scale plate and weld manufacturing may be the most effective RPV manufacturing system now possible.

6.8.1 Part Integration and Weld Removal

An AM vessel could remove the need for in-service weld inspections offering, one of the few inspection events occurring during micro reactor operations. Reducing or removing the need for inspection events will be decisive for future fully autonomous reactor operations. AM vessels may allow for cost reductions in manufacturing by removing the weld and inspection steps associated with added brackets and penetrations. Brackets and alignment features on internal and external surfaces can be printed in a single print rather than welded after. There may also be an opportunity to combine the RPV and CBA into a single component, simplifying the assembly of the reactor and reducing reactor assembly steps. In particular, the CBA for MMR is nearly 60% of the mass of the RPV itself. Integrating the two components, while maintaining the CBA and RPV's functions could reduce the total mass of the CBA and RPV system by up to 40%. The CBA functions primarily as a flow separator and structural support for the core, and both roles could be partially supported by a more capable RPV design. RPV cooling could be achieved by adding internal cooling channels similar to rocket nozzles.

Some HTGR reactor designs may use direct Brayton cycles [53] in a horizontal or vertical co-axial configuration, the main benefit being simplification, part removal, thermal and structural symmetry. Similar horizontal co-axial configurations have also been proposed for a horizontal steam generating HTGR [64]. The main drawback may be more involved turbomachinery or HX servicing, due to the proximity to the nuclear core and possible activation. In both cases, complex flow manifolds and support structures may be useful to achieve co-axial configuration and AM methods like WAAM may aid the prototyping and final component manufacture of these structures.

6.8.2 Topological Design for Mass Reduction

AM-enabled vessels may take advantage of mass reduction techniques from aerospace like isogrids or orthogrids which suggest 15-30% mass reductions compared to a standard vessel in various aerospace applications.[162][163][50] Reduced mass vessels will reduce material costs and could have knock-on cost benefits on transport, civil, and structural costs. For most manufacturing processes, mass reduction of final component is equivalent to a reduction in feedstock cost. Isogrids are usually machined in plate and bent to shape, and savings must be obtained by recycling chips. However, for AM processes like WAAM or LPBF, mass savings would reduce the primary feedstock, albeit with some powder recycling inefficiency. AM vessels can further reduce mass with optimized shapes that maximize volume/mass for a given pressure. Just using spheres versus cylinders achieves a 15-25% (see Appendix: 10.9) mass and feedstock reduction for the same enclosed volume and pressure. Spherical reactors and cores are only likely to be an option for AM fuel/moderator blocks designed to sit in spherical surfaces with new TH designs for cooling channels and plenums. In total, there is potential for 30-55% pressure boundary mass reduction that could achieve a similar percentage feedstock and manufacturing cost change for AM-enabled vessels. Still, a 50% RPV cost reduction yields only a 2.5% LCOE reduction (see Figure 49) in our model.

Beyond reducing the vessel cost associated with mass, lower vessel mass reduces the thermal resistance for decay heat transfer, potentially allowing for some power uprate unless the decay heat accident is limited by the thermal mass of the system. See Figure 50 for a pertinent trade.

6.8.3 Topological Design for flow (CBA, plenums, orificing, veins)

AM offers new design opportunities like optimized plenums or vein features that could reduce pressure drops, and improve flow conditions and temperature distributions.[164] Lower pressure drops reduce circulator size and power draw. Improved temperature distributions will reduce peaking factors and hot streaks and could improve fuel utilization and safety. Figure 49 shows the LCOE changes from reduced pressure drops for different pressure boundary cost factors. The circle represents the possibility of reduced pressure drops from integrated vessels with AM-enabled flow features and plenums. The cost of the AM-vessel is unclear as per kg costs are near or greater than traditional methods but could be offset by part integration. Even so, AM startups interviewed by the author claimed costs per kg can be reduced by a factor of 3 compared to forging, with sufficient R&D and scale production. Perhaps more relevant than predicted LCOE changes, is the extra design space allowed by adding flow features and engineered plenums to achieve improved margins.

6.8.4 On-site RPV or large steel component manufacturing

Additive Manufacturing techniques for large components may offer significant cost, performance, and supply chain advantages over traditional vessel manufacturing techniques. An additive vessel could allow for on-site manufacturing of the vessel, removing the need for transport and related inspection requirements. For example, a large WAAM or wire weld system used by Relativity Space weighs less than 5 tons and could create steel structures of on the order 50m in height with sufficient material feedstock. It's an open question if heat treatments can be effectively applied at that scale. That said, transport accounts for up to 1-2% of the micro reactor capital costs with the RPV making up roughly just 2% of the transport cost, so RPV mass reductions will have small effects on transport costs, at least for terrestrial micro systems.

A larger on-site manufactured AM-enabled vessel was not considered in this model. If the micro reactor is sized for relatively available transport methods by road and rail, this will limit the diameter and length of the vessel, with significant drawbacks on achievable burnups, total power level, vessel radiation damage, and fuel loadings. There may be significant burn-up and power rating benefits from a vessel built on-site with reduced size limitations.

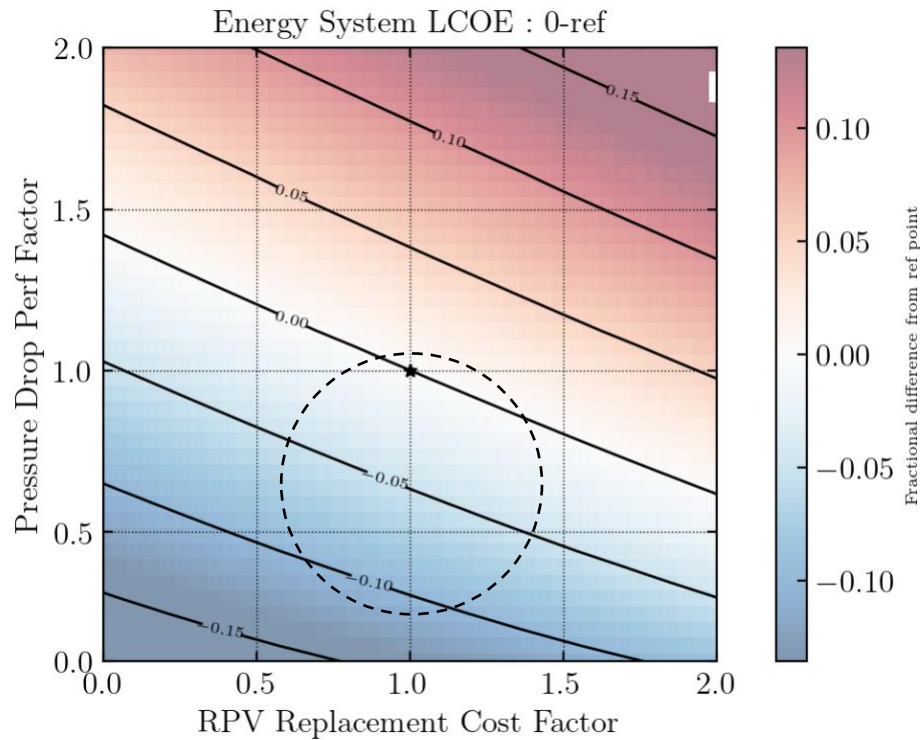


Figure 49 Pressure Boundary Cost vs Pressure Drop factor.

6.8.5 Heat Transfer Features

AM vessels could also incorporate new thermal design features to enhance heat transfer during accidents. These features could be turbulence inducing flow structures, features that increase surface area, or topologically optimized structures for natural circulation [165] under the particular accident conditions. For small CA-HTGR, the RPV heat flux can be the power limiting component. Figure 50 gives the pressure boundary cost traded with RX power rating, showing steep advantage for power uprates even at up to a relative 2x the factor for the RPV.

Another possibility is thermally expanding features that increase heat transfer between the core and RPV, either by conduction or convection aiding flow structures. Designers should be aware that reactivity will increase with reducing temperature of the core, potentially leading to a cyclically criticality if the decay heat is extracted from the core too effectively. There is a careful balance between 1) removing heat from the core to prevent meltdown and 2) preventing the reactor from achieving criticality or exceeding temperature and temperature gradient tolerances in concrete cavity structures or other safety related systems. As a result, AM-enabled vessels might simply be higher temperature rated with insulative properties to keep the core warm. This requires careful analysis beyond the scope of this work. Overall, vessel heat transfer features could improve temperature margins during accidents or could be used to increase the reactor power rating while maintaining the same temperature margins.

We note the power uprates in this analysis would represent safety reduction because the reactor dimensions are not changed to conserve surface area to power ratio and RCCS or large thermal mass systems are not added to compensate for the higher power rating and proportionally larger decay heat source. Perhaps an AM-component may allow for power uprates without a safety downrate or extra RCCS capability, as in the case of a RPV thermal features or higher temperature fuels. Future work will consider power uprates at the same safety level, which means power uprates require reactor upsizing and possibly a power density reduction.

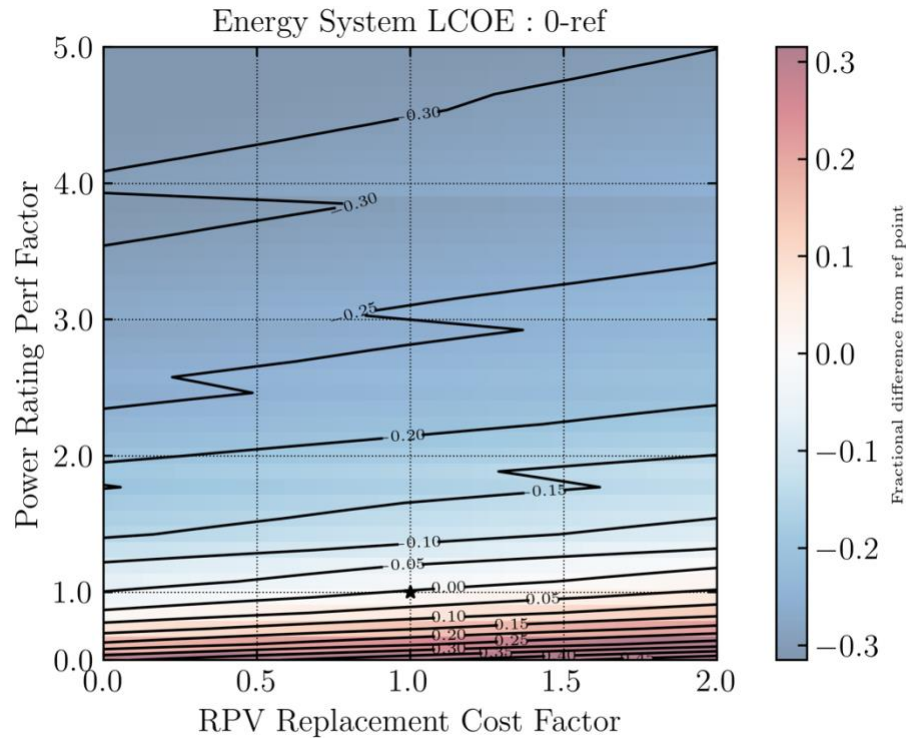


Figure 50 Pressure Boundary Cost vs RX Power rating.

6.8.6 Vessel Replacement Cost vs Damage Threshold

Micro reactor vessels experience higher dpa per energy produced than conventional large reactor vessels owing to greater neutron leakage from the core. A USNC MMR 3.2m diameter RPV is expected to last at least 40 years at 15 MWth, after which the vessel must be replaced or annealed – corresponding to 2 to 3 core’s worth of damage. A higher damage threshold can be bought at higher cost through greater margins like increased vessel thickness or increased shielding. Thermal annealing can reduce LCOEs even at lower radiation damage thresholds. The cost of annealing the micro reactor pressure vessel may be even lower than a 20% guess as the annealing may occur in-place with nuclear heat without removing the core or adding heaters. These results could change significantly when accounting for vessel disposal charges.

6.9 2D Trade Conclusions

These relatively simple 1- or 2-dimensional trade studies can be misleading as the analysis ignores multi-parameter change such as different enrichments and packing fractions at a different core diameter, pressure or temperature difference. The analysis is also limited by how the comparisons are made to the baseline design, and it is not obvious how similar trade studies would look like at a different design point. Regarding the LCOE effect magnitudes, it is note that many small effects can add up to significant effects. While 1-5% effects seem low priorities, achieving just a few of those effects can yield significant improvements.

7 Design Search and Populations

7.1 Problem Statement

The model outlined in Figure 22 constitutes a multi-input model with both continuous and discrete variables constrained to a specific range or set of options and produces various outputs. I use the model in a multi-input optimization problem to minimize just one of the outputs – the NOAK LCOE. Alternative value metrics to optimize could be the FOAK LCOE, the LCOE integrated over a planet wide deployment. I could also optimize with a multi-objective value function, such as minimum LCOE for at least a certain refueling interval or a maximum site area. The inputs include both the model world parameters like interest rates and feedstock costs and scaling rules, as well as the design-specific inputs. The model is deterministic with an unquantified uncertainty due to model assumptions and some unknowable error compared to future real-world implementations. I formally state the problem as follows:

Let the model be defined as a function:

$F: X \rightarrow C$, where X is the input space and C is the output space.

The optimization problem can be expressed as:

Minimize $F(x_1, x_2, \dots, x_n) = y$

subject to:

1. For continuous variables: $a_i \leq c_i \leq b_i, i = 1, 2, \dots, m$
2. For discrete variables: $d_j \in S_j, j = 1, 2, \dots, p$

where a_i and b_i are the lower and upper bounds of the continuous variables, respectively, and S_j represents the set of options for each discrete variable d_j .

$F(x)$ contains many discontinuities and conditional evaluations. Gradients are not easily obtainable, especially if I use more detailed calculations in the design estimates. Beyond the 2d trades in Section 6, I used grid evaluations and genetic algorithms (GA) to explore the input space in a few chosen worlds.

7.2 Random Sampling and Genetic Algorithm Populations

To explore the design space, I used uniform random sampling of the ranges for the base set of free parameters reported in Table 38, which is a significantly limited set of the available inputs but sufficient to observe the model's capabilities and limitations. All other input parameters were fixed, which defines the world and a large portion of the design inputs, as reported in Appendix 10.1 Table 41. Random sampling produces a diverse population of results compared to a discrete grid but does not guarantee evaluation of some desired combinations, such as the extrema of the ranges for each free parameter. Figure 51 and Figure 52 shows the LCOE distribution for 20,000 random sampling. Figure 53 to Figure 55 report the population of samples produced by a genetic algorithm (GA) with mutation and selection rate of 0.5, which concentrates the samples towards the minimizing fronts. The GA population history contains 64,000 samples.

I provide a few histograms of the GA population and resulting LCOEs in Appendix 10.3, filtered and colored by a given design parameter, both for free or dependent parameters. Because this is random sampling, the shape and magnitude of the resulting distributions are not particularly telling other than what could happen if designs were ever randomly selected, which does sometimes seem to be the case in the real world. The ranges of the resulting distributions are more interesting, reflecting rough bounds on what may be possible under a selected design choice.

Viewing LCOE against various design parameters in the following figures shows the large spread in possible outcomes and the existence of minima. there are plenty of ways to design a reactor with near equivalent LCOE, but many more ways to end up with much higher LCOE, even with this limited set of free parameters. However, when I constrain certain parameters further, for example by requiring a certain enrichment or refueling interval, the solution space thins out with fewer viable designs. This can be seen by constraining parameters in a parallel coordinate plot.

Table 38 Base set of free parameters and ranges for Random Sampling and GA evaluations.

Parameters	Range / Options
Net Electrical Power Target (MWe)	(5, 2000)
Project Lifetime	(60)
Operating Model	Low, Medium, High
Safety Class	Passive Class A, Passive Class B
Core Diameter (m)	(1, 5)
Reactor Aspect Ratio	(1, 5)
Reactor Shape	Cylinder
Reactor Orientation	Vertical
Average Enrichment	(0.05, 0.2)
TRISO Volume Packing Fraction	(0.1, 0.65)
Fuel Volume Fraction	(0.01, 0.1)
Turbine Max Size [MWth]	(5, 3000)
Primary Operating Pressure	(1, 15)
Primary Maximum Fluid Velocity	(20, 100)
Primary Inlet Temperature	(573,750)
Primary Outlet Temperature	(850,1200)
TRISO kernel material	UO2, UN

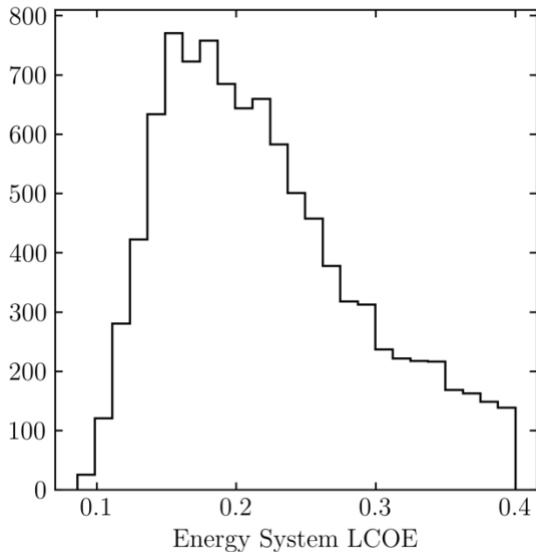


Figure 51 Distribution of NOAK LCOEs for uniform random sampling of the free parameters on the range [0,4] \$/kWehr.

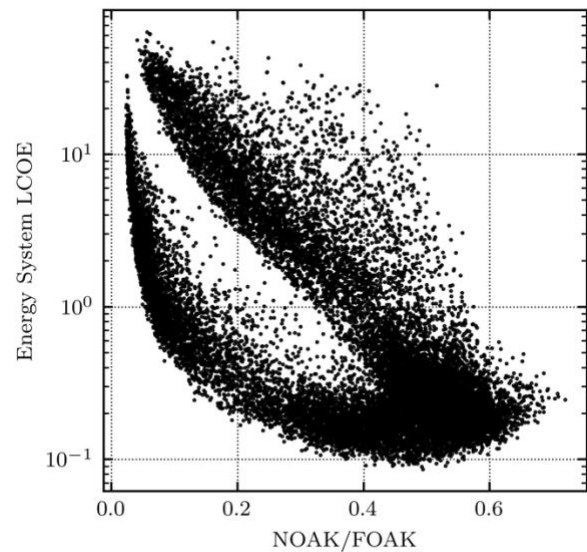


Figure 52 LCOE against NOAK/FOAK for random sampling suggesting optimal learning possibilities.

A few observations can be made for this specific world and the allowed free parameters. Economies of production are balanced by economies of scale in the power plant to create performative solutions in the middle, both through the design scaling and the cost scaling. LCOEs decrease for larger targeted electrical power for the Energy System. Larger power rating is favored with limited gains past 60 MWth, as shown in Figure 55. In terms of reactor dimensions, Figure 53 shows larger core diameters are favored but with diminishing best returns past 2.5 meters, if other parameters are free. Maximized aspect ratio gives the lowest LCOEs, sometimes to unrealistic lengths that would face control and TH challenges, not to mention transport limitations.

Low pressure is favored, as shown in Figure 55, perhaps an artifact of how the HX pressure drops are favorably estimated while RPV recurring expense are conservatively estimated. Reducing Helium pressure would be expected to increase OPEX through higher pumping power, increase CAPEX through larger circulator, and decrease CAPEX and OPEX through a reduced pressure boundary. It could be that the last trend is dominant in a high interest rate world and for the model's estimate of the pumping power, RPV costs, and circulator cost.

The solutions favor middling fuel loadings and refueling intervals on the order of 2-5 years, probably due to the high interest rate of 10%. Figure 54 shows minima in core energy content, core energy density, and the refueling intervals. High burnup is favored with limited gains past 60 MWd/kgU if other parameters are free. Packing fraction, fuel moderator ratio, and enrichment can be tuned for better results in a given financial world. It is not always best to maximize all three. UN is always favored, though the model includes no cost disadvantages for the use of UN over UO₂. Deviating from typical LWR LCOE, fuel cost is a large component of the LCOE in these solutions. This is due to the high starting price of TRISO-based fuels, and the fact I did not include learning effects on the OPEX including fuel and RPVs. The fuel cashflows are also debt financed, adding to the cost. UNF charges are also large, as I assumed the same dry-cask cost structure and volume packing as conventional LWR fuel.

To show the effects of a change in model assumptions, Figure 56 and Figure 57 show the randomly sampled populations under interest rates of 1% and 10%. The lines represent LCOE minima on a binned x-axis. Lower interest rates reduce the interest costs related to fuel, allowing longer refueling cycles to be more cost effective. In Figure 56, the LCOE minimizing refueling interval is longer for a lower interest rate. Figure 57 suggests that larger power levels are favored regardless of the interest rate, but with different dependence. This example shows that the characteristics of LCOE minimizing designs will be sensitive to the model assumptions. Claims of "best" designs and cost minimizing design parameters should be generally ignored unless they are supported by significant analysis across the model assumptions.

Overall, the population scatterplots show a wide range of possible designs and their resulting LCOEs which span about two orders of magnitude for the GA population and three orders of magnitude for random sampling. A closer look at LCOE against various design parameters suggests non-obvious trends and cost minimizing trades. It is also clear that there are cost minimizing designs in the given world and that costs will be sensitive to the various model assumptions.

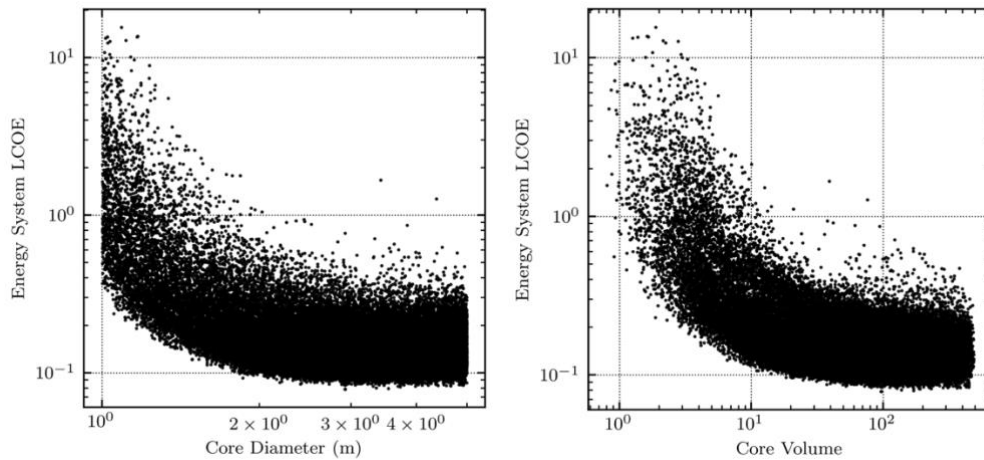


Figure 53 GA population scatter plots showing LCOE against reactor size parameters.

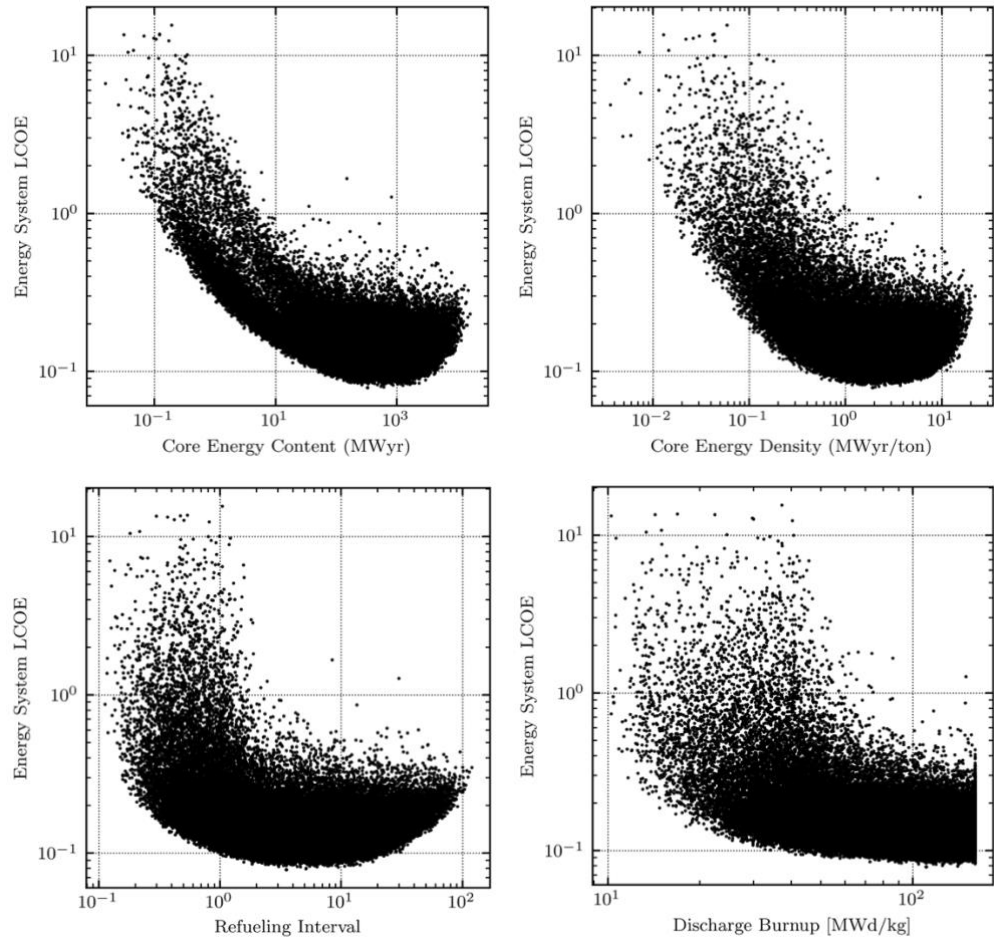


Figure 54 GA population scatter plots showing LCOE against core and fuel design parameters. Refueling Interval in years.

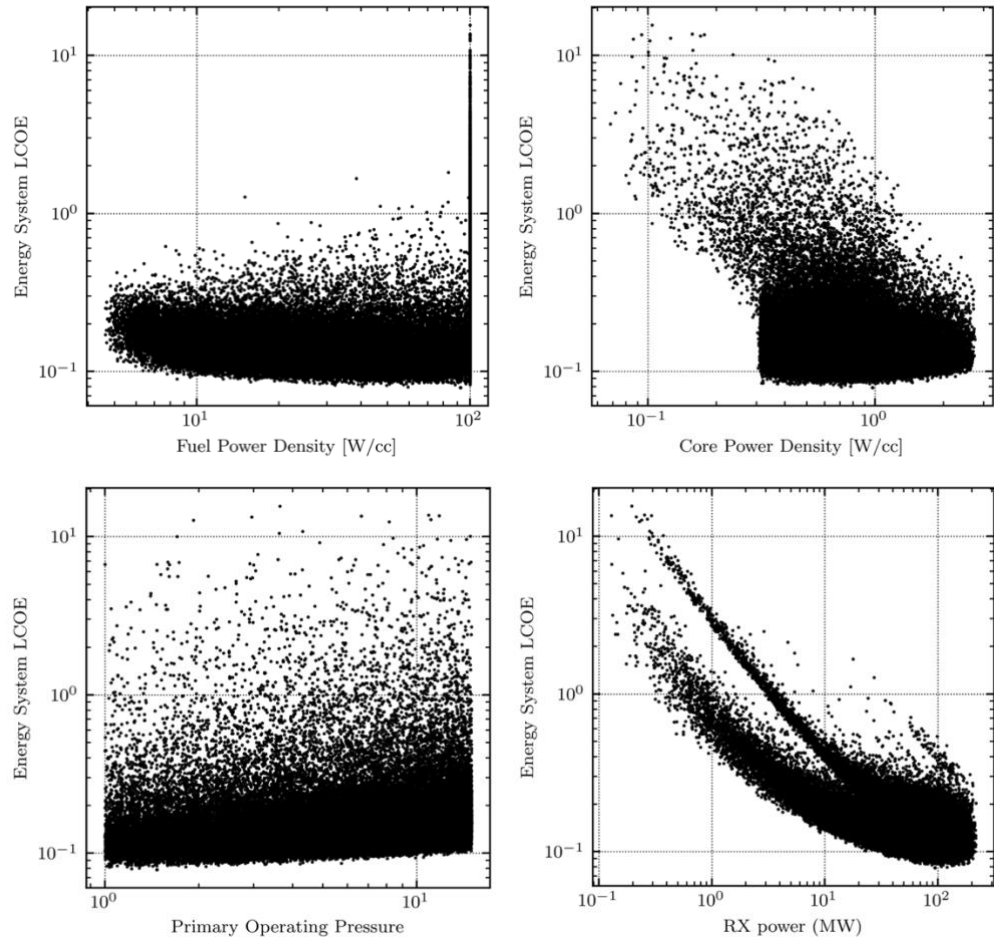


Figure 55 GA population scatter plots showing LCOE against thermal hydraulic design parameters.

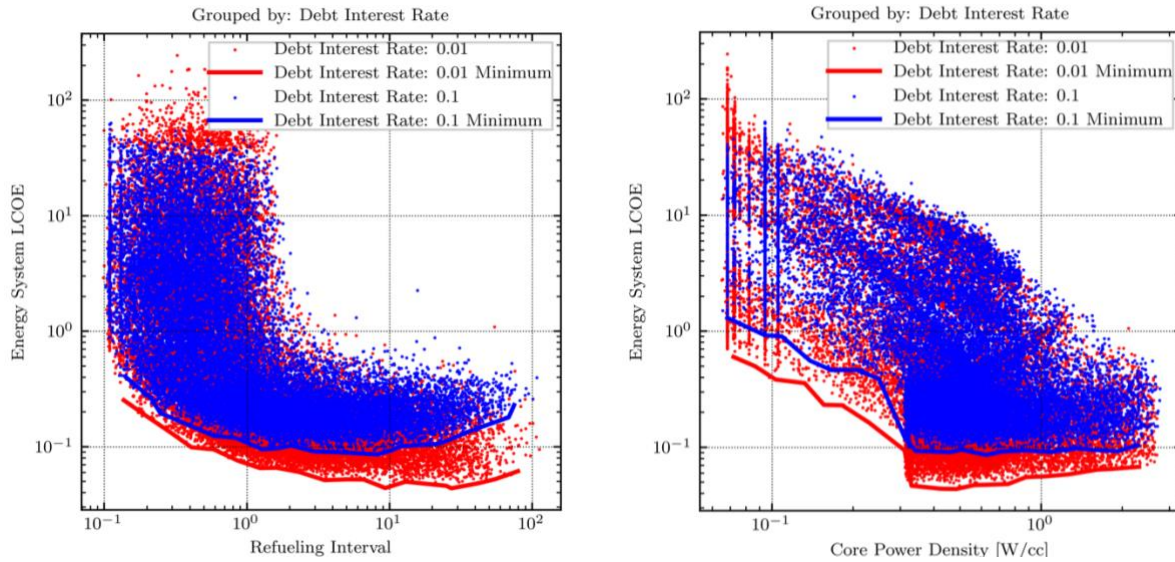


Figure 56 Random sample of the population of designs grouped by Debt Interest Rates, showing LCOE against refueling interval in years and core power density.

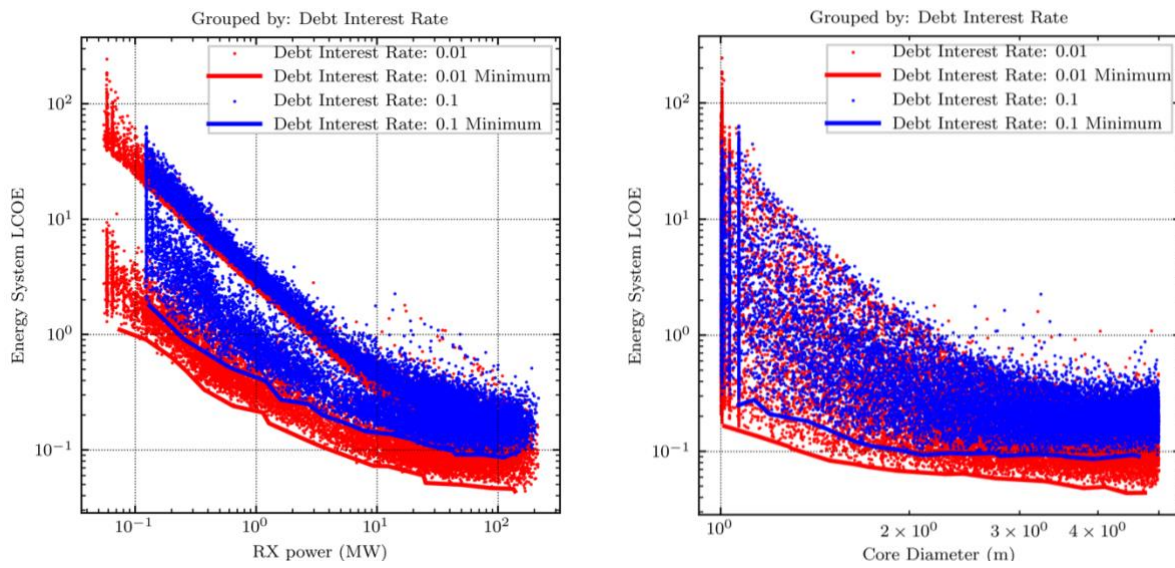


Figure 57 Random sample of the population of designs grouped by Debt Interest Rates, showing LCOE against reactor power and diameter.

7.3 Genetic Algorithm Search

GA is applied on the free parameters to find low LCOE designs with the specifications defined by Table 41. Starting with the base set of free parameters in Table 38, I defined the free parameter configurations listed in Table 39. The configurations explore some of the basic questions of the design space. How do low LCOE designs compare when constrained to different safety classes or different targeted Energy System power levels? What about different interest rates and core diameter constraints? The GA was run with a population of 1000, mutation and selection rate of .5, and usually converged after 15 generations but did not generally find strictly repeatable solutions as many of the inputs are continuous.

Table 39 Free parameter configurations.

Configuration	Base Set	Parameters Free Parameters	Constrained Value or Range
Active	Base	Safety Class, Operating Model	Active; Low
Passive Class A	Base	Safety Class	Passive Class A
Passive Class B	Base	Safety Class	Passive Class B
3.2m Diameter	Passive Class A	Core Diameter (m)	(1, 3.2)
High Interest	Passive Class A	Debt Interest Rate, Core Diameter (m)	(0.1), (1, 3.2)
Low Interest	Passive Class A	Debt Interest Rate, Core Diameter (m)	(0.02), (1, 3.2)
Target 10 MWe (Class A)	3.2m Diameter	Net Electrical Power Target (MWe)	(10)
Target 20 MWe (Class A)	3.2m Diameter	Net Electrical Power Target (MWe)	(20)
Target 50 MWe (Class A)	3.2m Diameter	Net Electrical Power Target (MWe)	(50)
Target 100 MWe (Class A)	3.2m Diameter	Net Electrical Power Target (MWe)	(100)
Target 200 MWe (Class A)	3.2m Diameter	Net Electrical Power Target (MWe)	(200)
Multi-unit MMR-like	MMR-like	Net Electrical Power Target (MWe)	(100)

The GA solutions for each configuration are shown in Table 40. Corresponding LCOE are shown in Figure 5. I can look at the design parameters in Table 40 and attempt to rationalize any trends and effects on LCOE. However, simple trends and explanations are not readily available given the large number of free and intermediate design parameters. I will prefer to conduct future statistical analysis for feature importance on uniformly random samples and populations of GA results.

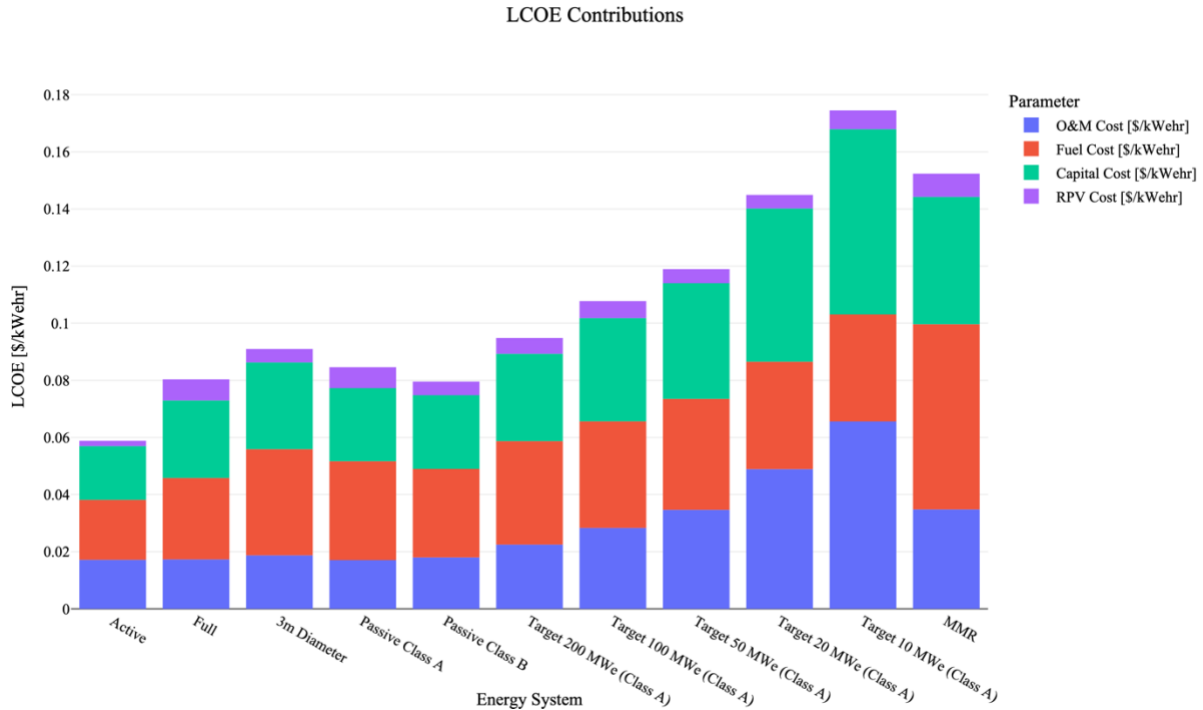


Figure 58 GA discovered Energy Systems under various free parameter configurations.

Table 40 Design and Cost Solution summaries. Free parameters highlighted. Unless specified, costs are for NOAK.

Parameter	Active	Full	Passive Class A	Passive Class B	Target 200 MWe	Target 100 MWe	Target 50 MWe	Target 20 MWe	Target 10 MWe	MMR
Total Plant Thermal Power (MWt)	5,561	4,320	3,676	1,772	612	306	170	80	47.8	309
Net Electrical Power Delivered (MWe)	1,801	1,378	1,178	568	198	97.9	54.3	25.6	15.1	96.6
Heat Rejected (MWt)	3,600	2,796	2,379	1,147	396	198	110	51.8	30.9	200
RX power (MW)	2,781	120	122	98.5	38.2	38.3	42.5	40	47.8	22.1
Number of RXs	2	36	30	18	16	8	4	2	1	14
Turbine Power [MWe/unit]	925	719	612	590	102	51	28.3	13.3	15.9	51.4
Number of Turbines	2	2	2	1	2	2	2	2	1	2
Net System Efficiency	0.324	0.319	0.321	0.321	0.323	0.32	0.319	0.32	0.316	0.313
Safety Class	Active	Passive Class B	Passive Class A	Passive Class B	Passive Class A	Passive Class A	Passive Class A	Passive Class A	Passive Class A	Passive Class A
Operating Model	Low	Medium	Medium	Medium	High	High	Medium	High	High	Medium
Reactor Shape	cyl	cyl	cyl	cyl	cyl	cyl	cyl	cyl	cyl	cyl
Core Diameter (m)	4.83	4.04	4.94	3.24	2.79	2.9	2.98	2.88	2.88	3
Core Height (m)	22.7	14.7	20.4	12.9	12.3	10.8	11.6	11.3	13.5	6
Active Core Volume	278	116	266	57.4	36.3	35.6	41.3	36.8	43.9	21.7
Coolant Volume Fraction	0.225	0.0583	0.0276	0.0416	0.0194	0.0215	0.0495	0.0188	0.00916	0.0139
RPV Diameter (m)	5.15	4.22	5.17	3.41	2.93	3.05	3.11	3.02	3.04	3.17
RPV Height (m)	34.5	23.8	31.7	20.4	18.7	17.4	18.4	17.9	20.4	12.7
RPV Thickness (m)	0.0775	0.0187	0.0261	0.0259	0.0186	0.0221	0.0143	0.0153	0.0267	0.0337
Vessel Mass (kg)	282,500	38,380	88,790	36,790	21,200	23,890	16,930	17,030	34,510	24,890
Core Power Density [W/cc]	6.71	0.637	0.313	0.928	0.51	0.537	0.523	0.54	0.541	0.52
Active Core Power Density [W/cc]	9.99	1.03	0.461	1.72	1.05	1.07	1.03	1.09	1.09	1.01
Core PSAR [W/cm ²]	809	64.3	38.6	75.1	35.6	39	39	39	39	39
Fuel Power Density [W/cc]	100	96.5	33.2	85.2	100	49.6	65.9	54.2	60	10.2
Fuel HM Power Density [kW/kgHM]	96.3	69.9	30.4	70.2	71.3	49.2	47.3	43.9	68.2	15.9
Discharge Burnup [MWd/kg]	160	132	154	119	105	114	76.9	110	108	59.9
Core Energy Content (MWyr)	9,814	584	1,659	440	152	238	180	269	205	224
Core Energy Density [MWh/kg]	111	15.4	21	20.5	10.1	16.5	11	18	11.5	25.2
Core Energy Density (MWyr/ton)	12.6	1.76	2.4	2.34	1.15	1.89	1.25	2.06	1.31	2.88
Core Energy Density (MWyr/m ³)	23.7	3.1	4.23	4.14	2.02	3.34	2.21	3.64	2.32	5.28
Refueling Interval	3.58	4.93	13.6	4.52	4.03	6.27	4.28	6.78	4.34	10.2
RPV Lifetime at Power Design (year)	0.324	7.5	7.34	9.14	23.5	23.5	21.2	22.5	18.8	40.8
Site Area	6.2	4.3	3.99	2.31	1.12	0.847	0.673	0.503	0.481	1.64
Project Lifetime	60	60	60	60	60	60	60	60	60	60
Construction duration (months)	45.9	43.8	39.4	29.4	19.9	15.3	12.5	10.3	8.98	16.2
Orders	17	22	26	53	152	307	553	1,174	1,985	311
Planet Scale RX Production [RX/yr]	1.7	39.6	39	47.7	122	123	111	117	99.2	218
Planet Scale RX Population	34	792	780	954	2,432	2,456	2,212	2,348	1,985	4,354
Peak Core Production Rate [core/year]	11.3	202	96.6	261	734	518	634	466	563	647
Labor Staff Total	547	51	66	27	13	12	14	11	11	16
Staff per MWth	0.0984	0.0118	0.018	0.0152	0.0213	0.0392	0.0824	0.138	0.23	0.0518
BoP Maintenance Staff	96	11	10	6	2	2	2	2	2	2
Reactor Maintenance Staff	35	33	49	15	6	5	6	4	4	8
Reactor Operation Staff	68	4	4	3	2	2	3	2	2	3
Security Staff	129	3	3	3	3	3	3	3	3	3
UNF Average Yearly [m ³ /ES]	15.8	9.19	8.18	4.66	1.54	0.995	0.609	0.219	0.186	3
Number of CRs per RX	37	26	39	17	13	14	14	14	14	15
Average Enrichment	0.172	0.163	0.156	0.184	0.189	0.196	0.129	0.19	0.186	0.0999
TRISO kernel material	UN	UN	UN	UN	UN	UN	UN	UN	UN	UO ₂
Core Average k	17.4	19.6	16.1	18.8	16.1	17.2	17.9	16.2	16.1	20.3
Core Average c	1.87	1.8	1.8	1.8	1.8	1.81	1.8	1.8	1.8	1.86
Smear Fuel Density	3,611	3,744	3,633	3,679	3,752	3,599	3,749	3,687	3,550	3,334
Core Fuel Mass [kgFuel]	100,400	4,654	13,410	4,252	1,434	2,782	2,415	2,722	2,826	7,240
Core Heavy Metal Mass	22,390	1,617	3,924	1,344	526	762	853	895	694	1,363
Total Core Mass	777,500	331,800	692,900	187,900	132,000	126,300	143,300	130,900	156,100	77,660
TRISO Volume Packing Fraction	0.467	0.621	0.492	0.546	0.631	0.453	0.626	0.556	0.396	0.4
TRISO [B particles/core]	30.8	1.83	4.31	1.5	0.573	0.832	0.958	0.974	0.749	2.06
Fuel Volume Fraction	0.0999	0.0107	0.0139	0.0201	0.0105	0.0217	0.0156	0.0201	0.0181	0.1
Primary Operating Pressure	4.51	1.15	1.38	2.08	1.64	1.94	1.12	1.26	2.42	3
Minimum Coolant Channel Diameter (m)	0.0247	0.0477	0.0195	0.0494	0.0103	0.0355	0.0256	0.0165	0.023	0.005
Primary Maximum Fluid Velocity	24.4	43.3	38.8	37.7	38.9	41.4	30.1	56.1	64.5	50
Primary Inlet Temperature	582	580	699	585	588	628	600	586	613	573
Primary Outlet Temperature	1,106	930	1,175	996	1,172	1,086	1,047	1,173	1,177	903
Loop 0: He, Mass Flow	2,040	2,373	1,486	832	201	129	73.2	26.2	16.3	180

Parameter	Active	Full	Passive Class A	Passive Class B	Target 200 MWe	Target 100 MWe	Target 50 MWe	Target 20 MWe	Target 10 MWe	MMR
Loop 0: He, Mass Flow per loop	1,020	65.9	49.5	46.2	12.6	16.1	18.3	13.1	16.3	12.9
Loop 0: He, delP [kPa]	68.8	18.3	21.8	32.8	26	31.3	17.4	21.6	44.7	60.6
Loop 0: He, Electrical Pumping Power per Loop	23.8	1.58	1.43	1.11	0.305	0.426	0.442	0.343	0.482	0.389
Loop 0: He, Electrical Pumping Power for Layer	47.5	57.1	42.9	20.1	4.88	3.41	1.77	0.685	0.482	5.45
Total TH Circulator Power (MWe)	50	59.2	44.9	21.5	5.77	4.07	2.29	1.06	0.79	6.12
Operating Labor Cost Energy System (\$M/yr)	82	7.65	9.9	4.05	1.95	1.8	2.1	1.65	1.65	2.4
Total fuel cost [\$/kgHM]	15,900	15,020	14,870	16,430	16,540	17,410	12,940	16,770	17,040	14,400
Moderator Cost [\$M/core]	10.7	5.17	10.7	2.9	2.06	1.95	2.23	2.03	2.42	1.11
Fresh Core Cost [\$M/core]	367	29.5	69.1	25	10.8	15.2	13.3	17	14.3	20.7
Refueling Cost / Core (\$M)	473	35.5	86.3	29.7	12.4	17.9	15.3	19.9	16.6	24.3
Capital Cost Total (\$M)	3,402	3,630	2,997	1,543	667	405	259	167	126	488
Capital Cost (\$/kWe)	1,889	2,634	2,543	2,714	3,371	4,139	4,768	6,546	8,368	5,047
RPV Cost [\$/kWehr]	0.00185	0.00735	0.00733	0.00477	0.00554	0.00594	0.00492	0.00475	0.00658	0.00813
O&M Cost [\$/kWehr]	0.0171	0.0173	0.017	0.018	0.0225	0.0283	0.0346	0.0489	0.0656	0.0348
Fuel Cost [\$/kWehr]	0.021	0.0285	0.0346	0.031	0.0363	0.0373	0.0389	0.0376	0.0375	0.0649
Capital Cost [\$/kWehr]	0.0188	0.0272	0.0256	0.0258	0.0306	0.0362	0.0405	0.0537	0.0649	0.0446
Energy System LCOE FOAK	0.089	0.161	0.16	0.164	0.236	0.29	0.344	0.507	0.678	0.402
Energy System LCOE NOAK	0.0588	0.0803	0.0846	0.0796	0.0948	0.108	0.119	0.145	0.175	0.152

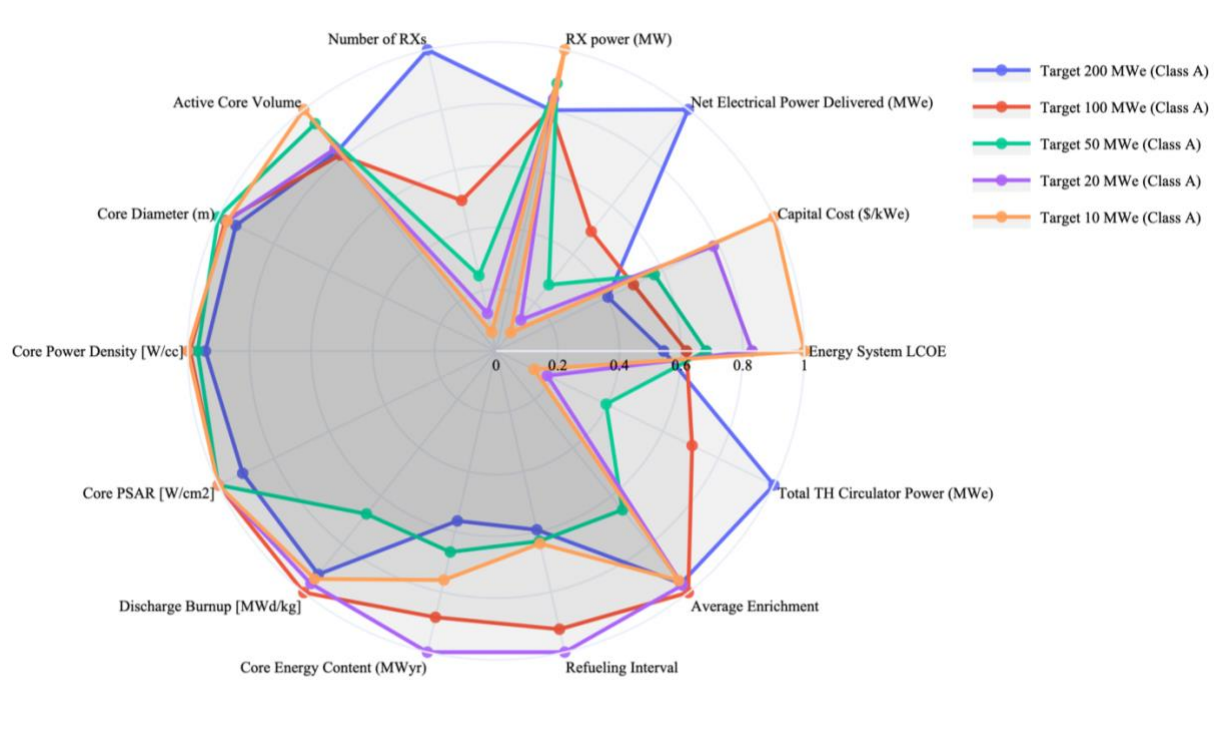


Figure 59 GA results for CA-HTGR at different Energy System electrical power.

8 Conclusions

This work first described potential avenues to achieve new planet wide deployments by reducing nuclear consequence. The space launch story served as inspiration for an approach to nuclear design in which many smaller reactors are factory produced to serve the full spectrum of end-users including single-unit isolated powerplants and parallel couplings to large balance of plants that benefit from physical economies of scale. I outlined a set of design principles to guide technology choice. I showed risk can be reduced by consequence reduction through passive mechanisms and inherent design characteristics that address the driving forces that turn fission products into consequences. I discussed some of the broad design choices, ultimately down selecting to HTGR. I then developed coupled design and cost codes for prismatic HTGR with Class A passive safety, verifying intermediate calculations with known results from the literature. Finally, I used the coupled model to explore the design space with 2-d trades, random sampling, and GA.

The two main findings are the feasibility of the approach and the existence of an optimization opportunity. Design-cost coupling is clearly possible at higher levels of detail than has usually been attempted. The design must be estimated with sufficient detail to evaluate costs, and the cost models should include established phenomena like cost scaling rules and learning experience curves which create the optimization potential. Despite the crude ROM approach for various design parameters, the framework produces designs that conform with the given architecture and the affecting physical laws and engineering codes. With an evaluation time of a few seconds on a laptop, the model can quickly produce thousands of cost estimates. Higher fidelity models can be configured and added. The ability to vary many input parameters across a wide range of options and produce consistent results is useful and necessary to explore the design space. Second, I have shown there are many feasible design solutions within a technology architecture and that the cost can vary widely amongst them. For a given set of assumptions, a GA finds performative solutions, but there are many designs with nearly equivalent performance. Changing the world and applying constraints to the free parameters can significantly change the optima and reduce the population of performative designs. I also suggested that finding performative designs should consider the rankings across a population of worlds instead of a single optimization in a single world.

All the results presented must be treated as merely indicative of trends and subject to large and even inverted changes under different financial conditions and modeling assumptions. The weights and trends can reveal relative importance of different design choices. The value of the work may lie most of all in the awareness that many knobs exist with many interactions and effects of varying importance. To have any meaning beyond the cognitive realm, this awareness can be integrated to affect a real-world implementation. The work may also be valuable because actual cost estimation goes along a similar route, perhaps with less detail and more broad stroked assumptions. Optimizing to the financial model only makes sense with sufficient design definition from physical and engineering considerations.

8.1 Model Shortcomings and Future Work

Particular designs still need careful definition of their unique features like a special building type to house dozens of reactors rather than a reactor building per reactor or the particular arrangement of heat sinks and loops inside the reactor building which can have effects on allowable power rating. The design abstraction sought in this thesis is perhaps naïve despite the initial technology down selection. Near-term improvements to the code are listed in Appendix 10.13. The envisioned use cases below would require even more significant code development. Most of the model weaknesses identified below favor smaller RX.

8.1.1 Design Code Shortcomings

- Pressure drop estimates and pumping power are somewhat lower than comparable estimates and do not punish high aspect ratio cores because of the thermal hydraulic assumption of channel lengths equal to the core diameter and insufficient estimation on pressure drops in plenums and the core barrel.
- In the evaluations presented, the RX temperatures were allowed to roam without increasing CAPEX or OPEX. The secondary and tertiary loops had fixed temperatures.
- Core energy content and power rating models are low fidelity with insufficient physical basis. In particular, core energy content has steep penalty for smaller cores.
- RPV lifetime estimate is based on dpa rate for a micro reactor reference and gives unrealistic replacement intervals for larger and higher power RX with lower leakage and dpa rates.

8.1.2 Cost Code Shortcomings

- EEDB is a 1980s cost reference for 1200 MWe plant. Forty years later, EEDB may be inadequate to estimate costs for a CA-HTGR architecture. For design purposes, future cost modeling should aim for bottom-up methods that disregard the nuclear cost escalations, cost category splits, etc and establish component cost curves based on industry quotes and material/energetic considerations.
- I used constant modularization relative to the reference design, but modularization potential should depend on the physical characteristics and system complexity and should favor smaller reactors.
- Indirect costs have strong dependence on construction time and only benefit from learning indirectly through CAPEX

- learning. The construction duration per unit power favors large reactors as smaller RX have large labor hours devoted to RX buildings which could be produced in parallel or enclosed in a single building.
- Safety class only offered minor CAPEX cost savings by dropping particular CAPEX accounts. However, CA-HTGR characteristics are the basis for the Medium and High Operating models and underpin the assumptions on learning. Active safety class should only be evaluated with low operating models and extensive learning. I can also imagine that CA-HTGR could have significant nuclear cost de-escalations.
- The aggressive learning without thresholds will be considered optimistic, but evaluations presented did not include fuel, RPV, and OPEX learning which will favor smaller RX which accumulate reactor years at rates proportional to the factor of reduced size. Figure 52 shows the large fractional change from FOAK to NOAK for very small systems, similar to solar and wind cost reduction over the last 40 years.

8.1.3 Search Code Shortcomings

- Many of the model evaluations are similar or repeated. Incremental calculations or asynchronous approach could be used to accelerate evaluation so that unique evaluations are run only once.
- As described in the uncertainty section, I should be designing for performative designs across range of markets and assumptions.

8.2 Envisioned Use

Various uses are envisioned for this design and cost code or similar DFC approaches to push advanced reactors to demonstration and planet wide deployment.

8.2.1 DFC Based on End-Users and Project Lists

A nuclear vendor might have a list of potential projects, each with particular needs and expected financial parameters. Chances are, the vendor, if not the regulatory body, lacks the resources for many customer-specific designs and licensing efforts. The vendor could specify the concept requirements for each customer such as net electrical power level, process heat amount and temperature, plant footprint, and other parameters that define the customer's envelope. This database can then be used to specify designs and projects that maximize profit across the end-users be it with one or multiple RX designs, including how to prioritize and charge customers. Projects with different interest rates or PPAs may benefit from different refueling cycles or deployment schedules. The current state of nuclear suggests a vendor has basically one shot at the RX design, while, if properly decoupled, can arrange for arbitrary BoPs specific to the customer.

Along similar lines, I could imagine the vendor seeking to license one RX design for multiple end-users with different power ratings and deployment needs. The goal could be to preserve a reactor architecture across different temperatures and power ratings. RPV, core geometry, and fuel loading would be the same, while power would decrease by lowering the flow velocity, pressure, or temperature difference across the core. The problem becomes finding the most profitable RX designs to service most of the end-users.

8.2.2 R&D and Technology Roadmaps

A nuclear vendor or R&D strategist has to plan for future technological and industrial capabilities. What R&D can have significant impact on performance and LCOE in the next 2 decades? Models like the one developed for this thesis can help explore the implications of certain performance or cost changes and direct R&D efforts, perhaps considering the magnitude of R&D or industrial expenditure required to deliver a particular change. Will lower LCOE be achieved by financing either a 100 \$M effort to develop and qualify a particular new moderator or a reactor demonstration? Similarly, a nuclear vendor may be able to identify particularly egregious cost contributors to focus their R&D and custom design efforts.

8.2.3 Integration with Standardized Modeling and Reporting Processes to Automate and Accelerate Reactor Design, Analysis, Licensing, and Business Development

Graduate students have been conducting design thesis for one-off designs of this sort since the 1950s. The calculations are more or less of the same variety, repeated ad nauseum: pick a technology architecture of fuel, coolant, moderator, and BoP; pick a power rating that limits peak temperatures; compute the energy balance, pressure drops, convection models, thermal conduction models, neutronic feasibility studies, etc. In some cases, a cost estimate is included. These are typically point designs with verifications, riddled with inherited assumptions. These studies may aim to introduce new materials and architectures or prove the potential for new capabilities in enrichment or power density. Vendors and government contractors will create conceptual design reports for specific designs, specifying the design parameters and conducting preliminary feasibility studies with higher level of detail. With sufficient MOUs, LOIs, and a full spigot of government financing, the paper pushing transitions to topical reports and licensing documents. Much of this work is of a highly repetitive and uncreative nature. Designs are, in a way, looked up in the annals of regulatory and engineering codes, and remaining design parameters can be codified with a particular design architecture.

Much of this can be automated using estimates like those in this thesis, integrated analysis tools, report templating techniques, and newly available Large Language Models (LLM). USNC's RAPTOR and ARMI are two industry codes that integrate nuclear modeling tools to define and analyze nuclear reactor configurations. It may be advisable to integrate the design and cost methods in this thesis into these established codes which have a high degree of integration with other nuclear analysis codes. These codes do not yet produce full human readable reports or studies and require full human control to specify the designs and analysis, run and rerun codes, and understand results to finally compile reports. Reporting techniques must be able to accurately reference the regulatory and engineering codes. While LLMs are likely to come short for licensing documents in the near future, licensing documents and explanations for a given design paradigm like HTGR can be templated and reused. A large part of the work can be done once if it is well defined and sufficiently abstracted, automated through code integration and testing, and templated for report generation. A nuclear vendor that takes licensing automation and standardized design methods seriously may be able to generate design and licensing documents on far shorter timelines than previously assumed. With a sound architecture, many design can be iterated and tuned to the population of the end users.

9 References

- [1] “The Future of Nuclear Energy in a Carbon-Constrained World AN INTERDISCIPLINARY MIT STUDY,” 2018.
- [2] J. Devanney, “The Two Lies that Killed Nuclear Power,” *Gordian Knot News*, 2022. [Online]. Available: <https://jackdevanney.substack.com/p/the-two-lies-that-killed-nuclear>.
- [3] J. Devanney, *Why Nuclear Power Has Been A Flop*. 2020.
- [4] J. J. Cardarelli and B. A. Ulsh, “It is time to move beyond the linear no-threshold theory for low-dose radiation protection,” *Dose-Response*, vol. 16, no. 3, pp. 1–24, 2018.
- [5] J. Devanney, “Can the NRC be Reborn?,” *Gordian Knot News*, 2023. .
- [6] N. Li, “New paradigm for civil nuclear energy . Perspectives from the hierarchy of energy sources and fundamental safety,” in *FORUM USPEKHI-2021’: CLIMATECHANGEAND GLOBAL ENERGYISSUES*, 2022, vol. 65, no. 11, pp. 1115–2287.
- [7] C. W. Forsberg and A. M. Weinberg, “ADVANCED REACTORS, PASSIVE SAFETY, AND ACCEPTANCE OF NUCLEAR ENERGY!,” 1990.
- [8] A. M. Weinberg, *The Second nuclear era: A new start for nuclear power*. 1985.
- [9] G. Dyson, *Darwin Among the Machines*. Basic Books, 1997.
- [10] H. W. Jones, “The Recent Large Reduction in Space Launch Cost,” *48th Int. Conf. Environ. Syst.*, no. July 2018, p. 81, 2018.
- [11] M. T. Wansley and S. N. Weinstein, *Venture predation*, no. forthcoming. 2023.
- [12] T. Dodd, *Starbase Tour with Elon Musk*. 2021.
- [13] A. Chaikin, “Is SpaceX Changing the Rocket Equation?,” *Air & Space Magazine*, 2012.
- [14] M. C. Weinzierl, K. Lucas, and M. Sarang, “SpaceX , Economies of Scale , and a Revolution in Space Access,” vol. 2020, no. JUNE, pp. 1–28, 2020.
- [15] A. Jonas *et al.*, “SpaceX : Raising Valuation Scenarios Following Key Developments,” pp. 1–16, 2020.
- [16] J. Wattles, “Elon Musk says SpaceX’s Mars rocket will be cheaper than he once thought,” *CNN Business*, 29-Sep-2019.
- [17] P. Eash-Gates, M. M. Klemun, G. Kavlak, J. McNERney, J. Buongiorno, and J. E. Trancik, “Sources of Cost Overrun in Nuclear Power Plant Construction Call for a New Approach to Engineering Design,” *Joule*, vol. 4, no. 11, pp. 2348–2373, 2020.
- [18] “Reinventing Construction: A Route to High Productivity,” 2017.
- [19] “By the numbers: The Space Launch System, NASA’s next Moon rocket,” 2022. [Online]. Available: <https://www.astronomy.com/space-exploration/by-the-numbers-the-space-launch-system-nasas-next-moon-rocket/>. [Accessed: 11-Aug-2023].
- [20] “Georgia nuclear plant again delayed at cost of \$200M more | AP News.” [Online]. Available: <https://apnews.com/article/georgia-power-co-southern-climate-and-environment-business-3b1d6c65353c6a65b1ccfdede753ab7>. [Accessed: 11-Aug-2023].
- [21] J. R. Lovering, A. Yip, and T. Nordhaus, “Historical construction costs of global nuclear power reactors,” *Energy Policy*, vol. 91, pp. 371–382, 2016.
- [22] Ray and Douglas, “Lazard’s Levelized Cost of Energy Analysis—Version 15.0,” 2021.
- [23] Helion Energy, “Helion FAQ,” 2023. [Online]. Available: <https://www.helionenergy.com/faq/>.
- [24] H. Ritchiem and M. Roser, “Modern renewables and nuclear energy are not only safer but also cleaner than fossil fuels,” *Our World in Data*, 2020. [Online]. Available: <https://ourworldindata.org/nuclear-energy#modern-renewables-and-nuclear-energy-are-not-only-safer-but-also-cleaner-than-fossil-fuels>.
- [25] S. Wheatley, B. K. Sovacool, and D. Sornette, “Reassessing the safety of nuclear power,” *Energy Res. Soc. Sci.*, vol. 15, pp. 96–100, 2016.
- [26] A. M. Weinberg, “Science and Trans-Science,” *Minerva*, vol. 10, no. 3, pp. 484–486, 1972.
- [27] P. Eash-gates, G. Kavlak, and J. Mcnerney, “Sources of cost overrun in nuclear power plant construction call for a new approach to reactor engineering design,” *Submitt. Prepr. to Joule*, 2020.

- [28] S. J. Zinkle, K. A. Terrani, J. C. Gehin, L. J. Ott, and L. L. Snead, "Accident tolerant fuels for LWRs: A perspective," *J. Nucl. Mater.*, vol. 448, no. 1–3, pp. 374–379, May 2014.
- [29] C. Forsberg and A. W. Foss, "Fission battery markets and economic requirements," *Appl. Energy*, vol. 329, no. June 2021, p. 120266, 2023.
- [30] G. Haratyk, "Early nuclear retirements in deregulated U.S. markets: Causes, implications and policy options," *Energy Policy*, vol. 110, no. August, pp. 150–166, 2017.
- [31] B. R. Sutherland, "Tax Carbon Emissions and Credit Removal," *Joule*, vol. 3, no. 9, pp. 2071–2073, 2019.
- [32] G. Haratyk, "Nuclear asset shutdown under uncertainty," *Massachusetts Inst. Technol.*, 2017.
- [33] S. Wang, D. Pasqualini, N. M. Urban, C. Co, R. Bent, and S. J. Mason, "An Optimization-Based Adaptation Framework for Coastal Electrical Infrastructure Resilience To Climate Change."
- [34] R. Lanza, "Fragility of Energy Networks," in *International Seminars On Planetary Emergencies And Associated Meetings*, 2014.
- [35] S. P. Burger, J. D. Jenkins, S. C. Huntington, and I. J. Perez-Arriaga, "Why distributed?: A critical review of the tradeoffs between centralized and decentralized resources," *IEEE Power Energy Mag.*, vol. 17, no. 2, pp. 16–24, Mar. 2019.
- [36] P. L. Joskow, "Challenges for Wholesale Electricity Markets with Intermittent Renewable Generation at Scale: The U.S. Experience Working Paper Series," 2019.
- [37] IAEA, "Safety Related Terms for Advanced Nuclear Plants," *Iaea-Tecdoc-626*, no. September, p. 20, 1991.
- [38] "Advanced Modular Reactors Technical Assessment," 2021.
- [39] E. (UCS) Lyman, "'Advanced' Isn't Always Better," 2021.
- [40] J. acopo Buongiorno, "Japan's Next Nuclear Energy System (JNext)," 2020.
- [41] K. Verfondern, H. Nabilek, and J. M. Kendall, "Coated particle fuel for HTGCR," *Nuclear engineering and technology*, vol. 39, p. 603, 2007.
- [42] "PELE PROGRAM PHASE I." Office of the Secretary of Defense Strategic Capabilities Office, 2019.
- [43] D. A. Petti, P. A. Demkowicz, J. T. Maki, and R. R. Hobbins, *Triso-coated particle fuel performance*, vol. 3. Elsevier Inc., 2012.
- [44] J. D. Hales, R. L. Williamson, S. R. Novascone, D. M. Perez, B. W. Spencer, and G. Pastore, "Multidimensional multiphysics simulation of TRISO particle fuel," *J. Nucl. Mater.*, vol. 443, no. 1–3, pp. 531–543, 2013.
- [45] L. L. Snead *et al.*, "Fully ceramic microencapsulated fuels: A transformational technology for present and next generation reactors-properties and fabrication of FCM fuel," *Trans. Am. Nucl. Soc.*, vol. 104, pp. 668–670, 2011.
- [46] B. Hiscox and K. Shirvan, "Reactor physics analysis of a new Accident Tolerant Fuel called Fuel-in-Fibers," *Ann. Nucl. Energy*, vol. 130, pp. 473–482, 2019.
- [47] K. A. Terrani *et al.*, "Architecture and properties of TCR fuel form," *J. Nucl. Mater.*, vol. 547, pp. 1–20, 2021.
- [48] L. L. Snead, T. Nozawa, Y. Katoh, T. S. Byun, S. Kondo, and D. A. Petti, "Handbook of SiC properties for fuel performance modeling," *J. Nucl. Mater.*, vol. 371, no. 1–3, pp. 329–377, 2007.
- [49] A. Glaser, "About the Enrichment Limit for Research Reactor Conversion: Why 20%?," *Reduc. Enrich. Res. Test React.*, pp. 1–12, 2005.
- [50] USNC-Tech, "USNC Pylon Design Review," 2022.
- [51] Aerojet-General Nucleonics, "Army Gas-Cooled Reactor Systems Program - The ML-1 Design Report," 1960.
- [52] S. K. Feng J, Baglietto E, Stewart WR, Velez-Lopez E, Wisner R, "Heat Transfer Analysis of a Conceptual Horizontally-Oriented High Temperature Gas-Cooled Reactor 2021," 2021.
- [53] C. Filippone and F. Venneri, "Modular Transportable Nuclear Generator," US 10 , 229 , 757 B2, 2019.
- [54] N. Li, "A paradigm shift needed for nuclear reactors: From economies of unit scale to economies of production scale," *Int. Congr. Adv. Nucl. Power Plants 2009, ICAPP 2009*, vol. 3, pp. 2568–2581, 2009.
- [55] Y. Someya *et al.*, "Management strategy for radioactive waste in the fusion demo reactor," *Fusion Sci. Technol.*, vol. 68, no. 2, pp. 423–427, 2015.
- [56] "IAEA Advanced Reactors Information System (ARIS) - Technical Data," IAEA, 2023. [Online]. Available:

- <https://aris.iaea.org/sites/overview.html>. [Accessed: 22-Aug-2023].
- [57] J. W. Sterbentz, J. E. Werner, M. G. McKellar, A. J. Hummel, and ..., "Special Purpose Nuclear Reactor (5 MW) for Reliable Power at Remote Sites Assessment Report," 2017.
- [58] "GE Hitachi Nuclear Energy BWRX-300 General Description," 2023.
- [59] J. R. Banavar, T. J. Cooke, A. Rinaldo, and A. Maritan, "Form, function, and evolution of living organisms," *Proc. Natl. Acad. Sci. U. S. A.*, vol. 111, no. 9, pp. 3332–3337, 2014.
- [60] F. J. Ballesteros, V. J. Martinez, B. Luque, L. Lacasa, E. Valor, and A. Moya, "On the thermodynamic origin of metabolic scaling," *Sci. Rep.*, vol. 8, no. 1, pp. 2–11, 2018.
- [61] "EPA eGRID Data Explorer." .
- [62] P. R. Wilding, N. R. Murray, and M. J. Memmott, "The use of multi-objective optimization to improve the design process of nuclear power plant systems," *Ann. Nucl. Energy*, vol. 137, 2020.
- [63] A. Abou-Jaoude, "An Economics-by-Design Approach Applied to a Heat Pipe Microreactor Concept," 2021.
- [64] W. R. Stewart, "Minimizing civil construction costs in nuclear : a horizontal, compact high temperature gas reactor," *Draft*, 2021.
- [65] C. Bolisetti, J. Coleman, W. Hoffman, and A. Whittaker, "Cost- and Risk-Based Seismic Design Optimization of Nuclear Power Plant Safety Systems," *Nucl. Technol.*, vol. 207, no. 11, pp. 1687–1711, 2021.
- [66] K. M. Lal *et al.*, "Reducing the capital cost of nuclear power plants using seismic isolation," no. March, 2020.
- [67] J. Buongiorno, B. Carmichael, B. Dunkin, J. Parsons, and D. Smit, "Can Nuclear Batteries Be Economically Competitive in Large Markets?," *Energies*, vol. 14, no. 14, p. 4385, 2021.
- [68] A. Kumar and P. V. Tsvetkov, "A new approach to nuclear reactor design optimization using genetic algorithms and regression analysis," *Ann. Nucl. Energy*, vol. 85, pp. 27–35, 2015.
- [69] X. Zhang, X. Sun, R. Christensen, I. Jantz, and M. Anderson, "Compact Heat Exchanger Design and Testing for Advanced Reactors and Advanced Power Cycles," 2018.
- [70] S. J. Ball, "GRSAC USERS MANUAL," 1999.
- [71] F. P. Incropera, *Fundamentals of Heat and Mass Transfer*, 6th ed. 2006.
- [72] H. Sato, H. Ohashi, Y. Tachibana, K. Kunitomi, and M. Ogawa, "Thermal analysis of heated cylinder simulating nuclear reactor during loss of coolant accident," *J. Nucl. Sci. Technol.*, vol. 51, no. 11–12, pp. 1317–1323, 2014.
- [73] M. Benson, D. Rudland, and M. Kirk, "Thermal-Mechanical Analysis of Pressure Vessels," *US Nucl. Regul. Comm.*, pp. 1–9.
- [74] I. Edwards *et al.*, "Htgr Core Thermal Design," vol. 12985, 1974.
- [75] G. Melese and R. Katz, *Thermal and Flow Design of Helium-Cooled Reactors*. 1984.
- [76] N. Todreas and M. Kazimi, *Nuclear Systems I Thermal Hydraulic Fundamentals*. 1990.
- [77] G. A. Johnson, H. Sundstrand, P. O. B. Mc, and A. RI, "Power Conversion System Evaluation For The Next Generation Nuclear Plant," 2010.
- [78] Q. Xinhe, Y. Xiaoyong, W. Jie, and Z. Gang, "Combined cycle schemes coupled with a Very High Temperature gas-cooled reactor," *Prog. Nucl. Energy*, vol. 108, no. April, pp. 1–10, 2018.
- [79] S. A. Wright, M. E. Vernon, and P. S. Pickard, "Concept Design for a High Temperature Helium Brayton Cycle with Interstage Heating and Cooling," no. December, 2013.
- [80] A. Moisseytsev and J. J. Sienicki, "Performance Improvement Options for the Supercritical Carbon Dioxide Brayton Cycle," *Argonne Natl. Lab.*, vol. ANL-GenIV-, pp. 1–52, 2007.
- [81] L. A. Porto-Hernandez *et al.*, "Fundamental optimization of steam Rankine cycle power plants," *Energy Convers. Manag.*, vol. 289, p. 117148, 2023.
- [82] C. R. Branan, *Rules Of Thumb For Chemical Engineers*. 2002.
- [83] M. Chen, X. Sun, R. N. Christensen, I. Skavdahl, V. Utgikar, and P. Sabharwall, "Fabrication and testing of a high-temperature printed circuit heat exchanger," *Int. Top. Meet. Nucl. React. Therm. Hydraul. 2015, NURETH 2015*, vol. 9, no. December 2017, pp. 7621–7636, 2015.

- [84] “Correspondence with Yue Jin at MIT.” 202AD.
- [85] Z. Zhang *et al.*, “Current status and technical description of Chinese 2×250 MWth HTR-PM demonstration plant,” *Nucl. Eng. Des.*, vol. 239, no. 7, pp. 1212–1219, 2009.
- [86] G. Zhao *et al.*, “Endurance test of full-scale mock-up helium circulator for HTR-PM,” *Nucl. Eng. Des.*, vol. 329, pp. 20–24, Apr. 2018.
- [87] F. K. Moore, “On the minimum size of large dry cooling towers with combined mechanical and natural draft,” *J. Heat Transfer*, vol. 95, no. 3, pp. 383–389, 1973.
- [88] G. Towler, *Chemical Engineering Design*. 2013.
- [89] W. R. Stewart and K. Shirvan, “Capital Cost Estimation for Advanced Nuclear Power Plants,” *Renew. Sustain. Energy Rev.*, vol. In Press, 2021.
- [90] F. Ganda, “Report on the ACCERT Cost Algorithms Tool: Nuclear Fuel Cycle and Supply Chain Prepared,” 2019.
- [91] A. M. Gandrick, “Assessment of High Temperature Gas-Cooled Reactor (HTGR) Capital and Operating Costs: INL-TEV-1196,” 2012.
- [92] M. A. D. Gandy, “Program on Technology Innovation: Small Modular Reactor Vessel Manufacture and Fabrication Phase 1- Progress (year 3),” no. 3002021037.
- [93] R. D’Aveni, “Economies of Integration Versus Bureaucracy Costs: Does Vertical Integration Improve Performance?,” *Acad. Manag. J.*, 1994.
- [94] J. Rose, “How Shifting Costs Are Altering the Math of Global Manufacturin,” 2018.
- [95] Y. Jie, “TSMC’s Arizona Chip Plant, Awaiting Biden Visit, Faces Birthing Pains,” *Wall Street Journal*, 05-Dec-2022.
- [96] J. Harper, “US, South Korean firms to run Polish nuclear plants,” *Deutsche Welle*, 28-Oct-2022.
- [97] ALL3DP, “Craftcloud,” 2023. [Online]. Available: <https://craftcloud3d.com>. [Accessed: 10-Jan-2023].
- [98] L. R. Lloyd CA, Roulstone T, “Transport, constructability, and economic advantages of SMR modularization.,” *Prog. Nucl. Energy*, vol. 134, 2021.
- [99] T. P. WRIGHT, “Factors Affecting the Cost of Airplanes,” *J. Aeronaut. Sci.*, vol. 3, no. 4, pp. 122–128, Feb. 1936.
- [100] E. S. Rubin, I. M. L. Azevedo, P. Jaramillo, and S. Yeh, “A review of learning rates for electricity supply technologies,” *Energy Policy*, vol. 86, pp. 198–218, 2015.
- [101] E. S. Rubin, S. Yeh, M. Antes, M. Berkenpas, and J. Davison, “Use of experience curves to estimate the future cost of power plants with CO₂ capture,” *Int. J. Greenh. Gas Control*, vol. 1, no. 2, pp. 188–197, 2007.
- [102] G. Kavlak, J. McNerney, and J. E. Trancik, “Evaluating the causes of cost reduction in photovoltaic modules,” *Energy Policy*, vol. 123, no. October, pp. 700–710, 2018.
- [103] M. R. Weimar, A. Zbib, D. Todd, J. Buongiorno, and K. Shirvan, “Techno-economic Assessment for Generation III + Small Modular Reactor Deployments in the Pacific Northwest,” no. April, 2021.
- [104] T. R. Mager, “Thermal Annealing Of An Embrittled Reactor Pressure Vessel,” no. 9, 1979.
- [105] R. K. Nanstad, “Reactor Pressure Vessel Task of Light Water Reactor Sustainability Program : Assessment of High Value Surveillance Materials June 2011,” 2011.
- [106] R. Wigeland *et al.*, “Nuclear Fuel Cycle Evaluation and Screening – Final Report,” 2014.
- [107] “UxC Uranium U3O8,” 2022. [Online]. Available: <https://www.cmegroup.com/markets/metals/other/uranium.html>.
- [108] S. Whitley, “Review of the gas centrifuge until 1962. part I: Principles of separation physics,” *Rev. Mod. Phys.*, vol. 56, no. 1, pp. 41–66, Jan. 1984.
- [109] K. A. Terrani, L. L. Snead, and J. C. Gehin, “Microencapsulated fuel technology for commercial light water and advanced reactor application,” *J. Nucl. Mater.*, vol. 427, no. 1–3, pp. 209–224, 2012.
- [110] S. Ray, E. Lahoda, and F. Franceschini, “Assessment of different materials for meeting the requirement of future fuel designs,” *2012 React. Fuel Perform. Meet.*, p. A0115, 2012.
- [111] G. K. Miller, D. A. Petti, J. T. Maki, D. L. Knudson, and W. F. Skerjanc, “PARFUME Theory and Model Basis Report,” 2018.
- [112] C. W. Kingsbury, “Fuel Cycle Cost And Fabrication Model For Fluoride- Salt High-Temperature Reactor (FHR) ‘ Plank ’

- Fuel Design Optimization,” 2015.
- [113] D. T. Blagoeva, “Stability of ferritic steel to higher doses: Survey of reactor pressure vessel steel data and comparison with candidate materials for future nuclear system,” *Int. J. Press. Vessel. Pip.*, vol. Volume 122, pp. 1–5, 2014.
- [114] M. Bunn, J. P. Holdren, S. Fetter, and B. Van Der Zwaan, “The economics of reprocessing versus direct disposal of spent nuclear fuel,” *Nucl. Technol.*, vol. 150, no. 3, pp. 209–230, 2005.
- [115] USNC, “Usnc Micro Modular Reactor (Mmr Block 1) Technical Information,” *usnc.com*, 2021. [Online]. Available: [https://usnc.com/assets/media-kit/\[022989\]\[01\] MMR Technical Information Document.pdf?v=4693eb5e69](https://usnc.com/assets/media-kit/[022989][01] MMR Technical Information Document.pdf?v=4693eb5e69).
- [116] M. S. Peterson, “Economic Impact Report Construction and Operation of a Small Modular Reactor Electric Power Generation Facility at the Idaho National Laboratory Site, Butte County, Idaho Prepared for Regional Economic Development for East Idaho (REDI),” 2019.
- [117] Dominion Energy Inc., Bechtel Power Corporation, TLG Inc., and MPR Associates, “Study of Construction Technologies and Schedules, O&M Staffing and Cost, Decommissioning Costs and Funding Requirements for Advanced Reactor Designs,” vol. 1, 2004.
- [118] IAEA, “Nuclear power plant outage optimisation strategy,” no. October, 2002.
- [119] “Nuclear Decommissioning: Decommission nuclear facilities - World Nuclear Association.” [Online]. Available: <https://world-nuclear.org/information-library/nuclear-fuel-cycle/nuclear-wastes/decommissioning-nuclear-facilities.aspx#:~:text=For US reactors the expected,to %241.22 million per MWe.> [Accessed: 21-Aug-2023].
- [120] M. Fisher, “Fort St. Vrain decommissioning project,” 1998.
- [121] L. D. D. Harvey, “Clarifications of and improvements to the equations used to calculate the levelized cost of electricity (LCOE), and comments on the weighted average cost of capital (WACC),” *Energy*, vol. 207, p. 118340, 2020.
- [122] A. Troi, “Historic buildings and city centres – the potential impact of conservation compatible energy refurbishment on climate protection and living conditions,” *Int. Conf. Energy Manag. Cult. Herit.*, no. March 2015, p. 10, 2011.
- [123] U. Hassler, “Long-term building stock survival and intergenerational management: The role of institutional regimes,” *Build. Res. Inf.*, vol. 37, no. 5–6, pp. 552–568, 2009.
- [124] L. M. Seymour, J. Maragh, P. Sabatini, M. Di Tommaso, J. C. Weaver, and A. Masic, “Hot mixing: Mechanistic insights into the durability of ancient Roman concrete,” *Sci. Adv.*, vol. 9, no. 1, Jan. 2023.
- [125] W. R. Stewart, “Capital cost evaluation of advanced reactor designs under uncertainty and risk By,” 2022.
- [126] Nuclear Energy Institute, “Roadmap for Regulatory Acceptance of Advanced Manufacturing Methods in the Nuclear Energy Industry,” 2019.
- [127] J. Simpson *et al.*, *Considerations for Application of Additive Manufacturing to Nuclear Reactor Core Components*. 2019.
- [128] J. Haley, K. Faraone, B. Gibson, J. Simpson, and R. Dehoff, *Review of Advanced Manufacturing Techniques and Qualification Processes for Light-Water Reactors: Laser-Directed Energy Deposition Additive Manufacturing*, no. September. 2021.
- [129] J. Simpson and R. Dehoff, *Review of Advanced Manufacturing Techniques and Qualification Processes for Light Water Reactors — Laser Powder Bed Fusion Additive Manufacturing*. 2020.
- [130] T. Koyanagi, K. Terrani, S. Harrison, J. Liu, and Y. Katoh, “Additive manufacturing of silicon carbide for nuclear applications,” *J. Nucl. Mater.*, vol. 543, 2021.
- [131] M. P. Trammell, B. C. Jolly, M. Dylan, R. Austin, T. Schumacher, and K. A. Terrani, “Advanced Nuclear Fuel Fabrication: Particle Fuel Concept for TCR,” no. July, 2019.
- [132] A. Nelson *et al.*, “Printed SiC for Nuclear Applications Transformational Challenge Reactor (TCR) Fuel,” 2022.
- [133] J. Hiemenz, “Electron beam melting,” *Adv. Mater. Process.*, vol. 165, no. 3, pp. 45–46, 2007.
- [134] H. Yeom and K. Sridharan, “Cold spray technology in nuclear energy applications: A review of recent advances,” *Ann. Nucl. Energy*, vol. 150, p. 107835, 2021.
- [135] K. A. Ross, J. P. Lareau, S. W. Glass, and R. M. Meyer, “Assessment Of Cold Spray Technology For Nuclear Power Applications,” 2021.
- [136] D. E. Shropshire *et al.*, “Advanced Fuel Cycle Cost Basis,” 2009.
- [137] C. Liu *et al.*, “Fully Ceramic Microencapsulated Fuels Fabricated by Tape Casting,” *J. Nucl. Mater.*, vol. 564, p. 153675, 2022.

- [138] X. Hu, C. Silva, and K. A. Terrani, "Development of yttrium hydride moderator for the transformational challenge reactor," *Trans. Am. Nucl. Soc.*, vol. 122, pp. 303–305, 2020.
- [139] P. Venneri, "Composite Moderator for Nuclear Reactor Systems;," 0027587 A1, 2020.
- [140] E. M. Duchnowski, R. F. Kile, L. L. Snead, J. R. Trelewicz, and N. R. Brown, "Reactor performance and safety characteristics of two-phase composite moderator concepts for modular high temperature gas cooled reactors," *Nucl. Eng. Des.*, vol. 368, no. August, 2020.
- [141] L. L. Snead *et al.*, "Development and potential of composite moderators for elevated temperature nuclear applications," *J. Asian Ceram. Soc.*, vol. 10, no. 1, pp. 9–32, 2022.
- [142] D. Gandy, "Development of a 316L SS Code Case Using Powder Metallurgy-Hot Isostatic Pressing," 2021.
- [143] C. Lewinsohn, "High-efficiency, ceramic microchannel heat exchangers," *Am. Ceram. Soc. Bull.*, vol. 95, no. 4, pp. 26–31, 2015.
- [144] A. T. Nelson, "Prospects for additive manufacturing of nuclear fuel forms," *Prog. Nucl. Energy*, vol. 155, no. October 2022, p. 104493, 2023.
- [145] C. Ang, L. Snead, and Y. Kato, "A logical approach for zero-rupture Fully Ceramic Microencapsulated (FCM) fuels via pressure-assisted sintering route," *J. Nucl. Mater.*, p. 151987, 2020.
- [146] K. A. Terrani, J. O. Kiggans, C. M. Silva, C. Shih, Y. Katoh, and L. L. Snead, "Progress on matrix SiC processing and properties for fully ceramic microencapsulated fuel form," *J. Nucl. Mater.*, vol. 457, pp. 9–17, 2015.
- [147] Y. Fukaya, N. Mizuta, M. Goto, H. Ohashi, and X. L. Yan, "Conceptual design study of a high performance commercial HTGR for early introduction," *Nucl. Eng. Des.*, vol. 361, no. February, 2020.
- [148] X. Hu, H. Wang, K. Linton, A. Le Coq, and K. A. Terrani, *Handbook on the Material Properties of Yttrium Hydride for High-Temperature Moderator Applications*, no. June. 2021.
- [149] C. Ang, L. Snead, and J. Trelewicz, "An Innovative Approach to Composite Moderators C ontaining Zirconium Hydrides," vol. 121, pp. 683–685, 2019.
- [150] S. Chabod, "Topology optimization in the framework of the linear Boltzmann equation – a method for designing optimal nuclear equipment and particle optics," *Nucl. Instruments Methods Phys. Res. Sect. A Accel. Spectrometers, Detect. Assoc. Equip.*, vol. 931, no. October 2018, pp. 181–206, 2019.
- [151] G. Ridley, L. Venneri, and B. Forget, "Topologically Optimal Nuclear Core Designs Using Deterministic Neutronics Gavin," in *ANS Summer, 2022*.
- [152] B. R. Betzler *et al.*, "Transformational Challenge Reactor preconceptual core design studies," *Nucl. Eng. Des.*, vol. 367, no. May, 2020.
- [153] D. Grossin *et al.*, "A review of additive manufacturing of ceramics by powder bed selective laser processing (sintering / melting): Calcium phosphate, silicon carbide, zirconia, alumina, and their composites," *Open Ceram.*, vol. 5, 2021.
- [154] J. Walker, J. R. Middendorf, C. C. C. Lesko, and J. Gockel, "Multi-material laser powder bed fusion additive manufacturing in 3-dimensions," *Manuf. Lett.*, vol. 31, pp. 74–77, 2022.
- [155] P. F. Venneri and Y. Kim, "A feasibility study on low enriched uranium fuel for nuclear thermal rockets - II: Rocket and reactor performance," *Prog. Nucl. Energy*, vol. 87, pp. 156–167, 2016.
- [156] J. Weinmeister and P. Jain, "Cooling channel optimization in additively manufactured gas cooled reactor core," 2020.
- [157] V. Sobes *et al.*, "AI-based design of a nuclear reactor core," *Sci. Rep.*, vol. 11, no. 1, pp. 1–9, 2021.
- [158] D. Southall, R. Le Pierres, and S. J. Dewson, "Design considerations for compact heat exchangers," *Int. Conf. Adv. Nucl. Power Plants, ICAPP 2008*, vol. 3, pp. 1953–1968, 2008.
- [159] J. Alexandersen and C. S. Andreasen, "A review of topology optimisation for fluid-based problems," *Fluids*, vol. 5, no. 1. MDPI AG, 2020.
- [160] M. A. SALAZAR DE TROYA, D. A. Tortorelli, and V. A. Beck, "Two dimensional topology optimization of heat exchangers with the density and level-set methods," *World Congr. Comput. Mech. ECCOMAS Congr.*, vol. 1300, pp. 1–25, 2021.
- [161] J. K. Wright, "Next Generation Nuclear Plant Steam Generator and Intermediate Heat Exchanger Materials Research and Development Plan," *ReVision*, no. September 2010, p. 217, 2010.
- [162] E. Ossola, J. P. Borgonia, M. Hendry, E. Sunada, E. Brusa, and R. Sesana, "Design of isogrid shells for venus surface

- probes,” *J. Spacecr. Rockets*, vol. 58, no. 3, pp. 643–652, 2021.
- [163] T. F. Johnson, D. W. Sleight, and R. A. Martin, “Structures And Design Phase I Summary For The Nasa Composite Cryotank Technology Demonstration Project.”
- [164] B. Betzler, J. Heinemann, P. Chesser, S. Cetiner, and N. See, “Pressure Vessel Design Optimization of the Transformational Challenge Reactor,” pp. 1619–1622, 2021.
- [165] T. Dbouk, “A review about the engineering design of optimal heat transfer systems using topology optimization,” *Applied Thermal Engineering*, vol. 112. Elsevier Ltd, pp. 841–854, 05-Feb-2017.
- [166] I. H. Bell, J. Wronski, S. Quoilin, and V. Lemort, “Pure and pseudo-pure fluid thermophysical property evaluation and the open-source thermophysical property library coolprop,” *Ind. Eng. Chem. Res.*, vol. 53, no. 6, pp. 2498–2508, 2014.
- [167] T. Drozda and C. Wick, *Tool and manufacturing engineers handbook : a reference book for manufacturing engineers, managers, and technicians*. 1983.
- [168] O. Stier, “Fundamental cost analysis of cold spray,” *J. Therm. Spray Technol.*, vol. 23, no. 1–2, pp. 131–139, 2014.
- [169] J. C. Zhao, “Additively Manufactured High Efficiency and Low-Cost sCO₂ Heat Exchangers,” in *The ARPA-E Energy Innovation Summit*, 2021.
- [170] M. Baumers, P. Dickens, C. Tuck, and R. Hague, “The cost of additive manufacturing: Machine productivity, economies of scale and technology-push,” *Technol. Forecast. Soc. Change*, vol. 102, pp. 193–201, 2016.
- [171] D. S. Thomas and S. W. Gilbert, “Costs and cost effectiveness of additive manufacturing: A literature review and discussion,” *Addit. Manuf. Costs, Cost Eff. Ind. Econ.*, pp. 1–96, 2015.
- [172] S. D. Williams, “An implicit-iterative solution of the heat conduction equation with a radiation boundary conditions,” *Numer. Methods Eng.*, vol. 11, no. August 1976, pp. 1605–1619, 1977.

10 Appendix

10.1 Base Inputs

Table 41 Base design and model inputs.

Parameter	Value	Unit	Group
BoP Type	3-loop subRankine	from dict	BOP
BoP Config	Shared Secondary	from dict	BOP
Ambient Temperature	300	K	BOP
Turbine Max Size [MWth]	3000	MWth	BOP
Primary Fluid Type	He	from dict	BOP
Primary Inlet Temperature	573	K	BOP
Primary Outlet Temperature	903	K	BOP
Primary Operating Pressure	3	MPa	BOP
Primary Maximum Fluid Velocity	50	m/s	BOP
Secondary Fluid Type	Solar Salt	from dict	BOP
Secondary Inlet Temperature	548	K	BOP
Secondary Maximum Fluid Velocity	10	m/s	BOP
Secondary Outlet Temperature	838	K	BOP
Steam Inlet Temperature	423	K	BOP
Steam Outlet Temperature	793	K	BOP
Secondary Operating Pressure	0.1	MPa	BOP
Steam Operating Pressure	12.5	MPa	BOP
HX Cost Factor	1	factor	BoP
Capital Cost Reference Name	EEDB	from dict	Capital Cost
Gen III+ or later	TRUE	bool	Capital Cost
Integral Vessel	FALSE	bool	Capital Cost
E-beam Welding	TRUE	bool	Capital Cost
Nuclear Superstructure Thickness [m]	1.2	m	Civil
Non-Nuclear Superstructure Thickness [m]	0.3	m	Civil
Nuclear Foundation Thickness [m]	1.2	m	Civil
Non-Nuclear Foundation Thickness [m]	1	m	Civil
Nuclear Below Grade	1	fraction	Civil
Bedrock Depth [m]	3	m	Civil
Decommissioning Period (months)	12	months	Decommissioning
Decommissioning Cost Fraction Reactor	0.15	fraction	Decommissioning
TRISO Volume Packing Fraction	0.4	fraction	Fuel
TRISO kernel radius [um]	255	um	Fuel
TRISO 1 radius [um]	355	um	Fuel
TRISO 2 radius [um]	390	um	Fuel
TRISO 3 radius [um]	425	um	Fuel
TRISO 4 radius [um]	465	um	Fuel
TRISO kernel material	UO2	from dict	Fuel
TRISO 1 material	BuC	from dict	Fuel
TRISO 2 material	PyC	from dict	Fuel
TRISO 3 material	SiC	from dict	Fuel
TRISO 4 material	PyC	from dict	Fuel
TRISO Matrix Material	SiC	from dict	Fuel
Max Fuel Temp [K]	2000	K	Fuel
Max Fuel Power Density [W/cc]	100	W/cc	Fuel
Average Enrichment	0.0999	fraction	Fuel
Burnup Perf Factor	1	factor	Fuel
TRISO matrix Material Cost (\$/kg)	1	\$/kg	Fuel Cost
Fuel Block Reuse (fraction old)	0	fraction	Fuel Cost
Fuel Compaction Cost [\$/ccFuel]	1.5	\$/ccFuel	Fuel Cost
TRISO Fabrication Cost [\$/particle]	0.0045	\$/particle	Fuel Cost
Core Cost Factor	1	factor	Fuel Cost
Nuclear Plant Site Labor Cost Learning	0.131	factor	Learning
Nuclear Plant Site Labor Hours Learning	0.131	factor	Learning
Nuclear Plant Site Material Cost Learning	0.071	factor	Learning
Nuclear Plant Factory Equipment Cost Learning	0.160	factor	Learning
Buildings Site Labor Cost Learning	0.131	factor	Learning
Buildings Site Labor Hours Learning	0.131	factor	Learning
Buildings Site Material Cost Learning	0.071	factor	Learning
Buildings Factory Equipment Cost Learning	0.160	factor	Learning
Adjacent Plant Site Labor Cost Learning	0.131	factor	Learning
Adjacent Plant Site Labor Hours Learning	0.131	factor	Learning
Adjacent Plant Site Material Cost Learning	0.071	factor	Learning
Adjacent Plant Factory Equipment Cost Learning	0.160	factor	Learning
Fuel Site Labor Cost Learning	0.131	factor	Learning

Parameter	Value	Unit	Group
Fuel Site Labor Hours Learning	0.131	factor	Learning
Fuel Site Material Cost Learning	0.071	factor	Learning
Fuel Factory Equipment Cost Learning	0.160	factor	Learning
Burnable Poison Material	Gd	from dict	Manufacturing
RPV Manufacturing Pathway	Forging - Ganda	from dict	Manufacturing
Fuel Manufacturing Pathway	FCM Sintering	from dict	Manufacturing
HX Manufacturing Pathway	Printed Circuit Diffusion Bonded	from dict	Manufacturing
Moderator Manufacturing Pathway	Machining Graphite - Quotes	from dict	Manufacturing
RPV Material	SA-533	from dict	Manufacturing
Moderator Material	C	from dict	Manufacturing
Stored Energy Model	crude1	from dict	Model
Power Rating Model	k-dominated	from dict	Model
A.212 Offsite Material Efficiency	1.1	factor	Modularization
A.221 Offsite Material Efficiency	1.1	factor	Modularization
A.223 Offsite Material Efficiency	1.1	factor	Modularization
A.226 Offsite Material Efficiency	1.1	factor	Modularization
A.227 Offsite Material Efficiency	1.1	factor	Modularization
A.23 Offsite Material Efficiency	1.1	factor	Modularization
A.24 Offsite Material Efficiency	1.1	factor	Modularization
A.212 Offsite Labor Efficiency	2.0	factor	Modularization
A.221 Offsite Labor Efficiency	2.0	factor	Modularization
A.223 Offsite Labor Efficiency	2.0	factor	Modularization
A.226 Offsite Labor Efficiency	2.0	factor	Modularization
A.227 Offsite Labor Efficiency	2.0	factor	Modularization
A.23 Offsite Labor Efficiency	2.0	factor	Modularization
A.24 Offsite Labor Efficiency	2.0	factor	Modularization
A.212 Fraction Offsite Work	0.5	factor	Modularization
A.221 Fraction Offsite Work	0.5	factor	Modularization
A.223 Fraction Offsite Work	0.5	factor	Modularization
A.226 Fraction Offsite Work	0.5	factor	Modularization
A.227 Fraction Offsite Work	0.5	factor	Modularization
A.23 Fraction Offsite Work	0.5	factor	Modularization
A.24 Fraction Offsite Work	0.5	factor	Modularization
Operating Model	Medium	from dict	Operating
Capacity Factor	1	fraction	Operating
Down time for refueling (months)	0.66	months	Operating
Nuclear Insurance Yearly	0.01	fraction/yr	Operating
Material and Supplies Yearly	0.025	fraction/yr	Operating
Cost of Uranium conversion	6.00	\$/kgu	Operating
Cost of Uranium (\$/lb)	40.00	\$/lb of U308	Operating
Cost of Uranium enrichment	160.00	\$/SWU	Operating
Wages per FTE	150,000.00	\$/yr	Operating
Average Annual Property Tax (\$M)	0.03	\$M	Operating
Natural Uranium enrichment	0.00711	fraction	Operating
Tailing enrichment	0.0027	fraction	Operating
UNF Dry Cask Volume Packing Fraction	0.33	fraction	Project
UNF Dry Cask Cost [\$/ccFuel]	0.244	\$/ccFuel	Project
Licensing Fees Yearly	0.01	fraction/yr	Project
Tax Rate	0	fraction	Project
Carbon Tax	0	\$/kg CO2e	Project
Tax Subsidy	0	fraction	Project
Tax Subsidy Period	0	years	Project
Inflation Labor	0.03	fraction	Project
Inflation Standard	0.03	fraction	Project
Debt Interest Rate	0.1	fraction	Project
Equity Interest Rate	0.1	fraction	Project
Reinvestment Interest Rate	0.05	fraction	Project
Debt Ratio	1	fraction	Project
Startup duration (months)	36	months	Project
Planet Scale Deployment (GWe)	30	Gwe	Project
Planet Scale Deployment Time (Years)	20	years	Project
Net Electrical Power Target (MWe)	100	MW	Project
Project Lifetime	60	yr	Project
Project Start Year	2024	years	Project
Cost of Land [\$/acre]	0.1	\$/acre	Project
Dry Cask Footprint [m2]	25	m2	Project
Payback Period	20	years	Project
Vessel Design Temperature	643.15	K	Reactor
Minimum Coolant Channel Diameter (m)	0.005	m	Reactor
Core Diameter (m)	3	m	Reactor
Reactor Technology	HTGR	from dict	Reactor
RX power (MW) desired	0	MW	Reactor
Reflector Thickness	0.3	m	Reactor

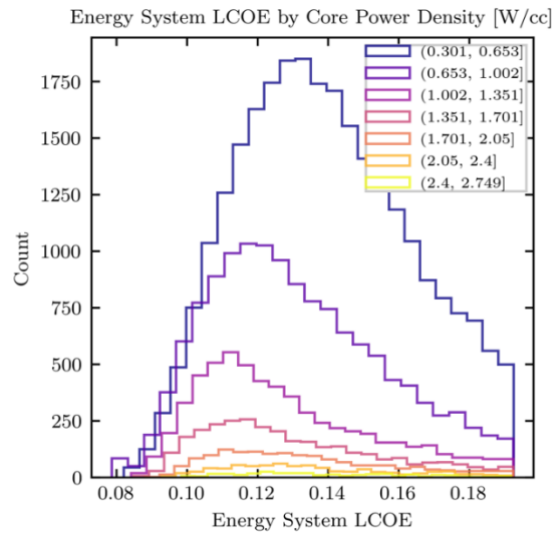
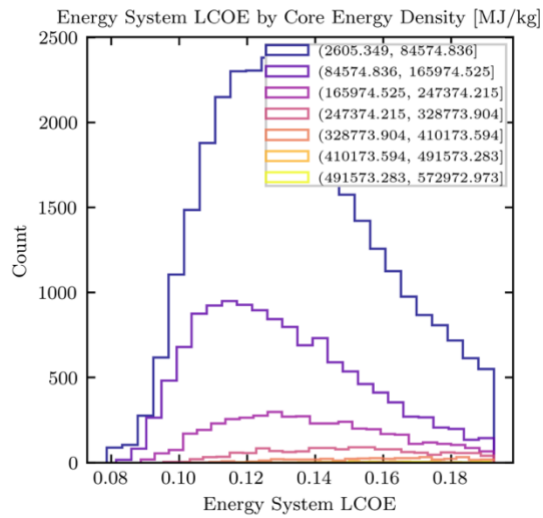
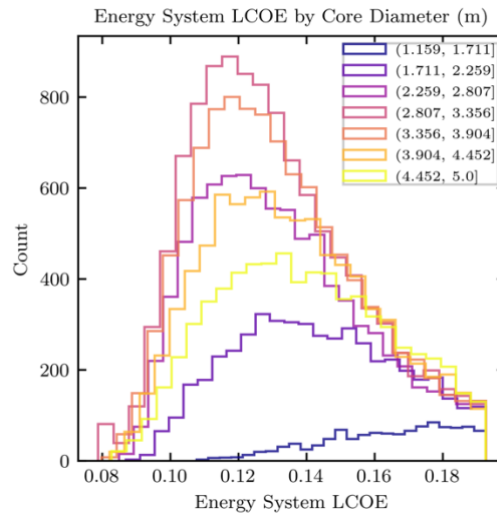
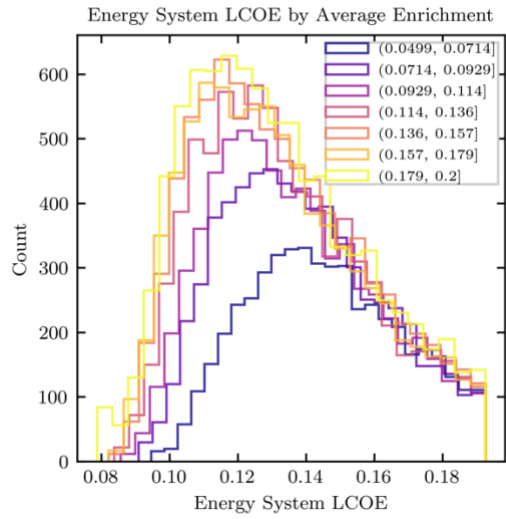
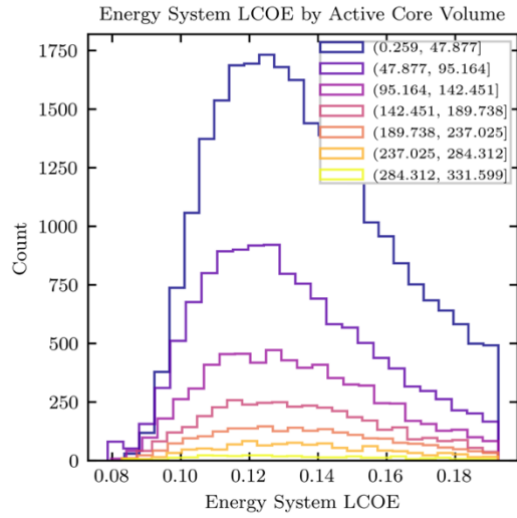
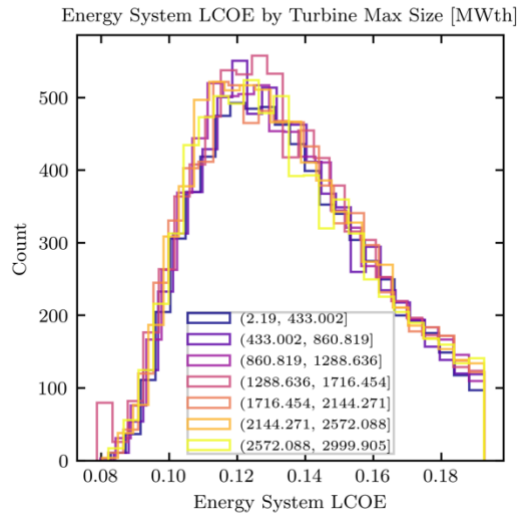
Parameter	Value	Unit	Group
Fuel Volume Fraction	0.1	fraction	Reactor
Reactor Aspect Ratio	2	float	Reactor
Reactor Shape	cyl	from dict	Reactor
Reactor Orientation	vert	from dict	Reactor
Pressure Vessel Design Method	ASME Sec III Div 5 Class A	from dict	Reactor
Shutdown System 1	rods	from dict	Reactor
Max Fuel Allowable Fuel Burnup	160	MWd/kgHM	Reactor
Plenum Volume Fraction	0.1	fraction	Reactor
Pressure Drop Perf Factor	1	factor	Reactor
RPV Damage Threshold Factor	1	factor	Reactor
Power Rating Perf Factor	1	factor	Reactor
Channel Count Factor	1	factor	Reactor
RPV Replacement Cost Factor	1	factor	Reactor
Safety Class	Passive Class A	from dict	Reactor
Coping Time	72	hr	Reactor
Safety Margin	1.3	factor	System
Standard Margin	1.2	factor	System
Primary Thermal Storage Hours	0	hr	Thermal Storage
Secondary Thermal Storage Hours	0	hr	Thermal Storage
[Simple] A.222.12: Reactor Coolant Piping	0.25		Cost Scaling
[Simple] A.223: Safeguards system	0.71		Cost Scaling
[Simple] A.224: Radwaste Processing	0.76		Cost Scaling
[Simple] A.225: Fuel Handling & Storage	0.52		Cost Scaling
[Simple] A.226: Other Reactor Equipment	0.5		Cost Scaling
[Electrical] A.241: Switchgear	0.5483		Cost Scaling
[Electrical] A.242: Station Service Equipment	0.2679		Cost Scaling
[Electrical] A.243: Switchboards	0.9062		Cost Scaling
[Electrical] A.244: Protective Equipment	1.01		Cost Scaling
[Electrical] A.245: Electrical Structures & Wiring Containter	0.5784		Cost Scaling
[Electrical] A.246: Power & Control Wiring	0.6051		Cost Scaling
222.13 Steam generators reduction mult	0.5		Cost Scaling
222.14 Pressurizer reduction mult	0.1		Cost Scaling
SPC steel cost escalation	1.48		Cost Scaling
SPC rebar reduction mult	0		Cost Scaling
SPC operating engineer lift time (per 30 m2)	8		Cost Scaling
SPC weld time (per 30 m2)	87		Cost Scaling
E-beam weld cost reduction mult	0.6		Cost Scaling
212.15 Factory cost mult	3.25		Cost Scaling
212.15 Labor hours mult	4.86		Cost Scaling
212.15 Labor cost mult	4.56		Cost Scaling
212.15 Material cost mult	28.98		Cost Scaling
Pool surface area cost	17,866		Cost Scaling
Structures - unit costs	1		Cost Scaling
Structures - plant power costs	0.8		Cost Scaling
Reactor equipment - plant power costs	0.8		Cost Scaling
Pressure vessel - exponent	0.85		Cost Scaling
RPV - nuclear escalation	34.4		Cost Scaling
RPV internals - exponent	0.85		Cost Scaling
RCP - exponent	0.92		Cost Scaling
RCP - nuclear escalation	39.7		Cost Scaling
Heat exchanger - exponent	1.2		Cost Scaling
Steam generator - nuclear escalation	17		Cost Scaling
Pressurizer - nuclear escalation	12.98		Cost Scaling
Fuel pool volume - exponent	0.75		Cost Scaling
Primary flow rate - exponent	0.75		Cost Scaling
Crane - exponent	1.26		Cost Scaling
Crane - nuclear escalation	1		Cost Scaling
NuScale containment vacuum pump - exponent	0.6		Cost Scaling
NuScale containment flooding drain - exponent	0.85		Cost Scaling
HTGR RCCS - exponent	1.21		Cost Scaling
HTGR refueling - exponent	1.31		Cost Scaling
HTGR He purification - exponent	0.6		Cost Scaling
HTGR circulator - exponent	0.6		Cost Scaling
HTGR circulator - nuclear escalation	0.5		Cost Scaling
BWR isolation condenser - exponent	0.8		Cost Scaling
Turbine equipment electric power - exponent	0.8		Cost Scaling
Electrical equipment electric power - exponent	0.6		Cost Scaling
Service system volume - exponent	1		Cost Scaling
Misc. equipment - exponent	0.8		Cost Scaling
Rejected thermal power - exponent	0.8		Cost Scaling
Heat rejection system - exponent	0.8		Cost Scaling

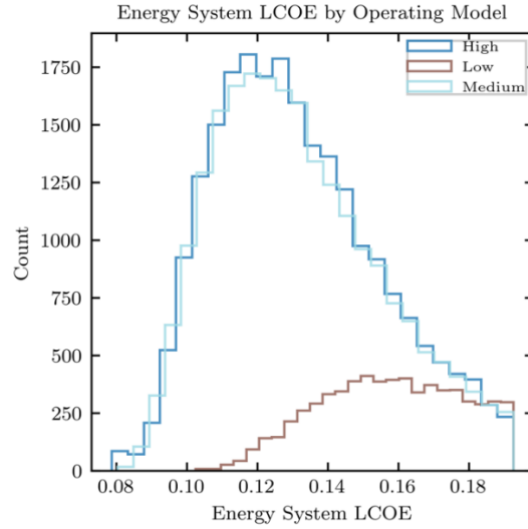
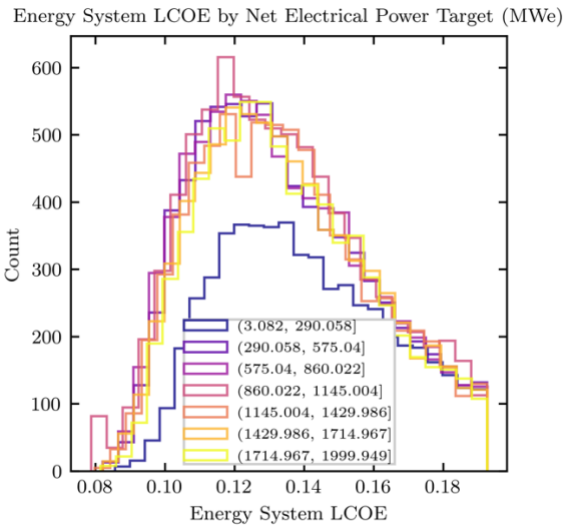
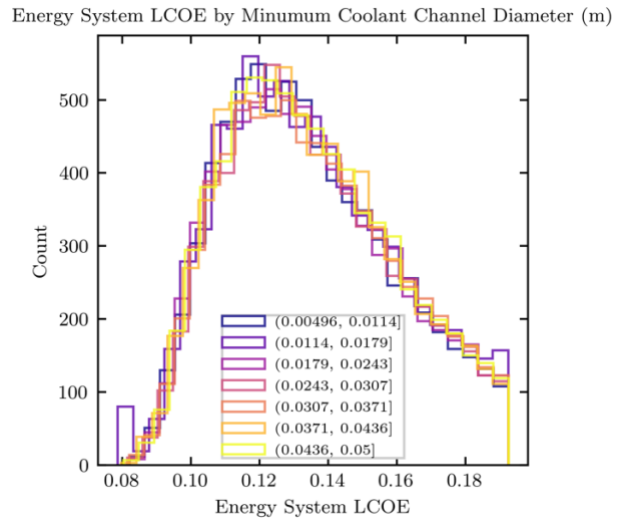
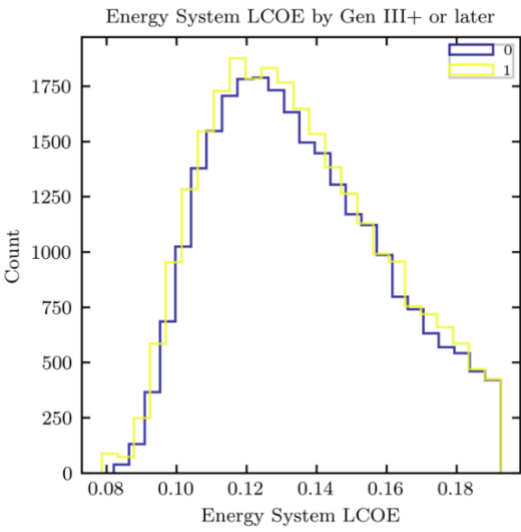
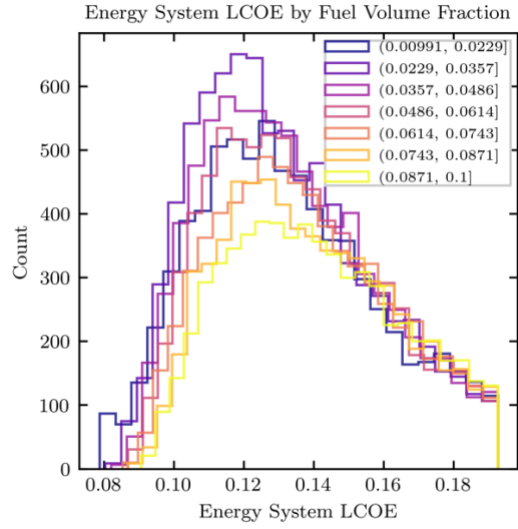
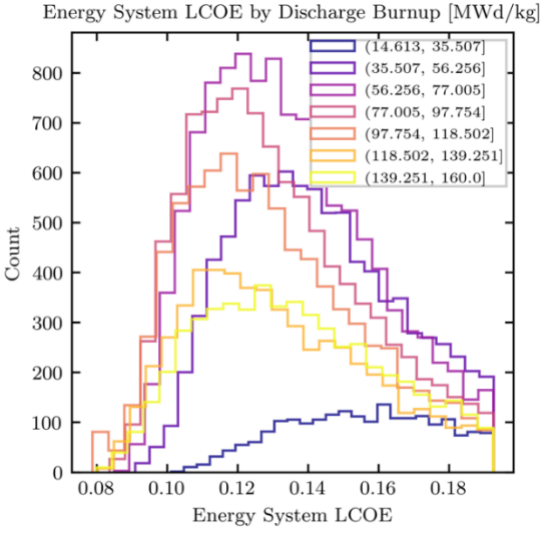
A.225.113	Constant	Structures - unit costs	Constant	Structures - plant power costs
A.225.114	Number of Refueling Systems	Structures - unit costs	Fuel cask capacity	Crane - exponent
A.225.12	Number of Refueling Systems	Structures - unit costs	Constant	Structures - plant power costs
A.225.13	Number of Refueling Systems	Structures - unit costs	Constant	Structures - plant power costs
A.225.3	Number of Refueling Systems	Structures - unit costs	Constant	Structures - plant power costs
A.225.4	Constant	Structures - unit costs	Fuel storage building - Spent fuel pool volume	Fuel pool volume - exponent
A.226.1	Constant	Structures - unit costs	Total Plant Thermal Power (MWt)	Structures - plant power costs
A.226.3	Constant	Structures - unit costs	Total Plant Thermal Power (MWt)	Structures - plant power costs
A.226.4	Constant	Structures - unit costs	Total Plant Thermal Power (MWt)	Structures - plant power costs
A.226.6	Constant	Structures - unit costs	Total Plant Thermal Power (MWt)	Structures - plant power costs
A.226.71	Constant	Structures - unit costs	Total Plant Thermal Power (MWt)	Reactor equipment - plant power costs
A.226.72	Constant	Structures - unit costs	Total Plant Thermal Power (MWt)	Structures - plant power costs
A.226.8	Constant	Structures - unit costs	Constant	Structures - plant power costs
A.226.9	Constant	Structures - unit costs	Constant	Structures - plant power costs
A.227.11	Number of RXs	Structures - unit costs	Constant	Structures - plant power costs
A.227.15	Constant	Structures - unit costs	Constant	Structures - plant power costs
A.227.16	Constant	Structures - unit costs	Constant	Structures - plant power costs
A.227.17	Constant	Structures - unit costs	Constant	Structures - plant power costs
A.227.18	Constant	Structures - unit costs	Constant	Structures - plant power costs
A.227.19	Constant	Structures - unit costs	Constant	Structures - plant power costs
A.227.2	Constant	Structures - unit costs	Constant	Structures - plant power costs
A.227.3	Constant	Structures - unit costs	Constant	Structures - plant power costs
A.227.4	Number of RXs	Structures - unit costs	Constant	Structures - plant power costs
A.227.5	Number of RXs	Structures - unit costs	Constant	Structures - plant power costs
A.227.9	Number of RXs	Structures - unit costs	Constant	Structures - plant power costs
A.228.1	Constant	Structures - unit costs	Constant	Structures - plant power costs
A.228.2	Constant	Structures - unit costs	Constant	Structures - plant power costs
A.228.4	Number of RXs	Structures - unit costs	RPV Surface Area (m2)	Structures - plant power costs
A.229.1	Number of RXs	Structures - unit costs	RX power (MW)	NuScale containment vacuum pump - exponent
A.229.2	Number of RXs	Structures - unit costs	RX power (MW)	NuScale containment flooding drain - exponent
A.229.3	Number of RXs	Structures - unit costs	RPV Surface Area (m2)	HTGR RCCS - exponent
A.229.4	Number of Refueling Systems	Structures - unit costs	Core Diameter (m)	HTGR refueling - exponent
A.229.5	Number of RXs	Structures - unit costs	He purif flow rate (kg/s)	HTGR He purification - exponent
A.229.6	Number of RXs	Structures - unit costs	Total Plant Thermal Power (MWt)	Structures - plant power costs
A.229.7	Number of RXs	Structures - unit costs	RX power (MW)	BWR isolation condenser - exponent
A.231.	Number of Turbines	Structures - unit costs	Turbine Power [MWt/unit]	Turbine equipment electric power - exponent
A.233.	Number of Turbines	Structures - unit costs	Turbine Power [MWt/unit]	Turbine equipment electric power - exponent
A.234.	Number of Turbines	Structures - unit costs	Turbine Power [MWt/unit]	Turbine equipment electric power - exponent
A.235.	Number of Turbines	Structures - unit costs	Turbine Power [MWt/unit]	Turbine equipment electric power - exponent
A.236.	Number of Turbines	Structures - unit costs	Turbine Power [MWt/unit]	Turbine equipment electric power - exponent
A.237.	Number of Turbines	Structures - unit costs	Turbine Power [MWt/unit]	Turbine equipment electric power - exponent
A.241.	Number of Turbines	Structures - unit costs	Turbine Power [MWt/unit]	Electrical equipment electric power - exponent
A.242.	Number of Turbines	Structures - unit costs	Turbine Power [MWt/unit]	Electrical equipment electric power - exponent
A.243.	Number of Turbines	Structures - unit costs	Turbine Power [MWt/unit]	Electrical equipment electric power - exponent
A.244.	Number of Turbines	Structures - unit costs	Turbine Power [MWt/unit]	Electrical equipment electric power - exponent
A.245.	Number of Turbines	Structures - unit costs	Turbine Power [MWt/unit]	Electrical equipment electric power - exponent
A.246.	Number of Turbines	Structures - unit costs	Turbine Power [MWt/unit]	Electrical equipment electric power - exponent
A.251.111	Constant	Structures - unit costs	TG crane capacity	Crane - exponent
A.251.112	Constant	Structures - unit costs	Heater bay crane capacity	Crane - exponent
A.251.12	Constant	Structures - unit costs	Containment crane	Crane - exponent
A.251.16	Constant	Structures - unit costs	Constant	Structures - unit costs
A.251.17	Constant	Structures - unit costs	Diesel building crane	Crane - exponent
A.252.1	Constant	Structures - unit costs	Volume of 212, 213, 215, 216, 217	Service system volume - exponent
A.252.2	Constant	Structures - unit costs	Volume of 212, 213, 215, 216, 217	Service system volume - exponent
A.252.3	Constant	Structures - unit costs	Volume of 212, 213, 215, 216, 217	Service system volume - exponent
A.252.4	Constant	Structures - unit costs	Constant	Structures - unit costs
A.253.	Constant	Structures - unit costs	Volume of 212, 213, 215, 216, 217	Service system volume - exponent
A.254.	Constant	Structures - unit costs	Volume of 212, 213, 215, 216, 217	Service system volume - exponent
A.255.	Constant	Structures - unit costs	Constant	Structures - unit costs
A.261.1	Constant	Structures - unit costs	Heat Rejected (MWt)	Rejected thermal power - exponent
A.261.2	Constant	Structures - unit costs	Heat Rejected (MWt)	Rejected thermal power - exponent
A.261.3	Constant	Structures - unit costs	Heat Rejected (MWt)	Rejected thermal power - exponent
A.262.11	Constant	Structures - unit costs	Heat Rejected (MWt)	Rejected thermal power - exponent
A.262.12	Constant	Structures - unit costs	T/B Bldg - Cooling source distance (m)	Structures - unit costs
A.262.13	Constant	Structures - unit costs	Heat Rejected (MWt)	Rejected thermal power - exponent
A.262.14	Constant	Structures - unit costs	Heat Rejected (MWt)	Rejected thermal power - exponent
A.262.15	Constant	Structures - unit costs	Heat Rejected (MWt)	Rejected thermal power - exponent
A.29111	Loop 0: He to Solar Salt, HX Count	Structures - unit costs	Constant	Structures - plant power costs
A.29112	Constant	Structures - unit costs	Constant	Structures - plant power costs
A.29113	Constant	Structures - unit costs	Constant	Structures - plant power costs
A.29114	Loop 0: He, Circ Count	Structures - unit costs	Constant	Structures - plant power costs
A.29115	Loop 0: He, Circ Count	Structures - unit costs	Constant	Structures - plant power costs
A.29116	Loop 1: Solar Salt to Steam, HX Count	Structures - unit costs	Constant	Structures - plant power costs
A.29117	Constant	Structures - unit costs	Constant	Structures - plant power costs
A.29118	Constant	Structures - unit costs	Constant	Structures - plant power costs
A.29119	Loop 1: Solar Salt, Circ Count	Structures - unit costs	Constant	Structures - plant power costs
A.29121	Constant	Structures - unit costs	Constant	Structures - plant power costs
A.29122	Constant	Structures - unit costs	Constant	Structures - plant power costs
A.29123	Loop 2: Steam, Circ Count	Structures - unit costs	Constant	Structures - plant power costs
A.11	Constant	Structures - unit costs	Constant	Structures - plant power costs

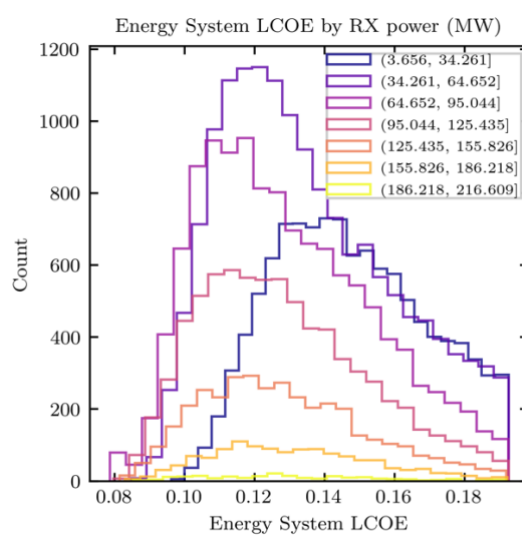
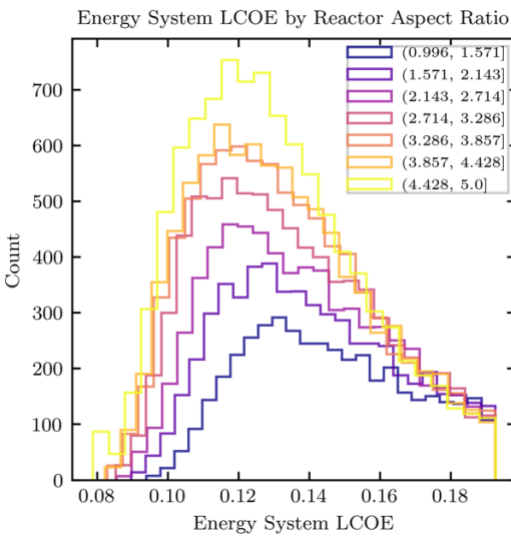
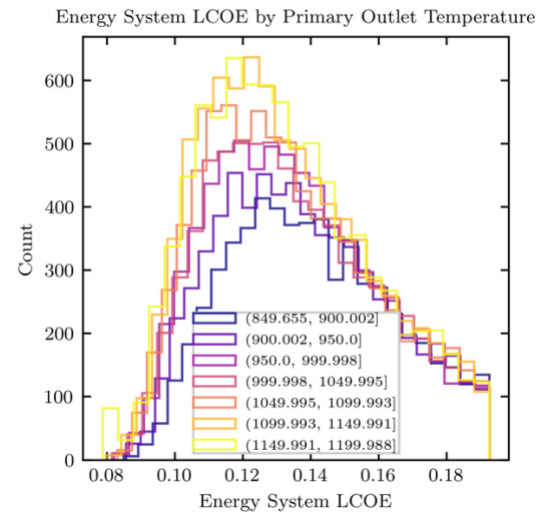
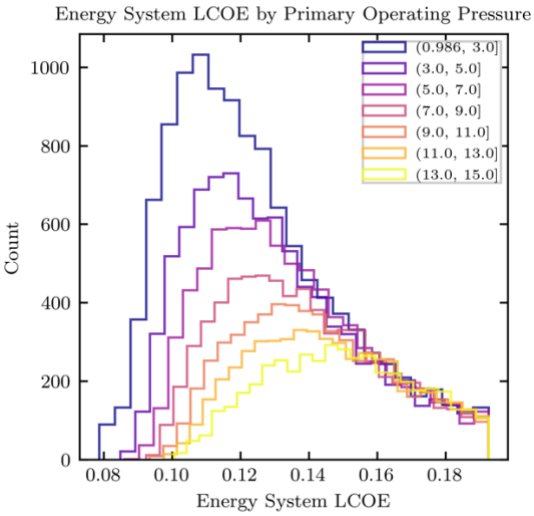
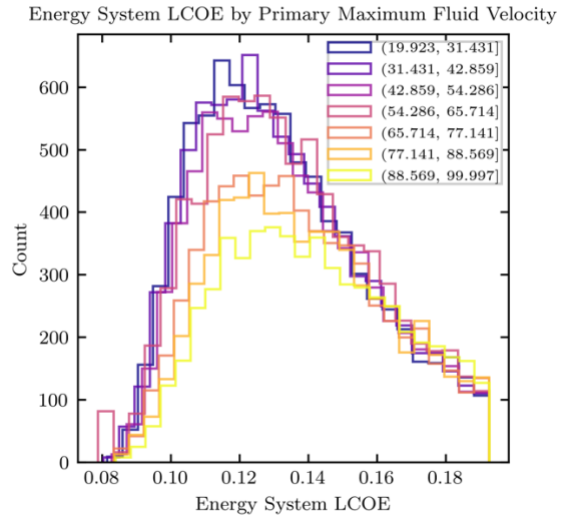
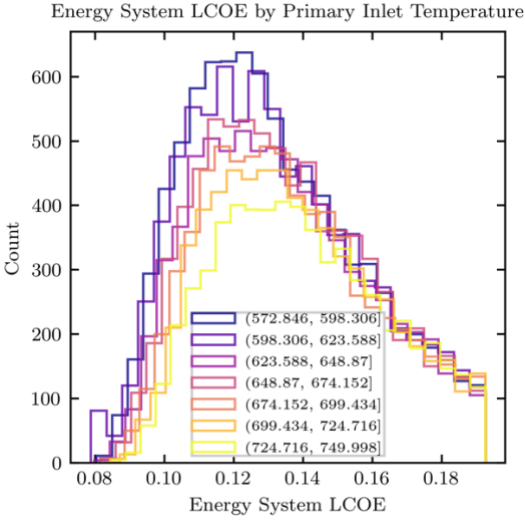
10.2.2 Special Rules

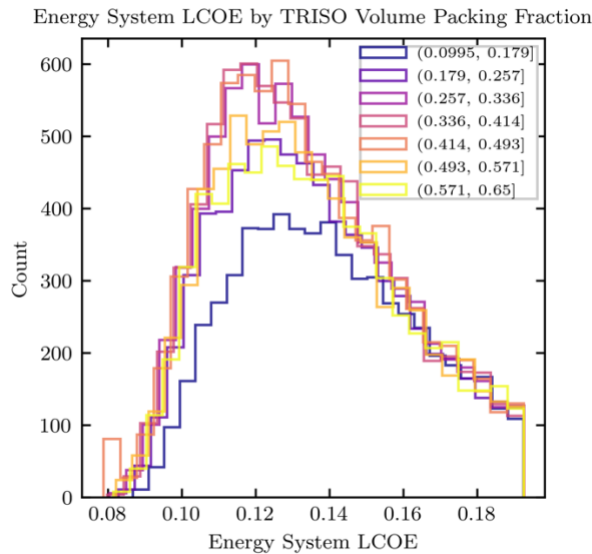
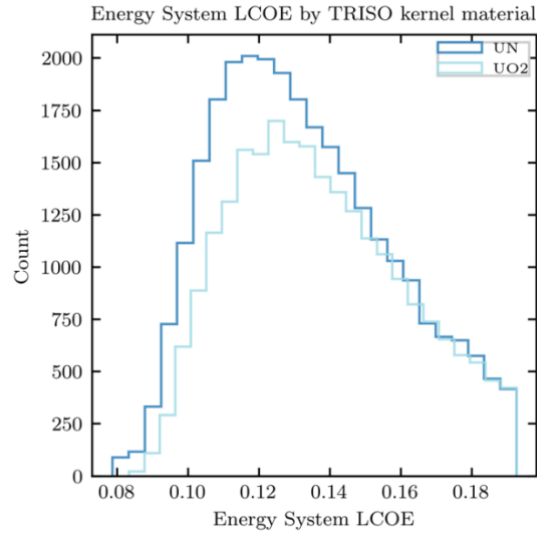
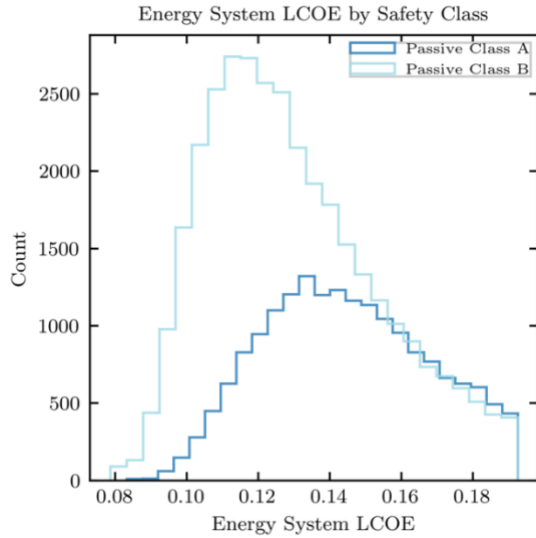
Account	Cost Categories	Function	Args
A.223	['Site Material Cost', 'Factory Equipment Cost', 'Site Labor Cost', 'Site Labor Hours']	Multiply	{'toggle_var': 'Safety Class', 'toggle_true': ['Passive Class A'], 'mult_true': 0}
A.224	['Site Material Cost', 'Factory Equipment Cost', 'Site Labor Cost', 'Site Labor Hours']	Multiply	{'toggle_var': 'Safety Class', 'toggle_true': ['Passive Class A'], 'mult_true': 0}
A.227.9	['Site Material Cost', 'Factory Equipment Cost', 'Site Labor Cost', 'Site Labor Hours']	Multiply	{'toggle_var': 'Safety Class', 'toggle_true': ['Passive Class A'], 'mult_true': 0}
A.212.15	['Site Material Cost', 'Factory Equipment Cost', 'Site Labor Cost', 'Site Labor Hours']	Multiply	{'toggle_var': 'Safety Class', 'toggle_true': ['Passive Class A'], 'mult_true': 0}
A.241	['Site Material Cost', 'Factory Equipment Cost', 'Site Labor Cost', 'Site Labor Hours']	Multiply	{'toggle_var': 'Safety Class', 'toggle_true': ['Passive Class A', 'Passive Class B'], 'mult_true': ['Electrical] A.241: Switchgear'}
A.242	['Site Material Cost', 'Factory Equipment Cost', 'Site Labor Cost', 'Site Labor Hours']	Multiply	{'toggle_var': 'Safety Class', 'toggle_true': ['Passive Class A', 'Passive Class B'], 'mult_true': ['Electrical] A.242: Station Service Equipment'}
A.243	['Site Material Cost', 'Factory Equipment Cost', 'Site Labor Cost', 'Site Labor Hours']	Multiply	{'toggle_var': 'Safety Class', 'toggle_true': ['Passive Class A', 'Passive Class B'], 'mult_true': ['Electrical] A.243: Switchboards'}
A.244	['Site Material Cost', 'Factory Equipment Cost', 'Site Labor Cost', 'Site Labor Hours']	Multiply	{'toggle_var': 'Safety Class', 'toggle_true': ['Passive Class A', 'Passive Class B'], 'mult_true': ['Electrical] A.244: Protective Equipment'}
A.245	['Site Material Cost', 'Factory Equipment Cost', 'Site Labor Cost', 'Site Labor Hours']	Multiply	{'toggle_var': 'Safety Class', 'toggle_true': ['Passive Class A', 'Passive Class B'], 'mult_true': ['Electrical] A.245: Electrical Structures & Wiring Containter'}
A.246	['Site Material Cost', 'Factory Equipment Cost', 'Site Labor Cost', 'Site Labor Hours']	Multiply	{'toggle_var': 'Safety Class', 'toggle_true': ['Passive Class A', 'Passive Class B'], 'mult_true': ['Electrical] A.246: Power & Control Wiring'}
A.221.12	['Site Material Cost', 'Factory Equipment Cost', 'Site Labor Cost', 'Site Labor Hours']	Multiply	{'toggle_var': 'E-beam Welding', 'toggle_true': [1], 'mult_true': 'E-beam weld cost reduction mult'}
A.222.13	['Site Material Cost', 'Factory Equipment Cost', 'Site Labor Cost', 'Site Labor Hours']	Multiply	{'toggle_var': 'Integral Vessel', 'toggle_true': [1], 'mult_true': '222.13 Steam generators reduction mult'}
A.222.14	['Site Material Cost', 'Factory Equipment Cost', 'Site Labor Cost', 'Site Labor Hours']	Multiply	{'toggle_var': 'Integral Vessel', 'toggle_true': [1], 'mult_true': '222.14 Pressurizer reduction mult'}
A.222.12	['Site Material Cost', 'Factory Equipment Cost', 'Site Labor Cost', 'Site Labor Hours']	Multiply	{'toggle_var': 'Gen III+ or later', 'toggle_true': [1], 'mult_true': ['Simple] A.222.12: Reactor Coolant Piping'}
A.223	['Site Material Cost', 'Factory Equipment Cost', 'Site Labor Cost', 'Site Labor Hours']	Multiply	{'toggle_var': 'Gen III+ or later', 'toggle_true': [1], 'mult_true': ['Simple] A.223: Safeguards system'}
A.224	['Site Material Cost', 'Factory Equipment Cost', 'Site Labor Cost', 'Site Labor Hours']	Multiply	{'toggle_var': 'Gen III+ or later', 'toggle_true': [1], 'mult_true': ['Simple] A.224: Radwaste Processing'}
A.225	['Site Material Cost', 'Factory Equipment Cost', 'Site Labor Cost', 'Site Labor Hours']	Multiply	{'toggle_var': 'Gen III+ or later', 'toggle_true': [1], 'mult_true': ['Simple] A.225: Fuel Handling & Storage'}
A.226	['Site Material Cost', 'Factory Equipment Cost', 'Site Labor Cost', 'Site Labor Hours']	Multiply	{'toggle_var': 'Gen III+ or later', 'toggle_true': [1], 'mult_true': ['Simple] A.226: Other Reactor Equipment'}
A.212	[]	Modularize	{}
A.221	[]	Modularize	{}
A.223	[]	Modularize	{}
A.226	[]	Modularize	{}
A.227	[]	Modularize	{}
A.23	[]	Modularize	{}
A.24	[]	Modularize	{}
A.21	['Site Material Cost', 'Factory Equipment Cost', 'Site Labor Cost', 'Site Labor Hours']	Learning	{'learning cat': 'Buildings'}
A.22	['Site Material Cost', 'Factory Equipment Cost', 'Site Labor Cost', 'Site Labor Hours']	Learning	{'learning cat': 'Nuclear Plant'}
A.23	['Site Material Cost', 'Factory Equipment Cost', 'Site Labor Cost', 'Site Labor Hours']	Learning	{'learning cat': 'Adjacent Plant'}
A.24	['Site Material Cost', 'Factory Equipment Cost', 'Site Labor Cost', 'Site Labor Hours']	Learning	{'learning cat': 'Adjacent Plant'}
A.25	['Site Material Cost', 'Factory Equipment Cost', 'Site Labor Cost', 'Site Labor Hours']	Learning	{'learning cat': 'Adjacent Plant'}
A.26	['Site Material Cost', 'Factory Equipment Cost', 'Site Labor Cost', 'Site Labor Hours']	Learning	{'learning cat': 'Adjacent Plant'}
A.29	['Site Material Cost', 'Factory Equipment Cost', 'Site Labor Cost', 'Site Labor Hours']	Learning	{'learning cat': 'Adjacent Plant'}

10.3 GA Population on Full Set









10.4 Materials and Fluids

Alexandria is a legacy python library developed by Dr. Christopher Morrison to create material cards in neutronic code inputs for a large library of custom or pre-built materials. The package provides an excellent way to define materials isotopically and because I envisioned using this code for coupled calculations at some point, I built in other material property data as a wrapper on Alexandria. I collected thermal property data across many sources for many materials, particularly the nuclear materials and civil materials that are required for the design estimates. Of particular interest were graphite, UO₂, UN, SiC, YH_x, ZrH_x, Be, carbon steel, stainless steel, concrete, and bedrock. Properties obtained included density, thermal conductivity, specific heat capacity, melting point, emissivity, and maximum temperature. The data came in the form of single values at known or unknown temperature or as functions of temperature. For many of the core materials, property data was found in the literature as irradiated and with temperature dependence. The wrapper conveniently uses whatever data is available for the material of interest starting with property fits and otherwise using available standalone values.

ASME Table 1A and 2A are used to look up stress intensity at the design temperature. Modulus, CTE, and Poisson's ratio and other material data have not yet been added.

The fluids of interest included helium and other noble gases, air, molten salt and water. I collected thermal and physical property data as functional forms of temperature and pressure, when available. CoolProps [166] was the source for water data.

10.5 AM Component Cost Estimation

Many AM methods are emerging technologies with different and evolving cost profiles, capabilities, maturity, and promise for use in nuclear reactor systems. Initial efforts by national labs, industry and NRC have focused on just five processes for the NRC's "Final Guidance on Initial AMTs"; namely Laser Powder Bed Fusion (LPBF), Directed Energy Deposition (DED), Cold Spray, Electron Beam Welding, and Power Metallurgy – Hot isostatic Pressing. Other AM methods are under development outside of the NRC's AMT Action Plan.

10.5.1 Bottom-Up Approaches

With sufficient process, cost, and component information, one could assemble bottom-up cost estimates for a particular method and component. The bottom-up approach can be applied to any manufacturing process by determining a manufacturing process's representative input parameters, step counts, and times. Similar adapted cost sums are available for most manufacturing techniques (e.g. traditional[167], cold-spray[168], HX[169]). Some other analysis on additive cost estimates can be found in [170], [171].

We can compute the costs for a generic additive printing process as below. The print is associated with N total parts ever produced with the machine, n parts produced per batch, and costs per part, and costs per kg of product. I can then normalize the cost by the n parts or the kg of finished product to find the cost per part or cost per kg. I combine all the costs, adjusted for a cost per part as below. The set of costs correspond to lifetime product costs, per batch costs, per part costs, and per kg costs.

$$c[\text{per part}] = \frac{1}{N} [c_{data}] + \frac{1}{n} [c_{prep} + c_{materials} + c_{run} + c_{clean} + c_{post}] \\ + [c_{heat} + c_{weld} + c_{assembly} + c_{inspection} + c_{testing} + c_x] + m_{part} [c_{transport}]$$

c_f , cost raw material \$/kg

v_f , final volume cm³ per part

v_p , printed volume cm³ per part, including final part and supports

$v_{enclosed} > v_p$, volume enclosed cm³ per part, including supports,

η , density

l_{build} , build volume side length

$l_{build}^3 = v_{build}$, build volume

$n = \lceil \text{floor}(l_{build}/v_{enclosed}^{1/3}) \rceil^3$, number of parts in build volume approximated by cubes of enclosed volume that fit inside build volume,

$c_{materials} = c_f \left(\frac{v_p}{\eta} + (v_{build} - \frac{v_p}{\eta})(1-r) \right)$, r the powder recycling rate (r is recovered). The powder in the printed volume is consumed as well as $1-r$ of the rest of the build volume.

$c_{prep} = (c_{machine} + c_{labor})t_{prep}$

$c_{run} = c_{machine}t_{run}$, $t_{run} = \frac{v_p}{\gamma}$,

γ , build rate

c_{post} , c_{weld} , $c_{assembly} \rightarrow c_x \approx c_{labor}t_x$

c_{heat} , a cost per heating treatment per part

The machine cost is made up of depreciation costs, overhead and maintenance costs, and power costs which be turned into hourly rates with an assumption of yearly utilization.

$$c_{machine} = \frac{c_{unit}r_d}{t_{year}f_{capacity}} + \frac{c_{unit}r_{OH}}{t_{year}f_{capacity}} + (P \cdot c_{electricity}).$$

$n_{part,yr} = \frac{t_{year}f_{capacity}}{t_{prep}+t_{run}}$, assuming the AM system is the rate limiting step

Using this model, I can estimate an AM HX cost and determine the cost drivers. For example, what happens as additive manufacturing technologies improve with faster build rates, larger volumes, or improved material reusability? What are the drivers of an AM component's cost in terms of material, machinery, labor, or other steps in the process? As an example, I use the reference estimate data for additively manufactured HX from [169] with other baseline assumptions like the machine utilization and the material cost. The reference cost composition is shown below and the reference cost data is given Table 42.

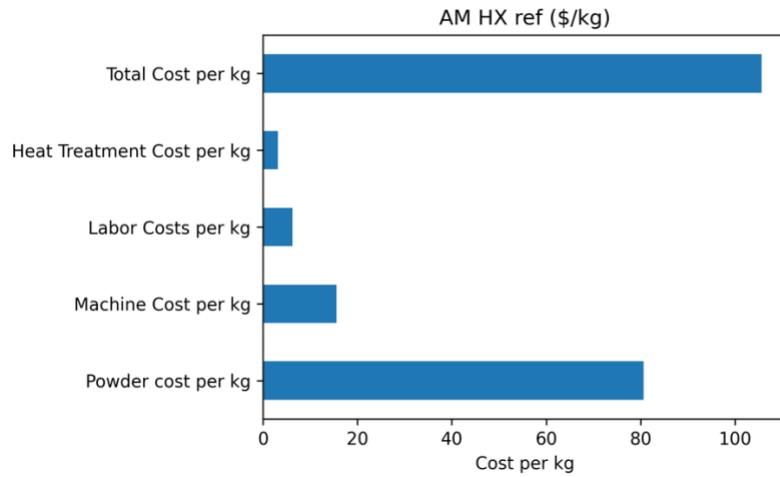


Figure 60 Cost composition of the reference additively manufactured steel HX at 300 cc/hr.

We then vary the a parameter like the build rate and observe the changes in cost composition. As expected from glancing at the cost equation above, I see that higher build rates at constant machine capital cost reduces costs asymptotically to the material and labor costs. In this case, material costs dominate, partly because unused powder recovery is low at 20%.

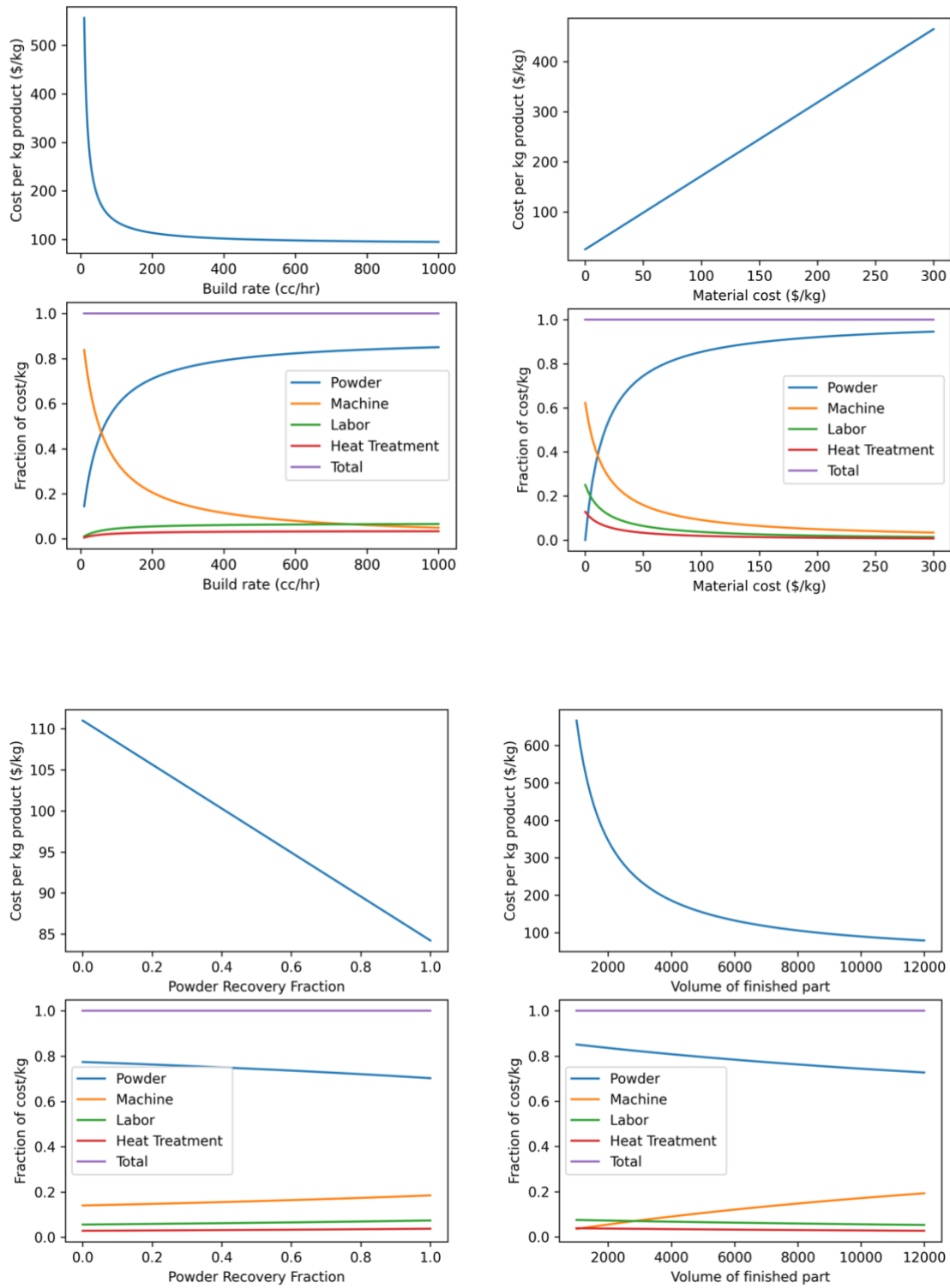


Figure 61 Effect of different parameters on cost per kg of product. As processes are finetuned and CAPEX is reduced, powder costs dominate the overall cost.

Table 42 Parameters used to evaluate AM costs.

Parameter	Value	Parameter	Value
Source	[169]	Total Cost per run \$	66081.70
Heat Treatment Cost (\$/part)	200.00	Powder cost per part	5041.49
Volume of finished part	8000.00	Powder cost per kg	80.59
Enclosed volume of finished part	12167.00	Powder cost per cc	0.63
Support fraction of enclosed volume	0.05	Powder cost per frac	0.76
Build Volume Side Length	50.00	Machine Cost per kg	15.59
Build rate (cc/hr)	300.00	Machine Cost per cc	0.12
Material Density	7.82	Machine Cost per frac	0.15
Material cost (\$/kg)	55.00	Labor Costs per part	391.25
Machine Cost (\$M)	0.70	Labor Costs per kg	6.25
Material Yield	0.85	Labor Costs per cc	0.05
Powder Recovery Fraction	0.20	Labor Costs per frac	0.06
Machine power consumption (kW)	10.00	Heat Treatment Cost per part	200.00
Time for data preparation (hr)	1.00	Heat Treatment Cost per kg	3.20
Time for machine preparation (hr)	0.75	Heat Treatment Cost per cc	0.03
Time to clean, remove any support (hr)	0.75	Heat Treatment Cost per frac	0.03
Time for part welding (hr)	1.00	Total Cost per part	6608.17
Time for part assembly (hr)	2.00	Total Cost per kg	105.63
Time for part testing (hr)	2.00	Total Cost per cc	0.83
Time for part inspection (hr)	2.00	Total Cost per frac	1.00
Mass of finished part (kg)	62.56		
Volume of support material	608.35		
Volume print per part	8608.35	Facility Parameters	Value
Void fraction	0.34	Electricity Rate (\$/kWh)	0.07
Build Volume	125000.00	Labor Rate (\$/hr)	50
n parts per run	10.00	Operating Capacity (days/yr)	310
n parts per run side fit	8.00	Machine Capacity Factor	0.85
Print Volume	86083.50	Annual Depreciation Rate	0.15
Powder Unused	38916.50	Annual Overhead Rate	0.15
Powder Recovery	7783.30		
Powder Volume Needed per run	117216.70		
Powder Mass Needed per run (kg)	916.63		
Powder cost per run	50414.90		
t _{run}	286.95		
Machine Hours per year	6324.00		
runs per year	21.98		
parts per year	219.82		
Machine Cost (\$)	700000.00		
Machine Depreciation Hourly Rate	16.65		
Machine Overhead Hourly Rate	16.65		
Machine Power Consumption Rate	0.70		
Machine Cost Hourly	33.99		
Machine Cost per run	9754.30		
Machine Cost per part	975.43		
Labor Costs per run	3912.50		
Heat Treatment Cost per run	2000.00		

10.6 Ultimate Cost Limits

Cost estimates include margin and biases of the current state of technology, regulation, and market which could be in its infancy as in the case of many AM techniques, or stagnant as in the case of nuclear components like Beryllium metal, helium circulators, and nuclear RPVs. At low quantities, overhead, tooling and factory cost is important, and the margin required to motivate a half-interested supplier for a one-off build can be breathtaking. To drive R&D decisions, it is useful to be able to predict the cost of a material or component in the limit of scaled up production and mature R&D and without the built-in discounts from market and policy distortions (e.g. using developing world labor or environmental regulations, tariffs, or subsidies). I can bypass current cost information that reflects decades and sometimes centuries of R&D on the extraction, processing, and forming of certain materials that were either the lowest hanging fruit or the most readily available with the highest utility for existing industries. To varying degree, these limits also avoid dealing with the details of good or bad design and present cost limits under equal design ability.

10.6.1 Cost Limit by Basic Inputs

The first approach to estimate cost limits is to sum up the basic inputs as they are available. These basic inputs are:

- Primary feedstock price and feedstock use efficiency
- Energy, equipment, labor costs to process, arrange and form, inspect, assemble components
- Paper costs
- Sales and transport costs

10.6.2 Cost limit by Crustal Abundance

In this case, I approximate cost by the crustal abundance corrected by a processing cost factor that captures the energy cost associated with refining and processing a component.

$$Cost_{system} \propto \sum_i^N \frac{m_i}{f_{Eart,i}} \alpha_i$$

Definitions:

m_i : mass of element or isotope i.

$f_{Eart,i}$: crustal abundance on Earth.

α_i : scaling factor for refining and processing energy cost per kg. Generally assume $\alpha_i = 1$.

This contains no information on the energy and cost to extract, transport, and process raw materials into useful feedstock. The cost of transforming feedstock into useful components, and assembling those components is assumed to be negligible. In a high production, high automation, advanced manufacturing environment, all other specific costs like processing, forming, assembly, and transport, will trend to zero per unit output. The material library already defines materials isotopically, so this estimation method can be done with crustal abundances in hand (e.g. Wolfram Database) and an approximate estimate of α_i using the melting temperature and heat capacity.

10.7 Levelized Cost on Long Time Horizons

Modern economies have a tendency to organize themselves to produce a larger volume of lower quality goods. This is a trade of lower upfront CAPEX for higher perpetual OPEX. A system has a CAPEX and OPEX. The CAPEX takes place at the beginning of the project. The OPEX takes place annually over the lifetime of the project. A large part of the OPEX is the CAPEX maintenance and replacement. Larger CAPEX can reduce the OPEX over the lifetime. Consider a 1950s refrigerator built like a tank with simple components and massive margin on the parts. The refrigerator is likely to still be functioning with original components and may require the occasional modular fix. Compare that to a 2020 refrigerator made of plastics, next to no margin, and basically designed for planned obsolescence. Similarly, consider a house made of brick or stone with a lifetime of 300-1000 years, and one built from plywood and plastics with a lifetime of 30-60 years. The upfront CAPEX is reduced by lowering quality, margins, and material capability. This leads to an overall reduction in the lifetime of the components and hence a higher OPEX to replace components or the system outright. While the reduced upfront CAPEX will expand the market and lead to more total refrigerators produced, the OPEX is higher. In many cases, the short-termism of the markets chooses short term gains at a long term loss. I analyze this situation briefly to show in what cases higher upfront CAPEX will lower the overall levelized cost.

For the case of no inflation and an interest rate d I have the levelized cost LC below, where the denominator is the equivalent years of revenue or service. The numerator has C_0 , the CAPEX and c_1 , the OPEX.

$$LC = \frac{CRF(d)C_0 + Nc_1}{N}$$

We consider that c_1 is function of the CAPEX with A and extra operations cost term such as refueling, labor, or cleaning. The second term is the CAPEX replacement cost per unit time, obtained by dividing the total CAPEX by the replacement time.

$$c_1 = f(C_0) = A + \frac{C_0}{t}$$

The replacement time is a function of the CAPEX with subscript r representing a reference point. Consider the cost and lifetime of a paper plate compared to a ceramic plate. α the scaling exponent for cost to obtain the replacement time.

$$t = t_r \left(\frac{C_0}{C_r} \right)^\alpha$$

What is α ? For many components, a cost and performance metric is sublinear or asymptotic. This is the case for luxury or military goods where spending 10x more will barely nudge the performance or utility. However, lifetime can often be a linear or higher power relation. The linear case can be considered redundancy. I can double the lifetime of a component by doubling the margin on the lifetime limiting parameter or adding the same component to the inventory for a simple replacement. Higher powers are common for simply using different materials. For example, a brick or stone house may have 2-3x higher upfront CAPEX but a 5-10x longer lifetime.

Substituting the replacement time and OPEX into the LC equation, I find

$$LC(C_0) = \frac{CRF(d) C_0}{N} + A + \frac{C_r^\alpha C_0^{1-\alpha}}{t_r}$$

And minimizing LC, I get the below, which has real solutions for $\alpha > 1$.

$$C_0 = C_r \left(\frac{N}{CRF(d)t_r} (\alpha - 1) \right)^{1/\alpha}$$

Without considering short term financing limitations, I have shown the existence of optimal CAPEX greater than 0 for $\alpha > 1$. Longer project lifetimes favor higher CAPEX. The non-CAPEX related OPEX cost (A) has no effect on the minima but can reduce the importance of the optimal CAPEX. Increasing real interest rates or lower inflation favors lower optimal CAPEX. I end by noting that in the evaluation of engineered systems and goods like buildings and cars, it should be required to include the price of having to look at the thing. A cost minimized monstrosity is still a monstrosity.

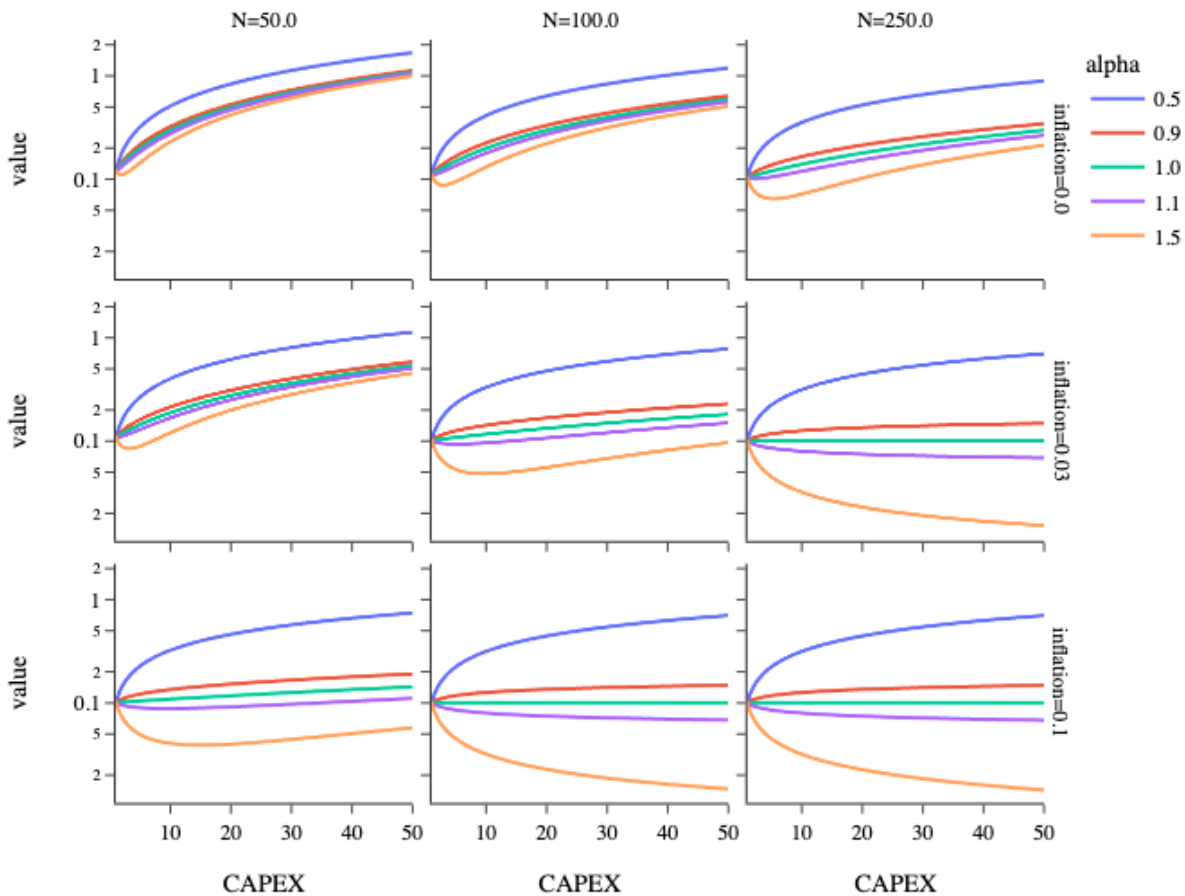


Figure 62 Levelized cost at 10% interest with different inflation rates and lifetimes. Alpha determines how OPEX varies with CAPEX.

10.8 Generalized Wright's Law

We suspect Wright's Law can be modified and generalized to capture the advantages of high production rates. There should be some consideration on the production per unit time so that units produced in short periods of time are rewarded relative to the same number of units produced over longer large periods of time. The idea is that learning only takes place under continuous and high cadence production executed by the same people or factories, on human or company learning timescales and will be less prevalent on widely separated projects executed by different companies or people on timescales that cannot reasonably be expected to yield learning. \dot{N} dependence is rooted in the limitations of knowledge and learning to persevere across production gaps, worker careers, company or product lifetimes, political and economic cycles.

This can be modeled with a modified Wright's law that considers the deployment rate. Interruptions to deployment are not considered but might be expected to reset learning. A few possibilities are shown below for production rate \dot{N} .

Production rate (units/year):

$$\dot{N} = \frac{N}{t_{deploy}}$$

Modified Wright's Law Option 1:

$$c_N = c_1 N^{-\alpha} \dot{N}^{-\beta}$$

Modified Wright's Law Option 2:

$$c_N = c_1 N^{-\alpha-\beta\dot{N}}$$

Modified Wright's Law Option 3:

$$c_N = c_1 N^{f(\dot{N})}$$

With $f(\dot{N})$ some transition function such as a logistic or arctangent, that defines a transition between no learning at low production rates to recover high learning Wright's law at very high production rates. The function could be a logistic with α defining the transition rate, β the transition midway point in years. Fitting these new laws to existing production and cost data remains a future work, albeit with questionable value.

$$c_N = c_1 N^{\left(\frac{-w}{1+e^{-\alpha(N-\beta)}}\right)}$$

10.9 Accident Pathways in CA-HTGR

The possibility of high consequence accidents for CA-HTGR still exists although it is limited to the realm of tampering and misuse. I need to carefully explore and analyze the possibility of new classes of accidents in CA-HTGR or other so-called meltdown proof reactors and consider mechanisms or design choices that may preclude those possibilities without side effects. I consider just three cases pertaining to CA-HTGR reactors. First, BDBA safety analysis makes assumptions about the steady state operating power which alters the stored and decay heat that the reactor has to deal with during accidents. What happens when the operator runs the reactor at four times the rated power level? Essentially, the meltdown proof claims are no longer valid because the reactor and its materials are not intended to dispense four times the rated decay heat. One way to limit power levels may passive heat transfer limiters built into fuel blocks that creates a step function in a HTC. This could be some kind differential CTE mechanism or nonlinear flow mechanism. This would make it impractical to increase the flow rate and operate the reactor at higher power.

Another accident source will come from insufficient fuel quality control. The fuel's ability to withstand extreme accidents relies on the assumption that the fuel in the reactor is the same as the fuel that was qualified. A high degree of QA in both fuel production and fuel loading is needed to have sufficient confidence that the fuel behaves as expected based on prior irradiations and characterization. Compared to the QA on reactor safety systems, lowering the probability out-of-spec fuel is a simpler task that can be approached in a factory environment.

Changes in emissivity of the reactor pressure vessel can also lead to accidents as this reduces the ability to radiatively cool. The outer wall emissivity can be tampered with simply by depositing an additional coating. For example, a high emissivity oxidation layer can be replaced with a low emissivity coating or polished metal finish. This accident possibility is somewhat mitigated by the fact that most metallic surfaces will oxidize, and coatings may decompose at high enough temperatures thus ensuring high emissivity. Also, most materials have an increasing emissivity with increasing temperature.[71] Concerns about emissivity go hand in hand with possible environment tampering such as reactor placement and ambient temperatures. In the first case, reactors might be placed too close to each other leading to shadowing which lowers the effectiveness of radiative cooling. In the second case, the ambient temperatures in the reactor chamber might be elevated due to fire conditions. Unless a bad actor intentionally creates furnace conditions, elevated ambient temperatures in the surrounding bedrock are unlikely because there is no combustible fuel source.

10.10 Spherical Vessel Opportunity

We estimate the mass advantage of a spherical vessel compared to cylindrical vessel for the same volume and pressure. First, I equate the enclosed volume for spherical and cylindrical geometries with parameterized aspect ratio, and then compute the pressure vessel mass ratio. I find a spherical pressure affords at most a 25% mass reduction in the limit of infinite aspect ratio, and a 20% mass reduction for aspect ratio (α) of 2. With W length of section of cylinder, I relate the radii for spherical and cylindrical pill vessels of the same volume,

$$\alpha = \frac{W}{2R_{cyl}}$$

$$V_{cyl} = \pi R_{cyl}^2 (\alpha 2R_{cyl} + R_{cyl} 4/3) = \pi R_{cyl}^3 (\alpha 2 + 4/3)$$

$$V_{sph} = 4/3 \pi R_{sph}^3$$

$$V_{cyl} = V_{sph}$$

$$R_{sph} = R_{cyl} (3/2\alpha + 1)^{1/3}$$

Assuming $t \ll R$, I find the mass of each vessel, using a vessel thickness estimate with stress limit σ ,

$$t_{sph} = \frac{PR}{2\sigma}, t_{cyl} = \frac{PR}{\sigma}$$

$$M_{sph} = 4\pi R_{sph}^2 \frac{PR_{sph}\rho}{2\sigma} = 2\pi R_{sph}^3 P \frac{\rho}{\sigma}$$

$$M_{cyl} = 2\pi R_{cyl}^3 (1 + 2\alpha) P \frac{\rho}{\sigma}$$

And find the ratio of masses,

$$\frac{M_{sph}}{M_{cyl}} = \frac{2\pi R_{sph}^3 P \frac{\rho}{\sigma}}{2\pi R_{cyl}^3 (1 + 2\alpha) P \frac{\rho}{\sigma}} = \frac{1 + 3/2\alpha}{1 + 2\alpha}$$

Note that the ratio is constant so that larger pressure vessels are not more efficient at using material to create a pressurized volume, at least without considering connections, flanges, and valves. As with TRISO particles, smaller vessels may offer benefits like subdivision and the ability to use more brittle or economical materials, but with greater irradiation and neutron leakage.

When the fluid is low pressure or atmospheric, the advantage of spherical vessels over cylindrical vessels is almost negligible, because most of the pressure vessel mass is structural mass.

10.11 Compact Heat Exchanger Design

Heat exchanger specification aims to achieve the needed thermal duty at the lowest cost. HX costs include the capital costs which scales with heat exchanger volume and mass, and operating costs taken as the pumping power requirements. The two cost components are opposed to each other, with smaller surface areas having lower capital costs but requiring higher pressure drops and pumping power. The literature is has many simplified cost models for optimally designing a C HX [69] and general guidelines for design [158].

There are many CHX design configurations that satisfy the required thermal conditions, and I will choose configurations that minimize cost. Particularly, there is a tradeoff between size and pressure drop within manufacturing constraints. The manufacturing constraints include considerations of reasonable aspect ratios, placement of manifolds, minimum channel diameters, maximum allowable stresses for the HX material, fouling and corrosion allowances. There are also fluid velocity considerations that can affect HX performance degradation.

10.11.1 CHX Specification

We need to specify:

- Cold and hot plate channel dimensions (often the same for hot and cold); here I consider just half circle channels
 - Plate thickness

- Channel radius
- Channel hydraulic diameter
- Channel pitch
- Channels can be zig zag, straight, S-shape, or airfoil fin
- Example channel unit area shown in Figure 63 with orange as the flow area.
- HX dimensions (d_{hot} , d_{cold} , d_{stack})
- Number of hot and cold channels
- Coolant channel length

The last three are tied up together, and I must decide which parameters are independent and which dependent. Table 43 shows how the HX parameters are defined indicating inputs and constraints.

Typical channels are half circles due to manufacturing process in etching metal plates. Channel diameters are usually limited to greater than 1 mm. Many channel paths are possible including straight, zig-zag, s-shaped, and airfoil. Plates are usually at least two half-circle radii in thickness to provide sufficient structural support and corrosion allowance. Adjacent channels typically have a half radii separation, and at least a two radii pitch. The plate thickness and channel pitches can be a function of the HX material, and the pressure difference between hot and cold sides. The thickness must be sufficient that maximum allowable stresses are not exceeded but was not addressed here.



Figure 63 Example Unit Area

Table 43 HX Parameters

Variable	Parameter	Definition	Constraint
R	Channel Radius	INPUT	$\geq .25mm$
t_{plate}	Plate Thickness	INPUT	$\geq R$
p	Channel Pitch	INPUT	$\geq 2R$
A_0	Repeating Unit Area	$A_0 = t_{plate} \times p$	
$A_{c,ch}$	Channel cross sectional flow area	$A_{c,ch} = \frac{\pi R^2}{2}$	
γ	Porosity	$\gamma = \frac{A_{c,ch}}{A_0}$	
P_w	Wetted Perimeter	$P_w = (\pi + 2)R$	
D_h	Hydraulic Diameter	$D_h = \frac{4A_c}{P} = \frac{4\pi R^2}{2(2 + \pi)R} = \frac{2\pi R}{(2 + \pi)}$	
d_{cold}	HX dimension; cold side manifold	INPUT	
d_{hot}	HX dimension; hot side manifold	INPUT	
N_{plate}	HX dimension; number of plates	INPUT	
d_z	HX dimension; plate height	$d_z = N_{plate} \times t_{plate}$	
A_{plate}	Plate area	$A_{plate} = d_{cold}d_{hot}$	
N_h, N_c	Number of hot and cold channels	INPUT	$\frac{N_h}{N_{plate}} \leq \frac{d_{hot}}{p}$
$N_{h,plate}, N_{c,plate}$	Number of hot and cold channels per plate	$N_{h,plate} = \frac{N_h}{N_{plate}}$	
L_h, L_c	Hot and cold channel lengths	$L_h = \frac{A_{plate}}{p \times N_{h,plate}} = \frac{A_{plate} N_{plate}}{p N_h}$	
$A_{s,ch,h}, A_{s,ch,c}$	Hot and Cold channel heat transfer area	$A_{s,ch} = P_w L_c = L_c(2 + \pi)R$	
$A_{s,tot}$	HX total heat transfer area (same for hot and cold)	$A_{s,total} = \frac{d_{hot}d_{cold}P_w N_{plate}}{p}$	
t_b	Border Thickness (extra HX solid volume)	$t_b = 0.05 m$	
$V_{HX,ch}$	HX channel volume	$V_{HX,ch} = d_{hot}d_{cold}d_z$	
$V_{HX,b}$	HX border volume	$V_{HX,b} = ((d_{hot} + 2t_b)(d_{cold} + 2t_b) - d_{hot}d_{cold})d_z$	
V_{HX}	HX total volume	$V_{HX} = V_{HX,ch} + V_{HX,b}$	
M_{HX}	HX Mass	$M_{HX} = \rho_m(V_{HX,ch}(1 - \gamma) + V_{HX,b})$	
ρ_{surf}	Total Surface Density	$\rho_{surf} = \frac{A_{s,tot}}{V_{HX}}$	
h	Heat transfer coefficient from Nusselt correlation (see below table)	$\dot{Q} = U A \Delta T_{im}$ $Nu_D = \frac{hD_h}{k} \rightarrow h = \frac{Nu_D k}{D_h}$	
U	Overall heat transfer coefficient (can be evaluated on each segment of channel length)	$U = \frac{1}{\frac{1}{h_c} + \frac{l}{k_{HX}} + \frac{1}{h_h}}$	

Thermal hydraulic correlations are needed to solve for the heat transfer coefficient. [69] created functional fits to the thermal hydraulic correlations for various geometries. This included the ability to change the angles of the geometry. They utilized these fits to optimize HX design including geometric parameters of the channels. This may prove useful in the future, but I limit ourselves here to a 52° zigzag channel as in the following table.

In practice, a gas plate will often have zigzag channels to enhance turbulence, while a liquid plate will be straight channeled to allow for drainage. It should also be noted these correlations are chosen from a population of sometimes conflicting correlations, and predictions rarely match measurements, especially regarding pressure drops.

Geometry	Regime	f correlation	Nu correlation
Straight Channel	Semi-circular, Laminar	$f \cdot Re = 15.78$	$Nu = 4.089$
	Semi-circular, Turbulent	$\frac{1}{\sqrt{f}} = -2.0 \log \left(\frac{e}{3.7} + \frac{2.51}{Re \sqrt{f}} \right)$	$Nu = 0.023 Re^{0.8} Pr^n$
Zigzag Channel	Angle 45°, laminar, helium	$f \cdot Re = 15.78 + 0.62339 Re^{0.78214}$	$Nu = 4.089 + 0.05988 Re^{0.66801}$
	Laminar Angle 52°, turbulent	$f = 0.1924 Re^{-0.091}$	$Nu = 0.1696 Re^{0.629} Pr^{0.317}$

10.11.2 CHX Design Solutions

Thus defined, I can solve for the heat transfer between the hot and cold fluids finding the HTC, heat transfer, and temperatures along the channels. This yields the total thermal duty of the CHX, pressure drop and pumping power for each fluid. I then adjust parameters to get to the required thermal duty. I also solve for HX parameters like CHX porosity, volume, mass, NTU, effectiveness; as well as overall HTC at primary side (kW/m²-°C) overall HTC at secondary side, total surface density (m²/m³), specific performance (MW/m³).

Assumptions:

- Negligible heat loss to the surroundings.
- Negligible kinetic and potential energy changes.
- Temperature dependence properties.
- Negligible fouling factors.
- Fully developed conditions.
- Negligible geometric and short circuit correction factors.

10.11.3 Cuboid Solution

Using logmean temperature method and assuming a cube with $L = d_{hot} = d_{cold} = d_{plate}$, I can find the heat exchanger side length as follow.

$$q = UA\Delta T_{lm}$$

$$L = \left(\frac{\dot{Q} 6R}{U(2 + \pi) \frac{\Delta T_2 - \Delta T_1}{\ln \left(\frac{\Delta T_2}{\Delta T_1} \right)}} \right)^{\frac{1}{3}}$$

10.11.4 Integrating Over the Channel Lengths

However, I have difficulties in evaluating the overall heat transfer coefficient U , because of changing conditions across the HX. Both the HTC and the temperature differences will vary across the HX. I segment the HX length in to $N_{segments}$.

For each segment, starting with the first, I find U , and solve for the next segment's fluid temperatures by energy conservation and Newton's law.

$$-\dot{q}_i = c_h \dot{m}_h (T_{h,i+1} - T_{h,i}), \dot{q}_i = c_c \dot{m}_c (T_{c,i+1} - T_{c,i})$$

$$\dot{q}_i = A_s h(v) (T_{wall} - T_{out})$$

For each fluid, I also find the pressure drop by summing the pressure drop in each segment. To achieve the required thermal duty, I use an iterative solver with an initial guess for the HX cuboid dimension, that changes to achieve the heat transfer and therefore the correct inlet and outlet fluid temperatures.

The two fluids will have different flow rates and pipe cross sectional area to maintain acceptable velocities. Over the course of the coolant loop, it may be beneficial to conserve bulk velocities, even as the temperatures change, to minimize pressure drops. The relative areas of the HX inlets is a good starting point for estimating the cross sectional area of the HX. If the cross sectional area of the hot fluid is 4x larger than the cold, the hot fluid should have 4x as many coolant channels as the cold fluid, and their length will be 4x shorter. The mass flow rate, \dot{m} , is constrained by the temperature inputs and total heat transfer required. I impose constraints on the velocity and hydraulic diameter. I solve with either constraint and pick the one that satisfies both.

Ratio of pipe areas for the two fluids at the HX is given by,

$$\alpha = \text{floor} \left(\frac{\max(D_{h,0}, D_{h,1})}{\min(D_{h,0}, D_{h,1})} \right)^2$$

We scale the smaller pipe to get an integer number of passes,

$$\min(D_{h,0}, D_{h,1}) = \frac{\max(D_{h,0}, D_{h,1})}{\alpha}$$

The channel length of the two fluids are related by the number of passes α . Note that the heat transfer area for both fluids is the same regardless of α .

10.11.5 HX dimensions and HX Containers

The dimensions of the HX depend on the deployment case and the thermal insulation requirements. Usually, the HX will just be a mounted component with hot and cold feeds and sufficient insulation. If the HX is being used for the primary intermediate HX, the HX should fit inside a PV that also contains the primary circulator. Hot primary coolant flows straight into the HX, to the circulator, and back around the HX, which is insulated. The dimensions of this pressure vessel can vary depending on the HX volume requirements, the circulator dimensions, and hot and cold fluid feed diameters. A good starting point would be to make the HX/circulator vessel the same diameter as the RPV, potentially allowing the two to be directly attached without a hot gas duct and reducing factory capital outlays.

10.12 Finite Difference Schemes for Unsteady Heat Equation with non-linear BC

We list the problem and results of the various finite difference schemes considered for the unsteady heat equation in cylindrical and spherical geometries. I first find an explicit solution to the cylindrical case, followed by an Crank-Nicholson implicit scheme with symmetric inner BC and explicit heat flux boundary conditions on the external surface. The heat flux boundary conditions at the core barrel and RPV surface include a non-linear radiative heat transfer which requires use of an explicit scheme.

Table 44 Unsteady Heat Equation and Conditions.

	Sphere	Cylinder (inf)
Unsteady 1-d Thermal Conduction $\rho C_p = \theta$	$\theta \frac{\partial T}{\partial t} = \frac{k}{r^2} \left[\frac{\partial}{\partial r} \left(r^2 \frac{\partial T}{\partial r} \right) \right] + q(r)$	$\theta \frac{\partial T}{\partial t} = \frac{k}{r} \left[\frac{\partial}{\partial r} \left(r \frac{\partial T}{\partial r} \right) \right] + q(r)$
RPV Surface Heat Flux BC (h fixed to 2.3 W m ⁻² K ⁻¹)	$-k \left(\frac{\partial T}{\partial r} \right)_s = h \left(\frac{T_s - T_a}{2} \right) + \sigma \varepsilon (T_s^4 - T_\infty^4)$	
r=0 BC	$\dot{Q} = A_s \left(h(T_{wall} - T_{inf}) + \sigma \varepsilon (T_{wall}^4 - T_{inf}^4) \right)$ $\left(\frac{\partial T}{\partial r} \right)_{r=0} = 0$	
Initial Conditions	T(r,0) = C, average core temperature.	T(r,0) =
Power Distribution	$P_0 = \frac{\sin(\frac{r-\pi}{R}) \cdot P}{4 \cdot R^2 \cdot r}$, within the active core, P total operating power	P_0 defined as 2 chopped cosines with a peaking factor
Power Decay		$Q(t, r) = 0.0622 P_0 (t^{-2} - (t_0 + t)^{-2})$

10.12.1 Cylindrical Geometry, C-N Scheme

We use a C-N semi-implicit scheme in time with explicit BC. I can follow [172] if further improvements in speed and accuracy are necessary.

$$\alpha [T]^{i+1} = \beta [T]^i + \gamma + f$$

With the variables defined as

$$\begin{aligned}
 A &= \frac{\Delta t k}{r_i 2\theta\Delta r}, B = \frac{\Delta t k}{\theta\Delta r^2} \\
 \alpha &= \frac{1}{k} - h(T_N - T_a) + \sigma(T_N^4 - T_\infty^4) \\
 \alpha &= \begin{pmatrix} 1+2B & -2B & 0 & 0 & 0 & 0 \\ \frac{A}{2} - \frac{B}{2} & 1+B & -\frac{A}{2} - \frac{B}{2} & 0 & 0 & 0 \\ 0 & \ddots & \ddots & \ddots & 0 & 0 \\ 0 & 0 & 0 & 0 & -B & 1+B \end{pmatrix} \\
 \beta &= \begin{pmatrix} 1-2B & 2B & 0 & 0 & 0 & 0 \\ -\frac{A}{2} + \frac{B}{2} & 1-B & \frac{A}{2} + \frac{B}{2} & 0 & 0 & 0 \\ 0 & \ddots & \ddots & \ddots & 0 & 0 \\ 0 & 0 & 0 & 0 & B & 1-B \end{pmatrix} \\
 \gamma &= \begin{pmatrix} -\frac{1}{2}(Q_0^{i+1} + Q_0^i) \frac{\Delta t}{\theta} \\ -\frac{1}{2}(Q_j^{i+1} + Q_j^i) \frac{\Delta t}{\theta} \\ \vdots \\ 0 \\ \vdots \\ \left(\frac{A}{2} + \frac{B}{2}\right) 2\Delta r(\alpha_N^i) \end{pmatrix} \\
 f &= \begin{pmatrix} 0 \\ \vdots \\ \left(\frac{A}{2} + \frac{B}{2}\right) 2\Delta r(\alpha_N^i) \end{pmatrix}
 \end{aligned}$$

10.12.2 Spherical Geometry, C-N Scheme

$$\begin{aligned}
 A &= \frac{\Delta t k}{r_i \theta\Delta r}, B = \frac{\Delta t k}{\theta\Delta r^2} \\
 \alpha &= \frac{1}{k} - h(T_N - T_a) + \sigma(T_N^4 - T_\infty^4) \\
 \alpha &= \begin{pmatrix} 1+3B & -3B & 0 & 0 & 0 & 0 \\ \frac{A}{2} - \frac{B}{2} & 1+B & -\frac{A}{2} - \frac{B}{2} & 0 & 0 & 0 \\ 0 & \ddots & \ddots & \ddots & 0 & 0 \\ 0 & 0 & 0 & 0 & -B & 1+B \end{pmatrix} \\
 \beta &= \begin{pmatrix} 1-3B & 2B & 0 & 0 & 0 & 0 \\ -\frac{A}{2} + \frac{B}{2} & 1-B & \frac{A}{2} + \frac{B}{2} & 0 & 0 & 0 \\ 0 & \ddots & \ddots & \ddots & 0 & 0 \\ 0 & 0 & 0 & 0 & B & 1-B \end{pmatrix} \\
 \gamma &= \begin{pmatrix} -\frac{1}{2}(Q_0^{i+1} + Q_0^i) \frac{\Delta t}{\theta} \\ -\frac{1}{2}(Q_j^{i+1} + Q_j^i) \frac{\Delta t}{\theta} \\ \vdots \\ 0 \\ \vdots \\ \left(\frac{A}{2} + \frac{B}{2}\right) 2\Delta r(\alpha_N^i) \end{pmatrix} \\
 f &= \begin{pmatrix} 0 \\ \vdots \\ \left(\frac{A}{2} + \frac{B}{2}\right) 2\Delta r(\alpha_N^i) \end{pmatrix}
 \end{aligned}$$

10.13 Code Improvements

1. Code Architecture
 - Bottom-up approach to build reactor COA without reference COA, using quote database and standalone component estimates. Quote database by component type ref design, amount by cost category, inflation indices, year, and the appropriate scaling laws to use.
 - Implement feedback mechanism to loop on sections of the code
 - Partitioning optimizations: system level vs subsystem/component level optimizations
2. Civil
 - Generic building cost estimate more accurate than the civil code requirements
 - Improve enclosure estimates with inspection and maintenance requirements
 - Analyze seismic isolation options and effects as additional components and effect on the civil / mechanical design
3. Cost Estimates
 - Detailed Spare and Maintenance cashflows based on part lifetimes rather than percentage of CAPEX
 - Input Parameter Inflation to accommodate dated cost inputs such as salary and feedstock or process costs
 - Other Cost Factors:
 - Account for Carbon Tax
 - Consider Tax Subsidy and period
 - Accounts to match Guidelines GENIV.
 - Heat Rejection Design and Cost Estimate
 - Conditional Operating Paradigms
 - Class A allows High and Medium Automation
 - Active requires Low Automation
 - Modularization as function of subsystem size
4. Materials
 - Data Consolidation:
 - Material databases.
 - ASME data; Dictionary between ASME materials and others.
 - Expand material data over temperature ranges.
5. RPVs
 - Expand the available material of construction, chosen to match the required contact temperatures with appropriate cost change.
 - Neutronic ROM to estimate dpa rate and RPV lifetime.
6. Thermal Hydraulics
 - Stress estimate on fuel elements during operations to affect the coolant channel and fuel thickness dimensions bounded by the manufacturing constraints.
 - Alternative geometric arrangements and TH design strategies
7. Balance of Plant
 - Solve for node temperatures.
 - Better estimate for BoP efficiency cycles
 - Concept design of turbo machinery including stages and dimensions
 - Better estimates for component temperature dependence based on material selection
 - Wider options for HX solver
 - Heat Rejection design and costing for Air-cooled Direct, Wet-cooled Direct, Air-cooled Indirect, Once Through Water, Radiative Heat sinks (space)
 - Expand feedstock and manufacturing method database.
8. UNF
 - ROM for decay heat curves at different burnups and fuel power densities for a set of different core configurations.
 - UNF heat transfer model for dry cask storage to determine packing arrangements and loading
9. Environmental impacts can be estimated based on land use, water use, carbon emission, and radiological exposure [106, Pt. Appendix C]
 - Table C-5.2. Summary of Land Use Impacts.
 - Table C-5.7. Summary of Water Use Impacts.
 - Table C-5.15. Summary of CO2 Impacts.
 - Table C-5.41. Summary of Radiologic Exposure - Total Estimated Worker Dose Impacts.
10. Core Design
 - More options for outer reflector, inner reflector, and core heterogeneity.
11. Power Rating

- Improve speed and numerical stability to utilize finite difference solution.
 - Operating power limit coupled to TH and fuel performance model (TRISO and fuel compact)
12. Core Energy Content
- ROM based on burnup evaluations across fuel/mod choices, enrichments, diameter, reflector thickness, and ratio.
13. Reporting
- Model status report to readily document how estimates are made over the design inputs available.
 - Full design report with trades, GA results, and model assumptions.
 - Improved component visualization to quickly seek the design dimensions of the full ES.

10.14 Improving Core Energy Content Models

The simple reduced order model discussed in Section 3.2 uses a reference point and a simple linear scaling for enrichment and diameter with a peak burnup. To be clear, this is a flawed and temporary solution until high fidelity reduced order models for best performance are built using more detailed burn up estimates across the design space. A burnup estimate for a given HTGR core using Serpent would be too time intensive for use in this code. Finding excellent heterogenous core designs for different enrichments, fuel types and definitions, moderators, and core diameters is even less feasible. I needed a way to estimate the possible burnup as a function of the enrichment, core diameter, fuel/moderator choice, and fuel/moderator ratio.

To that end, I used Serpent to evaluate burnup for a periodic pin cell across the design space consisting of pin radius, fuel moderator ratio, pin shape, pin height, and lattice type. These inputs fully define the pin including the lattice edge. The possible lattice types were: 2D hexagonal and cubic; 3D FCC, HCP, or cubic. This was done only for 20% enriched UO₂ pins in graphite with results in Figure 64 and Figure 65. I measured the burnups and volumetric energy density.

The characteristic performance curve for the given fuel/moderator choice is defined by maximal fuel utilization: the highest burnup achievable for each fuel/mod ratio considered. I find that for this fuel/mod choice and enrichment in a periodic pin geometry, one can achieve very high burnup with only minor penalties at high fuel/mod ratio up to 0.2. Cores of the same volume and fuel/mod ratio are considered the same cost regardless of the pin dimensions or counts. The volumetric energy content will correspondingly peak at a higher fuel moderator ratio than the ratio that maximizes burnup. I only looked at 20% enriched UO₂ in graphite and therefore limited the moderator option to just graphite. I also did not analyze the effects of varying reflector thickness, core minimum dimension, or more complex core geometries with variable pitch, variable F/M ratio, or variable enrichment.

Future efforts can be made to expand the choices into new fuel/moderator combinations and enrichments and provide characteristic performance curves across core diameter and reflector thickness. The latter task will prove challenging as smaller cores will require more careful design choices to reach their highest burnup potential. I am referring to heterogenous cores with radially varying enrichment, pitch, and pin radius.

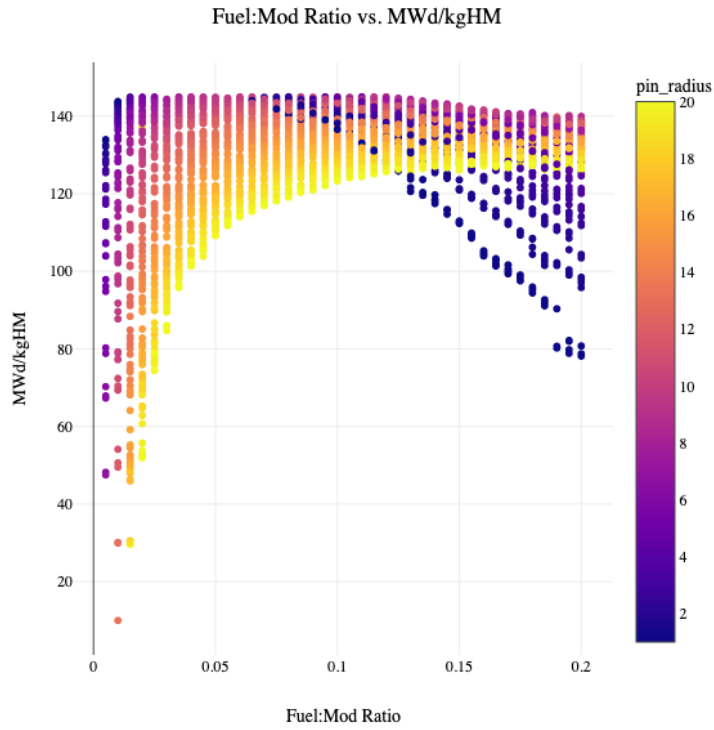


Figure 64 Showing the characteristic performance limit for periodic pins of UO₂ in graphite. Radius in cm.

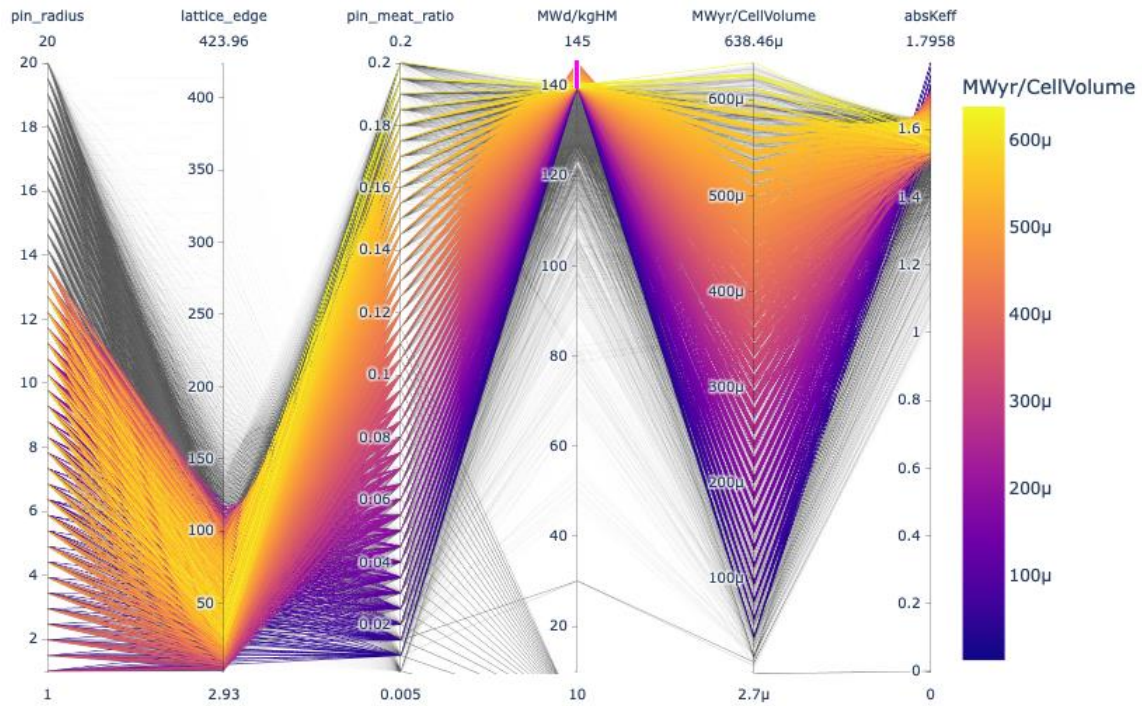


Figure 65 Performance results for grid evaluation of periodic pins of 20% enriched UO₂ in graphite. Radius and edge in cm.